INFORMATION TO USERS

This material was produced from a microfilm copy of the original document. While the most advanced technological means to photograph and reproduce this document have been used, the quality is heavily dependent upon the quality of the original submitted.

The following explanation of techniques is provided to help you understand markings or patterns which may appear on this reproduction.

1. The sign or "target" for pages apparently lacking from the document photographed is "Missing Page(s)". If it was possible to obtain the missing page(s) or section, they are spliced into the film along with adjacent pages. This may have necessitated cutting thru an image and duplicating adjacent pages to insure you complete continuity.

2. When an image on the film is obliterated with a large round black mark, it is an indication that the photographer suspected that the copy may have moved during exposure and thus cause a blurred image. You will find a good image of the page in the adjacent frame.

3. When a map, drawing or chart, etc., was part of the material being photographed the photographer followed a definite method in "sectioning" the material. It is customary to begin photoing at the upper left hand corner of a large sheet and to continue photoing from left to right in equal sections with a small overlap. If necessary, sectioning is continued again — beginning below the first row and continuing on until complete.

4. The majority of users indicate that the textual content is of greatest value, however, a somewhat higher quality reproduction could be made from "photographs" if essential to the understanding of the dissertation. Silver prints of "photographs" may be ordered at additional charge by writing the Order Department, giving the catalog number, title, author and specific pages you wish reproduced.

5. PLEASE NOTE: Some pages may have indistinct print. Filmed as received.

Xerox University Microfilms
300 North Zeeb Road
Ann Arbor, Michigan 48106

75-20,402

MATHEWS, Alexander Piravonu, 1944-
MATHEMATICAL MODELING OF MULTICOMPONENT
ADSORPTION IN BATCH REACTORS.

The University of Michigan, Ph.D., 1975
Engineering, civil

Xerox University Microfilms, Ann Arbor, Michigan 48106

THIS DISSERTATION HAS BEEN MICROFILMED EXACTLY AS RECEIVED.

MATHEMATICAL MODELING OF MULTICOMPONENT ADSORPTION IN BATCH REACTORS

by
Alexander Piravonu Mathews

A dissertation submitted in partial fulfillment
of the requirements for the degree of
Doctor of Philosophy
(Civil Engineering: Water Resources Engineering)
in The University of Michigan
1975

Doctoral Committee:

Professor Walter J. Weber, Jr., Chairman
Professor Jack A. Borchardt
Associate Professor Jonathan W. Bulkley
Associate Professor Raymond P. Canale
Associate Professor Norman D. Weiner

ACKNOWLEDGEMENTS

I would like to thank the members of the dissertation committee for their guidance in the conduct of this research. In particular, I would like to thank the Chairman of the committee, Professor Walter J. Weber, Jr., for his advice and suggestions during the course of the investigation. Acknowledgement and thanks are also due to all those who directly or indirectly assisted me in this research, and in the preparation of the dissertation.

I would also like to thank my wife, Shyla, for her patience, and her encouragement.

TABLE OF CONTENTS

	Page
ACKNOWLEDGEMENTS	ii
LIST OF TABLES	vi
LIST OF ILLUSTRATIONS	vii
NOMENCLATURE	xii
1. INTRODUCTION	1
2. SINGLE COMPONENT ADSORPTION	9
Reaction Rate Model	10
Pore Diffusion Model	14
Solid Phase Diffusion Model	17
Model Development	18
Numerical Procedure	21
Selection of Grid Size	25
3. EXPERIMENTAL MATERIALS AND ANALYTICAL METHODS	28
Adsorbent	28
Adsorbates	28
Adsorbate Mixtures	30
Analytical Methods	32
4. ADSORPTION EQUILIBRIA	38
Single Component Adsorption Equilibria	38
Experimental Procedure	40

TABLE OF CONTENTS (continued)

	Page
Experimental Results	41
Multicomponent Adsorption Equilibria	47
Correlation of Mixture Equilibria	55
Experimental Results	61
5. ESTIMATION OF RATE PARAMETERS	72
Mass Transfer - General Considerations	72
Mass Transfer to Suspended Solid Particles	75
Sensitivity Analysis	80
Mass Transfer in Adsorption Systems	83
Parameter Estimation	95
Experimental Method	97
Experimental Results	97
Conclusions	111
6. MULTICOMPONENT ADSORPTION	114
Mathematical Development	114
Numerical Procedure	118
Experimental Results	122
Phenol - p-Toluene Sulfonate Mixtures	123
Phenol - p-Bromophenol Mixtures	130
Phenol - Dodecyl Benzene Sulfonate Mixtures	139
Comparison to Single-Resistance Model	150

TABLE OF CONTENTS (continued)

	Page
7. SUMMARY AND CONCLUSIONS	156
APPENDICES	163
Appendix A: Finite Difference Approximation to Adsorption Rate Equations	163
Appendix B: Newton-Raphson Method Computations for Rate and Equilibrium Models	165
Appendix C: Computer Programs for Parameter Estimation and Multi-Solute Rate and Equilibria Prediction	167
BIBLIOGRAPHY	185

LIST OF TABLES

Table	Title	Page
3-1	Properties of Filtrasorb Carbon	29
3-2	Physical Properties of Solutes	31
3-3	Mixture Compositions	33
3-4	Molar Absorptivities for Solutes	34
4-1	Isotherm Constants	46
4-2	Equilibrium Data for Phenol-p-Bromophenol Mixtures: Phenol(1) - p-Bromophenol (2)	62
4-3	Equilibrium Data for Phenol-p-Toluene Sulfonate Mixtures: Phenol (1) - p-Toluene Sulfonate (2)	63
4-4	Equilibrium Data for Phenol (1) - Dodecyl Benzene Sulfonate Mixtures (2)	64
5-1	Mass Transfer and Surface Diffusion Coefficients	112

LIST OF ILLUSTRATIONS

Figure	Title	Page
2-1	Comparison of Numerical and Analytical Solutions	26
3-1	Calibration Curve for Phenol (268 and 282 mμ)	35
3-2	Calibration Curve for Phenol (215 and 223 mμ)	36
4-1	Adsorption Isotherm: Phenol	42
4-2	Adsorption Isotherm: p-Bromophenol	43
4-3	Adsorption Isotherm: p-Toluene Sulfonate	44
4-4	Adsorption Isotherm: Dodecyl Benzene Sulfonate	45
4-5	Comparison of Models for Mixture Equilibria Prediction: p-Cresol-p-Chlorophenol	56
4-6	Comparison of Models for Mixture Equilibria Prediction: p-Cresol-p-Chlorophenol	57
4-7	Comparison of Models for Mixture Equilibria Prediction: Acetone-Propionitrile	58
4-8	Comparison of Models for Mixture Equilibria Prediction: Acetone-Propionitrile	59
4-9	Correlation of Mixture Equilibria: Phenol-p-Bromophenol	65
4-10	Correlation of Mixture Equilibria: Phenol-p-Bromophenol	66
4-11	Correlation of Mixture Equilibria: Phenol-p-Toluene Sulfonate	67
4-12	Correlation of Mixture Equilibria: Phenol-p-Toluene Sulfonate	68
4-13	Correlation of Mixture Equilibria: Phenol-Dodecyl Benzene Sulfonate	69

LIST OF ILLUSTRATIONS (Continued)

Figure	Title	Page
4-14	Correlation of Mixture Equilibria: Phenol-Dodecyl Benzene Sulfonate	70
5-1	Sensitivity of Predicted Profile to Variation in Mass Transfer Coefficient, k_f. p-Bromophenol	81
5-2	Sensitivity of Predicted Profile to Variation in Mass Transfer Coefficient, k_f. Dodecyl Benzene Sulfonate	82
5-3	Sensitivity of Predicted Profile to Variation in Mass Transfer Coefficient, k_f. Phenol	84
5-4	Sensitivity of Predicted Profile to Variation in Mass Transfer Coefficient, k_f. p-Toluene Sulfonate	85
5-5	Effect of Intraparticle Diffusion on the Initial Uptake Rate for Phenol	89
5-6	Effect of Intraparticle Diffusion on the Initial Uptake Rate for Phenol	90
5-7	Effect of Intraparticle Diffusion on the Initial Uptake Rate: p-Toluene Sulfonate	91
5-8	Effect of Intraparticle Diffusion on the Initial Uptake Rate: p-Bromophenol	92
5-9	Effect of Intraparticle Diffusion on the Initial Uptake Rate: p-Bromophenol	93
5-10	Effect of Intraparticle Diffusion on the Initial Uptake Rate: Dodecyl Benzene Sulfonate	94
5-11	Concentration-Time Profile: p-Bromophenol (C_o=5 x 10^{-4}M, Carbon=0.33 g/l, 650 RPM)	99

LIST OF ILLUSTRATIONS (Continued)

Figure	Title	Page
5-12	Concentration-Time Profile: p-Bromophenol (C_o=5 x 10^{-4}M, Carbon=0.25 g/l, 650 RPM)	100
5-13	Concentration-Time Profile: p-Toluene Sulfonate (C_o=10^{-4}M, Carbon=0.33 g/l, 650 RPM)	102
5-14	Concentration-Time Profile: p-Toluene Sulfonate (C_o=10^{-4}M, Carbon=0.5 g/l, 650 RPM)	103
5-15	Concentration-Time Profile: Dodecyl Benzene Sulfonate (C_o=10^{-4}M, Carbon=0.5 g/l, 650 RPM)	105
5-16	Concentration-Time Profile: Dodecyl Benzene Suflonate (C_o=10^{-4}M, Carbon=0.33 g/l, 650 RPM)	106
5-17	Concentration-Time Profile: Phenol (C_o=5 x 10^{-4}M, Carbon=0.67 g/l, 650 RPM)	108
5-18	Concentration-Time Profile: Phenol (C_o=5 x 10^{-4}M, Carbon=0.67 g/l, 1670 RPM)	109
5-19	Concentration-Time Profile: Phenol (C_o=5 x 10^{-4}M, Carbon=0.5 g/l, 1670 RPM)	110
6-1	Rates of Adsorption from Mixtures: Phenol-p-Toluene Sulfonate (C_{10}=C_{20}=10^{-4}M, Carbon= 0. 67 g/l, 650 RPM)	124
6-2	Total Concentration Profile: Phenol-p-Toluene Sulfonate (C_{10}=C_{20}=10^{-4}M, Carbon=0.67 g/l, 650 RPM)	125
6-3	Rates of Adsorption from Mixtures: Phenol-p-Toluene Sulfonate (C_{10}=C_{20}=5 x 10^{-5}M, Carbon=0.33 g/l, 650 RPM)	126
6-4	Total Concentration Profile: Phenol-p-Toluene Sulfonate (C_{10}=C_{20}=5 x 10^{-5}M, Carbon=0.67 g/l, 650 RPM)	127

LIST OF ILLUSTRATIONS (Continued)

Figure	Title	Page
6-5	Rates of Adsorption from Mixtures: Phenol-p-Toluene Sulfonate ($C_{10}=5 \times 10^{-5}$M, $C_{20}=2.5 \times 10^{-5}$M, Carbon=0.33 g/1, 650 RPM)	128
6-6	Total Concentration Profile: Phenol-p-Toluene Sulfonate ($C_{10}=5 \times 10^{-5}$M, $C_{20}=2.5 \times 10^{-5}$M, Carbon=0.33 g/1, 650 RPM)	129
6-7	Rates of Adsorption from Mixtures: Phenol-p-Bromophenol ($C_{10}=C_{20}=5 \times 10^{-4}$M, Carbon=0.67 g/1, 650 RPM)	131
6-8	Total Concentration Profile: Phenol-p-Bromophenol ($C_{10}=C_{20}=5 \times 10^{-4}$M, Carbon=0.67 g/1, 650 RPM)	132
6-9	Rates of Adsorption from Mixtures: Phenol-p-Bromophenol ($C_{10}=C_{20}=5 \times 10^{-4}$M, Carbon= 0.5 g/1, 650 RPM)	134
6-10	Total Concentration Profile: Phenol-p-Bromophenol ($C_{10}=C_{20}=5 \times 10^{-4}$M, Carbon=0.5 g/1, 650 RPM)	135
6-11	Rates of Adsorption from Mixtures: Phenol-p-Bromophenol ($C_{10}=2.5 \times 10^{-4}$M, $C_{20}=5 \times 10^{-4}$M, Carbon=0.33 g/1, 650 RPM)	137
6-12	Total Concentration Profile: Phenol-p-Bromophenol ($C_{10}=2.5 \times 10^{-4}$M, $C_{20}=5 \times 10^{-4}$M, Carbon=0.33 g/1, 650 RPM)	138
6-13	Rates of Adsorption from Mixtures: Phenol-Dodecyl Benzene Sulfonate ($C_{10}=C_{20}=5 \times 10^{-5}$M, Carbon=0.33 g/1, 650 RPM)	140
6-14	Total Concentration Profile: Phenol-Dodecyl Benzene Sulfonate ($C_{10}=C_{20}=5 \times 10^{-5}$M, Carbon=0.33 g/1, 650 RPM)	141

LIST OF ILLUSTRATIONS (Continued)

Figure	Title	Page
6-15	Rates of Adsorption from Mixtures: Phenol-Dodecyl Benzene Sulfonate ($C_{10}=C_{20}=10^{-4}$ M, Carbon=0.67 g/l, 650 RPM)	142
6-16	Total Concentration Profile: Phenol-Dodecyl Benzene Sulfonate ($C_{10}=C_{20}=10^{-4}$ M, Carbon=0.67 g/l, 650 RPM)	143
6-17	Rates of Adsorption from Mixtures: Phenol-Dodecyl Benzene Sulfonate. Predicted Profiles Using k_{fi} from Mixture Rate Data	146
6-18	Total Concentration Profile: Phenol-Dodecyl Benzene Sulfonate. Predicted Profile Using k_{fi} from Mixture Rate Data	147
6-19	Rates of Adsorption from Mixtures: Phenol-Dodecyl Benzene Sulfonate. Predicted Profiles Using k_{fi} from Mixture Rate Data	148
6-20	Total Concentration Profile: Phenol-Dodecyl Benzene Sulfonate. Predicted Using k_{fi} from Mixture Rate Data	149
6-21	Effect of Intraparticle Diffusion on Rates of Adsorption from Mixtures: Total Concentration Profile for Phenol-p-Toluene Sulfonate Mixture	151
6-22	Effect of Intraparticle Diffusion on Rates of Adsorption from Mixtures: Phenol-p-Toluene Sulfonate	152
6-23	Effect of Intraparticle Diffusion on Rates of Adsorption from Mixtures: Total Concentration Profile for Phenol-Dodecyl Benzene Suflonate	153
6-24	Effect of Intraparticle Diffusion on Rates of Adsorption from Mixtures: Phenol-Dodecyl Benzene Sulfonate	154

NOMENCLATURE

ROMAN

Symbol	Description and Units
A	Surface area of adsorbent
A_i	Absorbance at wavelength λ_i
a	Isotherm constant, three parameter equation
a_f	Interfacial area for mass transfer through the film surrounding the particle (cm^2/cm^3)
a_p	Interfacial area for mass transfer within the particle (cm^2/cm^3)
b	Isotherm constant, three parameter equation
b'	Langmuir isotherm constant (liter/mole)
C	Concentration of solute in the fluid phase
C_e	Concentration of solute in the fluid phase in equilibrium with the solid phase concentration
C_i	Chapter 4: Equilibrium concentration of species i when adsorbing from a mixture
C_i	Chapter 6: Concentration of solute i in the fluid phase (moles/liter)
C_p	Concentration of solute in the fluid phase in the pores of the particle
C_s	Concentration of solute in equilibrium with the amount adsorbed q_s on the surface of the particle
C_o	Influent concentration in flow through sytems, and concentration at t=0 in batch reactor
D	Surface diffusion coefficient (cm^2/sec)
D_I	Impeller diameter

NOMENCLATURE (Continued)

Symbol	Description and Units
D_G	Ratio of equilibrium solute distribution between the solid and fluid phases ($q_\infty \rho_b / C_o \epsilon_b$). dimensionless
D_T	Diameter of reactor vessel
D_p	Pore Diffusivity (cm^2/sec)
D_v	Free liquid diffusivity (cm^2/sec)
d	Particle diameter
F	Volumetric flow rate (cm^3/min)
F^a	Helmholtz free energy for the adsorbed phase
f_i	Fugacity of solute i in mixture
f_i^o	Pure component fugacity
J_i	Flux of species i ($moles/cm^2$ sec)
K	Forward reaction rate constant (lit/mol sec)
K'	Reverse reaction rate constant (1/sec)
K_F	Freundlich isotherm constant
K_l	Linear isotherm constant
k_f	Liquid phase mass transfer coefficient (cm/sec)
k_f'	Liquid phase mass transfer coefficient (liter/sec)
k_f^*	Mass transfer coefficient for particle falling at its terminal velocity (cm/sec)
k_p	Mass transfer coefficient for solid-phase diffusion in the particle (cm/sec)

NOMENCLATURE (Continued)

Symbol	Description and Units
L	$k_f R/D$, dimensionless
$\frac{M_t}{M_\infty}$	Fractional approach to equilibrium
Q	Ultimate capacity, Langmuir isotherm constant
q	Concentration of solute on the solid phase (moles/gm)
q_e	Equilibrium concentration on the solid phase
q_i	Chapter 4: Equilibrium concentration of solute i when adsorbing from a mixture
q_i	Chapter 2: Concentration of solute on the solid phase, at any point in the particle
q_{ii}	Concentration of solute i on the solid phase at any point in the particle
q_i^a	Moles of i adsorbed relative to the solid phase
q_i^m	Invariant adsorption of solute i
q_T^m	Total amount adsorbed from mixture
q_s	Equilibrium concentration on the surface of the particle
q_∞	Equilibrium concentration corresponding to C_o
R	Radius of particle
r	radial coordinate
Re	Reynolds number = lu/ν, where, l is a length parameter, dimensionless.
Sc	Schmidt number = ν/D_v, dimensionless

NOMENCLATURE (Continued)

Symbol	Description and Units
Sh	Sherwood number = $k_f d/D_v$, dimensionless
t	time
u	Transformed solid phase concentration, $u=q_i x$
$\hat{u}$	Relative velocity between phases
V	Reactor volume
V_p	Volume of particle of radius R
v	Volume of bed in column
W	Weight of carbon
x	Dimensionless distance, r/R
y_i	Mole fraction of solute i in the adsorbed phase

GREEK

β	Isotherm constant, three parameter equation
γ	Freundlich isotherm constant
δ	Thickness of hydrodynamic film
ρ	Particle Density (gm/cm^3)
ρ_b	Density of bed (gm/cm^3)
ν	Kinematic viscosity (cm^2/sec)
$\bar{\nu}$	Ratio of surface diffusion coefficients, D_2/D_1
ν'	$\bar{\nu}\lambda$
ϵ	Porosity of particle
ϵ_b	Porosity of bed

NOMENCLATURE (Continued)

Symbol	Description and Units
ϵ_{ij}	Molar absorptivities
$\bar{\epsilon}$	Agitation power input per unit mass
μ_i^a	Chemical potential of adsorbed species i
μ_s^a	Chemical potential of solvent in the adsorbed phase
μ^l	Chemical potential of solute in the liquid phase
μ_i^o	Chemical potential of the pure component i
λ	$\Delta\tau/2\,\Delta x^2$
π	Spreading pressure
η_i	Interaction terms for mixture equilibria
$\bar{\eta}$	Scale of turbulence
τ	Dimensionless time, Dt/R^2

Subscripts

i	Solute i, or interior of the particle
s	Solvent, or surface of the particle

Superscripts

a	Adsorbed phase
m	Invariant adsorption
l	liquid phase
o	Equilibrium adsorption of pure component

CHAPTER 1

INTRODUCTION

Increases in population and industrial growth in the last few decades have had unprecedented impacts on the quality of the nation's water resources. Advances in manufacturing technology have tended to generate wastes with contaminants that are not affected by conventional methods of treatment.

The Advanced Waste Treatment Program was initiated in 1960 in recognition of the need for new technology for water pollution control. The stated objectives of the program were to develop alternative treatment methods to alleviate the nation's growing water pollution problems, and to renovate wastewater for direct reuse. Among the various methods studied over the last few years, adsorption on activated carbon has been shown by extensive laboratory and pilot-plant studies, and full scale development, to be a feasible process for the removal of organic compounds from aqueous solution (31,32,33,51,73,79).

Activated carbon adsorption can be used as a tertiary treatment method for effluents from existing secondary treatment plants, or as an integral part of a physico-chemical treatment system. Tertiary treatments of effluents from conventional biological treatment operations have

shown definite improvement in the effluent quality (50, 51,57), with some leakage of unadsorbed organic material. This unadsorbed fraction consists chiefly of low molecular weight polar organic compounds and high molecular weight humic carbohydrate-like material (10).

Physicochemical treatment of municipal wastewaters, encompassing chemical clarification, filtration, and adsorption, is an economically feasible process for meeting current high effluent standards. The significant advantages of this method over biological treatment are in the flexibility of design and operation, reduced sensitivity to toxic substances and to variations in flow and concentration, potential for heavy metal removal, removal of inorganic algal nutrients, and greater removal of organic wastes. Currently, a number of municipal wastewater treatment plants are under construction, or in operation, using activated carbon for tertiary treatment, or as an integral part of physicochemical treatment of raw wastewater. A wide variety of industrial wastes have also been shown to be amenable to treatment using activated carbon adsorption (15,16,55,80).

The cost of carbon is sufficiently high to warrant the regeneration and reuse of the exhausted carbon. This is usually done by controlled heating in rotary kilns or multiple-hearth furnaces in the presence of steam. The

capital costs for the regenerating equipment, and the added operating costs are high enough to make tertiary treatment with carbon uneconomical for small treatment plants. However, partial self-regeneration can be achieved by allowing biological growth on the surface of carbon (51, 71). Weber, et. al., (71) have found that the carbon exhaustion rate can be substantially reduced with biologically-extended adsorption systems.

Various contacting systems are available for adsorption on granular activated carbon (5). However, continuous operation in a packed or expanded bed has been shown to be the most advantageous in terms of ease of operation and economy (32,33,48,75,77). The expanded-bed mode of operation has several advantages over the packed bed system (68,69, 73). The most significant advantage is that the capacity of the carbon can be increased by allowing biological growth on the surface of the carbon. In packed beds, this may result in operational difficulties due to air-binding and high pressure drop. It is possible to use smaller size carbon particles in an expanded bed and take advantage of the higher adsorption rates possible with smaller particles.

The effective application of adsorption in tertiary and physicochemical treatments requires a thorough understanding of the process itself. Otherwise, plant design will

have to be based on expensive pilot-plant data for breakthrough profiles for various operating conditions. A mathematical model for the process will facilitate the establishment of systematic design procedures, and will also help delineate the control variables in the process. To this end, Keinath and Weber (36) developed a model for predicting breakthrough profiles for single solute adsorption in expanded bed adsorbers. This model is based on the second order reaction rate method of Thomas (62) for adsorption or ion-exchange reaction, and extended to diffusion-controlled adsorption by Hiester and Vermuelen (24). Its applicability is restricted to solutes exhibiting Langmuir-type adsorption isotherm.

DiGiano and Weber (12,13) studied the adsorption rates of solutes in finite and infinite bath systems. In the finite bath system, assumptions of irreversible immobilization and quasi-steady state in the solid phase were made. Thus, the model is suitable for solutes satisfying the dual criteria of irreversible adsorption and large solid to liquid equilibrium solute distribution. The latter condition is necessary to satisfy the assumption of quasi-steady state, that is, the rate of immobilization of the solute is rapid compared to the motion of the solute front in the solid. In the infinite bath system, mathematical

simplifications were achieved by maintaining constant solute concentration in the reactor. This method is suitable for solutes that can be analyzed continuously, for example, by visible spectrophotometry, or titrimetry. However, it poses serious experimental difficulties for multi-solute systems.

The single solute rate mode developed in this study is patterned after the homogeneous solid phase diffusion model proposed by Rosen (58) for solutes described by a linear isotherm. The model takes into account the diffusional processes within the solid and fluid phases, and is sufficiently general to be valid for a variety of solutes, since no restrictive assumptions are made. Several workers have noted the inadequacy of Langmuir and Freundlich isotherms in describing equilibrium data over a wide concentration range (30,76). An empirical equation is proposed and utilized in this study to represent adsorption equilibrium data over wide concentration ranges. However, any isotherm expression can be used in the rate model.

Industrial and domestic wastewaters typically contain a wide spectrum of compounds in differing concentrations. Even in single solute systems, biological decay may result in end products that compete with the solute for the available sites on the surface of the carbon. It is

therefore, important to develop a model to describe the adsorption of mixtures of organic compounds by activated carbon.

Usinowicz and Weber (67) used the Keinath-Weber model in attempting to predict breakthrough profiles for organic mixtures in expanded bed operations. The mixtures were represented by a single concentration parameter, COD, and column and isotherm data were obtained as for a single solute. The model was satisfactory upto about 50% of the breakthrough curve. Beyond that, the removal of solute in the column was better than predicted. Gariepy and Zwiebel (19) modeled the adsorption of bisolute systems using the equilibrium model of Michaels (46), for each solute. The Langmuir isotherm for mixtures was used to obtain the necessary equilibrium data for mixtures. The experimental data from fixed beds did not conform very well to the predicted values due to the simplicity of the model.

It is apparent that the treatment of multicomponent systems as single solute systems, or the use of simplified rate models does not provide an accurate representation of the physical process. To describe multicomponent adsorption by a mathematical model, it is necessary to consider the various diffusional rate processes occurring in the fluid

and solid phases, and the equilibrium adsorption of mixtures. The multicomponent rate model developed herein, is an extension of the single solute model described earlier. Diffusional rate equations are written for each species for the solid and fluid phases, and coupled by the adsorption equilibrium relation for mixtures.

Several models were evaluated to obtain a satisfactory description of adsorption equilibria for mixtures. The method of Radke and Prausnitz (53) using the principles of dilute solution thermodynamics, is particularly suitable for solutes that do not adsorb strongly. However, the computational effort required in utilizing this model in a multicomponent rate model is substantial. In this investigation, the empirical equation for single solutes discussed earlier, is extended to predict multi-solute equilibria. For systems that can not be adequately described by this method, a procedure is developed to correlate multi-solute equilibrium data. This allows the use of experimental equilibrium data in the mixture rate model.

The multicomponent rate model requires several input parameters. Mass transfer coefficients and solid phase diffusion coefficients for each solute are obtained from single solute rate data using a direct-search parameter

estimation procedure. The procedure can be utilized in future analyses of batch reactor data for different solutes. The solid diffusion coefficient obtained is a necessary input parameter for the prediction of multi-solute breakthrough profiles from columns. The numerical method developed for the single and multicomponent systems can be used, with minor modifications, to simulate adsorption in fixed and fluidized beds.

Adsorption is a surface phenomenon characteristic to many physical, chemical and biological processes. It has several applications in chemical processing, particularly in the purification of gases and liquids. In the environmental area, activated carbon adsorption can be used for water and wastewater treatment, and the removal of pollutants from air. The developments reported in this study, therefore, may be of significance to these diverse fields employing adsorption as a separation process.

CHAPTER 2

SINGLE COMPONENT ADSORPTION

The removal of adsorbate from the fluid phase on to the solid phase in a batch reactor results in progressive enrichment of the solid phase until equilibrium between the two phases is attained. The concentration-time profile that results is called a kinetic curve, and it describes the overall adsorption behavior. In non-flow agitated systems, the following mechanistic processes have to be considered: (1) diffusion through the hydrodynamic boundary layer or film surrounding the particle, (2) diffusion on the surface of the particle, (3) diffusion through the pores of the particle, and (4) adsorption on the surface. All these processes may occur at comparable rates, in which case, the mathematical representation becomes extremely complex. However, in many cases, some of the rate processes are rapid compared to the others, and can be neglected. In wastewater applications, the adsorption reaction is sufficiently rapid to allow the assumption of local equilibrium between the phases.

The simplest model that can be considered is one in which there are no mass transfer resistances in the fluid and solid phases. DeVault (9) and Glueckauf (20) have

considered this case for the solution of problems involving chromatography. More recently, Klein and Helfferich (23) have developed a theory of multicomponent chromatography for this case.

Basically there are three different models available for representing adsorption with significant mass transfer resistances. One uses a reaction rate approach in approximating mass transfer, and the other two are based on different representations of diffusion within the particle.

Reaction Rate Model

The reaction rate approach of Thomas (62) seeks to describe the process of adsorption or ion-exchange as a second order reaction between the adsorbent and the adsorbate.

$$\text{Adsorbent} + \text{Adsorbate} \rightleftharpoons (\text{Adsorbate.Adsorbent}) \quad (2\text{-}1)$$

If C is the concentration of the solute in the liquid phase, q is the amount adsorbed, and Q is the monolayer capacity of the adsorbent, the second order reaction rate expression for 2-1 is

$$\frac{dq}{dt} = K\left((Q-q)C - \frac{K'}{K}q\right) \quad (2\text{-}2)$$

K and K' are the forward and reverse reaction rate constants, and (Q-q) is the unused capacity of the adsorbent at any

time t. At equilibrium, equation 2-2 reduces to the Langmuir isotherm.

The material balance relationship for a solute of concentration C in the fluid phase and q on the solid phase in a packed or expanded bed reactor, is given by equation 2-3.

$$F \frac{\delta c}{\delta v} + \varepsilon_b \frac{\delta C}{\delta t} + \rho_b \frac{\delta q}{\delta t} = 0 \qquad (2\text{-}3)$$

F is the fluid flow rate into the column, and v, ϵ_b, and ρ_b are volume, pososity, and density of the bed respectively. By using linear and nonlinear transformations, Thomas solved the continuity equation of 2-3, and the adsorption reaction equation 2-2, and obtained an analytical expression for the effluent concentration profile for columnar operation.

Hiester and Vermuelen (24) adapted the method of Thomas to solute adsorption involving mass transfer resistances in the fluid and solid phases. In the case where external film diffusion is controlling mass transfer, equation 2-4 is used to represent solute transport.

$$\frac{dq}{dt} = k_f a_f \frac{\varepsilon_b}{\rho_b}(C - C_e) \qquad (2\text{-}4)$$

The equilibrium concnetration C_e is given by the Langmuir

(2-5)

isotherm as

$$q_e = \frac{Qb'C_e}{1+b'C_e} \qquad (2\text{-}5)$$

and, the ultimate equilibrium concnetration corresponding to an influent concentration C_o is given by

$$q_\infty = \frac{Qb'C_o}{1+b'C_o} \qquad (2\text{-}6)$$

Substituting 2-5 and 2-6 in 2-4, and comparing the resulting expression with 2-2, Hiester and Vermuelen obtained an expression relating the film transfer coefficient and the reaction rate constant.

$$K_f = \frac{k_f a_f}{(1+(b'C_o/(1+b'C_o))q/q_\infty} \qquad (2\text{-}7)$$

This equation is further simplified to 2-8 by assuming that the average value of q/q_∞ for the bed may be taken as 0.5.

$$K_f = \frac{2k_f a_f}{(2+b'C_o/(1+b'C_o))} \qquad (2\text{-}8)$$

For intraparticle diffusion controlled adsorption, a linear driving force is assumed to represent the transport rate as

$$\frac{dq}{dt} = k_p a_p (q_e - q) \qquad (2\text{-}9)$$

Substitution of 2-5 and 2-6 in 2-9 and comparison with 2-2 results in an expression 2-10 relating the reaction rate constant to the intraparticle diffusion rate constant.

$$K_p = \frac{k_p a_p D_G}{((\dot{b}C_o/(1+\dot{b}C_o))C/C_o + 1/(1+\dot{b}C_o))} \qquad (2\text{-}10)$$

D_G is the limiting solute distribution between the two phases, and is given by

$$D_G = \frac{q_\infty \rho_b}{C_o \varepsilon_b} \qquad (2\text{-}11)$$

The assumption that the average value of C/C_o for the bed may be taken as 0.5 reduces 2-10 to 2-11.

$$K_p = \frac{2k_p a_p D_G}{(1 + 1/(1+\dot{b}C_o)} \qquad (2\text{-}12)$$

For cases where external and internal diffusion rates are comparable, the resistances may be combined to give an overall reaction rate constant to be used in equation 2-2.

$$K = \frac{2}{((1+(1/1+\dot{b}C_o))(1/k_f a_f + 1/k_p a_p D_G)}$$

Keinath and Weber (36) utilized the second order reaction rate approach in developing a model for adsorption in expanded beds. The input parameters of film and intraparticle diffusion coefficients were obtained from correlations for mass transfer coefficients and from batch

experiments.

The limitations of the Thomas' model arise from the fact that it is essentially valid only for slow adsorption or ion-exchange reactions, rather than finite mass transfer rates. In relating the reaction rate to mass transfer rates, Hiester and Vermuelen made a number of assumptions. Linear driving was assumed within the particle, and q/q_{∞} and C/C_o for the bed and the fluid were assumed to 0.5. The adsorption equilibrium relationship that can be used is restricted to the Langmuir isotherm for the second order reaction, and linear equilibrium for the first order reaction.

Pore Diffusion Model

The pore phase diffusion model pictures the adsorbent particles as consisting of a solid phase interspersed with very small pores. The adsorbate diffuses into the pores in the fluid phase, and adsorption occurs at the internal surfaces. If C_p is the concentration of the solute in the fluid phase in the pores, and q is the concentration on the solid phase, the transport within the particle is represented by

$$\varepsilon \frac{\delta C_p}{\delta t} + (1-\varepsilon) \frac{\delta q}{\delta t} = D_p \left(\frac{\delta C_p}{\delta r^2} + \frac{2}{r} \frac{\delta C_p}{\delta r}\right) \qquad (2\text{-}14)$$

D_p is the pore diffusivity of the solute, and ϵ is the porosity of the particle. The condition at the surface r=R, of the spherical particle when there is an external mass transfer resistance is given by

$$-D_p\left(\frac{\delta C_p}{\delta r}\right)_{r=R} = k_f a_f (C-C_p) \qquad (2\text{-}15)$$

Edeskuty and Amundson (14) considered the case of intraparticle diffusion with external diffusion for batch systems where the solute isotherms are linear. Kasten et. al. (34) used the same model and obtained an analytical solution for adsorption in fixed beds. Weber and Rumer (78) considered the case of nonlinear isotherm to represent equilibrium, and obtained intraparticle diffusion coefficients assuming cylinderical particles, and neglecting external mass transfer resistance.

DiGiano and Weber (12) showed that external resistance may be important even in rapidly agitated systems, and obtained diffusivities for spherical particles under the assumption of quasi-steady state and irreversible immobilization. The assumptions of irreversible immobilization and quasi-steady state afford considerable simplification to the mathematical analysis. Equation 2-14 reduces to an ordinary differential equation and can be solved to obtain

the solute concentration as a function of the radius of the particle and the solute front. However, the applicability of the model is restricted to solutes exhibiting irreversible adsorption, and the success of the model in fitting the experimental data was shown to depend strongly on the initial and final equilibrium concentrations selected for the rate study. For solutes with nonlinear equilibria, the fluid phase concentration was maintained constant by using an infinite bath system. With this simplification in the boundary condition, equation 2-14 was solved numerically to obtain diffusion constants for solutes that may be analyzed using visible spectrophotometry.

A variety of cases have been considered where one rate step has been assumed to conrol the transfer process. Hougen and Marshall (26) considered the case of film diffusion controllling mass transfer for solutes with linear equilibria. Kyte (38) obtained numerical solutions for the same case of external mass transfer controlling adsorption in a fixed bed, with the Freundlich isotherm to represent equilibrium. Masamune and Smith (44,45) obtained analytical solutions for film and pore diffusion controlling mass transfer, and the three resistance case of film, pore and surface diffusion acting simultaneously. However, a linear isotherm was assumed.

Solid Phase Diffusion Model

The homogeneous solid phase diffusion model proposed by Rosen (57) pictures the phase separation to be occurring by adsorption on the surface and subsequent transport into the particle by surface diffusion. Rosen solved the system of transport and material balance equations for fixed beds, coupled with linear equilibrium analytically, and presented the solution in the form of an infinite integral. Subsequently, Rosen (58) developed a method to evaluate the integrals numerically. Tien (63,64) solved the diffusion equation analytically, and used a numerical method to solve the system of equations for a fixed bed adsorber, for the cases of linear equilibrium and the Freundlich isotherm. Stuart and Camp (61) utilized the same model and reported good success in representing experimental data.

The two diffusional models were compared by Dedrick and Beckman (8) using a series of batch experiments. For the pore phase model however, irreversible isotherm was assumed even though the isotherm was actually described by Freundlich equation. Both the models were found to fit the data equally well. Hsieh, Turien and Tien (28) conducted batch studies to correlate diffusivity data based on both models. They found less scatter in the data with the solid phase diffusion model, and concluded that it is simpler

and possibly a better model for describing intraparticle diffusion. The mathematical development in this study utilizes the homogeneous solid phase diffusion model approach to obtain representation of adsorption with an arbitrary equilibrium isotherm.

Model Development

The mechanisitic processes that are considered in representing single component adsorption are (1) film diffusion from the fluid phase to the surface of the particle, (2) adsorption on the surface, and (3) diffusion on the surface of the particle. In addition, a material balance equation for the reactor system is necessary to describe the adsorption process.

Interphase transport from the fluid to the solid phase is obtained by equating the rate of change of concentration of the solid phase to the rate of mass transfer of the solute from the fluid phase through the film, as in equation 2-16. The average concentration of the particle is obtained

$$\frac{dq}{dt} = \frac{k'_f}{V_p \rho (1-\varepsilon)} (C-C_s) \qquad (2-16)$$

by averaging the point concentration over the volume of the particle, and is given by equation 2-17. Any arbitrary

$$q = \frac{3}{R^3}\int_0^R q_i r^2 dr \qquad (2\text{-}17)$$

isotherm can be used to represent the equilibrium adsorption at the surface of the particle. In this study, a three parameter equation, 2-18, developed in Chapter 4 is used.

$$q_s = \frac{aC_s}{1+bC_s^{\beta}} \qquad (2\text{-}18)$$

C_s and q_s are equilibrium concentrations in the fluid and solid phases respectively at the surface, and a, b, and β are isotherm constants.

For a spherical particle, assuming symmetry in two directions, the variation of the solid phase concentration in the radial direction is given by 2-19.

$$\frac{\delta q_i}{\delta t} = D\left(\frac{\delta q_i}{\delta r^2} + \frac{2}{r}\frac{\delta q_i}{\delta r}\right) \qquad (2\text{-}19)$$

Material balance for the solute in the batch reactor is represented by equation 2-20. The initial conditions for

$$V\frac{dC}{dt} = -W\frac{dq}{dt} \qquad (2\text{-}20)$$

the system of equations is given by the concentrations in the solid and fluid phases at time t=o. These are,

$$q_i(r,0) = 0 \qquad (2\text{-}21)$$

$$C(0) = C_o \qquad (2\text{-}22)$$

The boundary conditions for the particle are specified as implicit functions of time. Also, the derivative of concentration at the center of the particle is zero.

$$q_i(R,t) = q_s(t) \tag{2-23}$$

$$\frac{\delta q_i}{\delta t}(0,t) = 0 \tag{2-24}$$

The independent variables in 2-19 can be changed to dimensionless variables by the following transformations.

$$\tau = \frac{Dt}{R^2} \tag{2-25}$$

$$x = r/R \tag{2-26}$$

Substitution of 2-25 and 2-26 in 2-19 results in 2-27.

$$\frac{\delta q_i}{\delta \tau} = \frac{\delta^2 q_i}{\delta x} + \frac{2}{x}\frac{\delta q_i}{\delta x} \tag{2-27}$$

Equation 2-27 is further simplified into 2-29 by the change of variable shown in equation 2-28.

$$u = xq_i \tag{2-28}$$

$$\frac{\delta u}{\delta \tau} = \frac{\delta^2 u}{\delta x^2} \tag{2-29}$$

The transformed initial and boundary conditions are,

$$u(0,\tau) = 0 = u(x,0)$$

$$u(b,\tau) = u_s(\tau) \tag{2-30}$$

Equations 2-16, 2-17, 2-25, and 2-26 can be combined to give equation 2-31.

$$\frac{\delta}{\delta \tau}\int_0^1 ux\, dx = \frac{k_f' R^2}{3V_p \rho D(1-\epsilon)}(C-C_s) \tag{2-31}$$

And by the Leibnitz theorem, this reduces to 2-32.

$$\int_0^1 \frac{\delta u}{\delta \tau} x \, dx = \frac{k_f' R^2}{3 V_p \rho D (1-\varepsilon)} (C - C_s) \qquad (2\text{-}32)$$

This equation can be used to replace the boundary condition for the surface in solving for the solid and fluid phase concentrations. Substituting equations 2-33 and 2-34 in 2-32 results in equation 2-35 as the boundary condition for the surface.

$$V_p = \frac{4\pi R^3}{3} \qquad (2\text{-}33)$$

$$k_f' = k_f \frac{4\pi R^2}{1000} \qquad (2\text{-}34)$$

$$\int_0^1 \frac{\delta u}{\delta \tau} x \, dx = \frac{k_f R (C - C_s)}{1000 \rho D (1-\varepsilon)} \qquad (2\text{-}35)$$

Equation 2-17 for the average solid phase concentration is transformed using the dimensionless variables to give equation 2-36.

$$q = 3 \int_0^1 ux \, dx \qquad (2\text{-}36)$$

Numerical Procedure

The system of equations 2-18, 2-20, 2-29, 2-30, 2-35 and 2-36 can not be solved analytically, and finite difference techniques must be employed. The solid phase equation and boundary conditions represented by equation 2-29, 2-30, and 2-35 were solved using the implicit finite

difference scheme of Crank-Nicholson. However, a simple tridiagonal matrix does not result due to the nonlinearity of the surface boundary condition.

As developed in Appendix A, the finite difference approximation for the solid phase represented by 2-29 is

$$-\lambda u_{j+1}^{n+1} + (1+2\lambda)u_j^{n+1} - \lambda u_{j-1}^{n+1} =$$

$$\lambda u_{j+1}^{n} + (1-2\lambda)u_j^{n} + \lambda u_{j-1}^{n}, \qquad \begin{matrix} j = 1,M \\ n = 1,N \end{matrix} \qquad (2\text{-}37)$$

where, n and j are subscripts referring to time and distance steps $\Delta\tau$ and Δx respectively, and $\lambda = (\Delta\tau/2(\Delta x)^2)$. An approximation to the surface boundary condition 2-35 is obtained by evaluating the integral on the left hand side in equation 2-35 using the Trapezoidal rule. The resulting equation is shown in 2-38. The subscript (M+1) refers to the surface of the particle, and M is one grid point inside the surface.

$$u_{M+1}^{n+1} + \frac{2}{M}\sum_{j=1}^{M} u_j^{n+1}\,(j-1) = \frac{4}{M}\,\frac{k_f R}{1000\rho D(1-\varepsilon)} + \frac{2}{M}\sum_{j=1}^{M} u_j^{n}\,(j-1) + u_{M+1}^{n} \qquad (2\text{-}38)$$

The concentration at the first distance step for any time grid point is given by equation 2-39, and the concentration for all distance grid points is given by 2-40.

$$u_1^n = 0 \tag{2-39}$$

$$u_j^1 = 0 \tag{2-40}$$

To obtain the equilibrium fluid phase concentration at the surface of the particle at each time step, equation 2-18 has to be inverted. Since the equation is implicit in C_s, the iterative procedure of Newton was used to invert 2-18. The equation can be written for the (k-1)th iteration as

$$C_s^{k-1} - \frac{q_s}{a}(1 + b(C_s^{k-1})^{\beta}) = 0 \tag{2-41}$$

The value of C_s for the (k)th iteration C_s^k is given from Newton's method by equation 2-42.

$$C_s^k = C_s^{k-1} - \frac{\frac{q_s}{a}(1 + b(C_s^{k-1})^{\beta})}{(1-(q_s/a)b\beta(C_s^{k-1})^{\beta-1})} \tag{2-42}$$

Starting with an initial guess for C_s, iteration is continued until $(C_s^k - C_s^{k-1})$ is sufficiently small. With the Newton's method, it is of particular importance that the initial guesses are suffciciently close to the root for convergence. For the first time step, the starting value was estimated from the equation 2-43.

$$C_s = \frac{q_s}{(a-bq_s^{\beta})} \tag{2-43}$$

For the subsequent time steps, the value of C_s at the

previous time step was used as the initial guess.

The average solid phase concentration is obtained by evaluating 2-36 using the Trapezoidal rule. The resulting equation is given in 2-44.

$$q = 3(\Delta x)^2 \sum_{j=2}^{M} u_j \, (j-1) + u_{M+1} \frac{M}{2} \qquad (2\text{-}44)$$

The fluid and solid phase concentrations are related by equation 2-45.

$$C^{n+1} = C^n - \frac{W}{V}(q^{n+1} - q^n) \qquad (2\text{-}45)$$

Equations 2-37 to 2-45 can be used to obtain the kinetic curve, given the necessary mass transfer and equilibrium parameters. The surface concentration is computed first using the equilibrium relationship. From this, and the initial conditions, the vector on the right hand side in equation 2-37 and 2-38 can be computed. The linear equations for (M+1) grid points in 2-37 and 2-38 are then solved to obtain concentrations at grid points within the particle. The average solid phase concentration is obtained from equation 2-44. The fluid phase concentration is obtained by using the computed value of the average solid phase concentration in equation 2-45. The procedure is repeated for successive time steps to obtain concentration-time profile.

Selection of Grid Size

The Crank-Nicholson finite difference approximation to equation 2-29 and a linear set of initial and boundary conditions is stable for any choice of λ. The error in the approximation is second order, and is given by by equation 2-46.

$$\epsilon_r = O(\Delta t)^2 + O(\Delta x)^2 \qquad (2\text{-}46)$$

The Trapezoidal rule approximation for the surface boundary condition is also second order correct.

To test the validity of the numerical procedure, analytical solutions for the solid phase in an infinite bath system were compared with the numerical solution. The solution for a spherical particle in an infinite bath with transfer from the surface at a linear rate is given by equation 2-47 (6).

$$\frac{M_t}{M_\infty} = 1 - \sum_{n=1}^{\infty} \frac{6L^2 \, e^{-\beta_n^2 Dt/R^2}}{\beta_n^2(\beta_n^2+L(1-1)} \qquad (2\text{-}47)$$

M_t is the total amount of substance entering the sphere, M is the final equilibrium concentration, $L=k_f R/D_v$, and β_n are the roots of

$$\beta_n \cot(\beta_n) + L-1 = 0 \qquad (2\text{-}48)$$

A comparison of the numerical and analytical solution is shown in Figure 2-1. To select a proper grid size, numerical

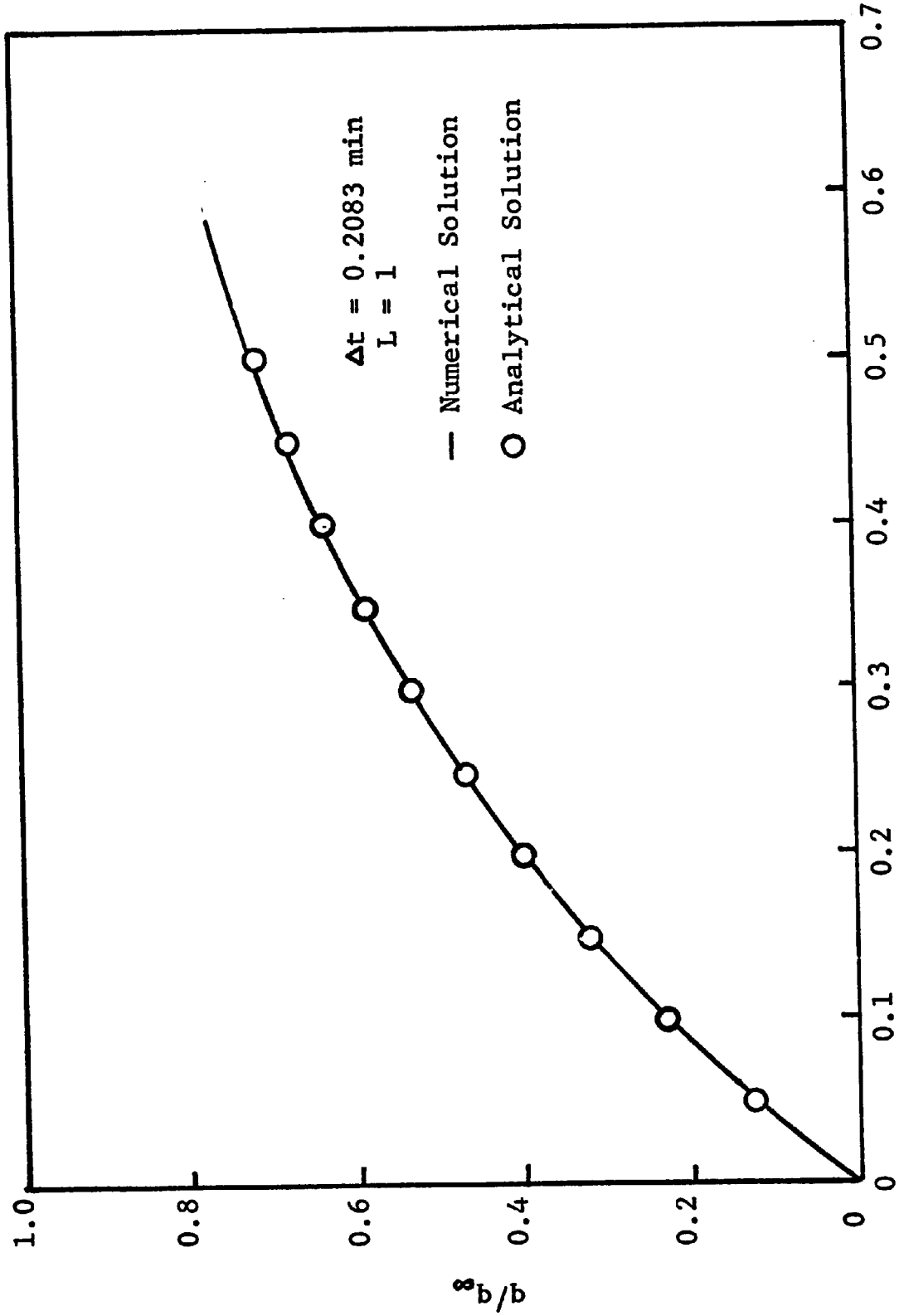


FIGURE 2-1. COMPARISON OF NUMERICAL AND ANALYTICAL SOLUTIONS

solutions were obtained for different values of Δt and Δx . The solutions were consistent with an error of less than 1% for Δt = 1.5 minutes, and Δx = 0.05. Grid sizes of Δx = 0.05, and Δt = 1 minute were chosen for use in the single solute and multicomponent rate programs.

CHAPTER 3

EXPERIMENTAL MATERIALS AND ANALYTICAL METHODS

Adsorbent

The adsorbent used in the experimental investigation is Filtrasorb 400 granular activated carbon obtained from the Calgon Corporation. The activated carbon is manufactured by high temperature steam activation of coal, and is particularly suitable for removing impurities from municipal and industrial wastewaters. Table 3-1 lists the properties of Filtrasorb 400 activated carbon given by the manufacturer. The carbon was sieved using U.S. Standard Sieves, and the size fraction 30/35 - particles passing 30 mesh sieve and retained on a 35 mesh sieve - was used in all the rate experiments. Adsorption equilibrium data were obtained with both 30/35, and 60/100 size fractions. The geometric mean particle diameter of the 30/35 size fraction is 0.548 mm, and of the 60/100 size fraction, 0.193 mm. The carbon was washed in distilled water repeatedly to remove fines and leachable materials, and dried at 105^{o} C to constant weight.

Adsorbates

The adsorbates for the study were selected to represent a broad spectrum of adsorption equilibrium and rate behavior.

TABLE 3-1

PROPERTIES OF FILTRASORB CARBON

Total Surface Area (m^2/gm) (N_2, BET method)	1000-1200
Bed Density, Backwashed and Drained (lbs/ft^3)	25
Particle Density, Wetted in Water (gm/ml)	1.35-1.40
Pore Volume (ml/gm)	0.94
Moisture	0.5%

The solutes studied, and their physical properties are listed in Table 3-2. The solute p-bromophenol has a high adsorption capacity, high energy of adsorption, and diffuses readily. On the other hand, dodecyl benzene sulfonate has a fairly large energy of adsorption, but has a much smaller diffusion coefficient. Phenol and p-toluene sulfonate have diffusion rates comparable to p-bromophenol, but have lower energies of adsorption. All the investigations were carried out at a pH of 7. At this pH, phenol and p-bromophenol are in the neutral form, and the sulfonates are in the anionic form. The equilibrium and rate behavior of these solutes are detailed in Chapters 4 and 5 respectively.

Crystalline p-bromophenol and p-toluene sulfonate were obtained in reagent grade form from the Eastman Kodak Company. Reagent grade phenol was obtained in crystalline form from the Mallinckrodt Chemical Works. Sodium dodecyl benzene sulfonate was obtained from K & K Laboratories, and consisted of a mixture of sulfonates. Its molecular weight was estimated to be 425 from its molar absorptivity at the wavelength of 223 millimicrons.

Adsorbate Mixtures

The adsorbate mixtures were designed to validate the rate and equilibrium models over a wide range of conditions. The p-bromophenol - phenol mixture system has two solutes

TABLE 3-2

PHYSICAL PROPERTIES OF SOLUTES

SOLUTE	FORMULA	SOLUBILITY (gm/100 gm)	IONIZATION CONSTANT
Phenol	C_6H_5OH	8.2 (15^oC)	9.89
p-Bromophenol	C_6H_4BrOH	1.4 (17^oC)	9.20
Sodium p-Toluene Sulfonate	$C_6H_4(CH_3)SO_3Na$	∞	0.7
Sodium Dodecyl Benzene Sulfonate	$CH_3(CH_2)_{11}C_6H_4 \cdot SO_3Na$	∞	1.5

with comparable diffusion coefficients and differing energies of adsorption. In the phenol - p-toluene sulfonate system, the two solutes have similar energies of adsorption and diffusion rates. The phenol - dodecyl benzene sulfonate system provides two solutes with differing energies of adsorption and markedly differing diffusion rates. The solid phase diffusion coefficient for dodecyl benzene sulfonate is about fourteen times smaller than that of phenol. The mixture concentrations studied for each system are shown in Table 3-3.

Analytical Methods

All the compounds investigated show peak absorption in the ultraviolet region, and were analyzed using ultraviolet absorption spectrophotometry. The wavelengths of maximum absorptivity for the solutes are listed in Table 3-4. Calibration curves for phenol at wavelengths of 268 and 282, and 215 and 223 are shown in Figures 3-1 and 3-2. The phenol and p-bromophenol mixtures were analyzed at wavelengths of 268 and 282 millimicrons and the phenol - sulfonate mixtures were analyzed at 215 and 223 millimicrons. A 10^{-2}M phosphate buffer solution of pH 7 was used as the reference in all the analyses. Particular care was taken in the analysis of sulfonates to rinse the absorption cell with the buffer solution since sulfonates adsorb onto quartz and glass

TABLE 3-3

MIXTURE COMPOSITIONS

MIXTURE COMPONENTS	CONCENTRATIONS (Moles/1)	CARBON (gm/1)
Phenol	5E-4*	
p-Bromophenol	5E-4	0.5
Phenol	5E-4	
p-Bromophenol	5E-4	0.67
Phenol	2.5E-4	
p-Bromophenol	5E-4	0.33
Phenol	5E-5	
p-Toluene Sulfonate	5E-5	0.33
Phenol	1E-4	
p-Toluene Sulfonate	1E-4	0.67
Phenol	5E-5	
p-Toluene Sulfonate	2.5E-5	0.33
Phenol	5E-5	
Dodecyl Benzene Sulfonate	5E-5	0.33
Phenol	1E-4	
Dodecyl Benzene Sulfonate	1E-4	0.67

*E-n = 10^{-n}

TABLE 3-4

MOLAR ABSORPTIVITIES FOR SOLUTES

SOLUTE	WAVELENGTH (mμ)			
	268	282	215	223
Phenol	1.445E+3*	0.260E+3	0.523E+4	0.260E+4
p-Bromophenol	0.810E+3	1.350E+3	-	-
p-Toluene Sulfonate	-	-	0.860E+4	1.080E+4
Dodecyl Benzene Sulfonate	-	-	0.796E+4	1.120E+4

*E+n = 10^n

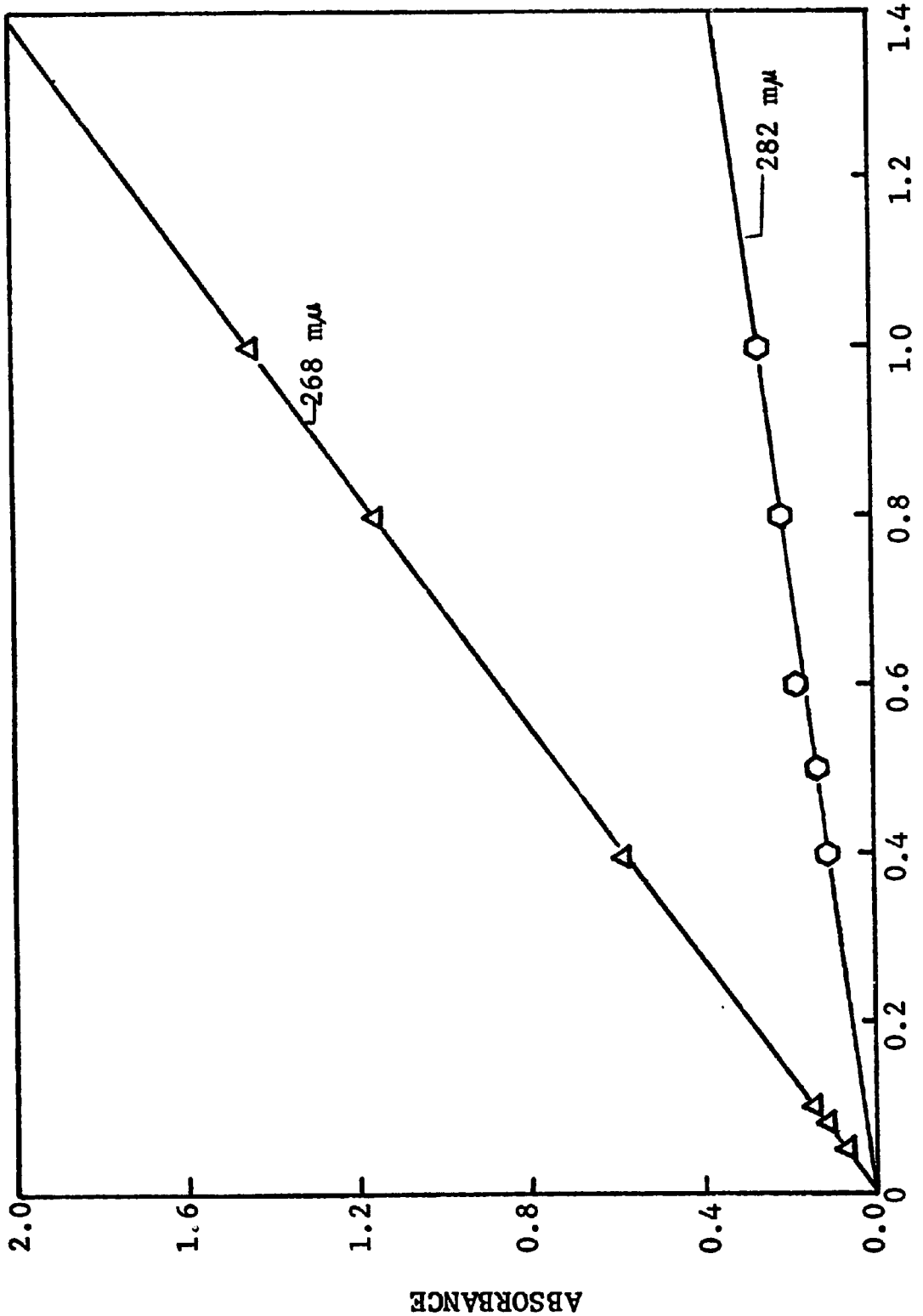


FIGURE 3-1. CALIBRATION CURVE FOR PHENOL (268 AND 282 mμ)

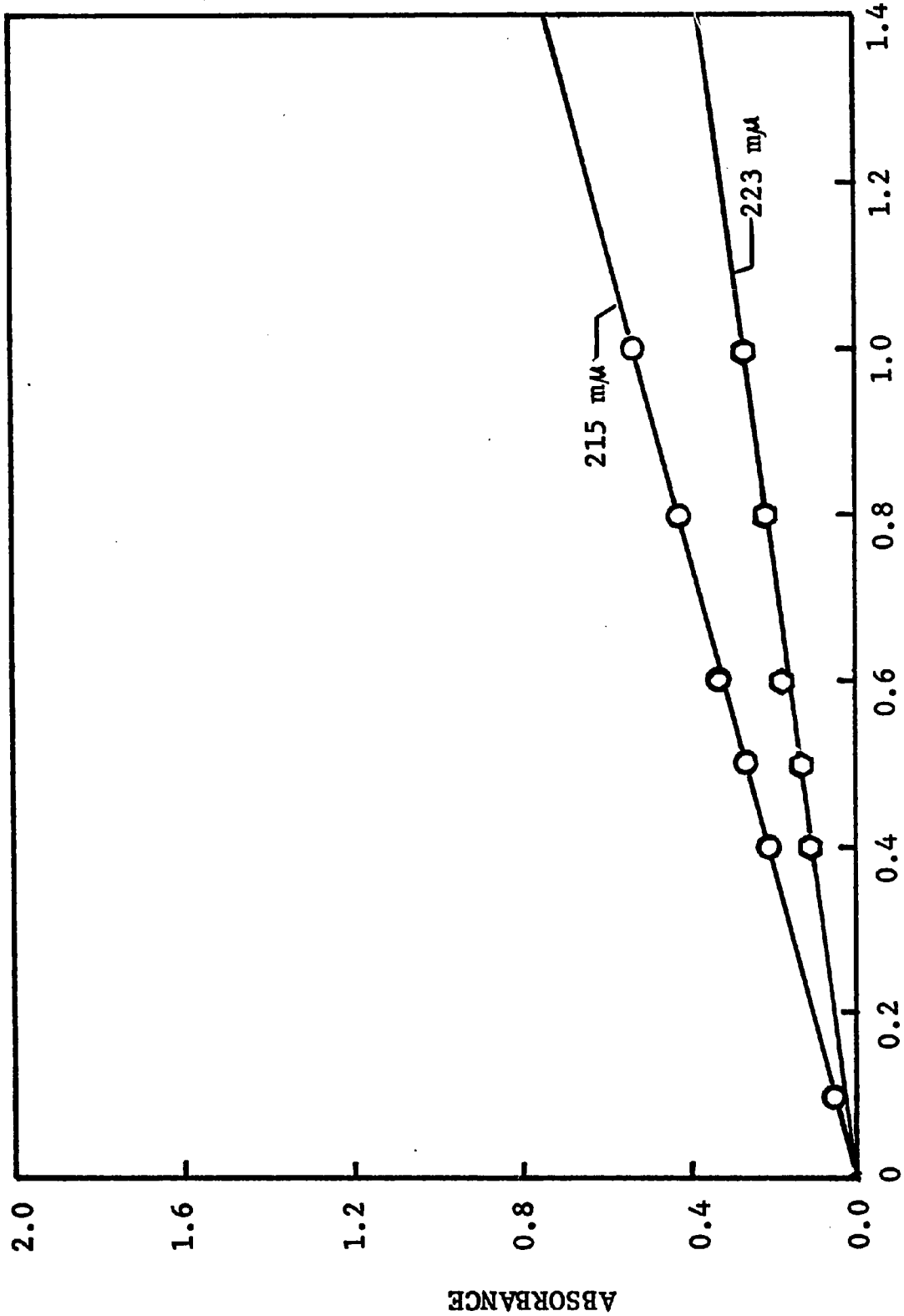


FIGURE 3-2. CALIBRATION CURVE FOR PHENOL (215 AND 223 mμ)

surfaces.

According to Beer's law, in a mixture of several adsorbing compounds, the total absorbance at any one wavelength is equal to the sum of the individual absorbances. This assumes that there are no chemical interferences and interactions between the solute species. The following two equations can be set up for a two component mixture at the wavelength of maximum absorption for each solute.

$$\varepsilon_{11}C_1 + \varepsilon_{12}C_2 = A_1 \qquad (3\text{-}1)$$

$$\varepsilon_{21}C_1 + \varepsilon_{22}C_2 = A_2 \qquad (3\text{-}2)$$

The molar absorptivities for solutes 1 and 2 at the wavelength λ_1 are ε_{11} and ε_{12} respectively, and the absorptivities at λ_2 are ε_{21} and ε_{22}. A_1 and A_2 are the absorbances at the wavelengths λ_1 and λ_2. The concentration of each solute in the mixture is obtained by solving equations 3-1 and 3-2.

CHAPTER 4

ADSORPTION EQUILIBRIA

The successful representation of dynamic adsorptive separation of solute from the fluid to the solid phase is contingent upon a satisfactory description of the equilibrium separation between the two phases. In this chapter, single component adsorption equilibrium models are reviewed and an empirical equation is proposed to represent the data over a wide concentration range. The empirical equation is extended for mixtures of solutes, and is compared with models available for predicting multicomponent equilibria.

SINGLE COMPONENT ADSORPTION EQUILIBRIA

Several empirical and theoretical equations are available to describe single component adsorption equilibria. These can be classified as irreversible, linear, and nonlinear isotherms, as shown in equations 4-1 to 4-3.

Irreversible	q_e = Constant	(4-1)
Linear	$q_e = K_1 C_e$	(4-2)
Nonlinear	$q_e = f(C_e)$	(4-3)

C_e and q_e are equilibrium concentrations of the solute in the liquid and solid phases respectively, and f is a nonlinear function of C_e.

Langmuir and Freundlich equations are two nonlinear isotherms that have been used widely to represent equilibrium data over small concentration ranges.

Langmuir Isotherm $$q_e = \frac{Qb'C_e}{1+b'C_e} \qquad (4\text{-}4)$$

Freundlich Isotherm $$q_e = K_F C_e^{\gamma} \qquad \gamma < 1 \qquad (4\text{-}5)$$

In the Langmuir isotherm 4-4, Q is the ultimate capacity of the adsorbent, and b' is a constant related to the energy of adsorption. A plot of $1/q_e$ against $1/C_e$ will yield a straight line with a slope of $1/Qb'$ and an intercept of $1/Q$. The constant K_F in the Freundlich isotherm is a rough indication of the adsorption capacity, and γ of the adsorption intensity. A logarithmic plot of q_e and C_e will yield a straight line with a slope of γ and intercept of K_F. The Freundlich equation agrees well with the Langmuir's equation over moderate concentration ranges, but unlike the Langmuir isotherm it does not reduce to the linear isotherm at low concentrations. Both the equations suffer from the disadvantage that equilibrium data over a wide concentration range can not be fitted with a single set of parameters. An empirical equation, 4-6, designated the three parameter equation is proposed and utilized in this study to represent adsorption equilibria over a wide concentration range.

$$q_e = \frac{aC_e}{1+bC_e^{\beta}} \qquad \beta \leq 1 \qquad (4\text{-}6)$$

The equation reduces to the linear isotherm at low concentrations, to the Freundlich isotherm at high concentrations, and to the Langmuir isotherm when $\beta = 1$. However, unlike the Langmuir and Freundlich isotherms, the three parameter equation can not be linearized, and the isotherm constants must be estimated by a least squares analysis of the experimental data.

Experimental Procedure

Adsorption equilibria for single-solute systems of phenol, p-bromophenol, p-toluene sulfonate and dodecyl benzene sulfonate were obtained over the concentration range 10^{-6} to 10^{-2}M. All the systems were maintained at a pH of 7 using a 10^{-2}M phosphate buffer. Thus phenol and p-bromophenol are in the neutral form, while p-toluene suflonate and dodecyl benzene sulfonate are in the anionic form.

The equilibrium points were obtained by contacting 100 ml aliquots of solution with carefully weighed amounts of carbon in 120 ml glass bottles. The bottles were tightly sealed with polyethylene-lined caps and placed in tumbler to provide agitation. Solute concentrations of 10^{-2}M to 10^{-4}M were used as starting concentrations in developing

equilibrium data over a wide range. In each case, blanks containing solution without carbon were included, and served as a check on degradation of organic material or adsorption on the glass. After equilibrium was attained, the carbon was allowed to settle, and the supernatant liquid analyzed to determine the decrease in concentration (C_o-C_e) by adsorption on W grams of carbon from V liters of solution. The equilibrium adsorbed phase concentration is computed from equation 4-7.

$$q_e = \frac{(C_o - C_e)\ V}{W} \qquad (4\text{-}7)$$

Experimental Results

The experimental isotherms for phenol, p-bromophenol, p-toluene sulfonate and dodecyl benzene suflonate are shown in Figures 4-1, 4-2, 4-3 and 4-4, respectively. The solid lines in the figures represent the best fit to the experimental points using the three parameter equation 4-6. The isotherm constants a, b, and β were estimated by minimizing the sum of the squares of percentage deviations of the experimental and estimated equilibrium solid phase concentration. The constants for the four solutes are listed in Table 4-1. In using the constants, the liquid and solid phase equilibrium concentrations must be expressed in millimoles/liter and millimoles/gram respectively.

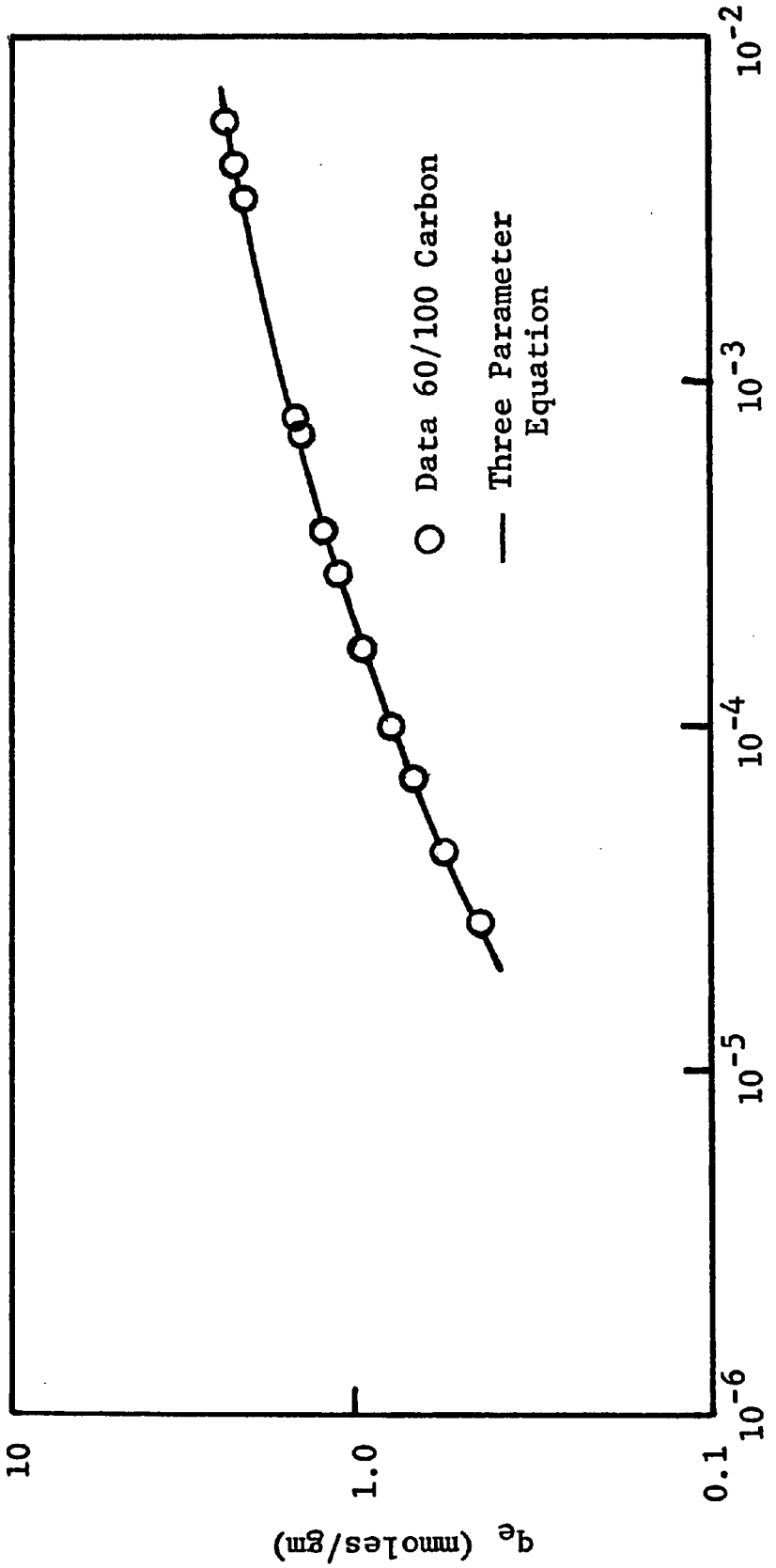


FIGURE 4-1. ADSORPTION ISOTHERM: PHENOL

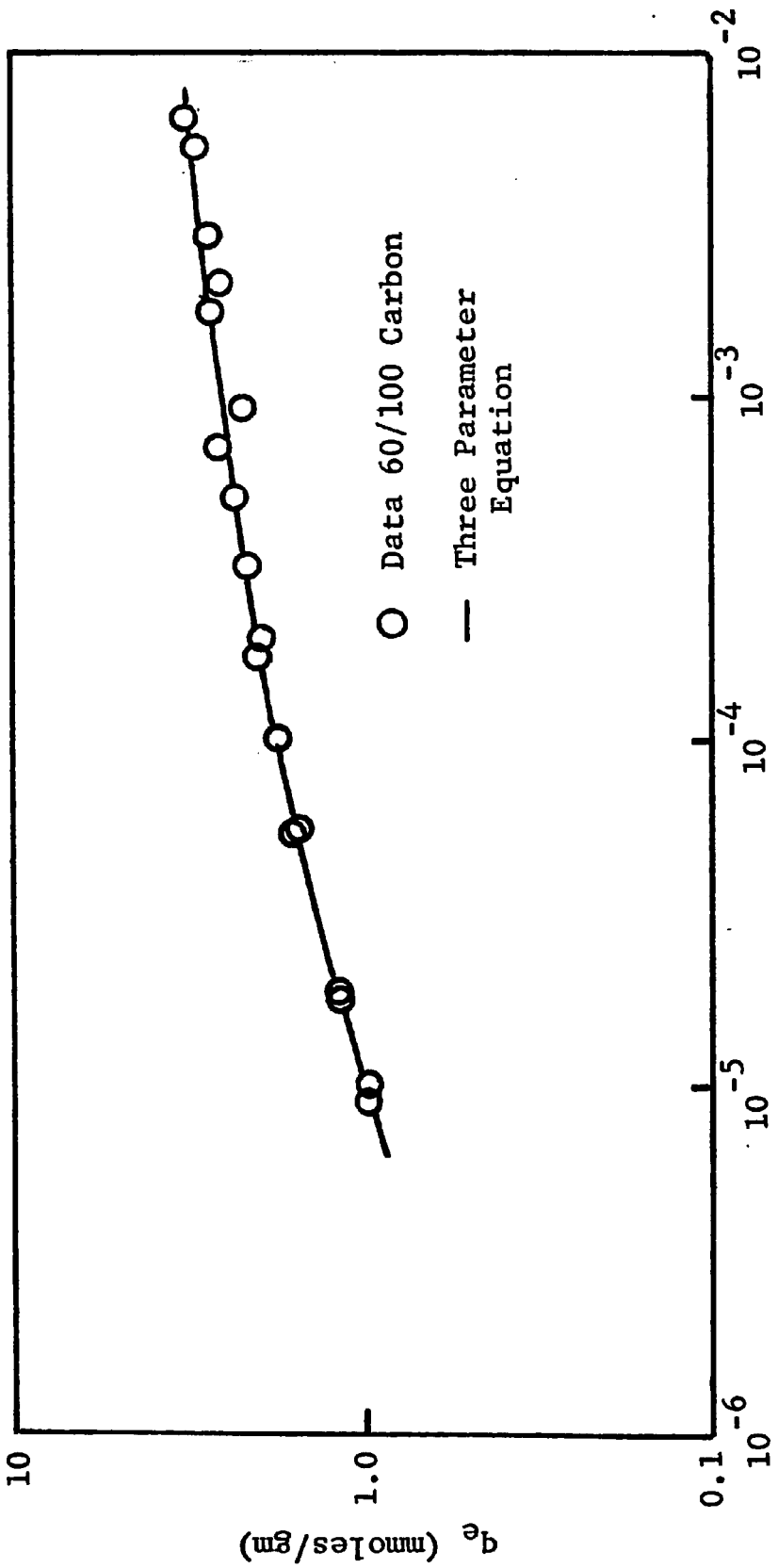


FIGURE 4-2. ADSORPTION ISOTHERM: p-BROMOPHENOL

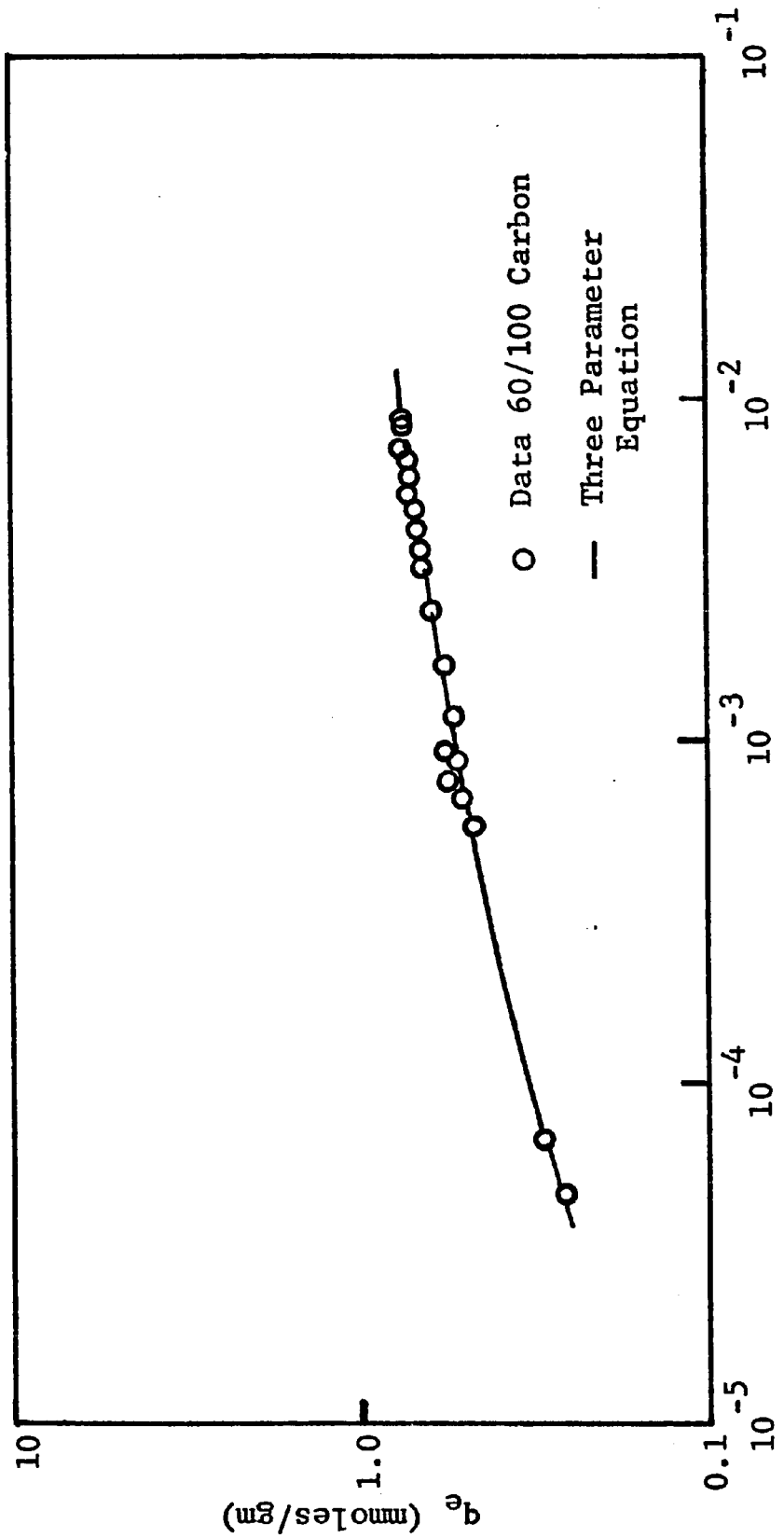


FIGURE 4-3. ADSORPTION ISOTHERM: p-TOLUENE SULFONATE

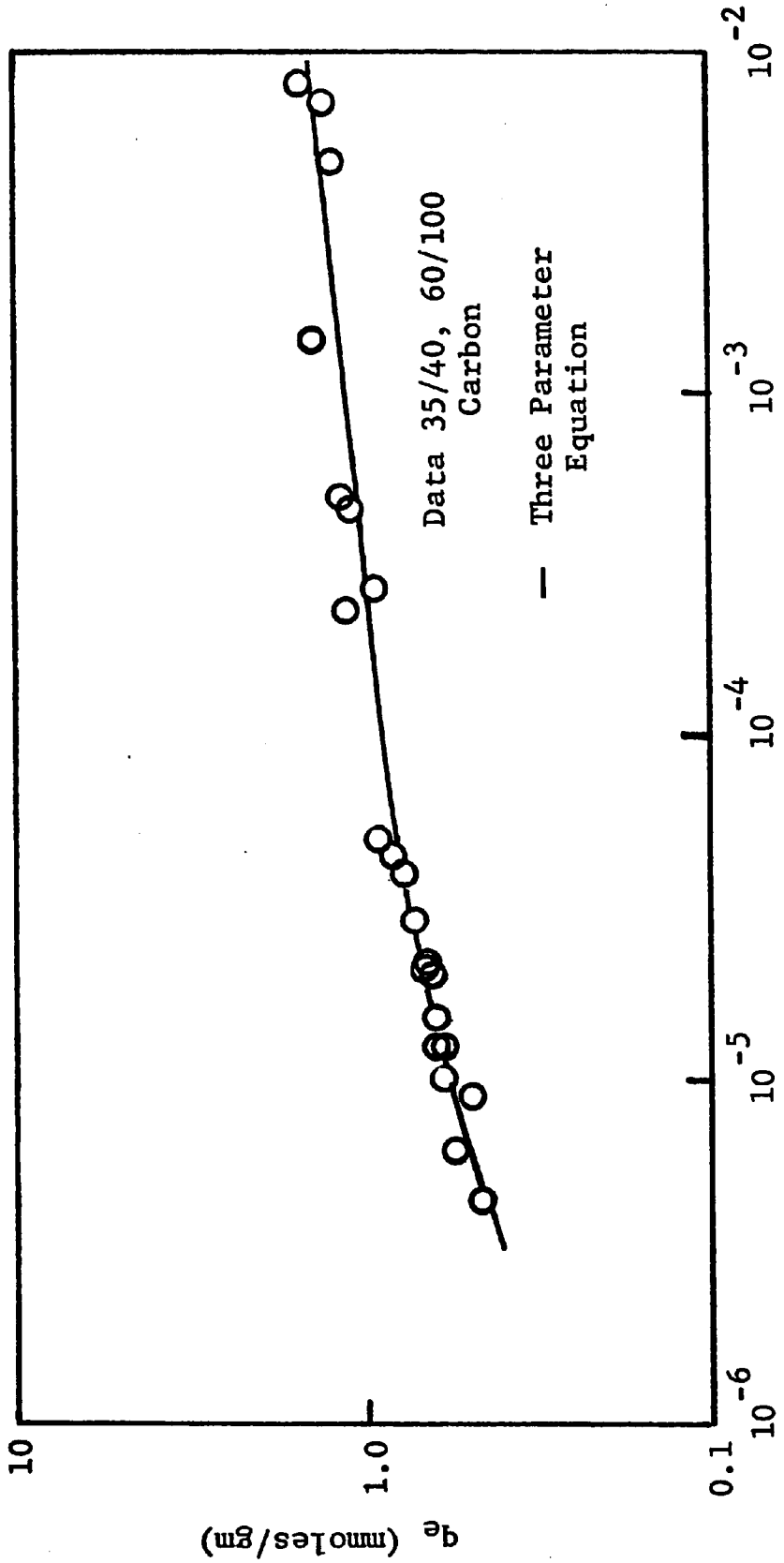


FIGURE 4-4. ADSORPTION ISOTHERM: DODECYL BENZENE SULFONATE

TABLE 4-1

ISOTHERM CONSTANTS*

SOLUTE	a	b	β
Phenol	43.29	26.34	0.7942
p-Bromophenol	333.4	133.5	0.8687
p-Toluene Sulfonate	22.23	40.41	0.8500
Dodecyl Benzene Sulfonate	284.7	248.5	0.9019

*Based on C_e and q_e expressed in mmoles/l and mmoles/gm respectively.

MULTICOMPONENT ADSORPTION EQUILIBRIA

The most common model used for representing multicomponent adsorption equilibria is the Langmuir mixture model shown in equation 4-8. This equation was developed

$$q_{ei} = \frac{Q_i b_i' C_i}{1+b_i' C_i} \qquad (4\text{-}8)$$

by Butler and Ockrent (3), and Markham and Benton (43) based on the same assumptions of monolayer surface coverage and surface homogeneity as for Langmuir's model for single solute adsorption. In this method, the Langmuir constants Q_i and b_i' from single solute isotherms are used to predict mixture equilibrium data using equation 4-8. An important difficulty with this method is that for many solutes the Langmuir isotherm does not provide an adequate fit to the data.

Snoeyink and Jain (30) modified the Langmuir relations for a binary system by hypothesizing that adsorption occurs without competition when the monolayer capacities Q_1 and Q_2 are unequal. Further, it was assumed that the number of sites for which there was no competition was equal to (Q_1-Q_2) when $Q_1 > Q_2$. The following set of equations were proposed for a binary system with $Q_1 > Q_2$.

$$q_{e1} = \frac{(Q_1-Q_2)b_1' C_1}{1+b_1' C_1} + \frac{Q_2 b_1' C_1}{1+b_1' C_1+b_2' C_2} \qquad (4\text{-}9)$$

$$q_{e2} = \frac{Q_2 b_2' C_2}{(1+b_2' C_2+b_1' C_1)} \qquad (4\text{-}10)$$

It may be noted that equation 4-10 is of the same form as the Langmuir mixture model equation 4-8. The equations 4-9 and 4-10 do not represent mixture equilibrium data satisfactorily, and extension of the development to more than two components is not readily apparent.

Radke and Prausnitz (53) applied the principles of ideal dilute solution thermodynamics in developing a method for predicting multicomponent adsorption equilibria from single solute isotherms for each species. This method is similar to the spreading pressure prediction method proposed by Myers and Prausnitz (49) for gases, and assumes an ideal adsorbed phase with no solute-solute interactions. With this assumption, the adsorbed phase fugacity of each component f_i can be expressed simply in terms of its pure component fugacity f_i^o as

$$f_i = y_i f_i^o \qquad (4\text{-}11)$$

In equation 4-11, y_i is the mole fraction of solute i in the adsorbed phase, and f_i^o is the fugacity of the solute i adsorbing singly from solution at the same temperature and pressure as that of the mixture.

The concept of a two-dimensional adsorbed phase adjacent to the surface of the particle was proposed by J.W. Gibbs, and the two-dimensional phase is deemed to have properties analogous to that of a three-dimensional fluid phase. However, the properties pressure and volume in the three-dimensional phase must be replaced by the spreading pressure π and the molar area A in the two-dimensional phase. Fundamental thermodynamic property relations (27) can be written for the adsorbed phase, and a relationship for the Helmholtz function F^a for isothermal conditions is shown in equation 4-12.

$$dF^a = -\pi dA + \sum_i \mu_i^a \, dq_i^a + \mu_s^a \, dq_s^a \qquad (4\text{-}12)$$

μ_i^a and μ_s^a are the chemical potentials of the solute and solvent respectively in the adsorbed phase, and q_i^a and q_s^a are the number of moles of solute and solvent in the adsorbed phase relative to the solid. Integration of 4-12 results in equation 4-13.

$$F^a = -\pi A + \sum_i \mu_i^a \, q_i^a + \mu_s^a q_s^a \qquad (4\text{-}13)$$

Taking the total differential of F^a in 4-12, equation 4-14

$$dF^a = -\pi dA - A d\pi + \sum_i \mu_i^a dq_i^a + \sum_i q_i^a d\mu_i^a + \mu_s^a dq_s^a + q_s^a d\mu_s^a \qquad (4\text{-}14)$$

is obtained. A comparison of equations 4-12 and 4-14 results in the Gibbs isothermal adsorption equation 4-15.

$$Ad\pi = \sum_i q_i^a d\mu_i^a + q_s^a d\mu_s^a \qquad (4\text{-}15)$$

At equilibrium, the chemical potentials of the adsorbed phase and the liquid phase are equal. That is,

$$\mu_i^a = \mu_i^l \qquad (4\text{-}16)$$

$$d\mu_i^a = d\mu_i^l \qquad (4\text{-}17)$$

If C_i and C_s are the solute concentrations in the liquid phase, the isothermal Gibbs-Duhem equation (27) can then be written as shown in equation 4-18.

$$\sum_i C_i d\mu_i^a + C_s d\mu_s^a = 0 \qquad (4\text{-}18)$$

Equations 4-18 and 4-15 can be combined to give 4-19.

$$Ad\pi = \sum_i (q_i^a - \frac{C_i}{C_s} q_s^a) d\mu_i^a \qquad (4\text{-}19)$$

Radke and Prausnitz (53) have shown that in dilute solutions, $(q_i^a - q_s^a C_i/C_s)$ can be related to the experimentally measurable quantity for the amount adsorbed, q_i^m, by equation 4-20.

$$q_i^m = V(C_o - C_e) = (q_i^a - \frac{C_i}{C_s} q_s^a) \qquad (4\text{-}20)$$

Then equation 4-19 reduces to 4-21.

$$A d\pi = \sum_i q_i^m d\mu_i^a \qquad (4\text{-}21)$$

The adsorbed phase fugacity is defined by equation 4-22.

$$d\mu_i^a = RT d\ln f_i^a \qquad (4\text{-}22)$$

Equations 4-11, and 4-22 can be combined to give equation 4-23.

$$\left(\frac{\delta \mu_i^a}{\delta \pi}\right)_{T,y_i} = \left(\frac{\delta \mu_i^o}{\delta \pi}\right)_T \qquad (4\text{-}23)$$

If q_T^m is the total amount adsorbed, equation 4-21 can be rearranged to give

$$\frac{A}{q_T^m} = \sum_i y_i \left(\frac{\delta \mu_i^a}{\delta \pi}\right)_{T,y_i} \qquad (4\text{-}24)$$

For a single solute 4-21 yields

$$\left(\frac{\delta \mu_i^o}{\delta \pi}\right)_T = \frac{A}{q_i^o} \qquad (4\text{-}25)$$

From 4-23, 4-24 and 4-25, a relation 4-26 between the total amount adsorbed from the mixture and the pure component adsorption of the solute species at the total spreading pressure of the mixture can be obtained.

In dilute solutions the activity coefficients can be neglected, and the chemical potential of the solute in the

$$\frac{1}{q_i^m} = \sum_i \frac{y_i}{q_i^o} \tag{4-26}$$

liquid phase can be expressed by equation 4-27.

$$d\mu_i^{\ell} = RT\ d\ln C_i \tag{4-27}$$

For the adsorbed phase, equation 4-28 results from 4-11 and 4-22.

$$d\mu_i^a = d\mu_i^o + RT\ d\ln y_i \tag{4-28}$$

For the pure component at the same total spreading pressure and temperature as that of the mixture equation 4-29 can be obtained from 4-17 and 4-22. Equations 4-27, 4-28, 4-29 and 4-17 can be combined to give the desired result relating the pure component liquid phase equilibrium concentration with the liquid phase mixture equilibrium concentration . This result is shown in equation 4-30.

$$d\mu_i^o = d\mu_i^{\ell} = RT\ d\ln C_i^o \tag{4-29}$$

$$C_i = C_i^o y_i \tag{4-30}$$

The pure component equilibrium concentrations C_i^o and q_i^o are evaluated at the same total spreading pressure as that of the mixture.

Thus, $$\pi_i = \pi_j = \pi \qquad (4\text{-}31)$$

The spreading pressure for the pure component may be evaluated from 4-21 and 4-29, and is given by equation 4-32.

$$\pi_i = \frac{RT}{A} \int_0^{C_i^o} \frac{q_i^o}{C_i^o} dC_i^o \qquad (4\text{-}32)$$

Equations 4-26, 4-30 and 4-31 can be used to predict mixture equilibria from single solute isotherms. The following set of equations are developed for a binary system. Equations 4-31 and 4-32 are combined to yield equation 4-33.

$$F(C_1^o, C_2^o) = \int_0^{C_1^0} \frac{a_1}{(1+b_1 (C_1^o)^{\beta_1})} dC_1^o - \int_0^{C_2^0} \frac{a_2}{(1+b_2 (C_2^o)^{\beta_2})} dC_2^o = 0 \qquad (4\text{-}33)$$

Writing equation 4-30 for each species

$$C_1 = C_1^o y_1 \qquad (4\text{-}34)$$

$$C_2 = C_2^o (1-y_1) \qquad (4\text{-}35)$$

Elimination of y_1 from 4-34 and 4-35 yields equation 4-36.

$$G(C_1^o, C_2^o) = C_2^o - \frac{C_1^o C_2}{C_1^o - C_1} \qquad (4\text{-}36)$$

Given the equilibrium concentrations C_1 and C_2 in the liquid phase, an initial estimate is made of the mole fraction y_1 in the adsorbed phase. C_1^o is then obtained from equation 4-34. Equations 4-33 and 4-36 are then solved for C_1^o using the Newton-Raphson iterative procedure. The adsorbed phase phase mole fraction can be obtained from

equations 4-34 and 4-35. And finally, the equilibrium adsorbed phase concentrations q_1 and q_2 are obtained from equations 4-26, 4-38 and 4-39.

$$q_1 = q_T^m y_1 \tag{4-38}$$

$$q_2 = q_T^m (1-y_1) \tag{4-39}$$

A computer program was written incorporating equations 4-33 to 4-39 to predict multi-solute equilibria. The integrals in equation 4-33 were evaluated using Romberg's method of Trapezoidal rule with end correction. The computations involved in the Newton-Raphson method are detailed in Appendix B. A listing of the program is given in Appendix C. The computational effort required in using the Radke and Prausnitz method is substantial since evaluations of the integrals are required at each iteration in the Newton-Raphson procedure. Therefore, its applicability to a multicomponent rate model is limited.

A simple extension of the three parameter equation is proposed in equation 4-44, and utilized in this study to predict multicomponent equilibria.

$$q_i = \frac{a_i C_i}{\sum_i 1+b_i C_i^{\beta_i}} \tag{4-44}$$

This equation was used to predict the equilibrium data of Radke and Prausnitz for p-chlorophenol and p-cresol mixtures, and for acetone-propionitrile mixtures. A comparison of the

models of Snoeyink and Jain, Radke and Prausnitz, and the three parameter equation are shown in Figures 4-5 to 4-8. The figures show a plot of the ratio of the predicted and experimental values of equilibrium adsorbed phase concentration of each solute against the equilibrium liquid phase concentration. From the figures it may be seen that equation 4-44 predicts the mixture equilibrium data better than the Snoeyink and Jain model for the two solute systems. The Prausnitz model gives somewhat better results,but the computational effort involved is greater.

Correlation of Mixture Equilibria

For solute systems that are not adequately described by the theoretical and empirical models described above, it may be necessary to develop correlational procedures so that the equilibrium data can be used in the multicomponent rate model. Schay et. al., (59) have proposed the use of interaction terms in correlating binary equilibrium data using the Langmuir's equations for mixtures. The Langmuir's equation is derived by considering the adsorbed phase as a two-dimensional mobile monolayer, and a correction term analogous to the Van der Waal's term in the three-dimensional gas phase is applied to correct for the surface area occupied by the adsorbed molecules. The resulting expression for the Langmuir isotherm is given by equation 4-45.

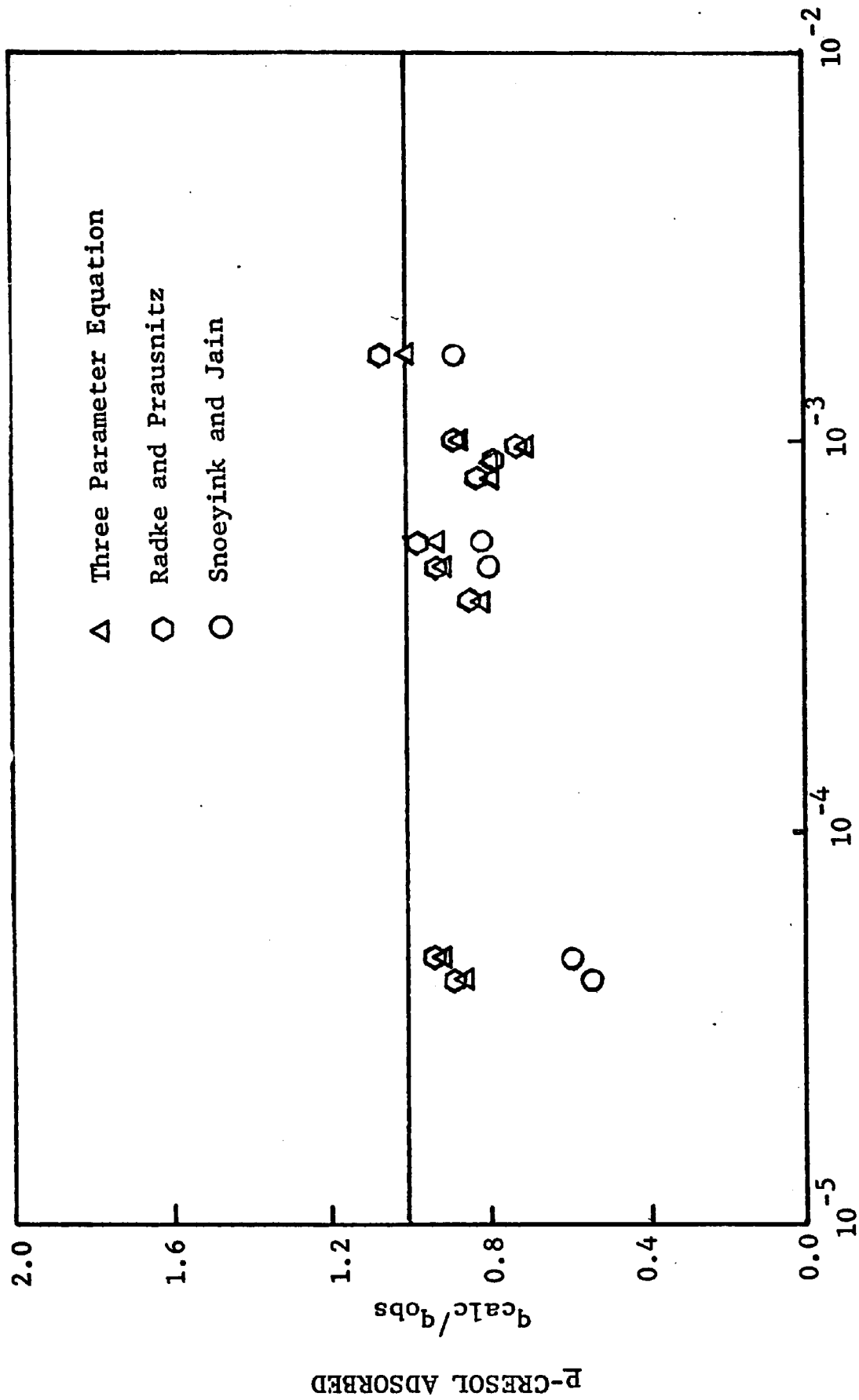


FIGURE 4-5. COMPARISON OF MODELS FOR MIXTURE EQUILIBRIA PREDICTION: p-CRESOL-p-CHLOROPHENOL

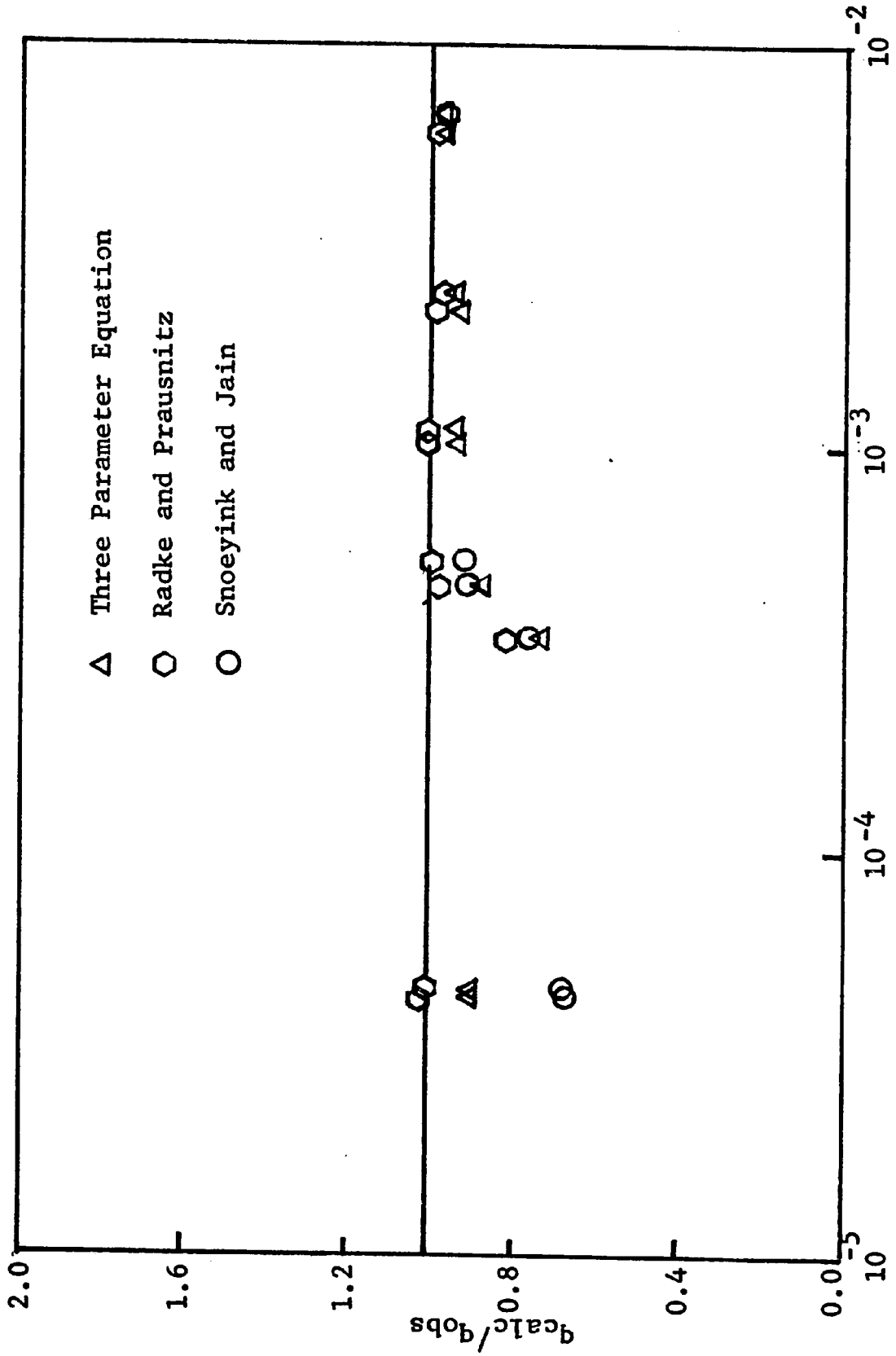


FIGURE 4-6. COMPARISON OF MODELS FOR MIXTURE EQUILIBRIA PREDICTION: p-CRESOL-p-CHLOROPHENOL

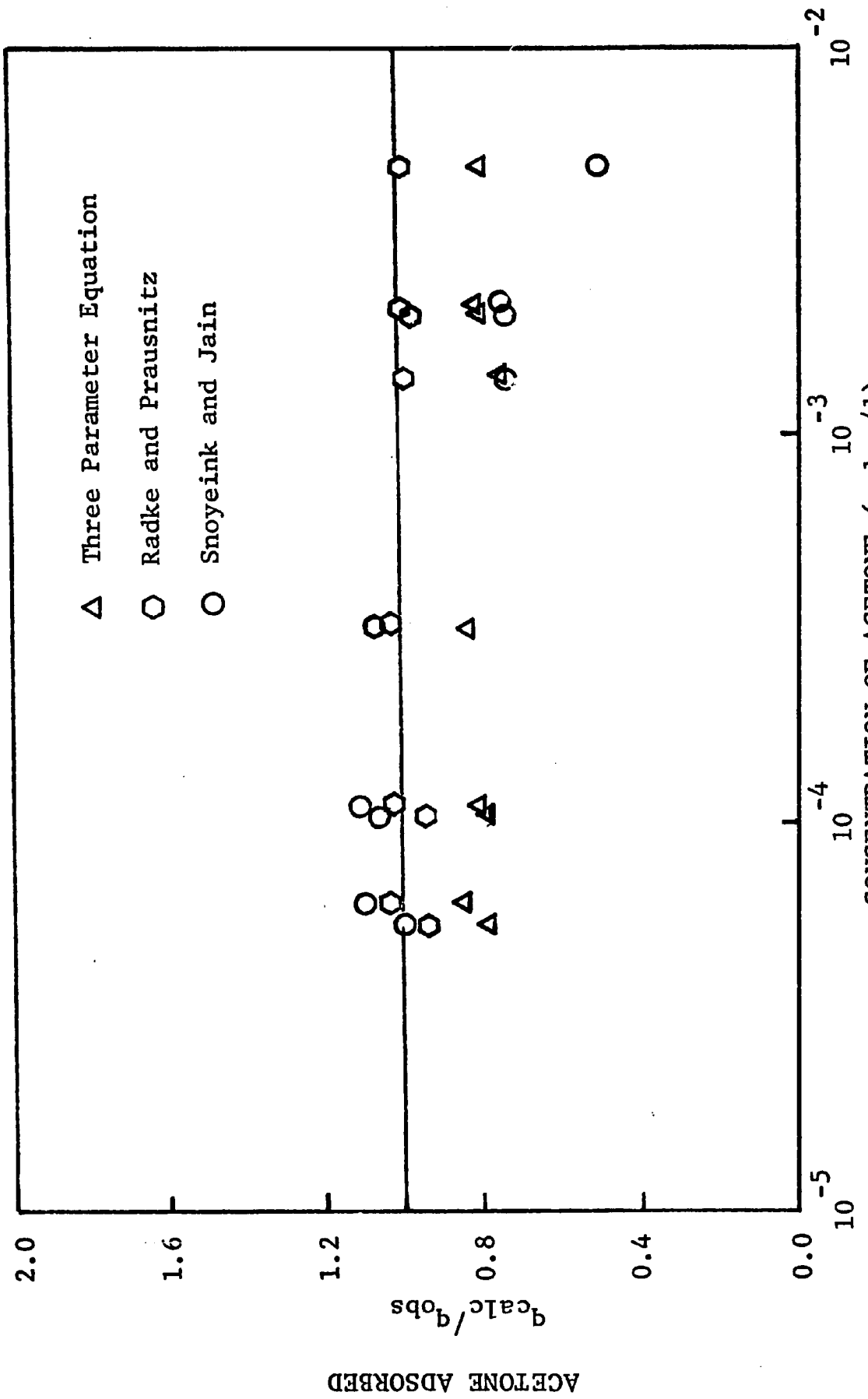


FIGURE 4-7. COMPARISON OF MODELS FOR MIXTURE EQUILIBRIA PREDICTION: ACETONE-PROPIONITRILE

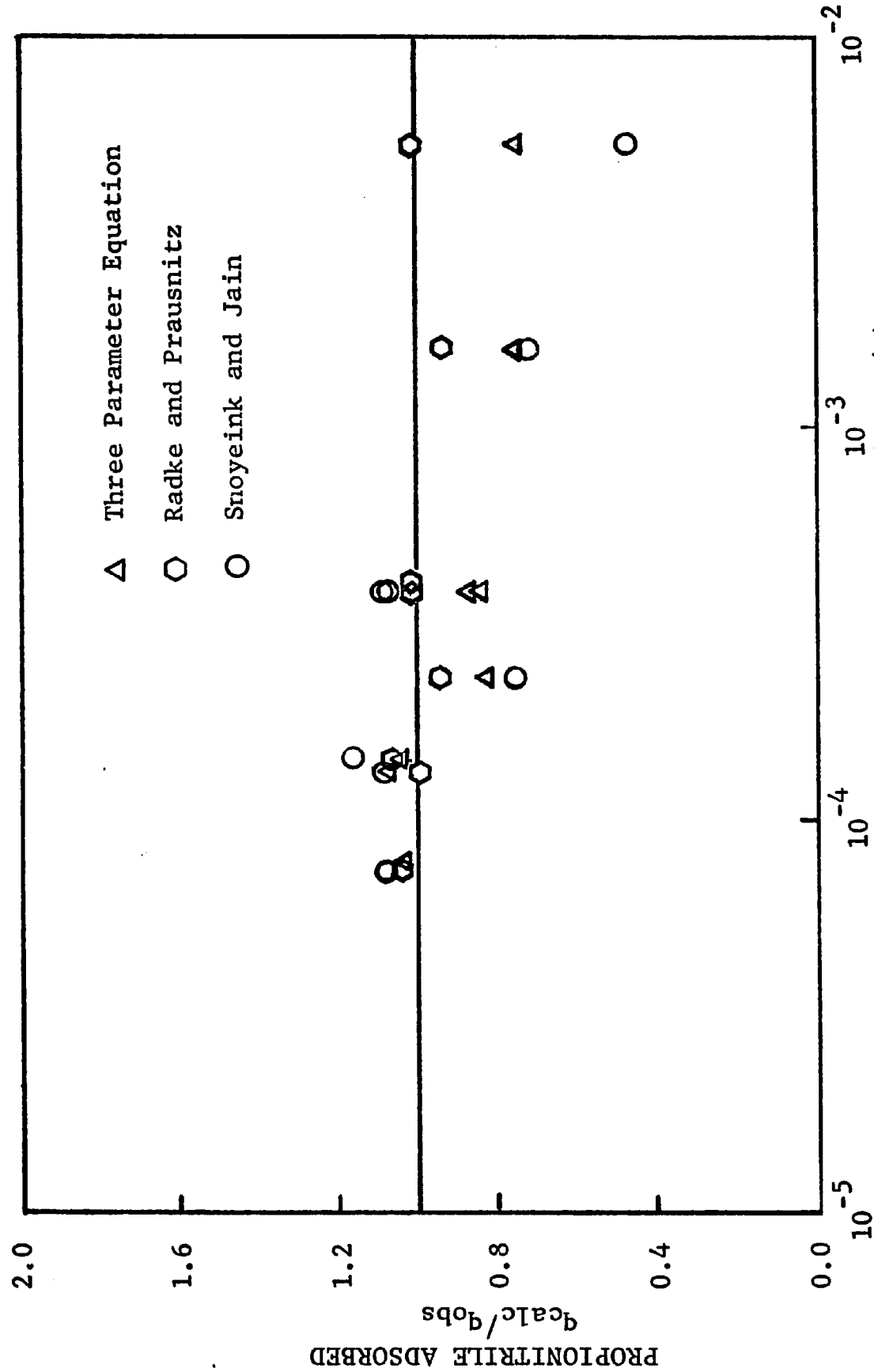


FIGURE 4-8. COMPARISON OF MODELS FOR MIXTURE EQUILIBRIA PREDICTION: ACETONE-PROPIONITRILE

$$q_i = \frac{Q_i b_i' (C_i/\eta_i)}{\sum_i 1+b_i' (C_i/\eta_i)} \qquad (4\text{-}45)$$

The η_i are interaction terms, one for each solute, and are obtained by correlating the multi-solute equilibrium data.

This approach was used by Yon and Turnock (81) to correlate equilibrium data for adsorption on molecular sieves. The application of this method to equation 4-44 results in euation 4-46.

$$q_i = \frac{a_i (C_i/\eta_i)}{\sum_i 1+b_i (C_i/\eta_i)^{\beta_i)}} \qquad (4\text{-}46)$$

This method, while strictly emperical, allows the use of mixture equillibrium data in the complicated multicomponent rate model discussed in Chapter 6. The constants ai, b_i and β_i for each solute are obtained from single solute equillibrium data. The η_i are obtained by minimizing the sum of the squares of percentage deviations between the experimental and calculated adsorbed phase concentrations for each solute. The objective function over which η_i are estimated is given by equation 4-47.

$$\sum_j \sum_i ((q_i - q_{c_i})/q_i)^2 \qquad (4\text{-}47)$$

The summation on j extends over the number of solutes, and the summation on i extends over the number of data

points. q_i and q_c are the experimental and calculated adsorbed phase concentrations for each solute in the mixture. A program was written to correlate the binary equillibrium data using equations 4-46 and 4-47.

Experimental Results

The experimental procedure described for single solute adsorption was used in developing equillibrium data for the binary systems. The results for phenol-p-bromophenol, phenol-p-toluene sulfonate, and phenol-dodecyl benzene sulfonate are tabulated in Tables 4-2, 4-3 and 4-4 respectively. The equation 4-44 was found inadequate to describe the data for each of the above systems. The data were correlated using equation 4-45. Correlaton coefficients of 0.868 and 0.399 were obtained for phenol and p-bromophenol respectively in the phenol-p-bromophenol system, 0.3425 for phenol and 0.5984 for p-toluene sulfonate in the phenol-p-toluene sulfonate system, and 0.5875 for phenol and 0.3641 for dodecyl benzene sulfonate in the phenol-dodecyl benzene sulfonate system.

The deviation of the equilibrium data predicted by the correlation from the experimental data is shown in Figures 4-9 and 4-10 for the phenol-p-bromophenol system. The ordinate in the figures is the ratio of the calculated equilibrium value to the experimental value. The abscissa

TABLE 4-2

EQUILIBRIUM DATA FOR PHENOL-p-BROMOPHENOL

MIXTURES: PHENOL (1) - p-BROMOPHENOL (2)

C_1 mmoles/l	C_2 mmoles/l	q_1 mmoles/gm	q_2 mmoles/gm
0.9542	0.5570	0.2289	0.2215E+1
0.9139	0.3758	0.2870	0.2081E+1
0.8652	0.2837	0.3371	0.1791E+1
0.7292	0.1410	0.4513	0.1432E+1
0.6180	0.9120E-1	0.5446	0.1298E+1
0.5750	0.8037E-1	0.5312	0.1150E+1
0.6374	0.1024	0.4942	0.1223E+1
0.6995	0.1349	0.4533	0.1305E+1
0.4756	0.2936	0.2284	0.1929E+1
0.3676	0.1048	0.4272	0.1275E+1
0.2442	0.3963E-1	0.4967	0.8939
0.4728	0.2764	0.2696	0.2214E+1
0.4554	0.1975	0.2974	0.2017E+1
0.4357	0.1339	0.3200	0.1822E+1
0.3657	0.6734E-1	0.4461	0.1437E+1
0.2766	0.2005E-1	0.5584	0.1200E+1
0.5770	0.9035E-1	0.4663	0.2105E+1
0.4408	0.9881E-1	0.5548	0.1886E+1
0.2557	0.5001E-1	0.6628	0.1736E+1
0.1995	0.1564E-1	0.6626	0.1643E+1
0.1043	0.2140E-1	0.6312	0.1394E+1
0.8115E-1*	0.1696E-1	0.5920	0.1278E+1
0.4427	0.1510	0.2618	0.1593E+1
0.3750	0.7666E-1	0.3857	0.1307E+1
0.3237	0.3989E-1	0.4219	0.1101E+1
0.2464	0.1740E-1	0.4794	0.9120
0.1880	0.1268E-1	0.5000	0.7810
0.3615	0.7111E-1	0.3784	0.1172E+1
0.3472	0.6201E-1	0.3819	0.1095E+1
0.3106	0.4462E-1	0.4153	0.9986

*E-n = 10^{-n}

TABLE 4-3

EQUILIBRIUM DATA FOR PHENOL-p-TOLUENE SULFONATE

MIXTURES: PHENOL (1) - p-TOLUENE SULFONATE (2)

C_1 mmoles/l	C_2 mmoles/l	q_1 mmoles/gm	q_2 mmoles/gm
0.1483	0.3773	0.5930	0.3090
0.7099E-1*	0.2903	0.4984	0.3220
0.3988E-1	0.2204	0.4040	0.3110
0.3303E-1	0.1413	0.3290	0.3120
0.2068E-1	0.8836E-1	0.2830	0.2960
0.1653E-1	0.5658E-1	0.2450	0.2720
0.1324E-1	0.3265E-1	0.2160	0.2500
0.1057E-1	0.1764E-1	0.1930	0.2290
0.8580E-2	0.1071E-1	0.1750	0.2080
0.1517	0.2250	0.7370	0.2503
0.1073	0.1919	0.5905	0.2903
0.7322E-1	0.1657	0.5070	0.2810
0.5122E-1	0.1340	0.4355	0.2901
0.2980E-1	0.1065	0.3910	0.2869
0.2047E-1	0.8013E-1	0.3360	0.2831
0.1590E-1	0.5581E-1	0.2990	0.2774

*E-n = 10^{-n}

TABLE 4-4

EQUILIBRIUM DATA FOR PHENOL (1) - DODECYL BENZENE SULFONATE (2) MIXTURES

C_1 mmoles/l	C_2 mmoles/l	q_1 mmoles/gm	q_2 mmoles/gm
0.3037	0.3664E-1	0.4572	0.6325
0.2682	0.3131E-1	0.4517	0.5980
0.2155	0.2676E-1	0.4545	0.5639
0.1888	0.1868E-1	0.4455	0.5389
0.1509	0.1998E-1	0.4212	0.4861
0.1627	0.1821E-1	0.4497	0.6424
0.9015E-1 *	0.8982E-2	0.4098	0.4910
0.6105E-1	0.5113E-2	0.3658	0.4124
0.2620E-1	0.2132E-2	0.3159	0.3319
0.2385	0.5285E-1	0.2615	0.9471
0.1667	0.4273E-1	0.2666	0.7658
0.8775E-1	0.2802E-1	0.2748	0.6480
0.5802E-1	0.1716E-1	0.2526	0.5616
0.3407E-1	0.8520E-2	0.2330	0.4957
0.2430E-1	0.6145E-2	0.2114	0.4417

*E-n = 10^{-n}

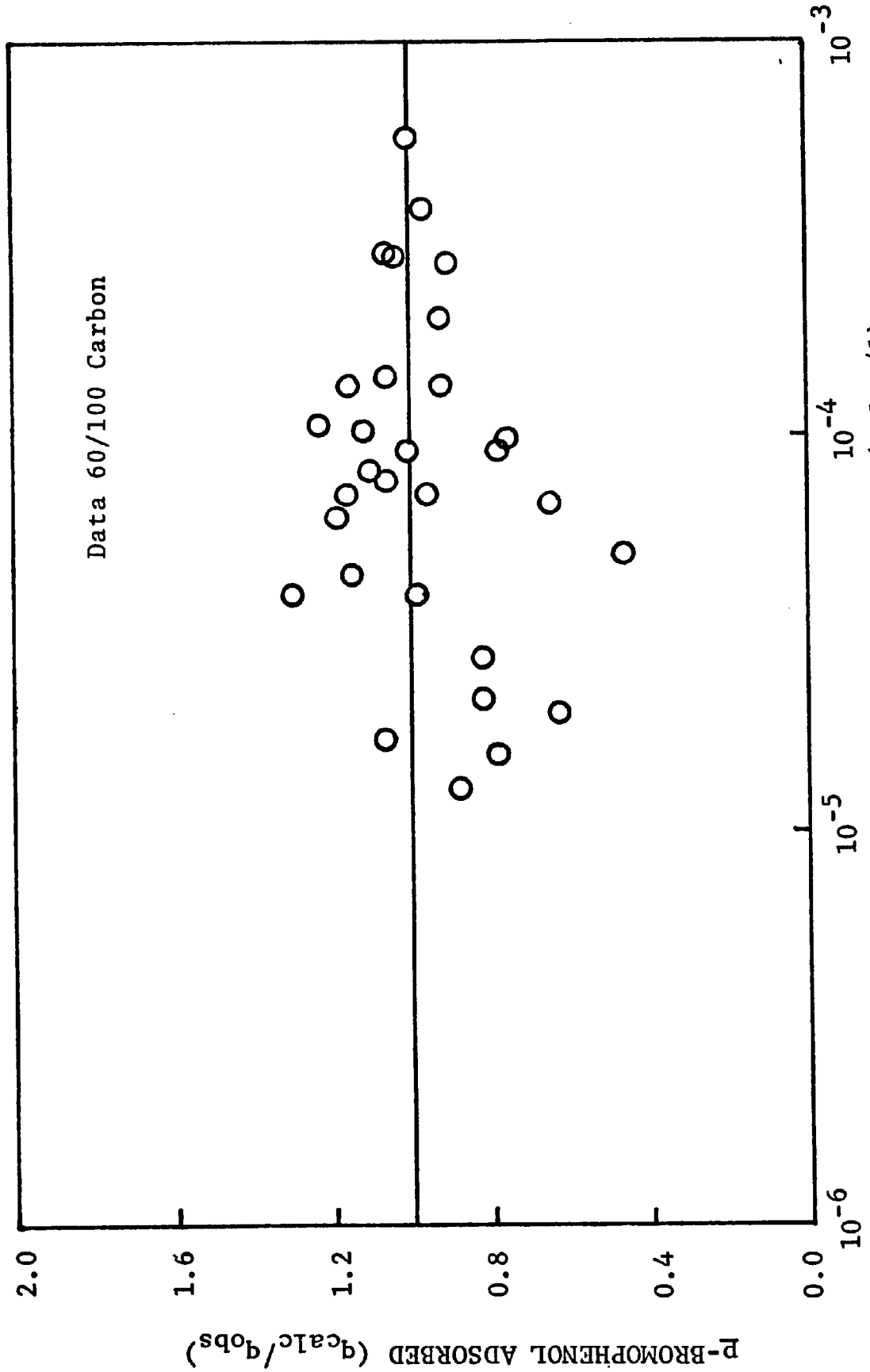


FIGURE 4-9. CORRELATION OF MIXTURE EQUILIBRIA:
PHENOL-p-BROMOPHENOL

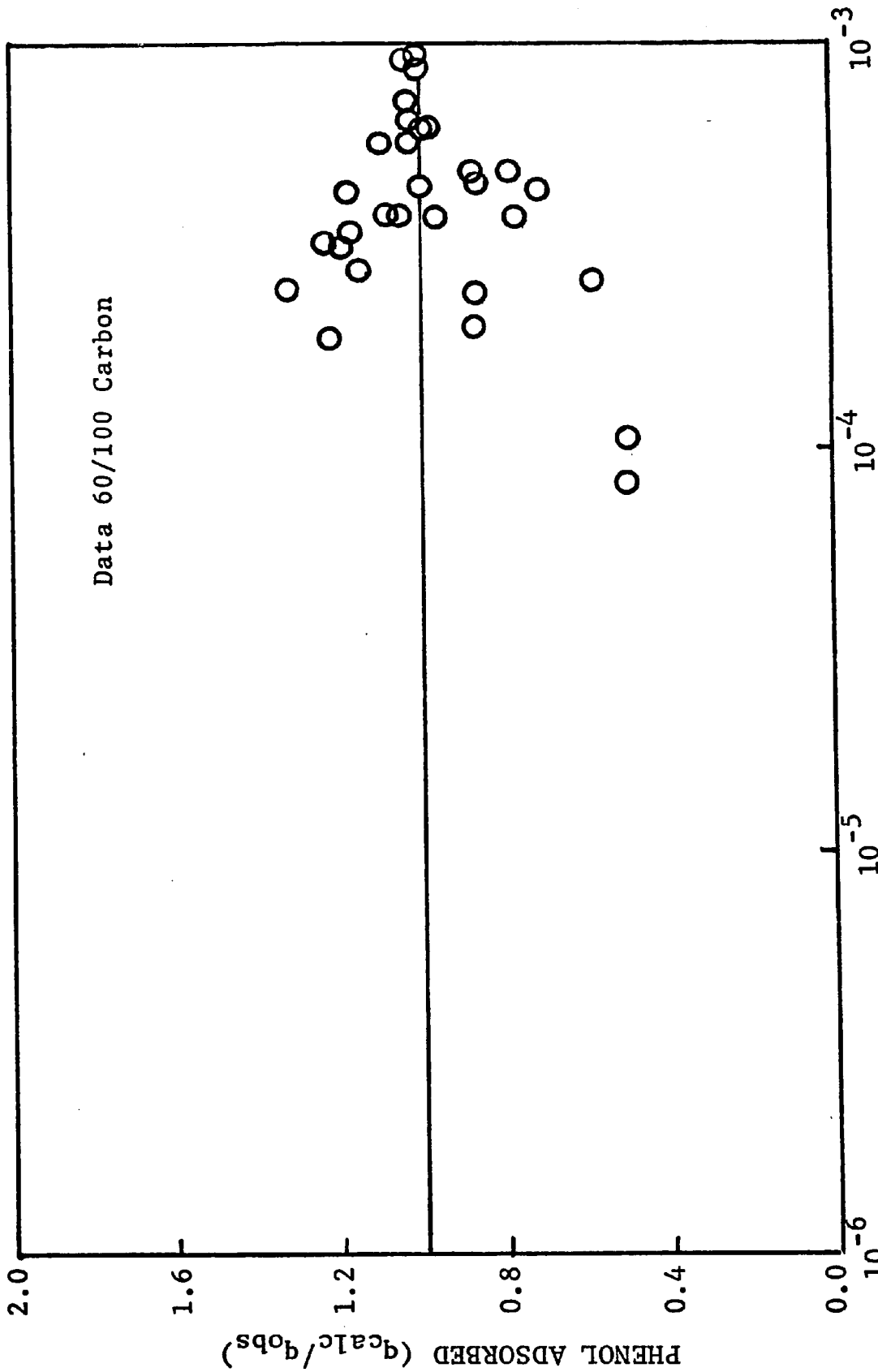


FIGURE 4-10. CORRELATION OF MIXTURE EQUILIBRIA: PHENOL-p-BROMOPHENOL

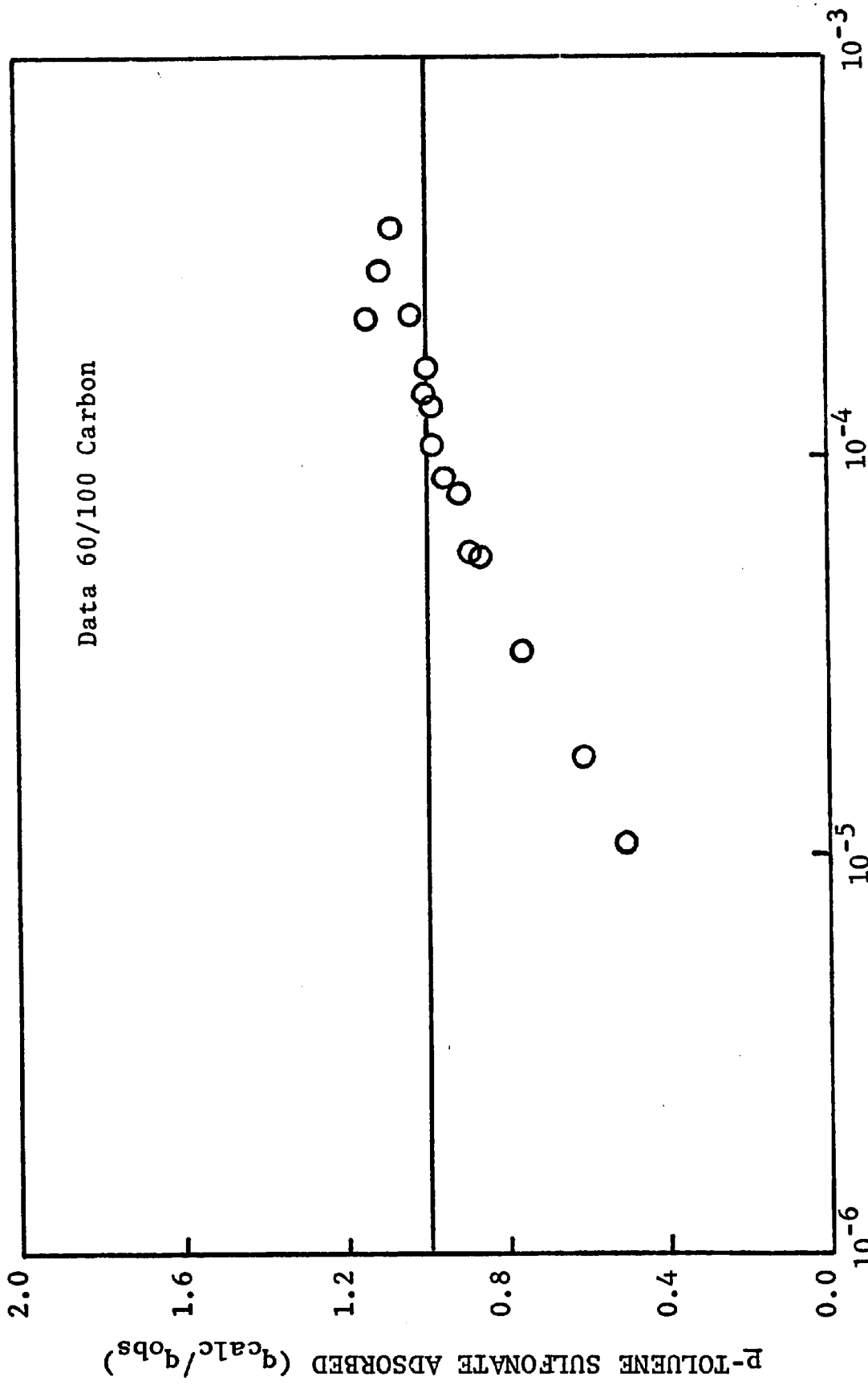


FIGURE 4-11. CORRELATION OF MIXTURE EQUILIBRIA: PHENOL-p-TOLUENE SULFONATE

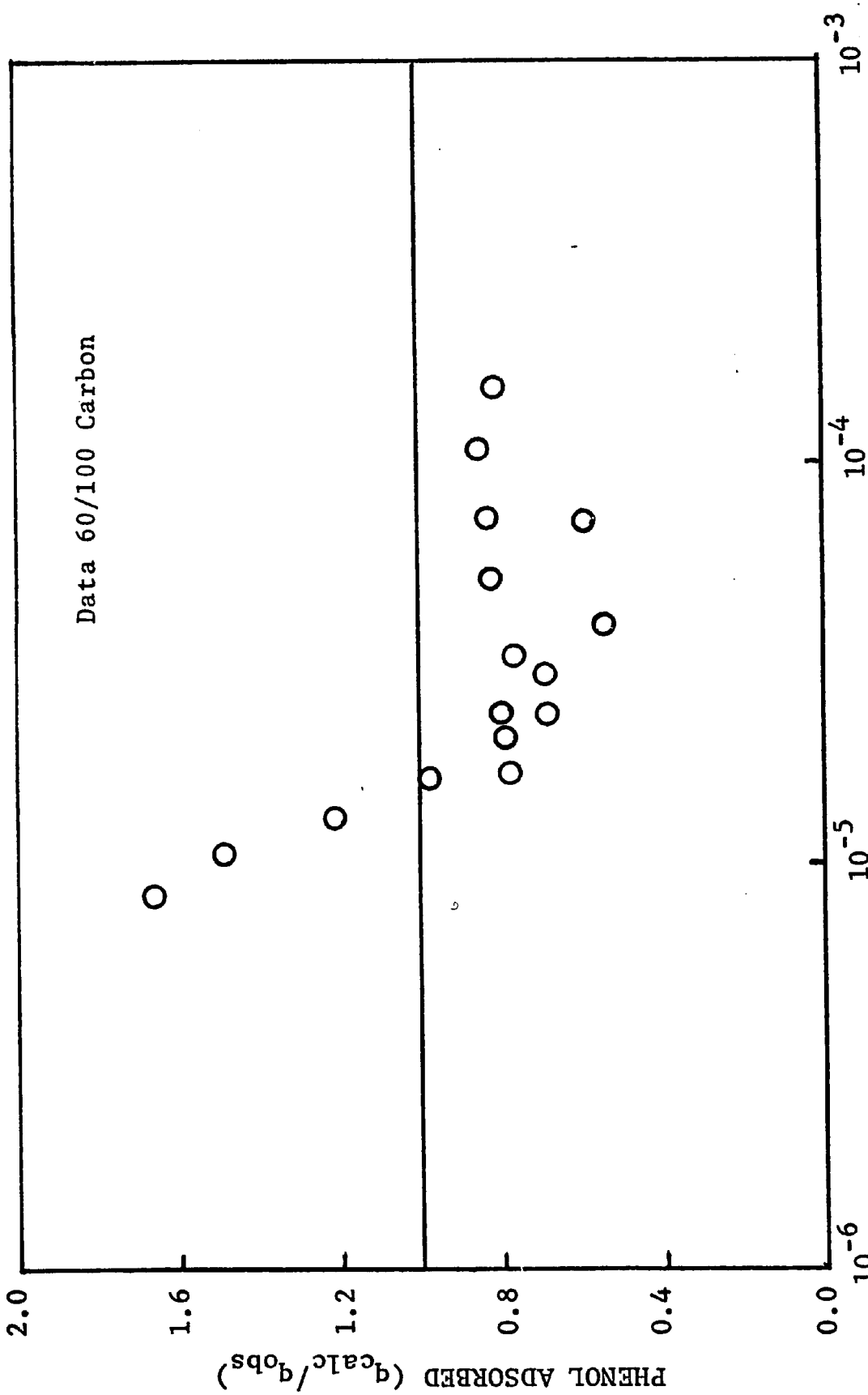


FIGURE 4-12. CORRELATION OF MIXTURE EQUILIBRIA: PHENOL-p-TOLUENE SULFONATE

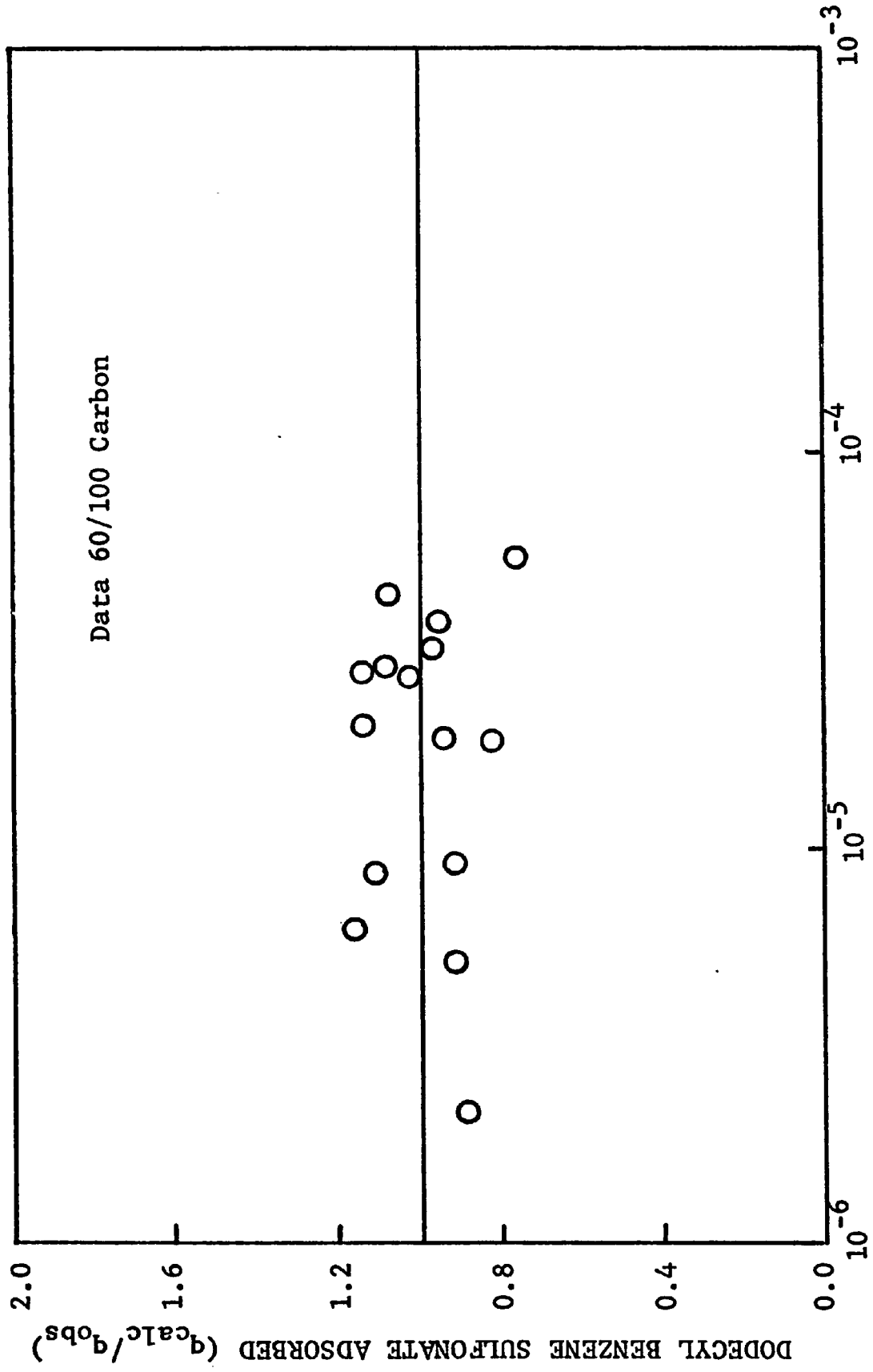


FIGURE 4-13. CORRELATION OF MIXTURE EQUILIBRIA:
PHENOL-DODECYL BENZENE SULFONATE

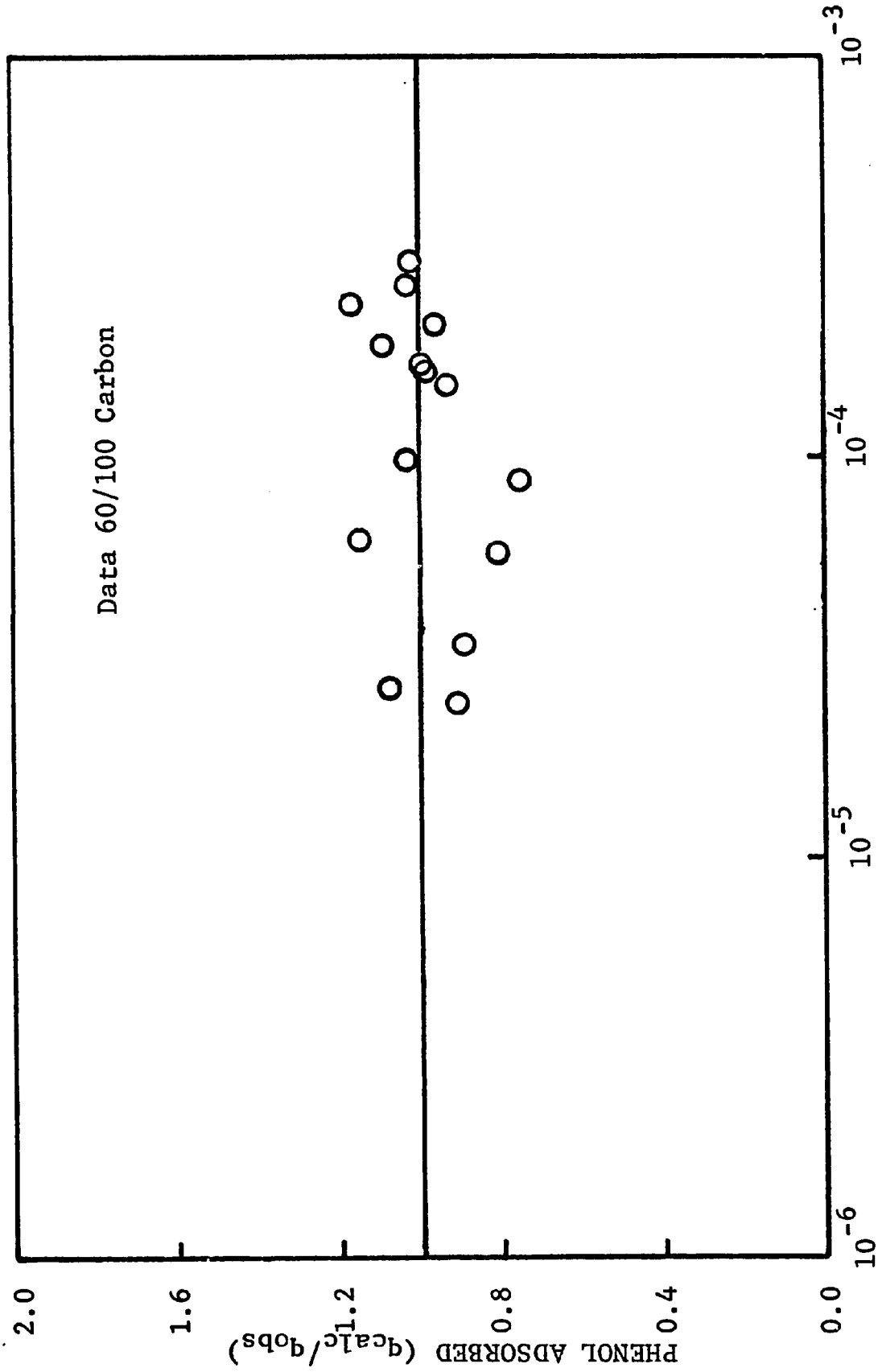


FIGURE 4-14. CORRELATION OF MIXTURE EQUILIBRIA:
PHENOL-DODECYL BENZENE SULFONATE

is the equilibrium concentration of the particular solute in the mixture. It is seen that most of the data points are well within a deviation of $\pm$ 20%. Similar results are shown for the p-toluene sulfonate-phenol system and phenol-dodecyl benzene sulfonate system. The results for these diverse solute systems indicate that equation 4-46 is suitable for correlating binary equilibrium data for use in multicomponent rate models.

CHAPTER 5

ESTIMATION OF RATE PARAMETERS

The solutions of the single and multicomponent adsorption equations developed in Chapters 2 and 6, provide a means for predicting concentration-time curves for single adsorbates and adsorbate mixtures. In order to utilize the model, a number of system parameters must be defined. Of primary importance are the mass transfer coefficients for each solute, the surface diffusion coefficients, and the equilibrium parameters. Estimation of single solute equilibrium constants and mixture equilibria predictions have been treated in Chapter 4. In this chapter, the determination of external mass transfer coefficients, and surface diffusion coefficients from single solute rate data will be discussed.

Mass Transfer - General Considerations

Interphase transport in fluid-fluid and fluid-solid systems has been the subject of intense study for several decades, and a number of theories have been advanced to describe the rate of transport. The film theory postulates the existence of a statioary film around the particle through which mass transfer occurs strictly by molecular diffusion. The fluid within the film is in laminar flow, and all velocity components are assumed to be parallel to the

interface. The mass transfer flux J_i, is represented by equation 5-1.

$$J_i = \frac{D_v(C-C_s)}{\delta} \qquad (5\text{-}1)$$

D_v is the free liquid diffusivity, and δ is the thickness of the stationary film around the particle. This theory is inadequate except for the simple case of mass or heat transfer from a stationary particle in a stagnant medium in the absence of natural convection. For this case, the Sherwood number, $Sh = k_f d/D_v$ is equal to 2.

If there is any relative motion between the phases, the film transfer coefficient will increase. The film theory does not provide any means for predicting the variation of the thickness of the film with changes in relative velocity. The penetration theory, introduced by Higbie (25), and modified by Danckwerts (7), postulates that fresh fluid is brought to the phase boundary in a random manner, and that transport occurs from this quiescent fluid at the interface by molecular diffusion. Further, it is assumed that the velocity gradients normal to the interface are equal to zero. This theory predicts that the mass transfer coefficient is proportional to the square root of the free liquid diffusivity, and has been shown to apply in certain types of contactors in which the bulk fluid is in turbulent flow.

The boundary layer theory has been used widely in predicting laminar and turbulent transport in recent years. It takes into account the important factor of bulk flow in the direction normal to the interface, and predicts that the mass transfer coefficient is proportional to the two-thirds power of the free liquid diffusivity. For convective diffusion in liquids, Levich (40) has shown that the thickness of the diffusion layer can be related to the diffusivity of the solute, a characteristic length of the system, 1, the kinematic viscosity of the liquid, ν , and the relative velocity between the phases, $\hat{u}$. The concentration is shown to change rapidly in the diffusion layer, but the concentration change can be considered linear and the mass transfer rate can be represented by equation 5-1.

Two dimensionless groups that represent the physical properties and flow characteristics that influence the diffsion layer, are the Schmidt number $Sc = \nu/D_v$, and the Reynolds number $Re = \hat{u}l/\nu$. Accordingly, several investigators have attempted to correlate heat and mass transfer coefficients by equations of the form

$$Sh = A + Const.Re^{a}Sc^{b} \qquad (5\text{-}2)$$

For heat transfer, the Sherwood and Schmidt numbers are replaced by analogous Nusselt and Prandtl numbers.

Mass Transfer to Suspended Solid Particles

Mass transfer to fixed spheres submerged in a flowing fluid is correlated well by equation 5-3 obtained by Ranz and Marshall (52).

$$Sh = 2 + 0.60\ Re^{1/2} Sc^{1/3} \qquad (5\text{-}3)$$

Marangozis and Johnson (42) plotted the ratio $Sh/Sc^{1/3}$ against Re for a large number of experimental systems. These data include rate studies such as dissolution of suspended cylinderical solutes, rotating cylinderical electrodes undergoing oxidation-reduction reactions, and agitated vessels in which pellets of solute were freely suspended. However, the length parameter used in the calculation of the Reynolds and Schmidt numbers was the impeller diameter in the case of particles suspended by agitation in liquids. The velocity for computation of the Reynolds number was taken to be the peripheral speed of the impeller. This is theoretically incorrect. From boundary layer theory the length parameter should be the distance over which a diffusion layer for continuous mass transfer is formed, and the velocity should be the relative velocity between the two phases. Nevertheless, the experimental points were correlated with a standard deviation of 17%.

Ideally, equations 5-1 and 5-2 can be applied only if the relative velocity between the particle and the fluid is known. To obviate this difficulty, Harriott (22) suggested that the mass transfer rates in agitated systems be estimated as a multiple of the rate for a particle falling through a stagnant medium at its terminal velocity. The terminal velocity can be obtained from Stoke's law, and is used in equation 5-1 to obtain the minimum value k_f^* for the film transfer coefficient. With turbulence due to agitation, k_f will be greater than k_f^*. Harriott, using his and other published data showed that the ratio k_f/k_f^* generally lies between 1 and 4. However, there is no reliable method for predicting this ratio exactly. Miller (47) has plotted k_f/k_f^* against the agitator power input per unit volume and has shown that the correlation has an average standard deviation of 39%.

A number of investigators (2,4) have used Kolmogorff's theory of local isotropic turbulence in correlating heat and mass transfer rates with agitation power per unit volume of liquid. According to Kolmogoroff's theory, turbulence results in a continuous transfer of energy from the primary eddies to intermediate and smaller eddies, until all the energy is dissipated by viscous flow. The primary eddies are continually created by the rotation of the impeller and has a definite orientation and a maximum

scale of turbulence similar to the dimension of the reactor. As the energy is transferred from large to small eddies, the geometric orientation of the primary eddies are lost. With sufficient interaction, a large number of eddies much smaller than the primary eddies are formed. The directional nature of the primary eddies is completely lost, and the turbulence is locally isotropic. The eddies formed are statistically independent of the primary eddies, and their properties are determined solely by the rate at which the energy is supplied, and the tendency of the eddies to dissipate energy viscously. The scale of the smallest eddies is given by Kolmogoroff as $\bar{\eta} = (\nu^3/\bar{\epsilon})^{1/4}$. The root mean square of the fluctuating velocity in turbulent flow over a length equal to the diameter of the particle is given as

$$\hat{u} = \text{Const.}(\bar{\epsilon}\, d)^{1/3} \qquad (5\text{-}4)$$

Calderbank and Moo-Young (4) used this velocity, $\hat{u}$, in defining the Reynolds number, and correlated experimental data over a seven fold range from heat and mass transfer studies by the following relation.

$$Sh = 0.13\left(\frac{\bar{\epsilon}\, d^4}{\nu^3}\right)^{1/4} Sc^{1/3} \qquad (5\text{-}5)$$

The mass transfer data were obtained from solute dissolution experiments and liquid-liquid extraction studies. The correlation did not include diameter as a variable, and

therefore, predicts that the mass transfer coefficient does not vary with particle size. This is contrary to the findings of Harriott, which indicate that k_f decreases as particle size is increased, linearly for particles less than approximately 100 microns in size, and as $d^{-\frac{1}{4}}$ for particles greater than 1000 microns. In the range of 100 to 1000 microns, Harriott's results do not show any appreciable variation in k_f^* with particle diameter. The Calderbank-Moo-Young correlation predicts mass transfer coefficients within a standard deviation of 66%.

Brian et. al., (2) measured heat transfer rates from water to melting ice spheres, and mass transfer rates from dissolving spheres of spivalic acid. From an analysis of the data using Kolmogoroff's theory, they conclude that the transport coefficients are a function of the agitator power input, but independent of agitator design or reactor geometry. The effect of solid-liquid density ratio on the correlation was estimated to be less than 12%, for density ratios between 0.75 and 1.25. In this range, the gravity group also seems to have little effect. Brian et. al., plotted their heat and mass transfer data and the data of Harriott with $Sh/Sc^{1/3}$ or $Nu/Pr^{1/3}$ as the ordinate, and $\epsilon d^4/\nu^3$ as the abscissa. The mass transfer data agree with that of Harriott for moderate values of the Schmidt number,

corresponding to high viscosity solutions, lie considerably below the mass transfer results for moderate values of the Schmidt number. Brian, et. al., in light of these results and the fact that the density and gravity groups have little effects on the correlation conclude that the exponent 1/3 for the Schmidt number is inadequate to describe the effect of the Schmidt number in mass transfer rates.

Levins and Glastonbury (41) critically examined the applicability of Kolmogoroff's theory to problems involving solid-liquid mass transfer. From a study of published data for mass transfer, and their own data, it was concluded that agitation power per unit volume is not a successful method for correlating mass transfer rates to particles suspended in agitated vessels. The study indicates that the impeller to reactor diameter ratio significantly affects the mass transfer rates. Further, the effect of this ratio appeared to be related to the solid-liquid density difference. From a statistical analysis of data for a number of systems with different impeller types, the following equation were proposed.

$$k_f = \text{Const.}(\bar{\epsilon})^{0.2}(D_I/D_T)^{0.12} \quad , \quad \Delta\rho = 0.1 \ \frac{gm}{ml} \qquad (5\text{-}6)$$

$$k_f = \text{Const.}(\bar{\epsilon})^{0.22}(D_I/D_T)^{0.27} \quad , \quad \Delta\rho = 0.28 \ \frac{gm}{ml} \qquad (5\text{-}7)$$

Sensitivity Analysis

It is apparent then, that the question of accurate prediction of mass transfer coefficients from correlation for dimensionless groups, is yet to be resolved. The slip velocity method of Harriott provides correlation with an average deviation of 39%. The correlation of Calderbank and Moo-Young based on Kolmogoroff's theory has a standard deviation of 66%. Brian and Hales did not obtain superimposable curves from heat and mass transfer studies, and from mass transfer data for high Schmidt numbers.

The effect of errors in the estimated values for the mass transfer coefficient on the concentration-time profile is shown for p-bromophenol in Figure 5-1. The solid line represents the concentration-time profile that is obtained by using the mass transfer coefficient of 5.4×10^{-3} cm/sec., and a surface diffusion coefficient of 1.58×10^{-8} $cm^2/sec.$, in the single solute rate equations developed in Chapter 2. The dotted lines above and below represent the predicted profiles that would result, if k_f is estimated with an error of -20%, and 30% respectively. It is apparent that substantially different predicted profiles could result, if k_f is estimated to be lower even by 20%. The effect of a higher k_f value than the actual is less pronounced, but is still substantial. Figure 5-2 shows similar results for dodecyl benzene sulfonate. The effect in this case,

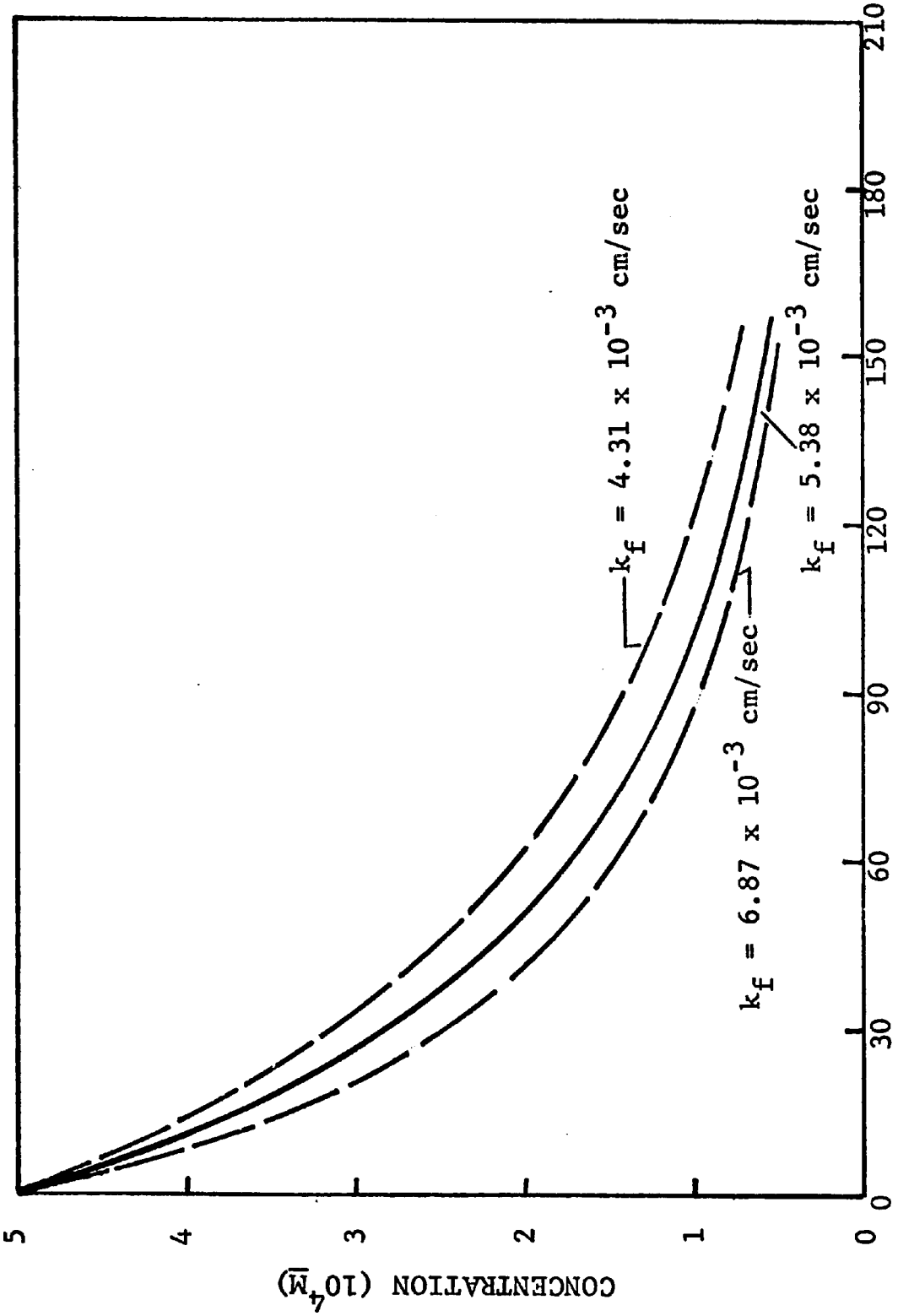


FIGURE 5-1. SENSITIVITY OF PREDICTED PROFILE TO VARIATION IN MASS TRANSFER COEFFICIENT, k_f
p-BROMOPHENOL

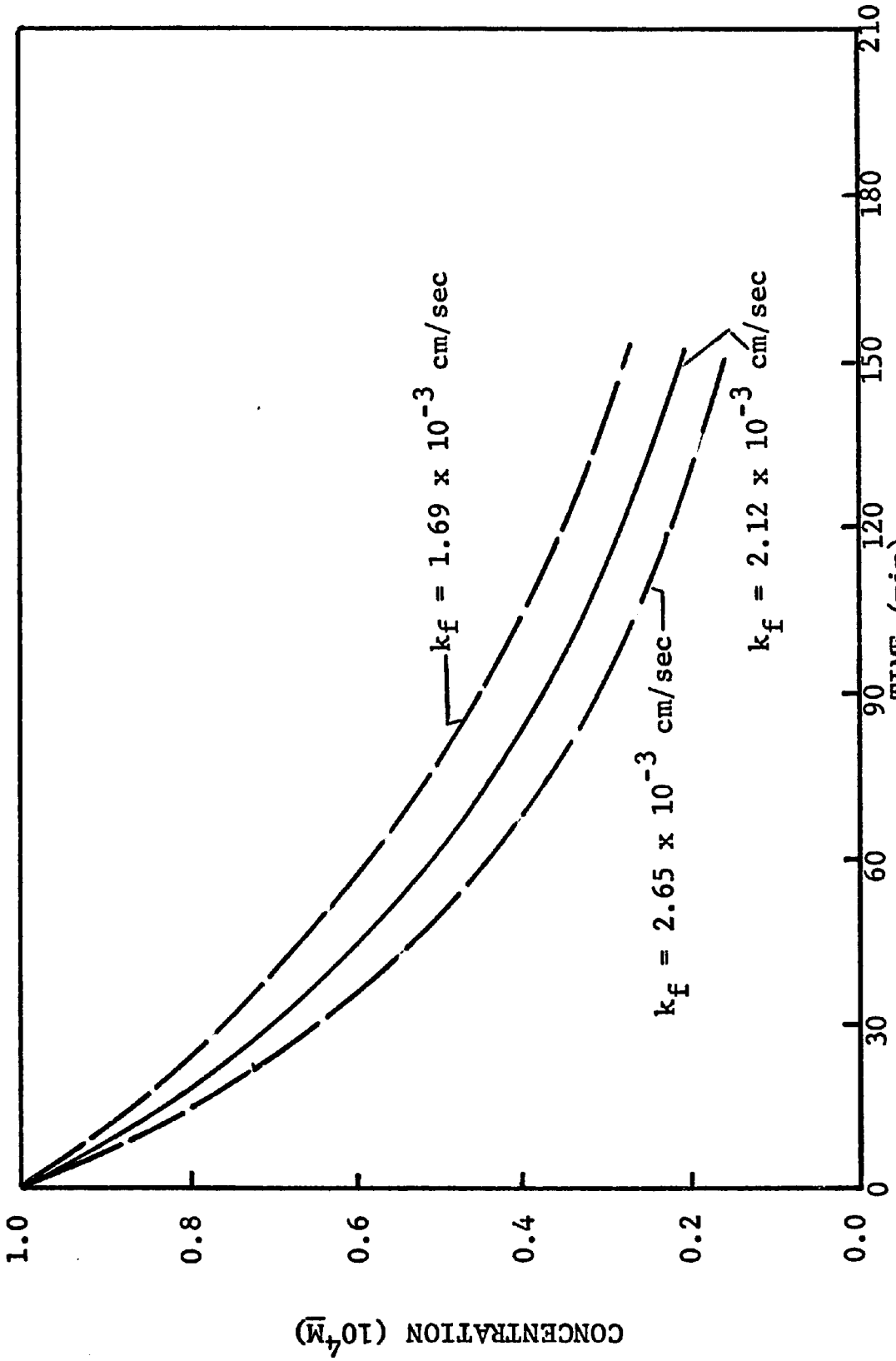


FIGURE 5-2. SENSITIVITY OF PREDICTED PROFILE TO VARIATION IN MASS TRANSFER COEFFICIENT, k_f
DODECYL BENZENE SULFONATE

is more pronounced than that of p-bromophenol, and extends over a longer period of time. The predicted concentration at the end of 150 minutes is less than the actual by 33%, if the k_f value used is less than the actual by 20%. Results for phenol and p-toluene sulfonate are shown in Figures 5-3 and 5-4, and the sensitivity to variation in mass transfer coefficients appears to be less pronounced for these solutes. In general, the generated profiles will be more sensitive to variations in the mass transfer coefficient for film-diffusion controlled systems than for intraparticle-diffusion controlled adsorption. The implications of these results for single and multi-solute adsorption rate simulation is self-evident. It will be necessary to have fairly accurate values for the film transfer coefficient to predict the concentration-time profiles satisfactorily.

Mass Transfer in Adsorption Systems

The studies on mass transfer to solid particles in an agitated system have mainly been restricted to experiments involving the dissolution of solid particles. Brian and Hales (1) have shown that, in such systems, particle shrinkage and transpiration could significantly affect the measured transport rates. There have been very few studies on fluid-particle transport rates in adsorption

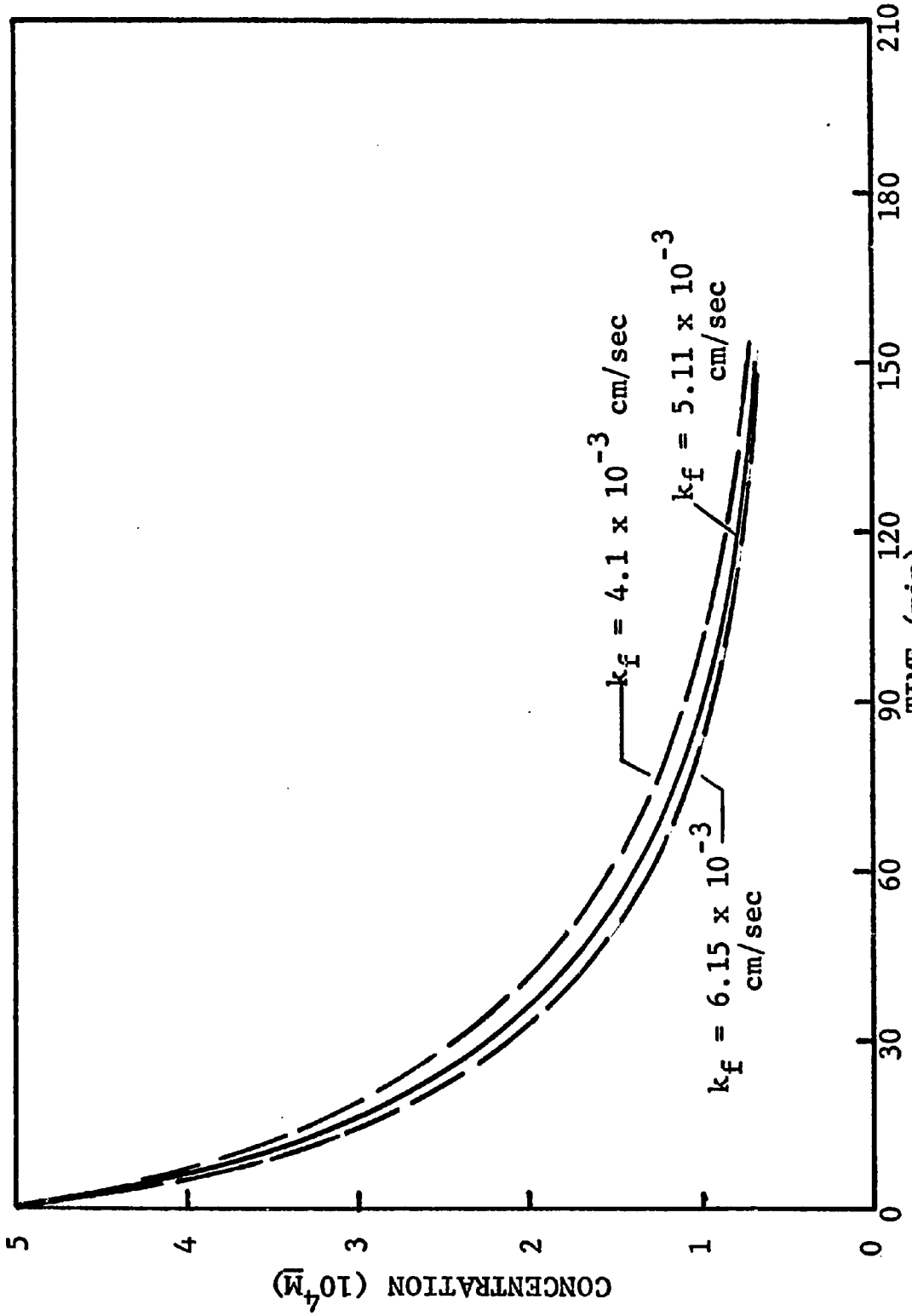


FIGURE 5-3. SENSITIVITY OF PREDICTED PROFILE TO VARIATION IN MASS TRANSFER COEFFICIENT, k_f PHENOL

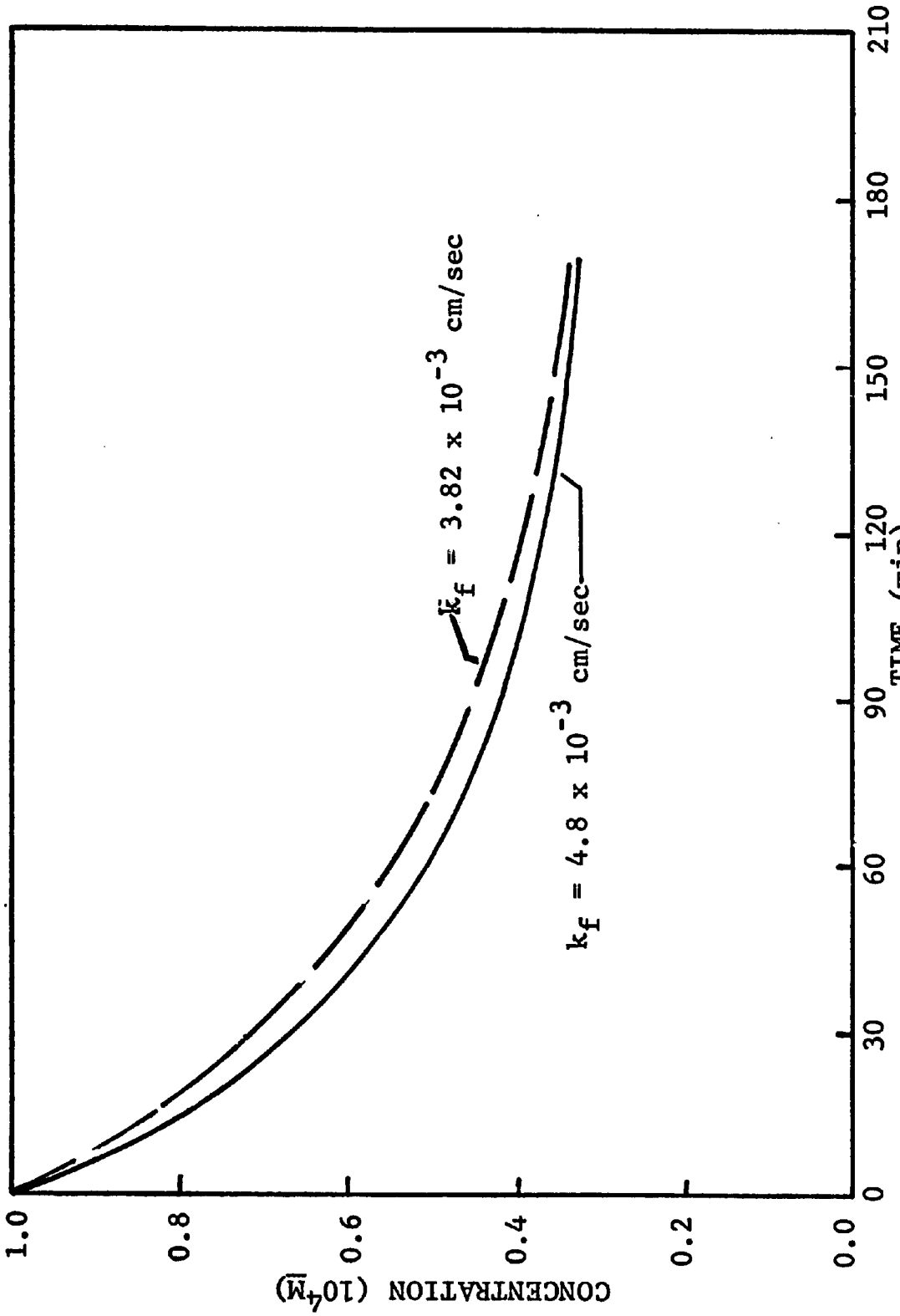


FIGURE 5-4. SENSITIVITY OF PREDICTED PROFILE TO VARIATION IN MASS TRANSFER COEFFICIENT, k_f
p-TOLUENE SULFONATE

systems. Furusawa and Smith (17,18) measured adsorption rates of benzene and benzaldehyde on activated carbon and amberlite particles. The isotherms of these solutes were described by the Langmuir equation. However, for estimating mass transfer coefficients, it was assumed that the isotherm is linear, and that the intraparticle diffusion resistance is negligible. The concentration-time profiles from estimated values of the mass transfer coefficients match the experimental curves only for the first two minutes for activated carbon, and for a much lesser time period for the amberlite particles. The k_f was used in a two-resistance model for the adsorption rate, to estimate pore diffusivities for the solutes. Pore diffisivities for solutes porous particles are generally lower than the corresponding free liquid diffusivities by an order of magnitude. However, the pore diffusivity values obtained by Furusawa and Smith are higher than the free liquid diffusivity, and they explain the discrepancy by including surface diffusion as a factor. Similar results were obtained by DiGiano (11) for the adsorption of neutral species of p-nitrophenol and dinitro pehnol on to activated carbon. These inconsistencies in the pore diffusivity values could be due to the inaccuracies in the estimation of mass transfer coefficients. If intraparticle diffusion is neglected in rapidly agitated

systems, the estimated value for k_f will be lower than the actual resulting in a concentration-time curve that is higher than the experimental curve in a two-resistance model. The estimated pore diffusivities would then have to be much higher to balance the effects of a lower mass transfer coefficient. The effect of a lower mass transfer coefficient on the overall profile in a two-resistance model can be observed in Figures 5-1 to 5-4.

Letterman et. al., (39) obtained mass transfer coefficients for phenol over a wide range of conditions of agitation power input. They assumed that the surface concentration is negligible,and used a first order rate equation, 5-8, in obtaining mass transfer coefficients from rate data extending to a period of ten minutes.

$$\frac{dC}{dt} = \frac{-k_f\ 3W\ C}{R\rho(1-\epsilon)} \qquad (5\text{-}8)$$

Equation 5-8 is strictly valid only for time t = 0, and its use for periods of time as in their study is justifiable only for small values of agitation power input. For large values of power input, intraparticle diffusion becomes controlling, and at such values, the assumption that the intraparticle diffusion resistance is negligible, or the assumption that the surface concentration is zero is obviously erroneous.

The effect of intraparticle diffusion on the initial adsorption rate is shown in Figures 5-5 and 5-6 for phenol. For moderate values of the film transfer coefficient, initial rates are not affected significantly by diffusion within the particle. For such cases, the assumption of negligible intraparticle resistance is valid in estimating the mass transfer coefficient. However, for large values of k_f as shown in Figure 5-6, the use of initial rate data beyond the first few minutes would result in large errors in computed values for k_f. Similar results are shown for p-toluene suflonate in Figure 5-7.

The initial rates are also a function of the equilibrium distribution of solute between the two phases. Results for p-bromophenol, for k_f values 5.4×10^{-3}, 7.8×10^{-3}, and 1.48×10^{-2} cm/sec are shown in Figures 5-8 and 5-9. The assumption of negligible intraparticle resistance does not seem to seriously affect the initial rate data for p-bromophenol. This can be explained on the basis of the fact that p-bromophenol has a high solid to liquid equilibrium solute distribution. Analogous results were obtained for dodecyl benzene sulfonate and are shown in Figure 5-10 for k_f values of 2.12×10^{-3}, 7.42×10^{-3} cm/sec.

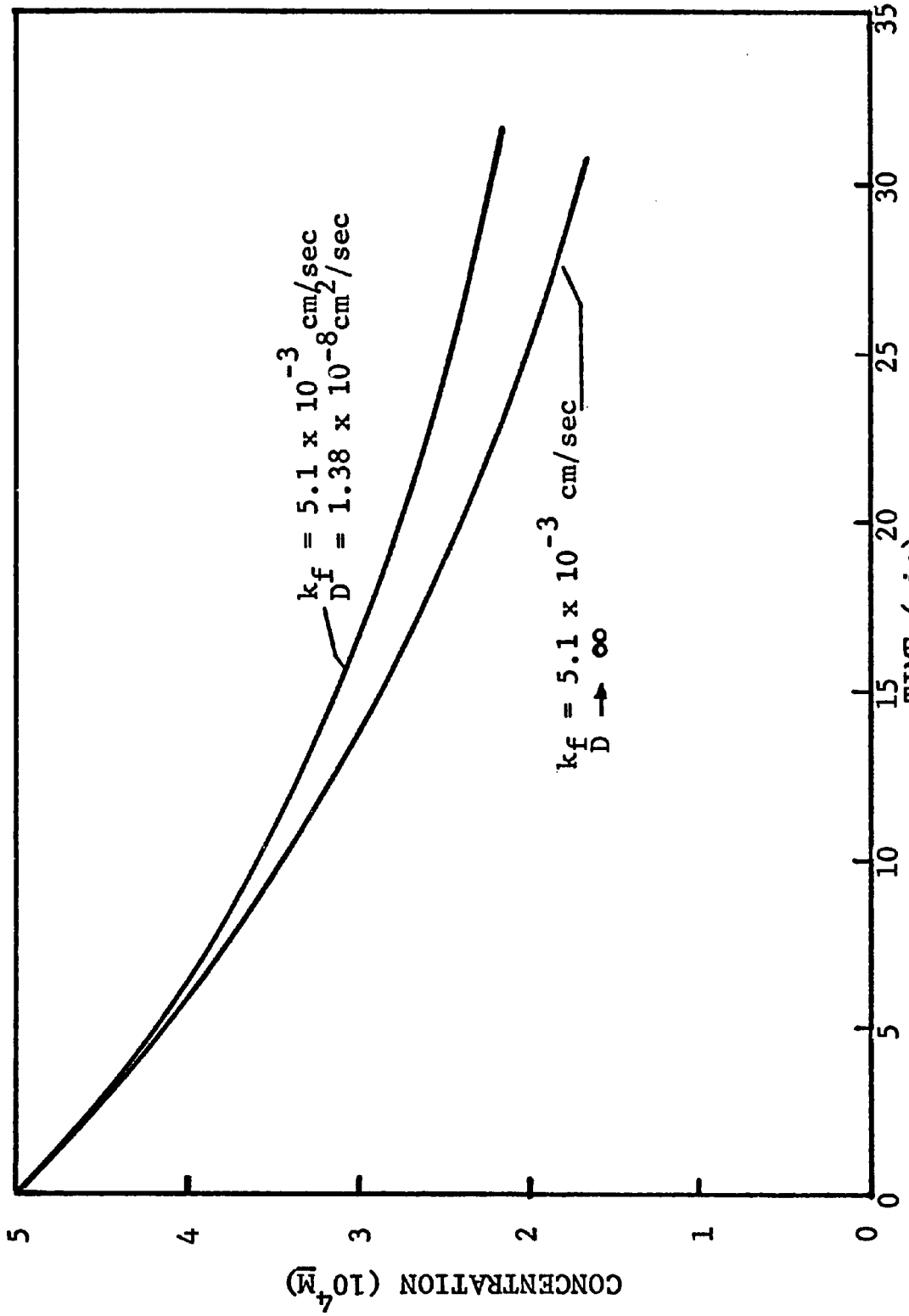


FIGURE 5-5. EFFECT OF INTRAPARTICLE DIFFUSION ON THE INITIAL UPTAKE RATE FOR PHENOL

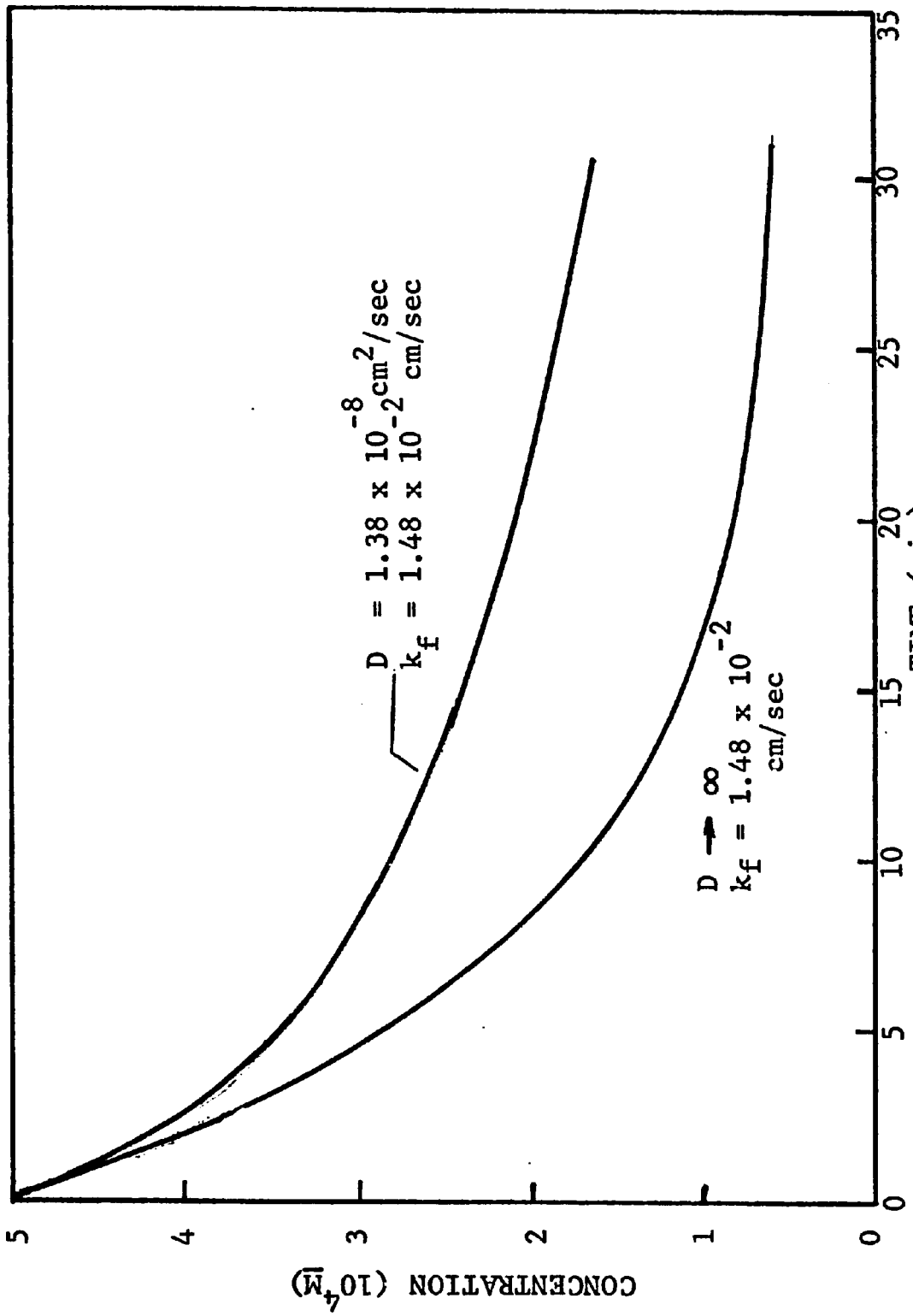


FIGURE 5-6. EFFECT OF INTRAPARTICLE DIFFUSION ON THE INITIAL UPTAKE RATE FOR PHENOL

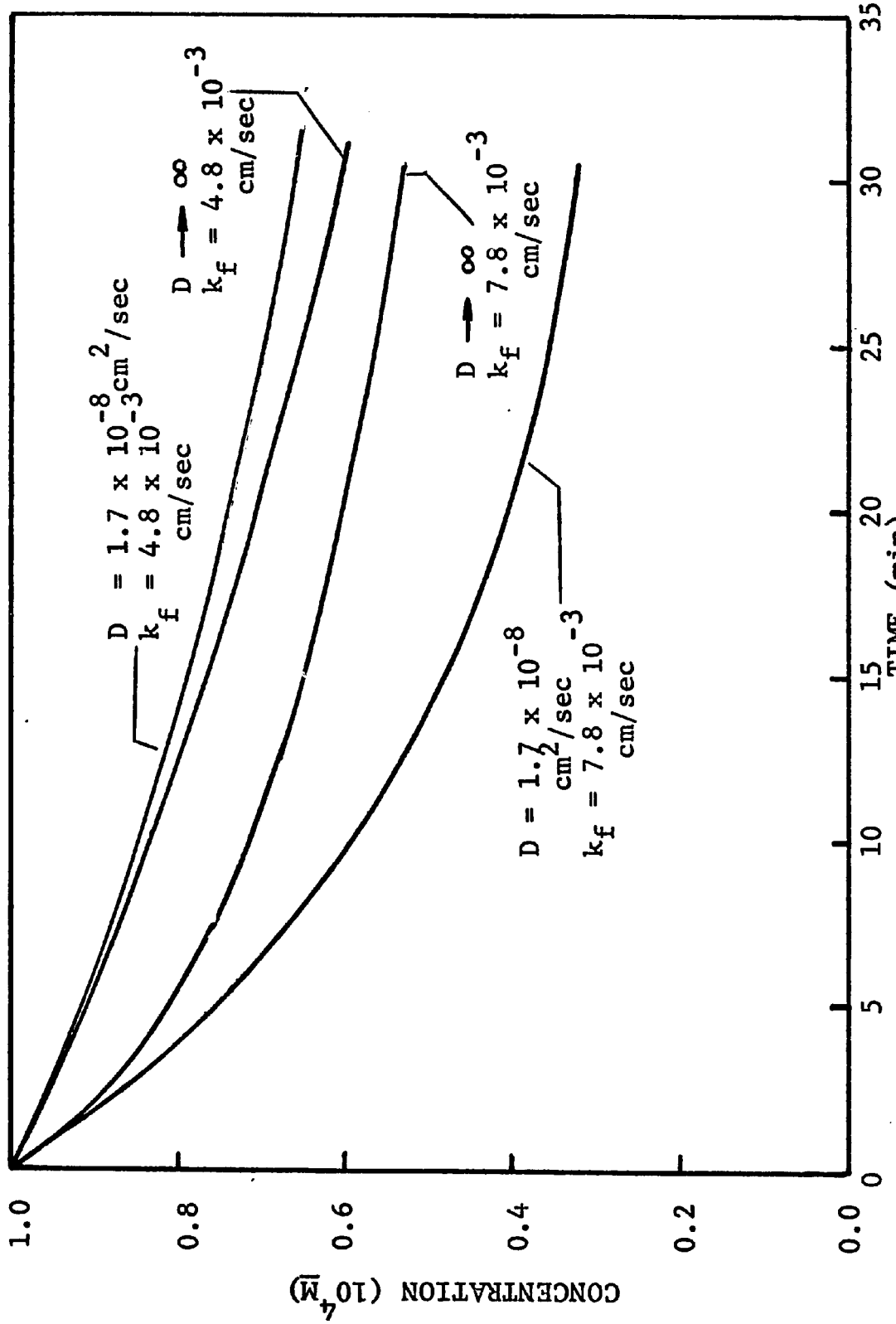


FIGURE 5-7. EFFECT OF INTRAPARTICLE DIFFUSION ON THE INITIAL UPTAKE RATE: p-TOLUENE SULFONATE

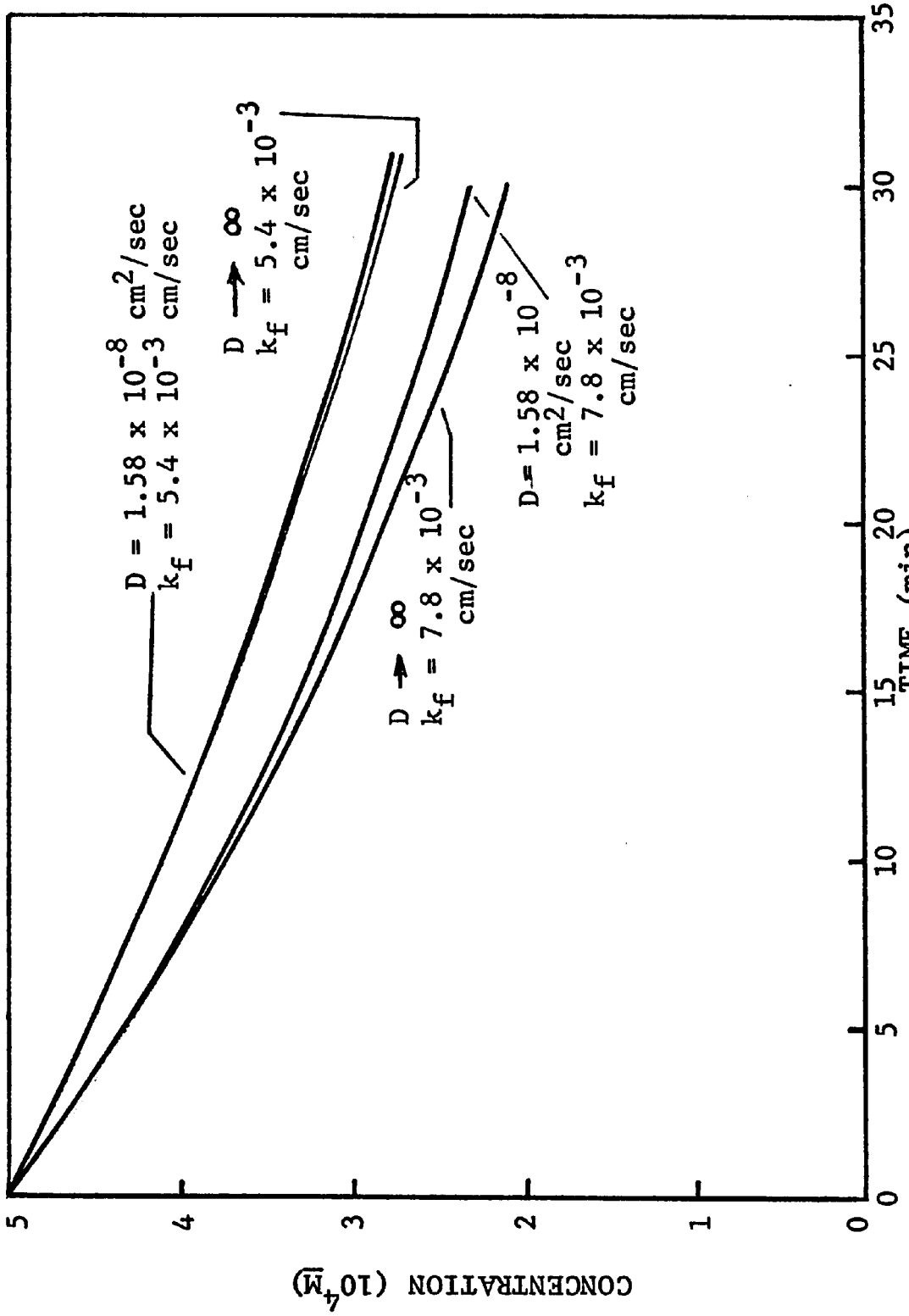


FIGURE 5-8. EFFECT OF INTRAPARTICLE DIFFUSION ON THE INITIAL UPTAKE RATE: p-BROMOPHENOL

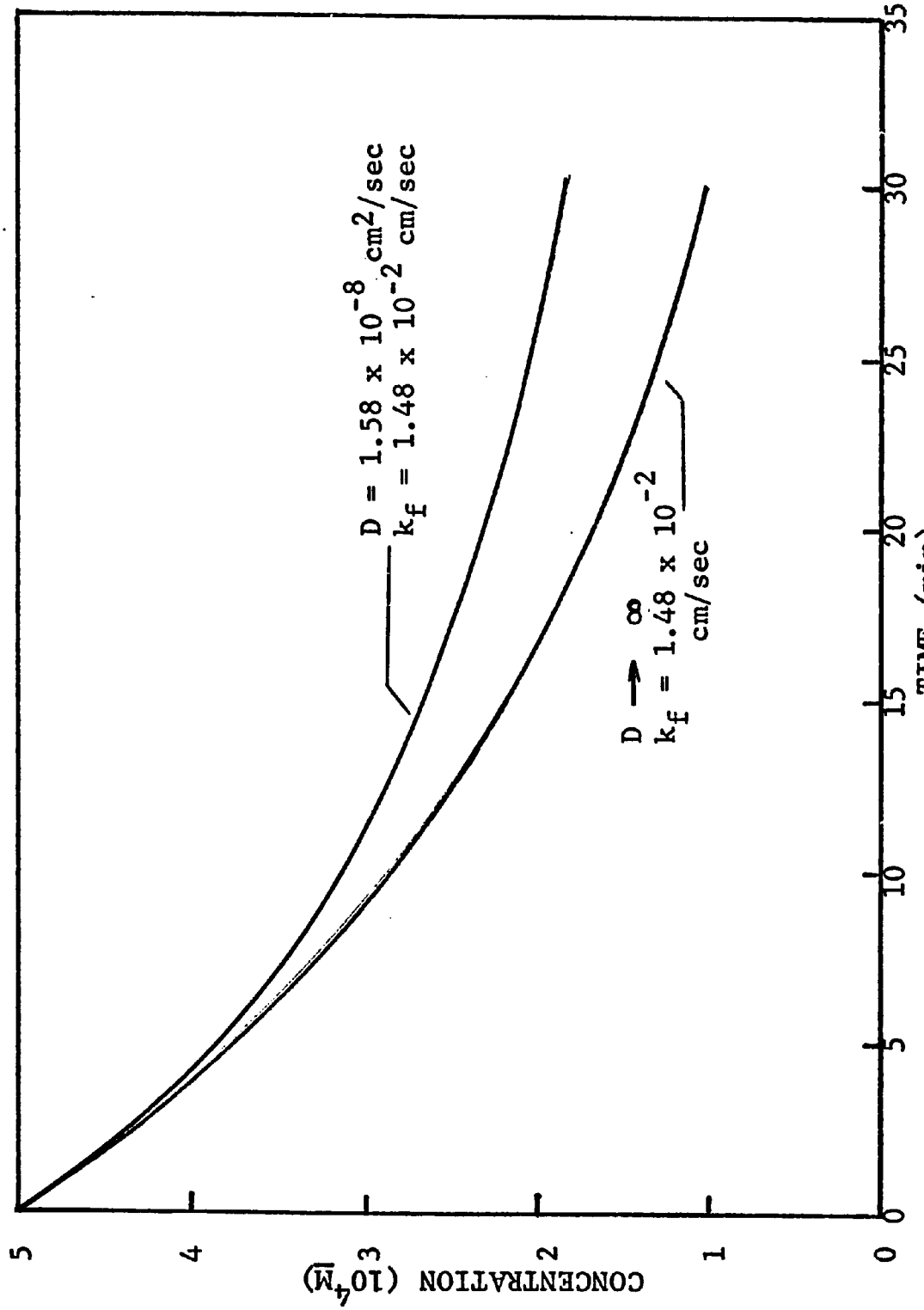


FIGURE 5-9. EFFECT OF INTRAPARTICLE DIFFUSION ON THE INITIAL UPTAKE RATE: p-BROMOPHENOL

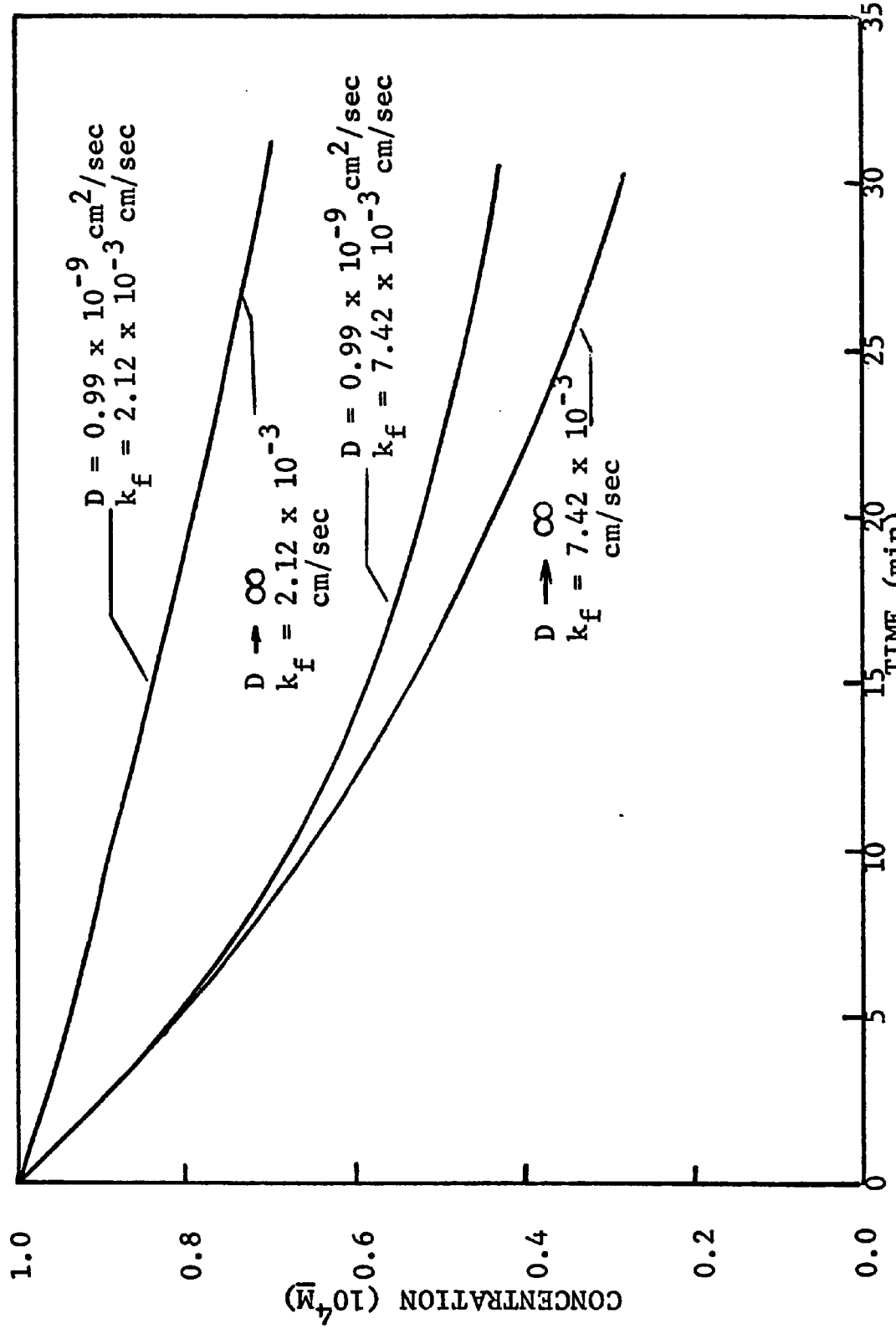


FIGURE 5-10. EFFECT OF INTRAPARTICLE DIFFUSION ON THE INITIAL UPTAKE RATE: DODECYL BENZENE SULFONATE

Parameter Estimation

It is apparent from the above considerations that the intraparticle diffusion resistance can not be neglected 'a priori' in estimating mass transfer coefficients in adsorption systems. Conversely, as DiGiano (11) has noted, the film transfer resistance may be significant even in rapidly agitated systems, and should be taken into account in batch reactor studies for the estimation of internal diffusion coefficients.

In this study, mass transfer and surface diffusion coefficients are estimated simultaneously from single solute rate data, taking into consideration both internal and external diffusion resistances. A direct-search parameter estimation procedure, PRAXIS, available on the Michigan Terminal System was used for this purpose. PRAXIS is a minimization procedure that does not require the computation of derivatives for the variables over which the objective function is being minimized. This should result in substantial savings in computation time, particularly since the objective function involves the complex rate equations developed in Chapter 2.

The objective function used in the program is the sum of the square of percentage deviations between the experimental and calculated data for the liquid phase

concentrations. The program developed allows the search for the variables within certain specified constraints. Search outside the constraints is limited by the use of penalty functions. The main components of the program are: (1) a main program to initiate the search procedure, given the initial estimates for k_f and D; (2) a function program containing the objective function and the penalty function for the constraints; (3) a subroutine to solve the single solute rate and equilibrium equations developed in Chapter 2; and, (4) a subroutine to estimate the equilibrium surface concentration needed in the rate subroutine.

The single solute rate subroutine involves the application of the numerical procedure developed in Chapter 2 for the differential equations, and the Newton's method for the estimation of the equilibrium surface concentration. The program was made interactive to allow input from the terminal, if the Newton's iterations did not converge, or if the constraints for the variables need to be changed. However, such difficulties were not encountered, with a time step of one minute, and reasonable estimates for the initial values and the constraints. A listing of the program is attached in Appendix 2.

Experimental Method

The single solute rate experiments were carried out in 3.5 liter glass jars covered with a plexiglass lid. Two baffles of 2 cm width extended from the lid to 1 cm from the bottom of the reactor. Agitation was provided by a stirring motor with polyethylene stirrers. The speed of the motor was controlled with a Variac, and measured using a strobe light. The speed was maintained at 650 rpm for all the rate studies. The pH of the solution was initially adjusted to 7. The pH was measured at the end of the experiment, and did not differ from the initial value. Three liters of solution without the adsorbent particles was agitated, and allowed to reach equilibrium with the vessel before withdrawing the initial sample for analysis. However, no measurable change in concentration was noticed. At time t=0, a measured quantity of activated carbon was introduced into the reactor and agitated. Samples were withdrawn periodically, until equilibrium was reached, and analyzed for the solute concentration in the liquid phase.

Experimental Results

The parameter estimation procedure using the homogeneous solid phase diffusion rate model was applied to the rate data for p-bromophenol presented in Figure 5-11. The experiment was carried out with an initial concentration of 5×10^{-4} M

p-bromophenol, and a carbon dosage of 0.33 gm/l. The solid line in Figure 5-11 is the predicted concentration-time profile, and appears to be in excellent agreement with the experimental points. The mass transfer coefficient is estimated to be 5.4×10^{-3} cm/sec. The dotted line in Figure 5-11 is the predicted concentration-time profile from a model with external film transfer controlled adsorption. It is apparent from the poor fit, that the single resistance model is inadequate in predicting concentration profiles beyond the initial time period.

The curve for the single resistance model was obtained by allowing $D \rightarrow \infty$, in the two-resistance model, and differs from the models of DiGiano (11), and Letterman, et. al. (39), where the surface concentration is assumed to be negligible. With such an assumption, the predicted profile would be even more at variance with the experimental data. However, such an approach may be valid in the initial time period for p-bromophenol, as discussed earlier. Integrating equation 5-8 from $(0,C_o)$ to $(t,0)$ results in equation 5-9 for the value of k_f.

$$k_f = \frac{R\rho}{3W}(1-\epsilon)\frac{\ln(C_o/C)}{t} \qquad (5\text{-}9)$$

A k_f value of 5.38×10^{-3} cm/sec was obtained for p-bromophenol using the rate data over the first 15 minutes, and is in good agreement with the value obtained

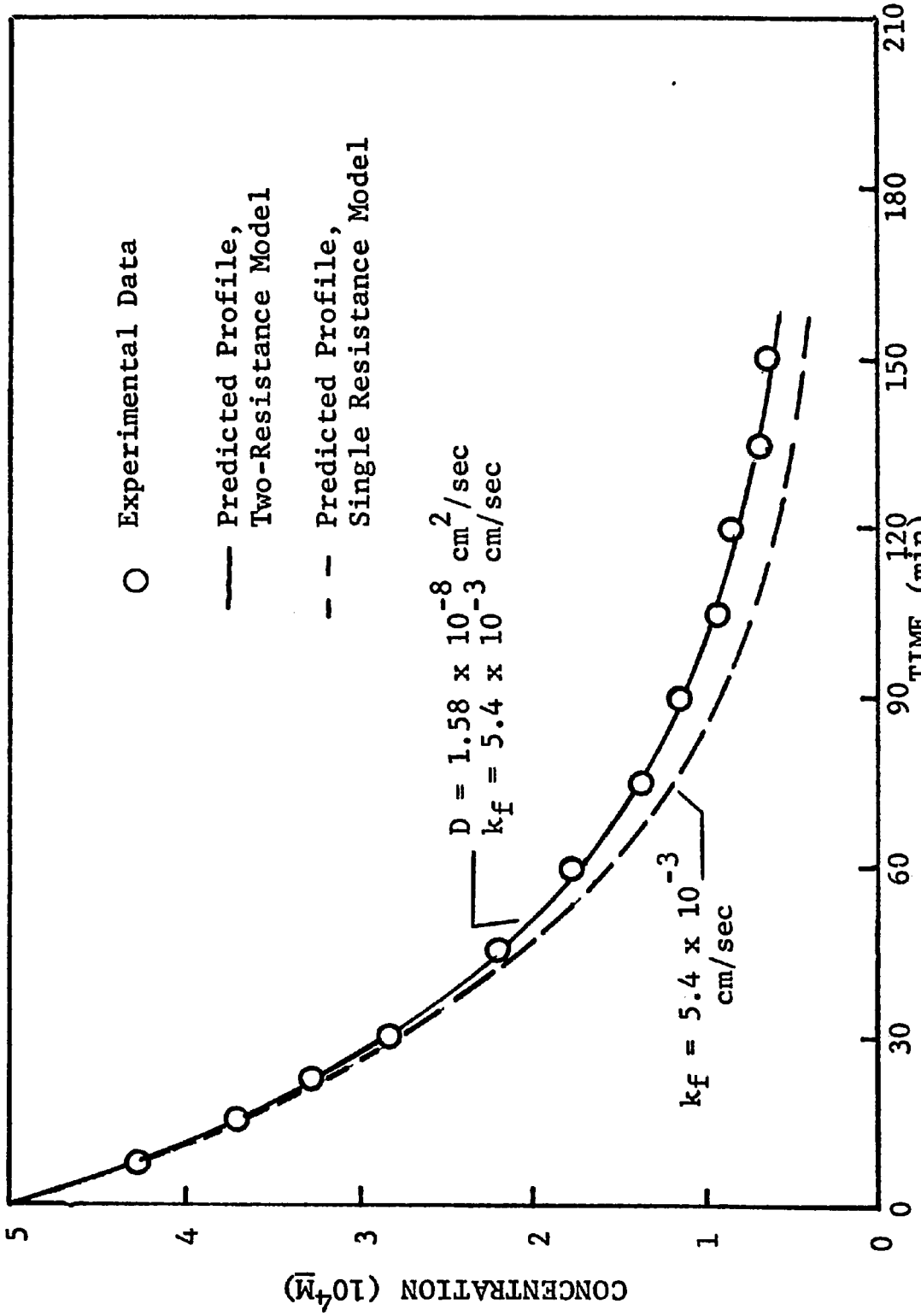


FIGURE 5-11. CONCENTRATION-TIME PROFILE: p-BROMOPHENOL
(C_o=5 x 10^{-4}M, CARBON=0.33g/1, 650 RPM)

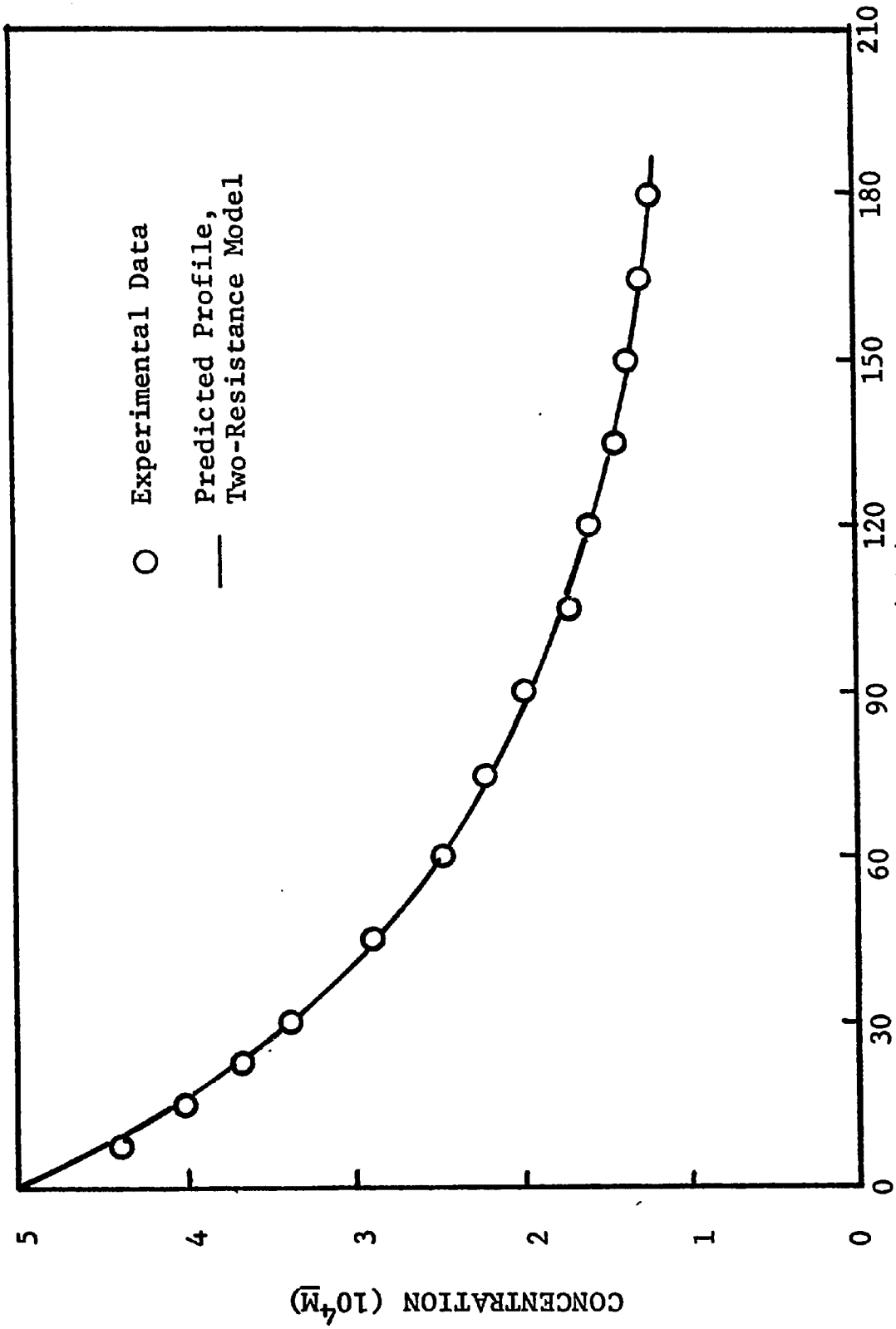


FIGURE 5-12. CONCENTRATION-TIME PROFILE: p-BROMOPHENOL
(C_o=5 x 10^{-4} M, CARBON=0.25 g/l, 650 RPM)

from the parameter estimation procedure.

The surface diffusion coefficient for p-bromophenol was estimated to be 1.58×10^{-8} cm^2/sec. This is in the broad range of surface diffusion values obtained by other workers (29,37). Adsorption rate data for p-bromophenol with an initial concnentration of 5×10^{-4} M and a carbon dosage of 0.25 gm/l, is shown in Figure 5-12. The solid line is the predicted profile using the rate parameters estimated from the data of Figure 5-11. The experimental and predicted profiles are in good agreement, and lend validity to the model, and the estimated values for the transport coefficients.

The experimental profile for p-toluene sulfonate with an initial concentration of 10^{-4} M, and a carbon dosage of 0.33 gm/l is shown in Figure 5-13. The mass transfer coefficient is estimated to be 4.8×10^{-3} cm/sec, and the diffusion coefficient 1.7×10^{-8} cm^2/sec. The mass transfer coefficient is calculated to be 4.4×10^{-3} cm/sec using equation 5-9. This denotes a difference of 10%, and could, as discussed earlier, explain in part the discrepancies in pore diffusivity values obtained by other workers. The dotted line represents the profile obtained by assuming negligible intraparticle diffusion resistance. This profile deviates more from the experimental curve than p-bromophenol

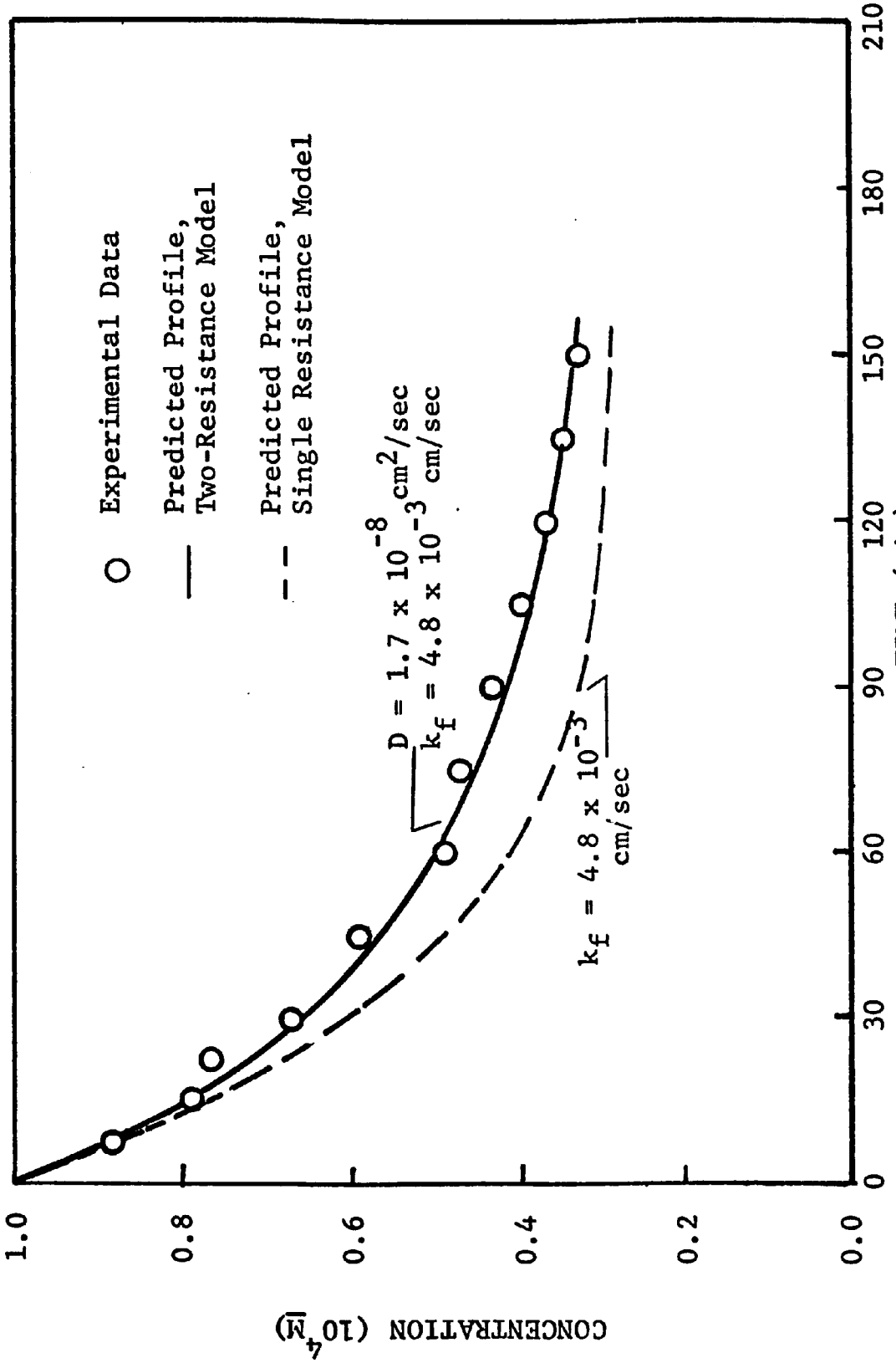


FIGURE 5-13. CONCENTRATION-TIME PROFILE: p-TOLUENE SULFONATE ($C_o=10^{-4}$M, CARBON=0.33 g/l, 650 RPM)

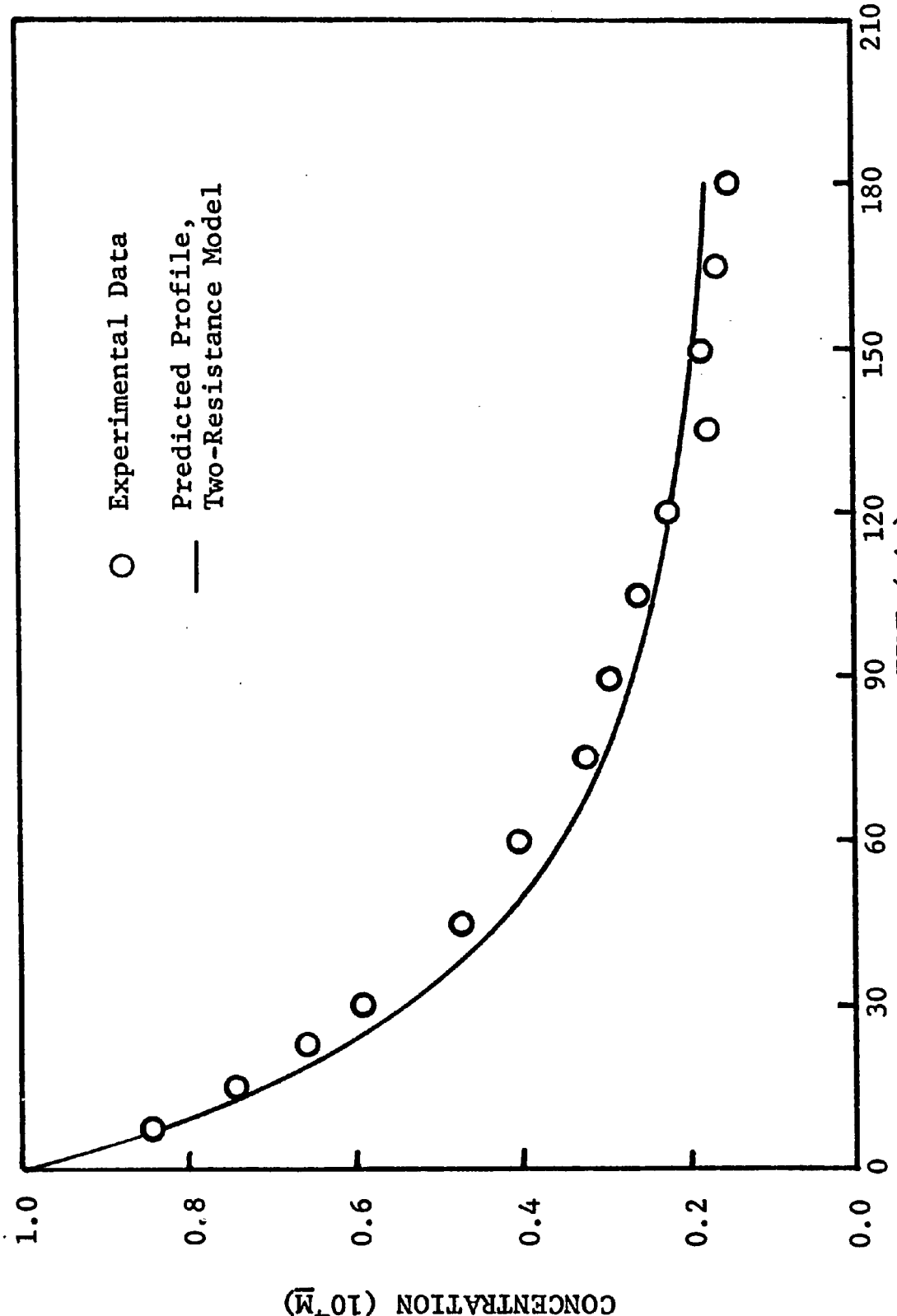


FIGURE 5-14. CONCENTRATION-TIME PROFILE: p-TOLUENE SULFONATE ($C_o=10^{-4}$M, CARBON=0.5 g/l, 650 RPM)

due to the comparatively low equilibrium solid to liquid solute distribution. The estimated coefficients are used to predict the experimental profile of Figure 5-14 for p-toluene sulfonate, with an initial concentration of 10^{-4}M, and a carbon dosage of 0.5 gm/1. Again, the experimental and predicted profiles are in good agreement.

The rate data of Figure 5-15 was used in estimating the diffusion coefficients for dodecyl benzene sulfonate. This solute has a substantially lower film transfer coefficient of 2.12×10^{-3} cm/sec due to the large size of the molecule. The surface diffusion coefficient is about fourteen times smaller than that of phenol, and is equal to 9.86×10^{-10} cm^2/sec. This would indicate that the adsorption rate for dodecyl benzene sulfonate would be film transfer controlled for a much longer initial time period than for the other solutes. This is evident from the close match obtained with a single resistance model, shown by the dotted line in Figure 5-15. However, for extended time periods, or an increased agitation power input, the simple film diffusion model will not be satisfactory, as may be seen from Figure 5-10. The rate parameters estimated from Figure 5-15 was used in predicting the profile of Figure 5-15, with an initial concentration of 10^{-4}M, and a carbon dosage of 0.33 gm/1.

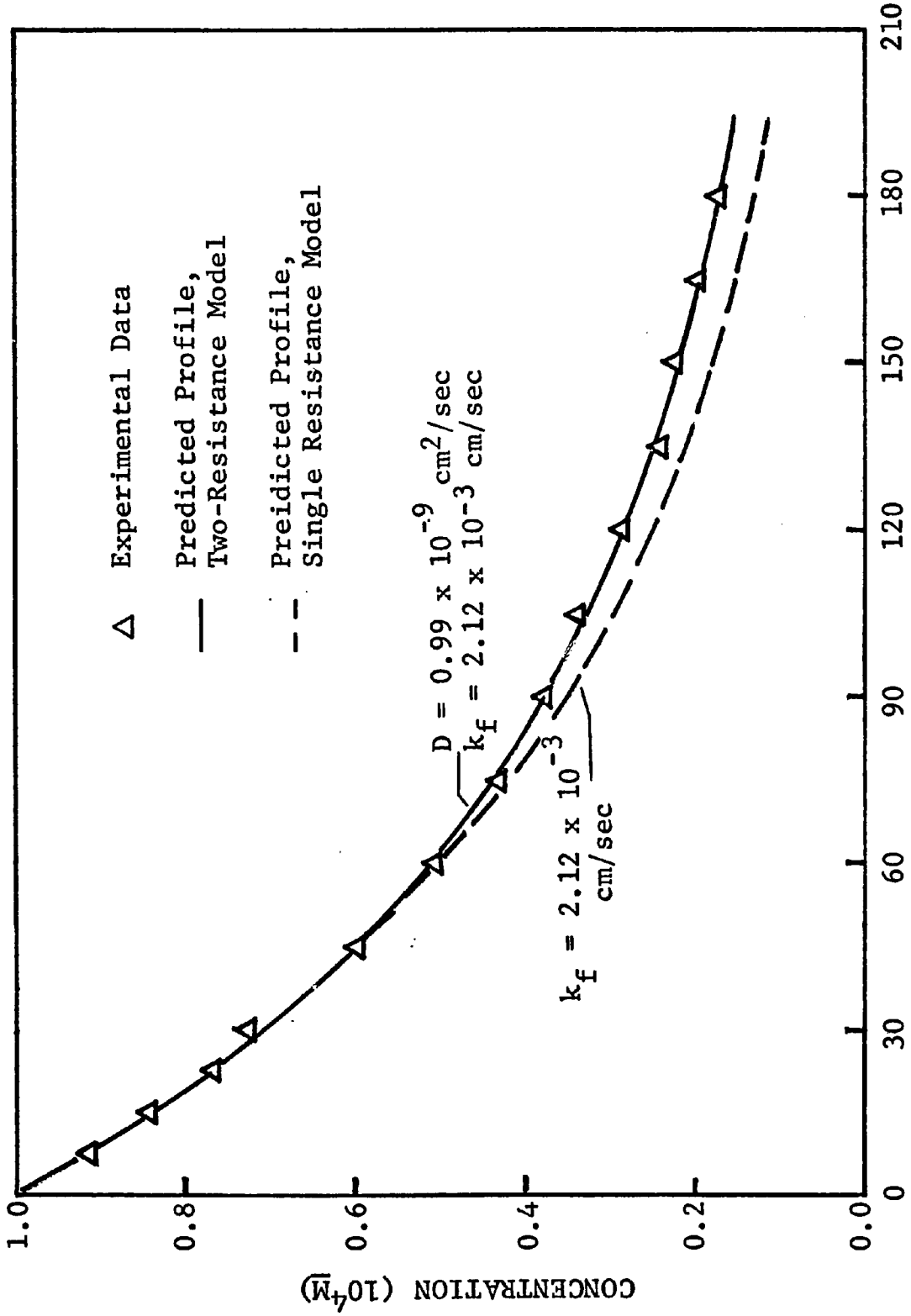


FIGURE 5-15. CONCENTRATION-TIME PROFILE: DODECYL BENZENE SULFONATE (C_o=10^{-4} M, CARBON=0.5 g/1, 650 RPM)

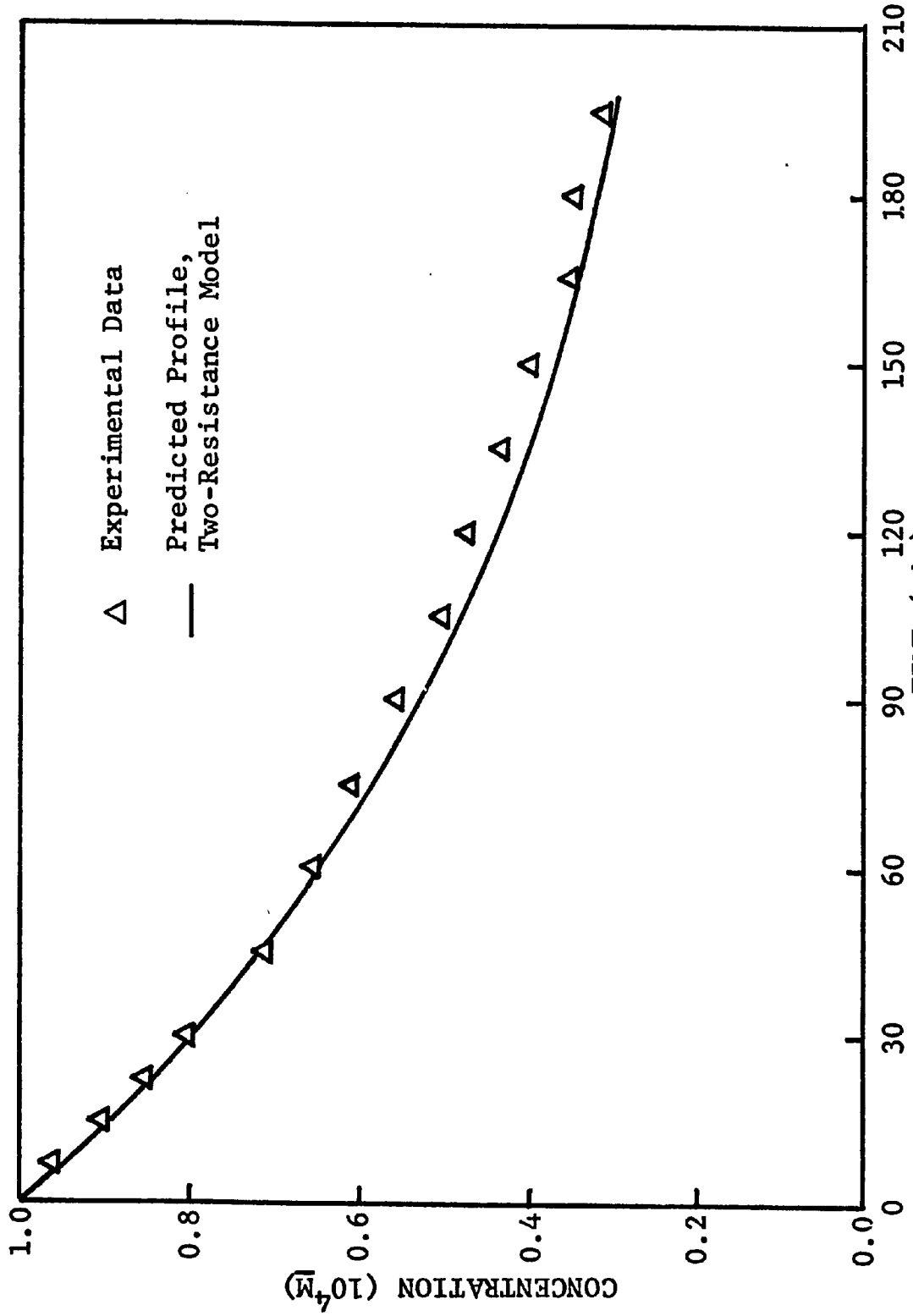


FIGURE 5-16. CONCENTRATION-TIME PROFILE: DODECYL BENZENE SULFONATE ($C_o=10^{-4}$M, CARBON=0.33 g/l, 650 RPM)

The experimental and predicted profile for phenol with an initial concnetration of 5×10^{-4} M, and a carbon dosage of 0.67 gm/l is shown in Figure 5-17. The mass transfer coefficient is estimated to be 5.1×10^{-3} cm/sec, and the surface diffusion coefficient, 1.38×10^{-8} cm^2/sec. The mass transfer coefficient is estimated from equation 5-9 to be 4.5×10^{-3} cm/sec. The predicted profile from the film resistance model is shown by the dotted lines, and shows substantial deviations from the experimental data points.

Two experimental runs were made at a higher speed of 1670 rpm. Figure 5-18 shows the experimental data for an initial concentration of 5×10^{-4} M, and a carbon dosage of 0.67 gm/l. The solid line is the predicted profile using the parameter estimation procedure. The mass transfer coefficient is estimated to be 1.13×10^{-2} cm/sec, and the surface diffusion coefficient, 1.29×10^{-8} cm^2/sec. This value is in close agreement with the value of 1.38 cm^2/sec obtained from the 650 rpm rate data. Figure 5-19 shows the experimental data, and the predicted profile, using the above values for the transport coefficients, for the rate of uptake from an initial concnetration of 5×10^{-4} M and a carbon dosage of 0.5 gm/l.

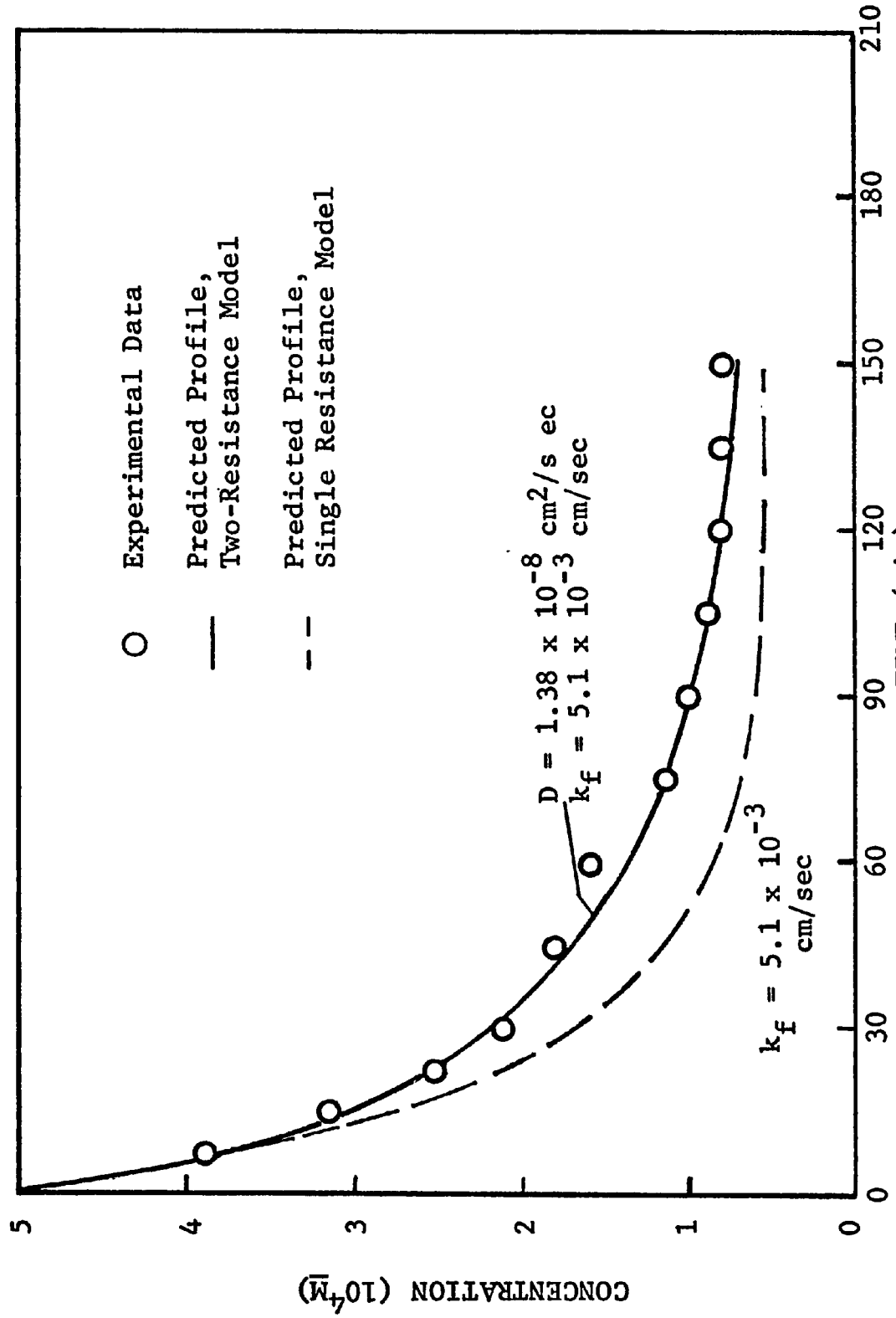


FIGURE 5-17. CONCENTRATION-TIME PROFILE: PHENOL (C_o=5 x 10^{-4} M, CARBON=0.67 g/1, 650 RPM)

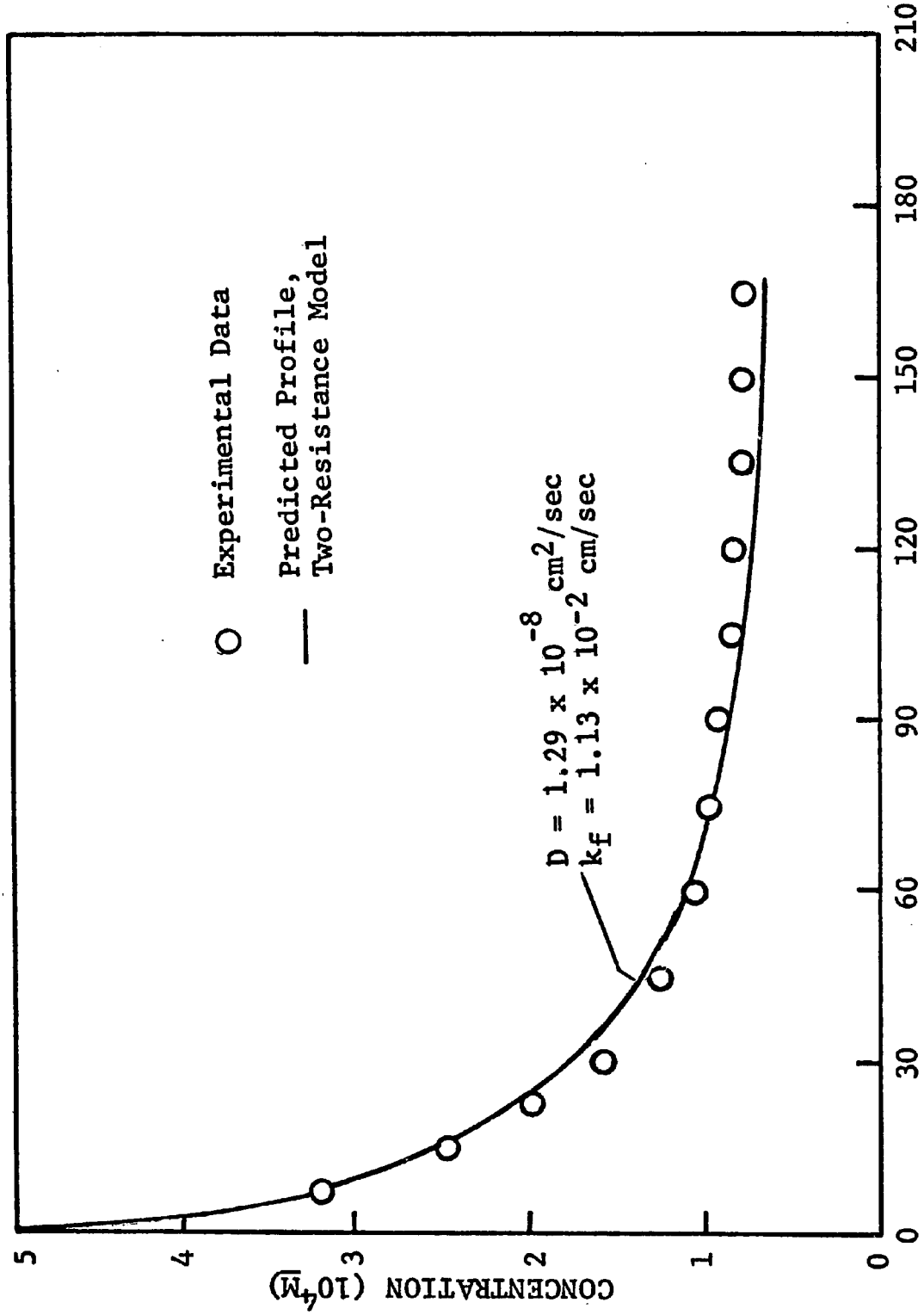


FIGURE 5-18. CONCENTRATION-TIME PROFILE: PHENOL (C_o=5 x 10^{-4}M, CARBON=0.67 g/l, 1670 RPM)

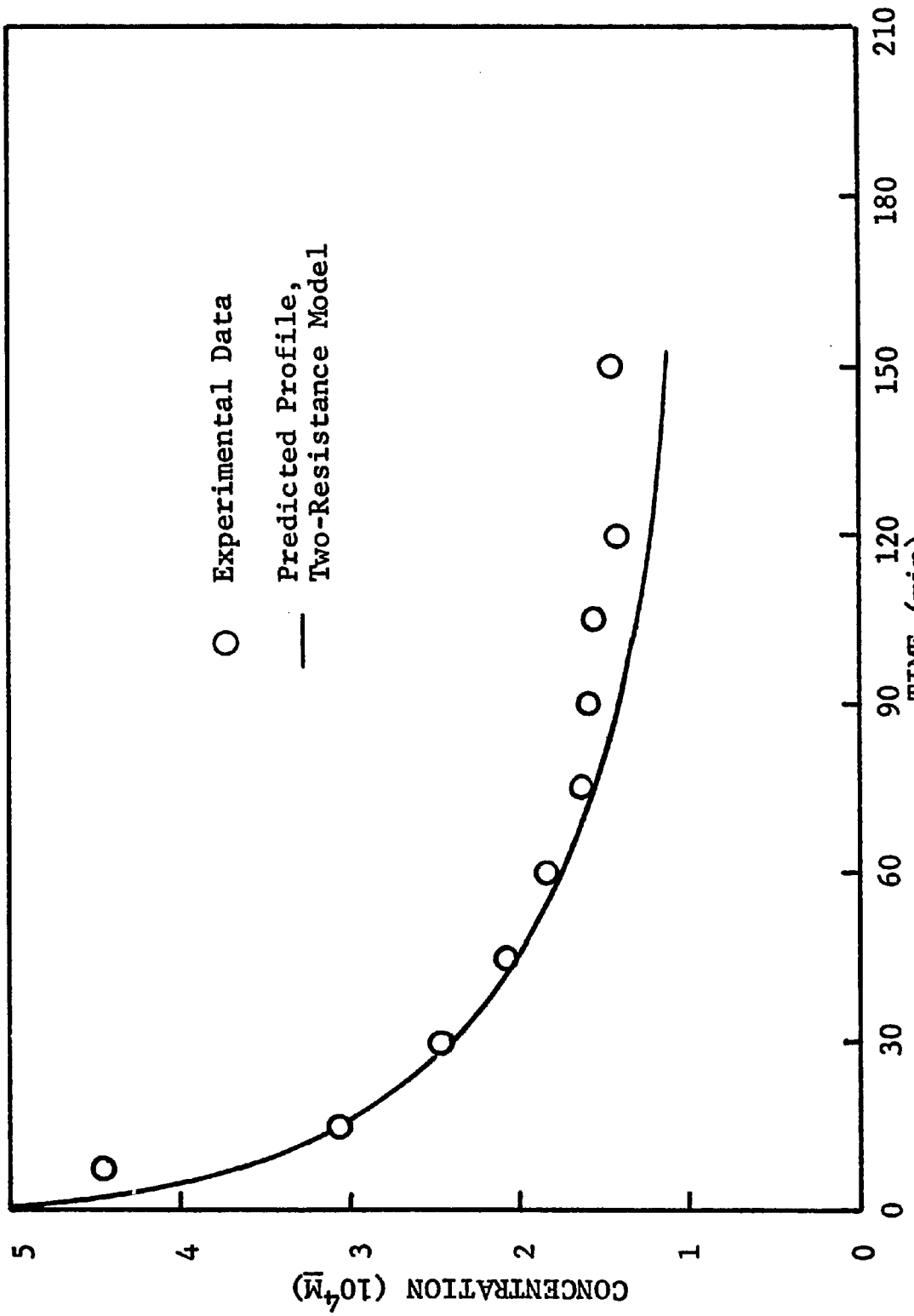


FIGURE 5-19. CONCENTRATION-TIME PROFILE: PHENOL (C_o=5 x 10^{-4}M, CARBON=0.5 g/l, 1670 rpm)

Conclusions

One of the main objectives of this investiagtion has been to develop a single solute rate model that will provide an accurate representation of the physical process. To this end, the overall rate has been represented by a nonlinear combination of the internal and external diffusion rates. The external mass transfer rate was assumed to be occurring at a linear rate, and represented by equation 2-16. This is a valid assumption, considering the small thickness of the hydrodynamic boundary layer, and the rapidity of the concentration change within the layer (40).

Hiester and Vermuelen (24), and several other investigators (35,67) have represented the internal diffusion rate by a steady state equation of the form

$$\frac{dq}{dt} = k_s a'(q_e - q) \qquad (5\text{-}10)$$

Hiester and Vermuelen subsequently suggested that a quadratic driving force, rather than a linear relation, as in equation 5-10, may better approximate the internal diffusion rate. Keinath (35) conducted "several hundred" rate experiments to correlate particle size and initial solute concentration with internal diffusion rates. For the solute dinitro-o-sec-butyl phenol, the following correlation was developed.

TABLE 5-1

MASS TRANSER* AND SURFACE DIFFUSION COEFFICIENTS

SOLUTE	k_f cm/sec	D cm^2/sec
Phenol	5.10×10^{-3}	1.38×10^{-8}
p-Bromophenol	5.40×10^{-3}	1.58×10^{-8}
p-Toluene Sulfonate	4.80×10^{-3}	1.70×10^{-8}
Dodecyl Benzene Sulfonate	2.12×10^{-3}	9.86×10^{-10}

* At 650 rpm

$$\frac{d(q)^2}{dt} = 2.08C_o/d^{1.4} \qquad (5\text{-}11)$$

Such correlations, particularly for the initial solute concentrations, are restricted to the solutes being studied. Other workers (21) have found that the internal diffusion rate is inversely proportional to $d^{1.6}$. In this study, diffusion within the particle is represented by the unsteady state equation 2-19, and obviates the necessity for correlations as discussed above.

The combined film and solid phase diffusion model was used in estimating mass transfer and diffusion coefficients from single solute rate data. The transport coefficients for the different solutes are listed in Table 5-1. The mass transfer coefficients listed, correspond to an agitation speed of 650 rpm and an agitation power input of 3.4×10^6 dyne-cm/sec (11). Film diffusion has been shown to control the transport rate in the initial time period, and internal diffusion during the latter part of the rate study. However, the extend of time over which each process controls the rate is governed by the magnitude of the transport coefficients.

CHAPTER 6

MULTICOMPONENT ADSORPTION

The diffusional processes that govern the overall adsorption rate for single solute systems have been examined in detail in Chapters 2 and 5. These considerations are extended to multicomponent systems in this chapter, and a general model is developed to predict multicomponent concentration-time profiles. The model is general in the sense that diffusion rates in both fluid and solid phases are considered, and no restrictions are made regarding adsorption equilibrium relationships. However, diffusional flows due to solute-solute interactions are assumed to be zero in both the fluid and solid phases.

MATHEMATICAL DEVELOPMENT

The multicomponent adsorption model considers the following mechanistic processes: (1) film diffusion of each species from the fluid phase to the solid phase; (2) adsorption on the surface from the solute mixture; and, (3) surface diffusion of the individual solute species into the interior of the particle. The mathematical development described below, closely parallels that discussed for single solute adsorption rate in Chapter 2.

Mass transfer of each of two solute species

is given by equations 6-1 and 6-2.

$$\frac{dq_1}{dt} = \frac{k'_f(C_1-C_{s1})}{V_p\rho(1-\varepsilon)} \tag{6-1}$$

$$\frac{dq_2}{dt} = \frac{k'_{f2}(C_2-C_{s2})}{V_p\rho(1-\varepsilon)} \tag{6-2}$$

The average concentration of each solute on the particle at any time is

$$q_1 = \frac{3}{R^3}\int_0^R q_{i1}r^2\,dr \tag{6-3}$$

$$q_2 = \frac{3}{R^3}\int_0^R q_{i2}r^2\,dr \tag{6-4}$$

Adsorption at the surface is governed by the mixture equilibrium relationship of equation 4-46, and may be written as

$$q_{s1} = \frac{a_1(C_{s1}/\eta_1)}{(1+b_1(C_{s1}/\eta_1)^{\beta_1}+b_2(C_{s2}/\eta_2)^{\beta_2})} \tag{6-5}$$

$$q_{s2} = \frac{a_2(C_{s2}/\eta_2)}{(1+b_1(C_{s1}/\eta_1)^{\beta_1}+b_2(C_{s2}/\eta_2)^{\beta_2})} \tag{6-6}$$

Diffusion to the interior of the particle is represented by the unsteady-state equations 6-7 and 6-8 for each solute.

$$\frac{\delta q_{i1}}{\delta t} = D_1\left(\frac{\delta^2 q_{i1}}{\delta r^2} + \frac{2}{r}\frac{\delta q_{i1}}{\delta r}\right) \tag{6-7}$$

$$\frac{\delta q_{i2}}{\delta t} = D_2\left(\frac{\delta^2 q_{i2}}{\delta r^2} + \frac{2}{r}\frac{\delta q_{i2}}{\delta r}\right) \tag{6-8}$$

The continuous mixed batch reactor material balance equations for each species are

$$V\frac{dC_1}{dt} = -W\frac{dq_1}{dt} \tag{6-9}$$

$$V\frac{dC_2}{dt} = -W\frac{dq_2}{dt} \tag{6-10}$$

At time t=0, the concentration of the solutes in the fluid phases are C_{1o} and C_{2o}, and the solid phase concentrations are equal to zero. Thus the initial conditions are

$$\begin{aligned} C_1(0) &= C_{10} \\ C_2(0) &= C_{20} \end{aligned} \tag{6-11}$$

$$\begin{aligned} q_{i1}(r,0) &= 0 \\ q_{i2}(r,0) &= 0 \end{aligned} \tag{6-12}$$

The boundary conditions are

$$\begin{aligned} q_{i1}(R,t) &= q_{s1}(t) \\ q_{i2}(R,t) &= q_{s2}(t) \end{aligned} \tag{6-13}$$

$$\frac{\delta q_{i1}(0,t)}{\delta t} = 0 = \frac{\delta q_{i2}(0,t)}{\delta t} \qquad (6\text{-}14)$$

By using the change of variables $\tau = D_1 t/R^2$, $x = r/R$, $u_1 = q_1 x$, and $u_2 = q_2 x$, and the relations 2-33 and 2-34, the equations 6-1 to 6-4, 6-7, 6-8, and 6-11 to 6-14 can be reduced to the following set for each component.

Component 1:

$$\frac{\delta u_1}{\delta \tau} = \frac{\delta^2 u_1}{\delta x^2} \qquad (6\text{-}15)$$

$$u_1(0,\tau) = 0$$
$$u_1(x,0) = 0 \qquad (6\text{-}16)$$

$$q_1 = 3 \int_0^1 u_1 x \, dx \qquad (6\text{-}17)$$

$$\int_0^1 \frac{\delta u_1}{\delta \tau} x \, dx = \frac{k_{f1} R}{1000\rho(1-\varepsilon)D_1} (C_1 - C_{s1}) \qquad (6\text{-}18)$$

Component 2:

$$\frac{\delta u_2}{\delta \tau} = \bar{\nu} \frac{\delta^2 u_2}{\delta x^2} \qquad (6\text{-}19)$$

where, $\bar{\nu} = D_2/D_1$

$$u_2(0,\tau) = 0$$
$$u_2(x,0) = 0 \qquad (6\text{-}20)$$

$$q_2 = 3\int_0^1 u_2 x\, dx \qquad (6\text{-}21)$$

$$\int_0^1 \frac{\delta u_2}{\delta \tau} x\, dx = \frac{k_{f2}R}{1000\rho(1-\varepsilon)D_1}(C_2 - C_{s2}) \qquad (6\text{-}22)$$

The equations 6-15 to 6-22 and 6-9 and 6-10, coupled with the equilibrium relations 6-5 and 6-6 can be solved numerically to predict the adsorption rate profile for each solute.

Numerical Procedure

As in the single solute rate model, the solid phase equations 6-15 and 6-20 are approximated using the Crank-Nicholson method. The procedure is similar to the development for single solute adsorption equations detailed in Appendix A. The resulting expressions for each solute are given by equations 6-23 and 6-24.

$$-\lambda u_{1_{j+1}}^{n+1} + (1+2\lambda)u_{1_j}^{n+1} - \lambda u_{1_{j-1}}^{n+1} =$$
$$\lambda u_{1_{j+1}}^{n} + (1-2\lambda)u_{1_j}^{n} + \lambda u_{1_{j-1}}^{n}, \qquad \begin{matrix} j = 1,M \\ n = 1,N \end{matrix} \qquad (6\text{-}23)$$

$$-\nu' u_{2_{j+1}}^{n+1} + (1+2\nu') u_{2_j}^{n+1} - \nu' u_{2_{j-1}}^{n+1} =$$

$$\nu' u_{2_{j+1}}^{n} + (1-2\nu') u_{2_j}^{n} + \nu' u_{2_{j-1}}^{n} \quad , \quad \begin{matrix} j = 1,M \\ n = 1,N \end{matrix} \tag{6-24}$$

where, $\nu' = \lambda\bar{\nu}$

The integrals in equations 6-17 and 6-18, and 6-21 and 6-22 are evaluated using the Trapezoidal rule. Equations 6-17 and 6-18 are then transformed to 6-25 and 6-26.

$$q_1 = 3(\Delta x)^2 \left(\sum_{j=2}^{M} u_{1_j} \, (j-1) + u_{1_{M+1}} \, \frac{M}{2} \right) \tag{6-25}$$

$$u_{1_{M+1}}^{n+1} + \frac{2}{M} \sum_{j=2}^{M} u_{1_j}^{n+1} \, (j-1) = \frac{(4\lambda/M) k_{f1} R}{1000\rho(1-\varepsilon) D_1} (C_1 - C_{s1}) + \frac{2}{M} \sum_{j=2}^{M} u_{1_j}^{n} \, (j-1) + u_{1_{M+1}}^{n} \tag{6-26}$$

The corresponding equations for solute 2 are,

$$q_2 = 3(\Delta x)^2 \left(\sum_{j=2}^{M} u_{2_j} \, (j-1) + u_{2_{M+1}} \, \frac{M}{2} \right) \tag{6-27}$$

$$u_{2_{M+1}}^{n+1} + \frac{2}{M}\sum_{j=2}^{M} u_{2_j}^{n+1}(j-1) = \frac{(4\lambda/M)k_{f2}R}{1000\rho(1-\varepsilon)D_1}(C_2-C_{s2}) + \frac{2}{M}\sum_{j=2}^{M} u_{2_j}^{n}(j-1) + u_{2_{M+1}}^{n} \tag{6-28}$$

The initial and boundary conditions for each solute are

$$u_{1_1}^{n} = 0 = u_{1_j}^{1} \tag{6-29}$$

$$u_{2_1}^{n} = 0 = u_{2_j}^{1} \tag{6-30}$$

The finite difference equations for the fluid phase equations 6-9 and 6-10 are given by equations 6-31 and 6-32.

$$C_1^{n+1} = C_1^{n} - \frac{W}{V}(q_1^{n+1} - q_1^{n}) \tag{6-31}$$

$$C_2^{n+1} = C_2^{n} - \frac{W}{V}(q_2^{n+1} - q_2^{n}) \tag{6-32}$$

The equilibrium surface concentrations q_{s1} and q_{s2} are given by equations 6-5 and 6-6. To obtain the equilibrium concentrations C_{s1} and C_{s2} in the fluid phase, 6-5 and 6-6 must be solved. The Newton-Raphson iterative procedure was used for this purpose, and is developed in Appendix B.

The equations 6-23 to 6-32 and 6-5 and 6-6 provide the basis for predicting multicomponent adsorption rate profiles. The input parameters required are the mass transfer and diffusion coefficients for each solute,

the single solute isotherm constants, and the mixture equilibria correlation coefficients. These have been developed in Chapters 4 and 5.

Given the initial conditions, the equation 6-5 and 6-6 are solved first to obtain the equilibrium fluid phase concentrations for each solute at the surface. The vectors on the right hand side in equations 6-23 and 6-28 for solute 1, and equations 6-24 and 6-30 for solute 2, are then computed and the linear system of equations solved to obtain the concentration distribution of each solute in the particle. The concentrations are averaged over the particle using equations 6-27 and 6-29. The fluid phase concentrations at the end of the time step are obtained from equations 6-31 and 6-32. The procedure is repeated for successive time steps to obtain the concentration-time profile for each solute.

A general computer program for a three component system was developed using the above concepts, and is attached in Appendix C. The program consists of a main section with the finite difference approximations to the rate equations, and a subroutine to compute the equilibrium concentrations from equations 6-5 and 6-6. The Newton-Raphson procedure used requires initial estimates for C_{s1} and C_{s2} at each time step. The values of the equilibrium

concentrations at the previous time step was used as the initial guess in the program. The program was made interactive to counter the possibility that the Newton-Raphson iterations may diverge. However, for moderate values of k_f, no difficulties were encountered with a time step of one minute.

EXPERIMENTAL RESULTS

The capability of the model to predict adsorption rates was examined for the three solute mixture systems and the initial concentrations listed in Table 3-3. The solutes exhibit a wide range of adsorption behavior, and allow testing of the ability of the model to predict adsorption rates when: (1) the solute species have comparable single solute equilibrium and rate characteristics; (2) comparable diffusion rates, but differing equilibrium characteristics; and, (3) differing diffusion rates and equilibria.

The input parameters required for model prediction are the single-solute film transfer and surface diffusion coefficients, the single-solute isotherm constants, and the mixture equilibria correlation coefficients. The rate parameters were obtained in Chapter 5 from single solute rate data, and the equilibrium parameters were obtained in Chapter 4 from single and multi-solute equilibrium data. These are listed in Tables 5-1 and 4-1.

The experimental reactors and procedure described for single solutes in Chapter 5 were used in generating mixture rate data. All the experiments were carried out at 650 rpm, with three liters of solution buffered at a pH of 7. The analytical procedure for multicomponent systems has been described in Chapter 3.

Phenol - p-Toluene Sulfonate Mixtures

The experimental data for adsorption rates of phenol and p-toluene sulfonate from an equimolar mixture of concentration 10^{-4} M are shown in Figure 6-1. The carbon dosage used is 0.67 gm/1. The solid and dotted lines are the model predictions for phenol and p-toluene sulfonate, respectively. The experimental and predicted profiles are in excellent agreement. The total mixture concentration in the liquid phase is plotted in Figure 6-2, and shows good agreement with the predicted curve. Initial concentrations of 5×10^{-5} M for each solute were used in the second rate study, with a carbon dosage of 0.33 gm/1. The data for this run are shown in Figures 6-3 and 6-4. The predicted component profiles, and the total concentration profiles closely match the experimental data. The results from the rate study with differing starting concentrations, 5×10^{-5} M for phenol and 2.5×10^{-5} M for p-toluene suflonate are shown in Figures 6-5 and 6-6. The predicted profiles

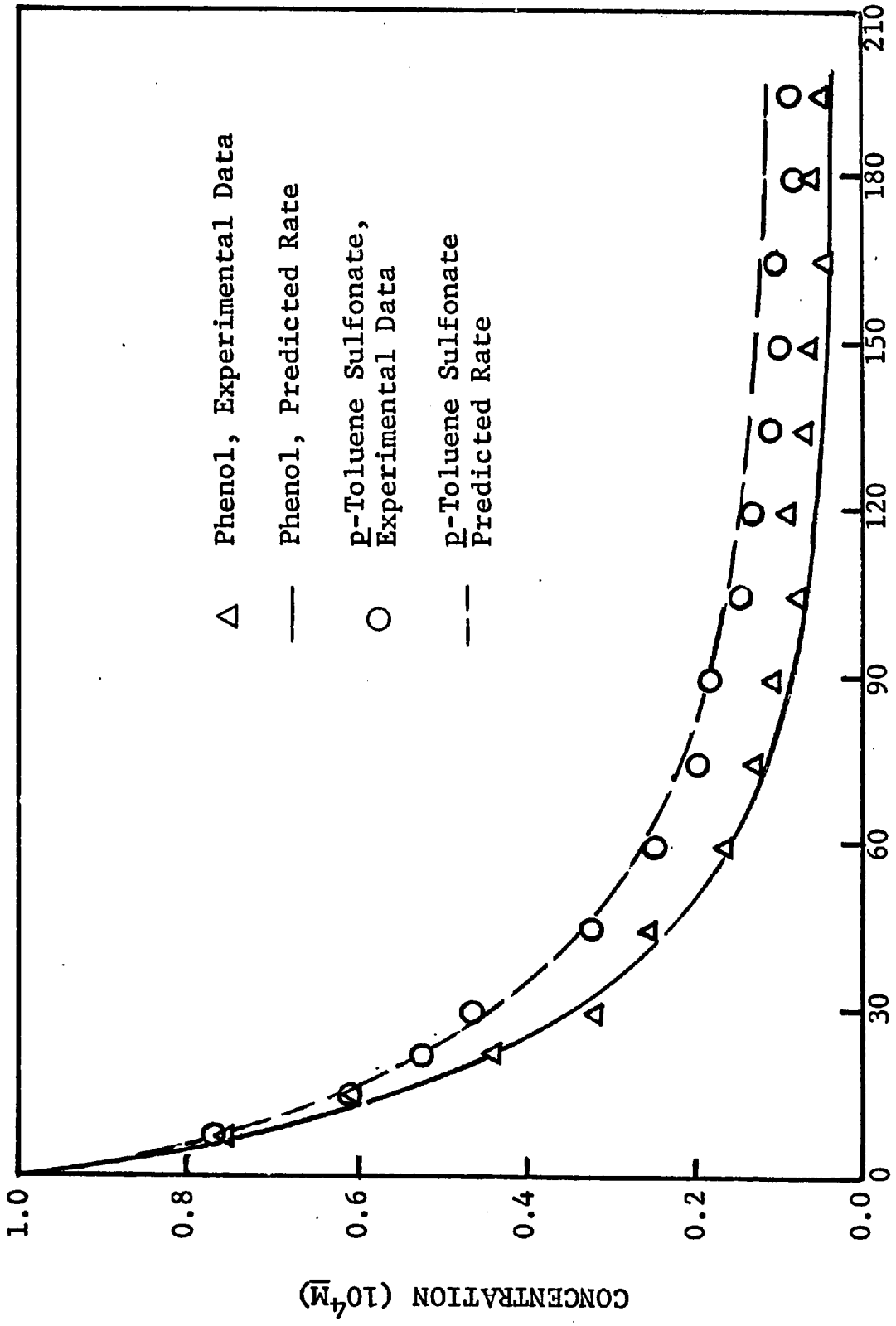


FIGURE 6-1. RATES OF ADSORPTION FROM MIXTURES: PHENOL-p-TOLUENE SULFONATE ($C_{10}=C_{20}=10^{-4}$M, CARBON=0.67 g/l, 650 RPM)

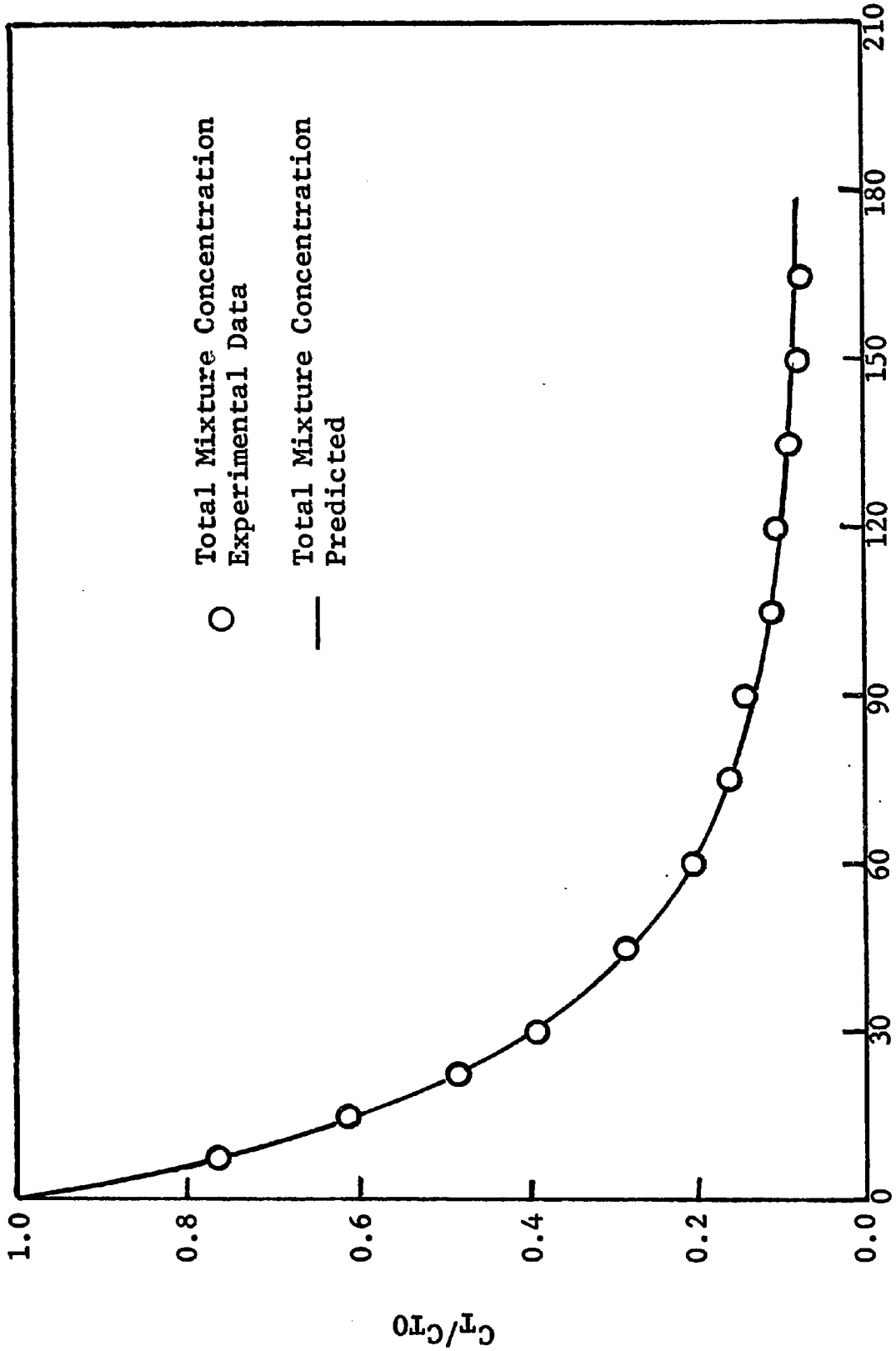


FIGURE 6-2. TOTAL CONCENTRATION PROFILE: PHENOL-p-TOLUENE SULFONATE ($C_{10}=C_{20}=10^{-4}$M, CARBON=0.67 g/l, 650 RPM)

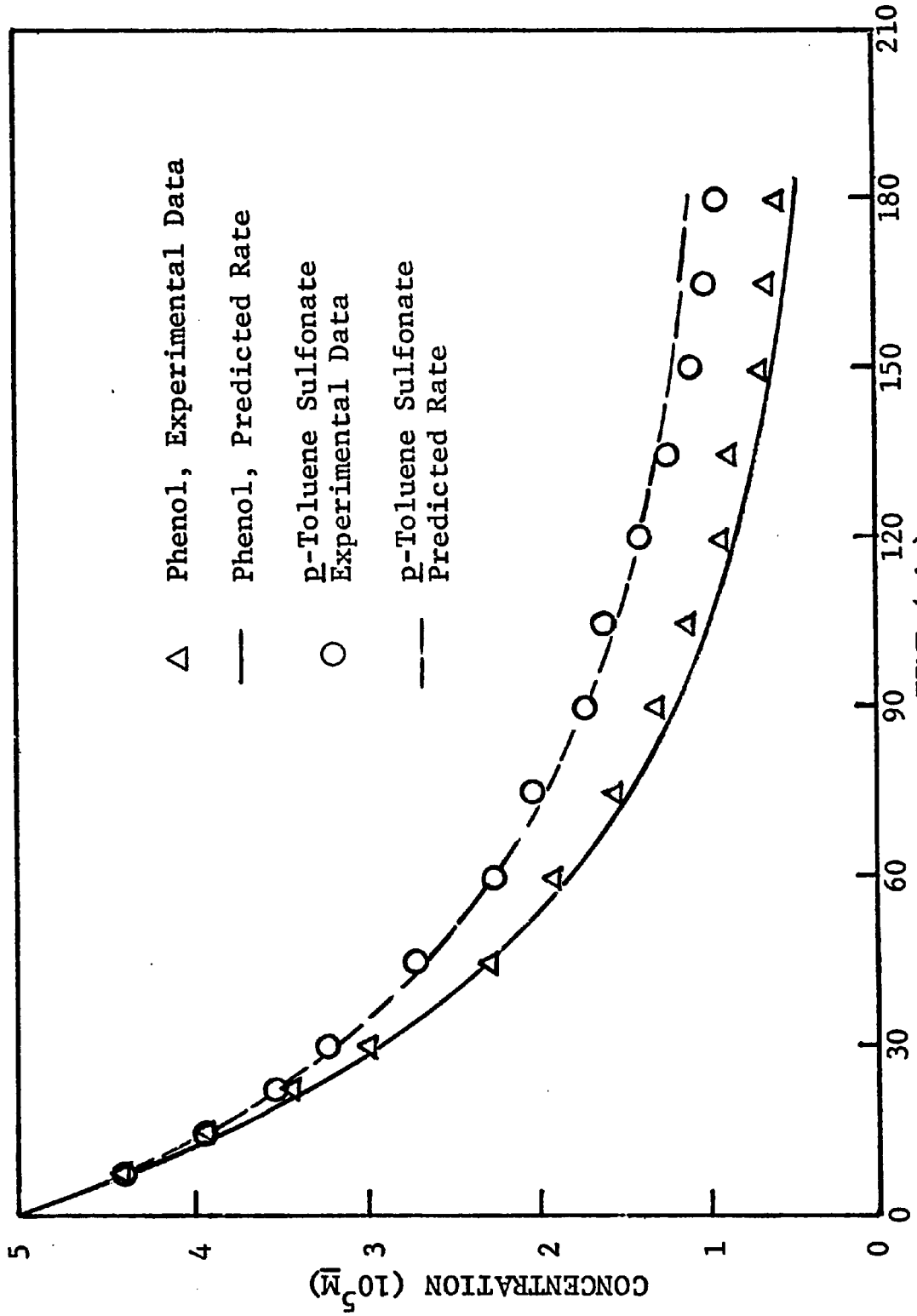


FIGURE 6-3. RATES OF ADSORPTION FROM MIXTURES: PHENOL-p-TOLUENE SULFONATE ($C_{10}=C_{20}=5 \times 10^{-5}$M, CARBON=0.33 g/1, 650 RPM)

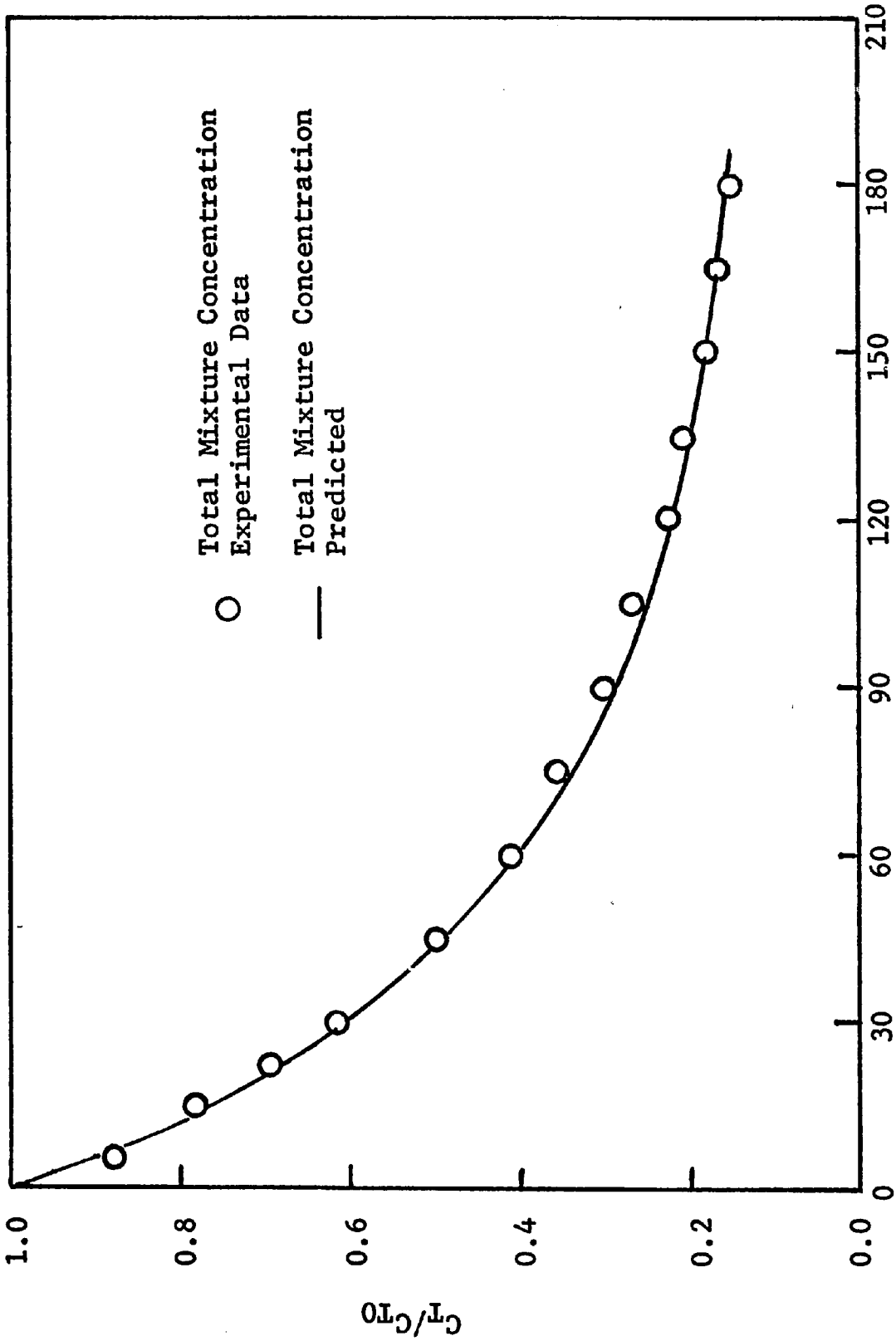


FIGURE 6-4. TOTAL CONCENTRATION PROFILE: PHENOL-p-TOLUENE SULFONATE ($C_{10}=C_{20}=5 \times 10^{-5}$ M, CARBON=0.67 g/1, 650 RPM)

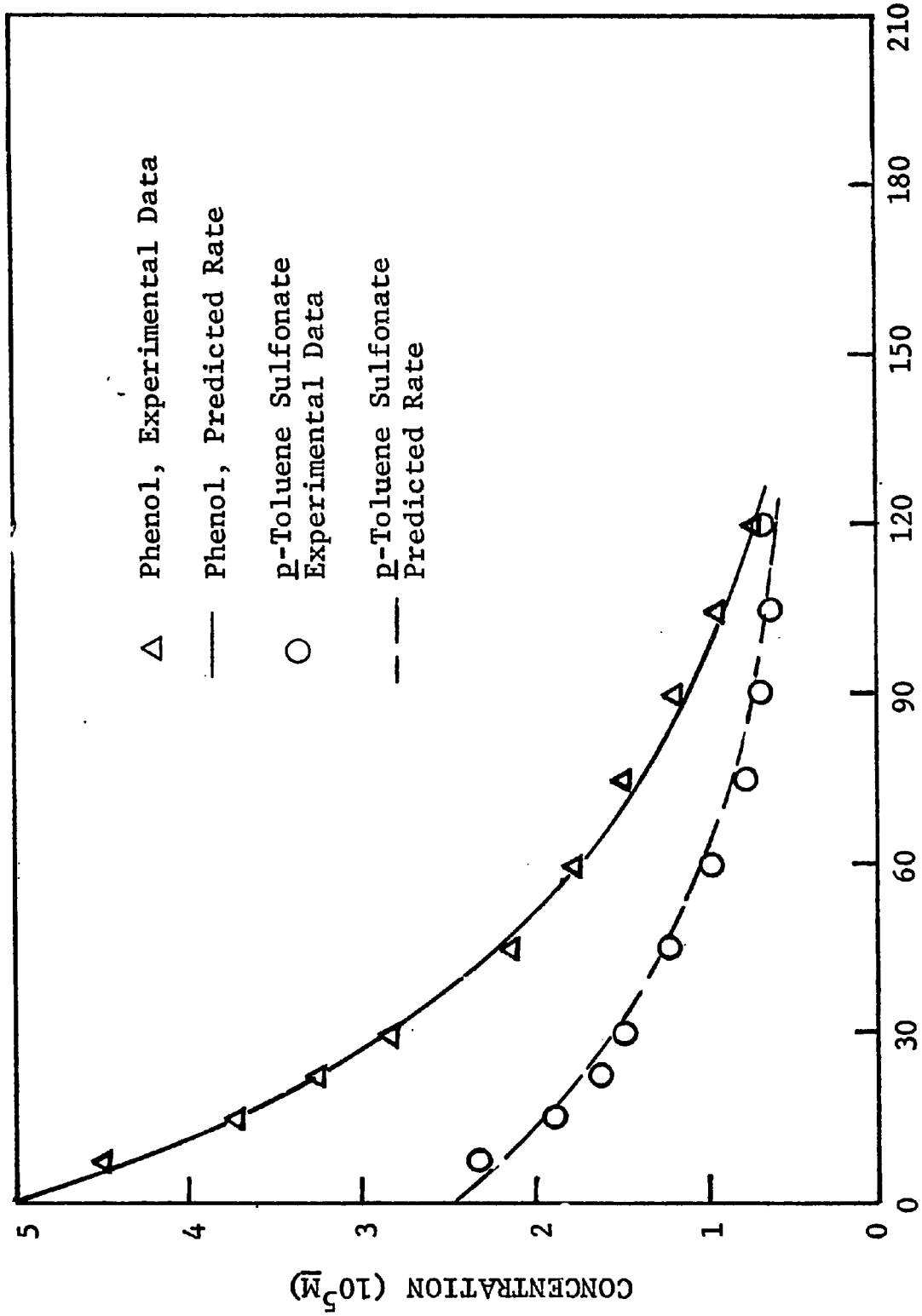


FIGURE 6-5. RATES OF ADSORPTION FROM MIXTURES: PHENOL-p-TOLUENE SULFONATE (C_{1O}=5 x 10^{-5}M, C_{2O}=2.5 x 10^{-5}M, CARBON=0.33 g/1, 650 RPM)

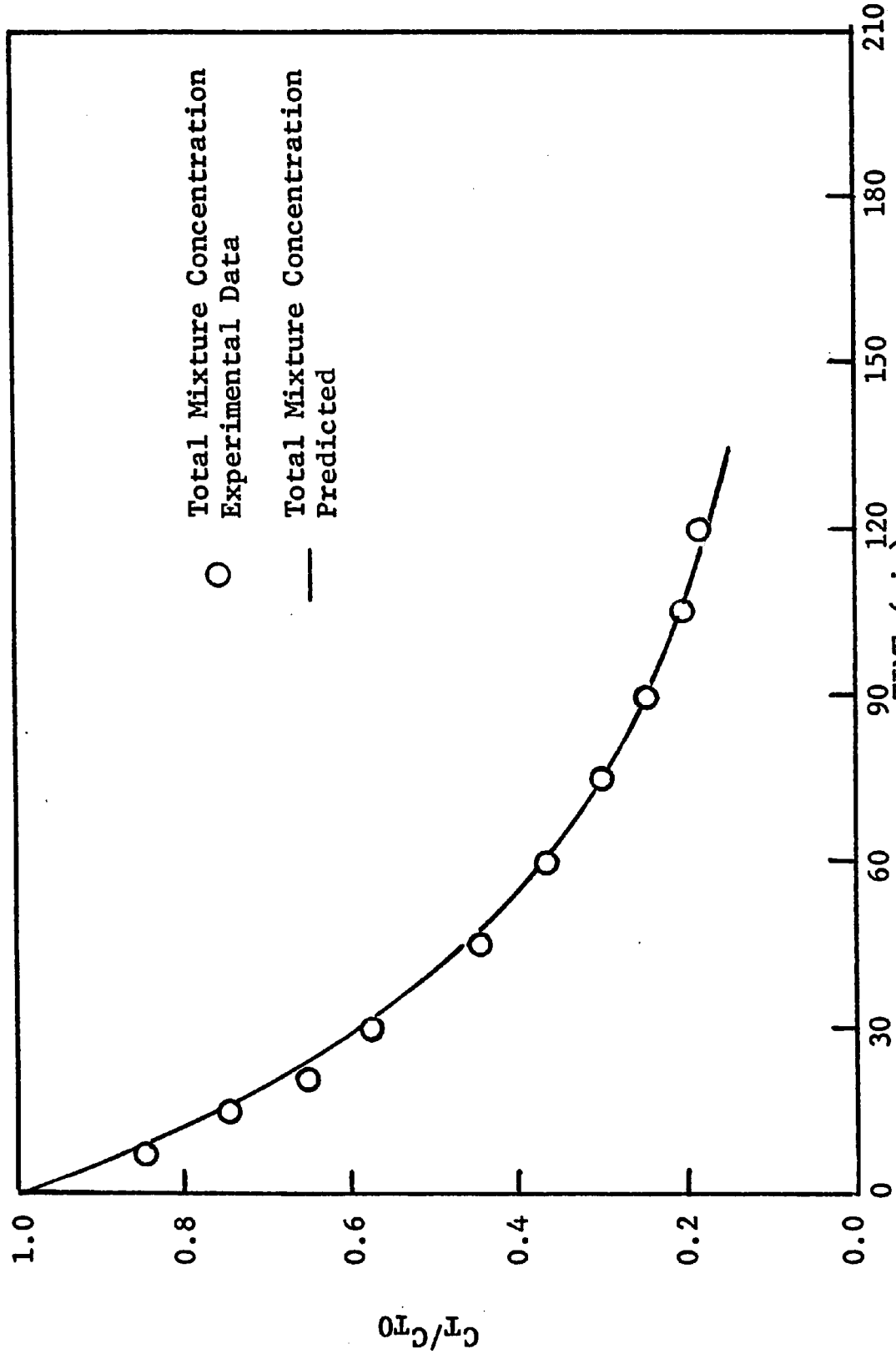


FIGURE 6-6. TOTAL CONCENTRATION PROFILE: PHENOL-p-TOLUENE SULFONATE (C_{10}=5 x 10^{-5}M, C_{20}=2.5 x 10^{-5}M, CARBON=0.33 g/l)

are in excellent agreement with the experimental curves.

Thus, for solutes with comparable rate and equilibrium characteristics, the model predictions are in excellent agreement with the experimental data. The results with different initial solute concentrations are particularly significant when compared with the reaction rate model. In the reaction rate model, the internal diffusion rate is assumed to be linear, and consequently, for cases where internal diffusion rate is rate limiting, it is necessary to correlate diffusion rates with the particle diameter and the initial solute concentrations. The extension of such a model to multicomponent systems will result in considerable difficulties in evaluating internal diffusion rates, and may be satisfactory only for the case of film-diffusion controlled adsorption.

Phenol - p-Bromophenol Mixtures

The experimental and predicted profiles for the adsorption rates of phenol and p-bromophenol from an equimolar mixture of concentration 5×10^{-4} M are shown in Figure 6-7. The predicted profile for p-bromophenol is in excellent agreement with the experimental data. However, for phenol there is some deviation after the initial time period. The experimental adsorption rate for phenol appears to be faster than predicted for about 60 minutes after the

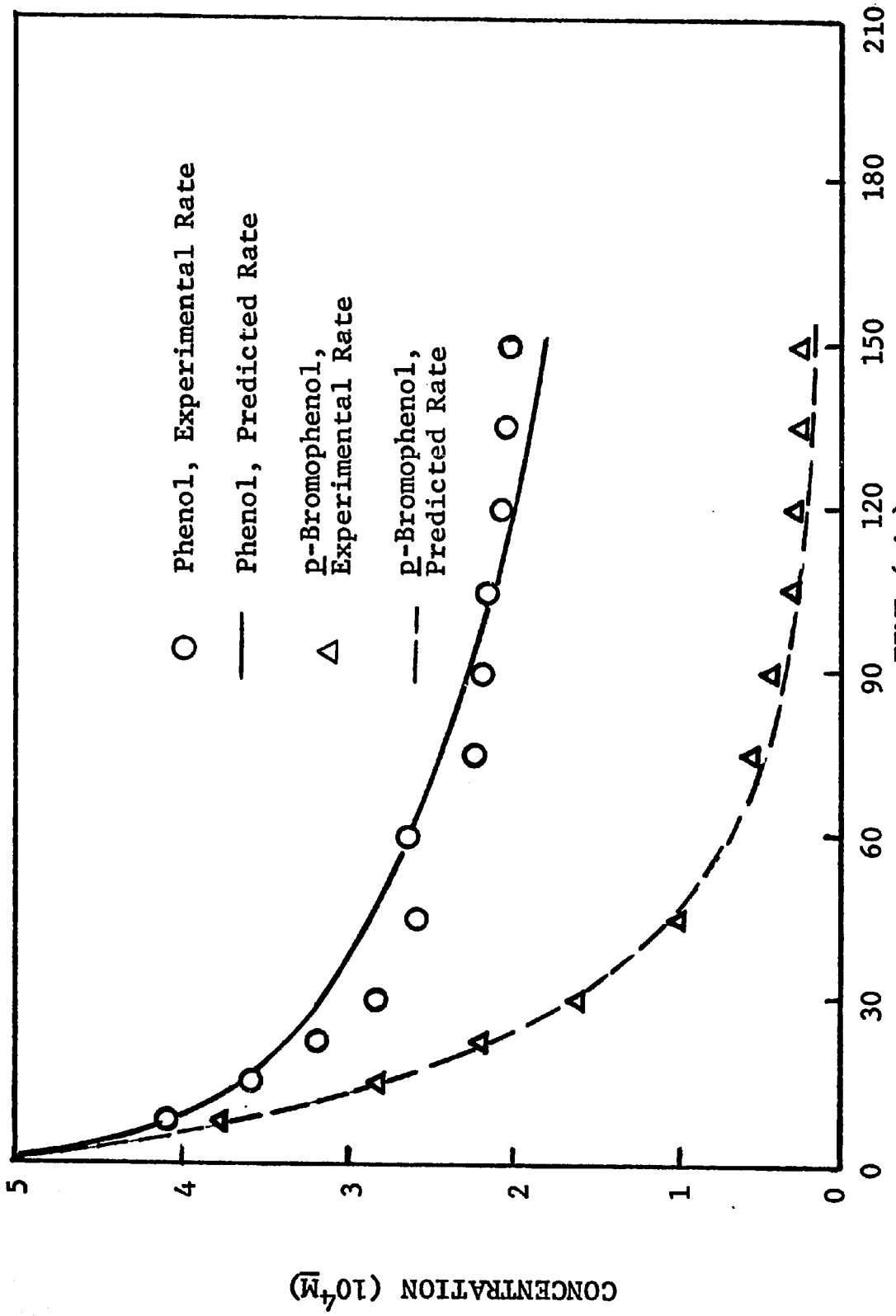


FIGURE 6-7. RATES OF ADSORPTION FROM MIXTURES: PHENOL-p-BROMOPHENOL ($C_{10}=C_{20}=5 \times 10^{-4}$M, CARBON=0.67 g/1, 650 RPM)

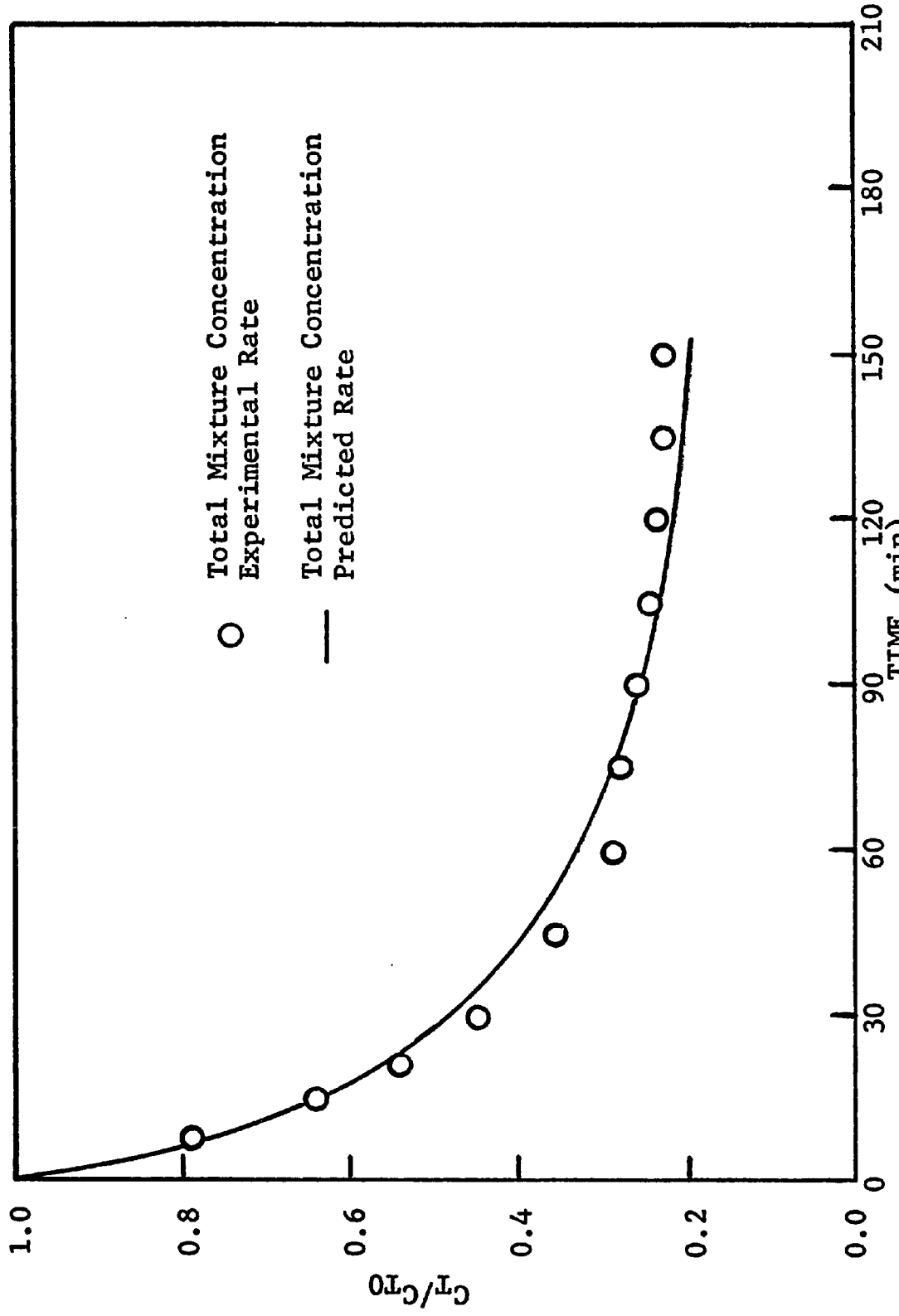


FIGURE 6-8. TOTAL CONCENTRATION PROFILE: PHENOL-p-BROMOPHENOL
($C_{10}=C_{20}=5 \times 10^{-4}$ M, CARBON=0.67 g/l, 650 RPM)

first 15 minutes. Thereafter, the rate is slightly slower than predicted. From an examination of the binary equilibrium data, this deviation may be attributed to the inadequate correlation of the mixture equilibrium data in this region. The correlation predicts lower than actual equilibrium concentrations for phenol, for the rate concentrations in the 15 - 60 minute period, and somewhat slightly higher values for the solute concentrations in the time period beyond the first 60 minutes. For p-Bromophenol, equilibrium adsorption from the solute mixture is predicted well by the correlation as may be seen from Figure 4-9. This is reflected in the good fit between the experimental and rate profiles in Figure 6-7.

The profile for the total concentration is shown in Figure 6-8. The fit between the experimental and predicted profiles is generally good. However, as may be expected from the component profiles, there is some deviation in the time period 15 - 60 minutes.

Figures 6-9 and 6-10 show the component and total concentration profiles for the adsorption rates from a solution 5×10^{-4} M in each solute, with a carbon dosage of 0.5 gm/l. As for the previous system, the predicted curve for p-bromophenol closely matches the experimental curve.

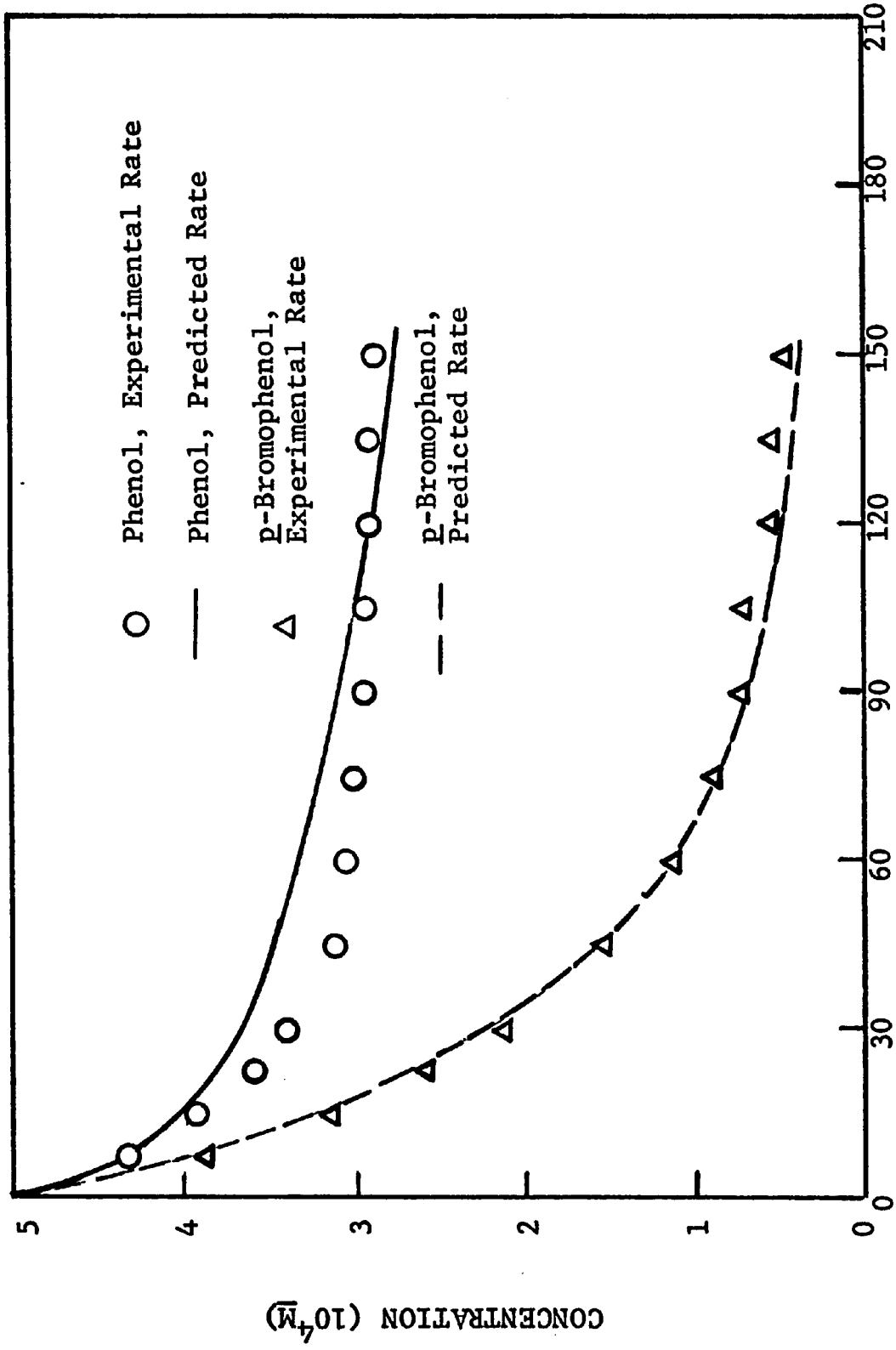


FIGURE 6-9. RATES OF ADSORPTION FROM MIXTURES: PHENOL-p-BROMOPHENOL ($C_{10}=C_{20}=5 \times 10^{-4}$M, CARBON=0.5 g/l, 650 RPM)

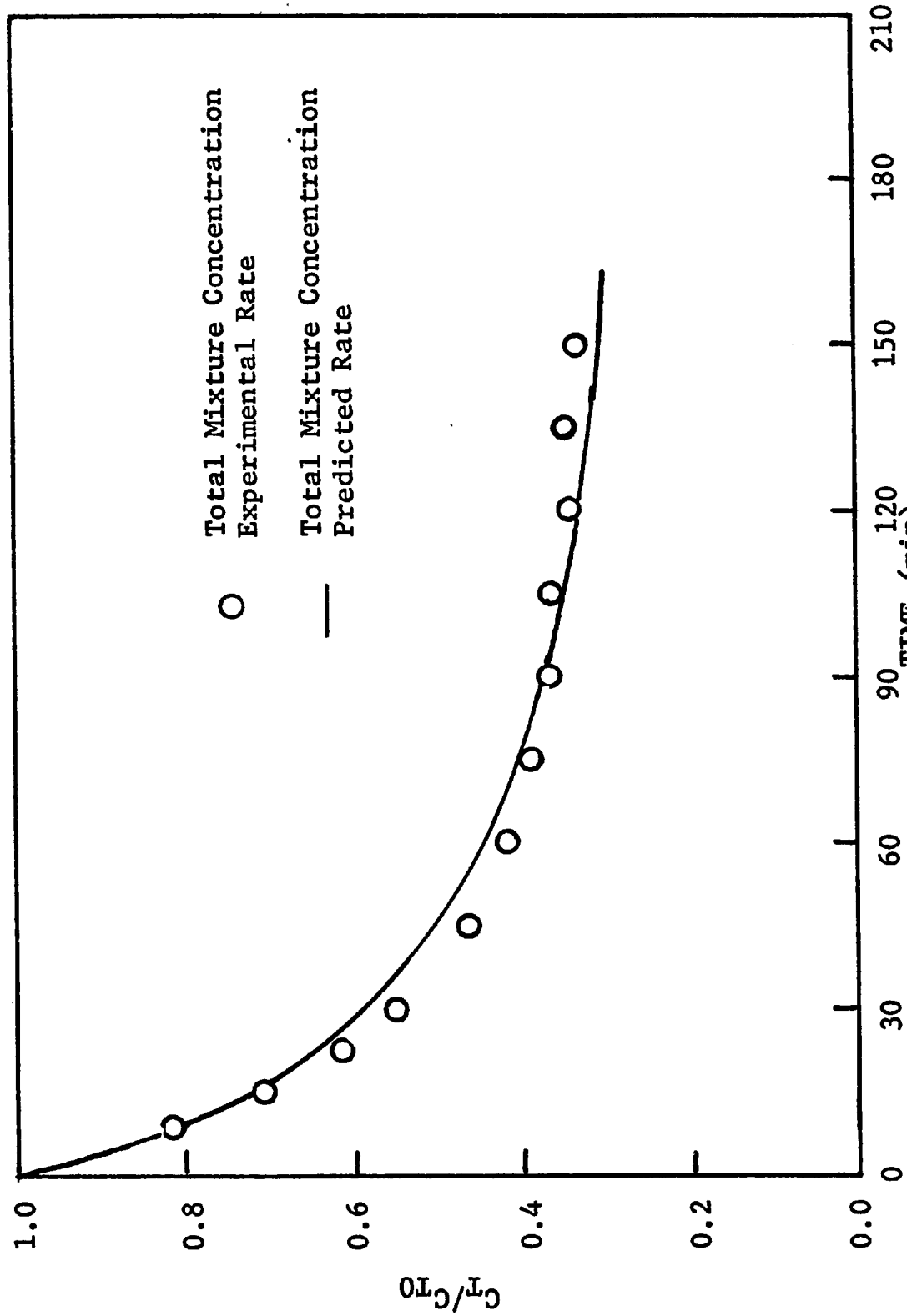


FIGURE 6-10. TOTAL CONCENTRATION PROFILE: PHENOL-p-BROMOPHENOL ($C_{10}=C_{20}=5 \times 10^{-4}$M, CARBON=0.5 g/l, 650 RPM)

For phenol, the predicted curve is slightly higher than the actual in the middle segment of the curve for reasons discussed above. Initial concentrations of 2.5×10^{-4}M for phenol, and 5×10^{-4}M for p-bromophenol were used in another rate study, the data from which are shown in Figures 6-11 and 6-12. The experimental and predicted curves are in fair agreement.

It is noteworthy that in all experiments, the single solute mass transfer coefficients predict the initial mixture rates satisfactorily. For p-bromophenol, the predicted profiles match the experimental data through the entire length of the rate study. Phenol and p-bromophenol have comparable diffusion rates, but different equilibrium characteristics. The equilibrium amount of p-bromophenol adsorbed from a mixture of these solutes is much larger than phenol, and has been satisfactorily correlated by the mixture equilibria correlation in Chapter 4. However, for phenol, the correlation is not completely satisfactory, and the impact of this is apparent in the rate profiles for phenol. The inability of the correlation program to represent data satisfactorily is in part due to the large equilibrium concentration ratios involved in the phenol-p-bromophenol system.

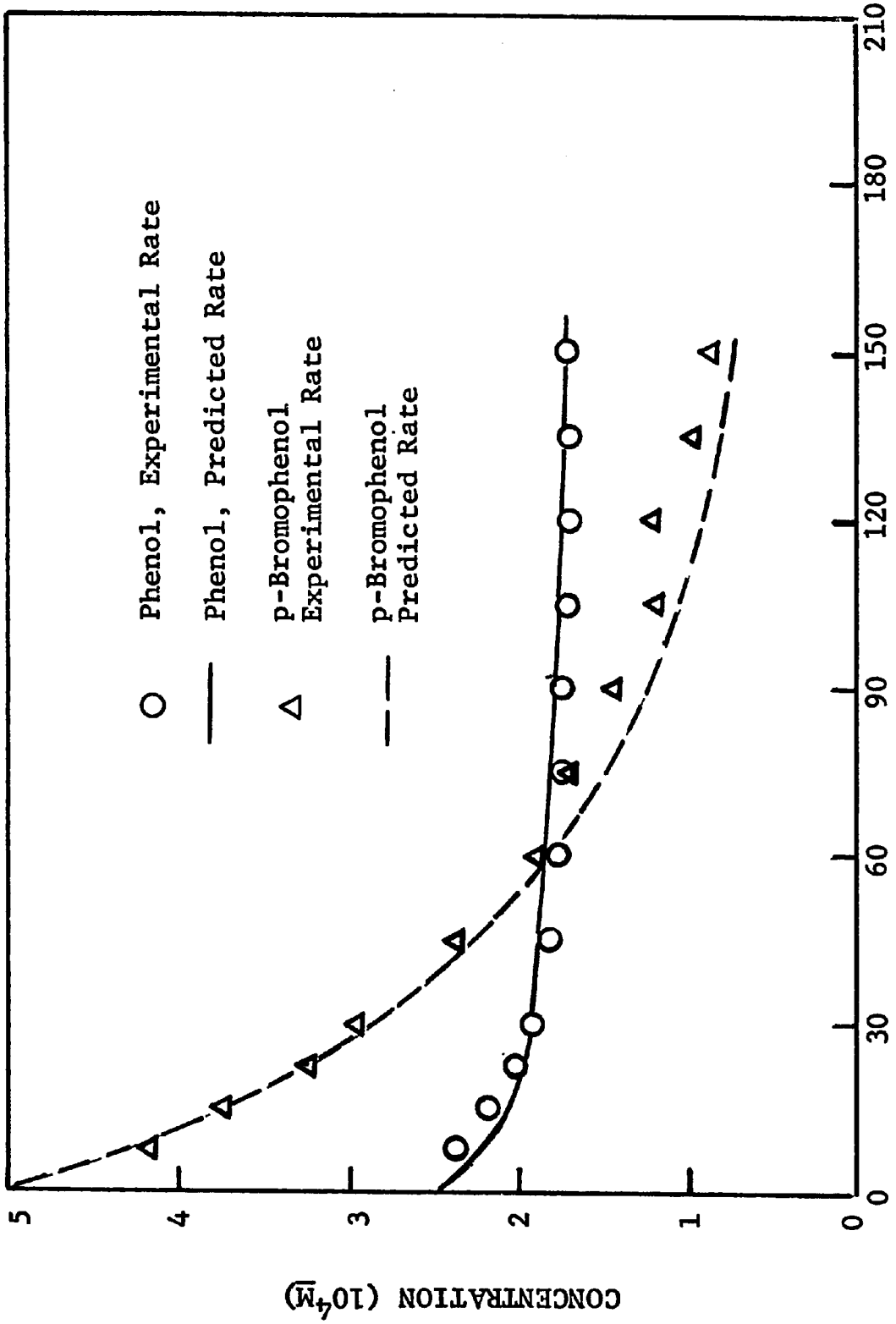


FIGURE 6-11. RATES OF ADSORPTION FROM MIXTURES: PHENOL-p-BROMOPHENOL (C_{10}=2.5 x 10^{-4}M, C_{20}=5 x 10^{-4}M, CARBON=0.33 g/l)

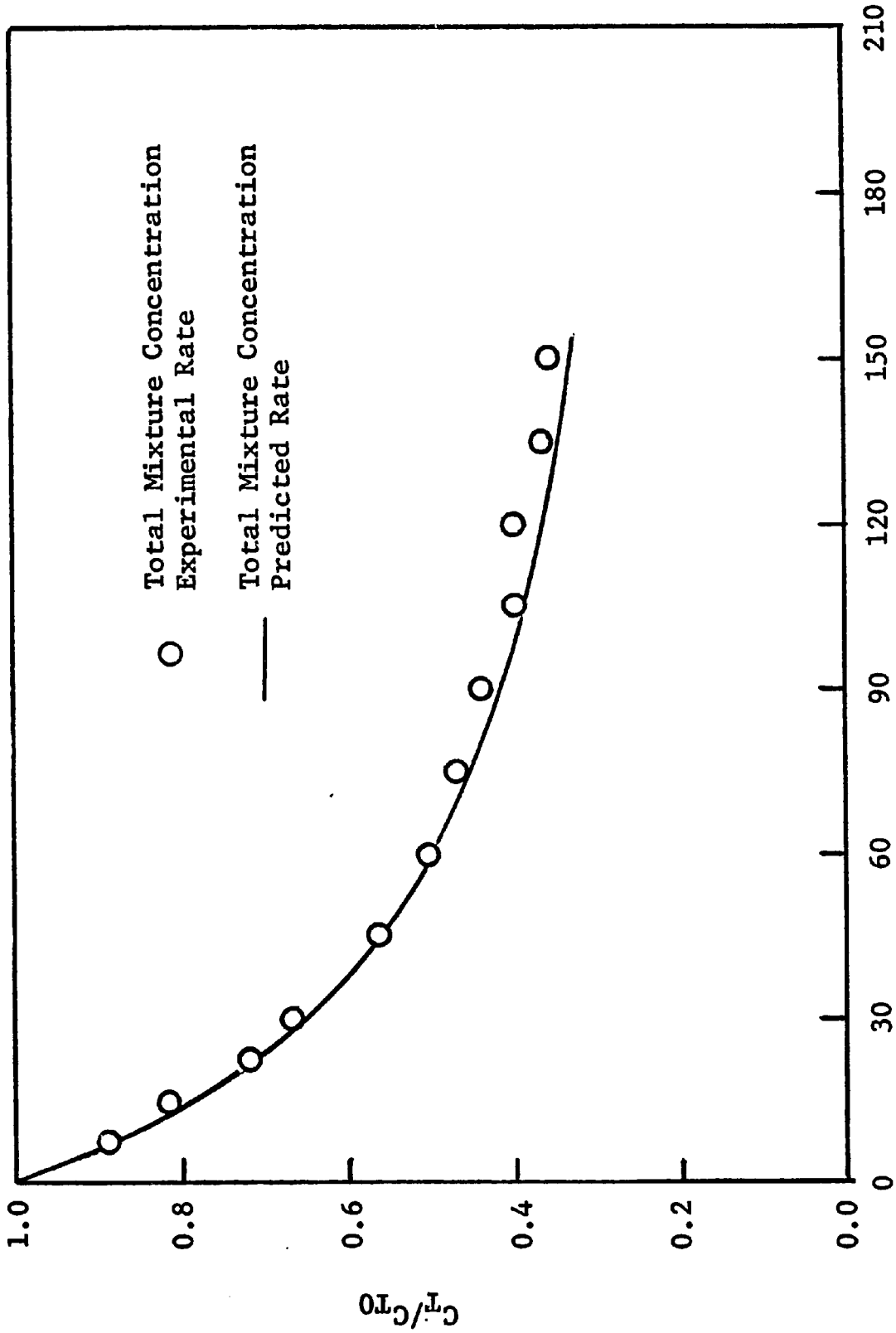


FIGURE 6-12. TOTAL CONCENTRATION PROFILE: PHENOL-p-BROMOPHENOL
(C_{10}=2.5 x 10^{-4}M, C_{20}=5 x 10^{-4}M,
CARBON=0.33 g/l, 650 RPM)

Phenol - Dodecyl Benzene Sulfonate Mixture

Phenol and dodecyl benzene sulfonate are two solutes that have markedly different adsorption characteristics. The surface diffusion coefficient of phenol is about fourteen times greater than that for dodecyl benzene sulfonate. The equilibrium adsorption constants indicate that dodecyl benzene sulfonate has a much higher energy of adsorption than phenol (76). The adsorption rates from a mixture of these solutes can be predicted accurately, if (1) an adequate representation is obtained for the mixture equilibria, and (2) the diffusion rates in the solid and fluid phases are not affected by solute-solute interactions.

The experimental and predicted profiles for adsorption from a mixture 5×10^{-5} M in phenol and 5×10^{-5} M in dodecyl benzene sulfonate are shown in Figure 6-13. The rate of adsorption of dodecyl benzene sulfonate is faster than predicted, and for phenol, the rate is slower than predicted. However, the shape of the predicted profiles for both solutes closely parallel the experimental curves. Similar trends may be noted in Figure 6-15 for the adsorption rates from a 10^{-4} M phenol and 10^{-4} M dodecyl benzene sulfonate mixture. As may be seen from Figures 4-13 and 4-14, the mixture equilibrium data have been correlated satisfactorily.

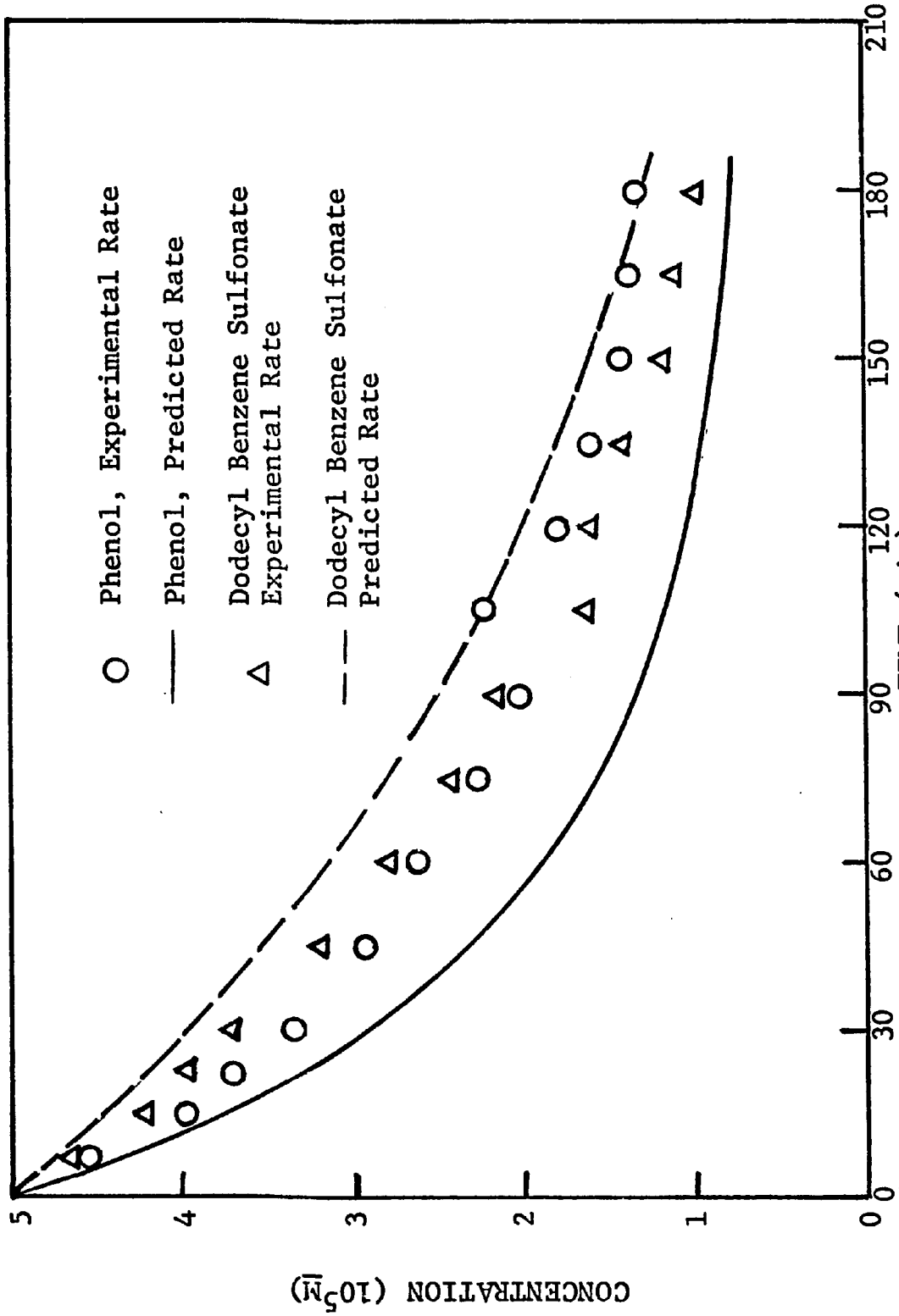


FIGURE 6-13. RATES OF ADSORPTION FROM MIXTURES: PHENOL-DODECYL BENZENE SULFONATE ($C_{10}=C_{20}=5 \times 10^{-5}$M, CARBON=0.33 g/l, 650 RPM)

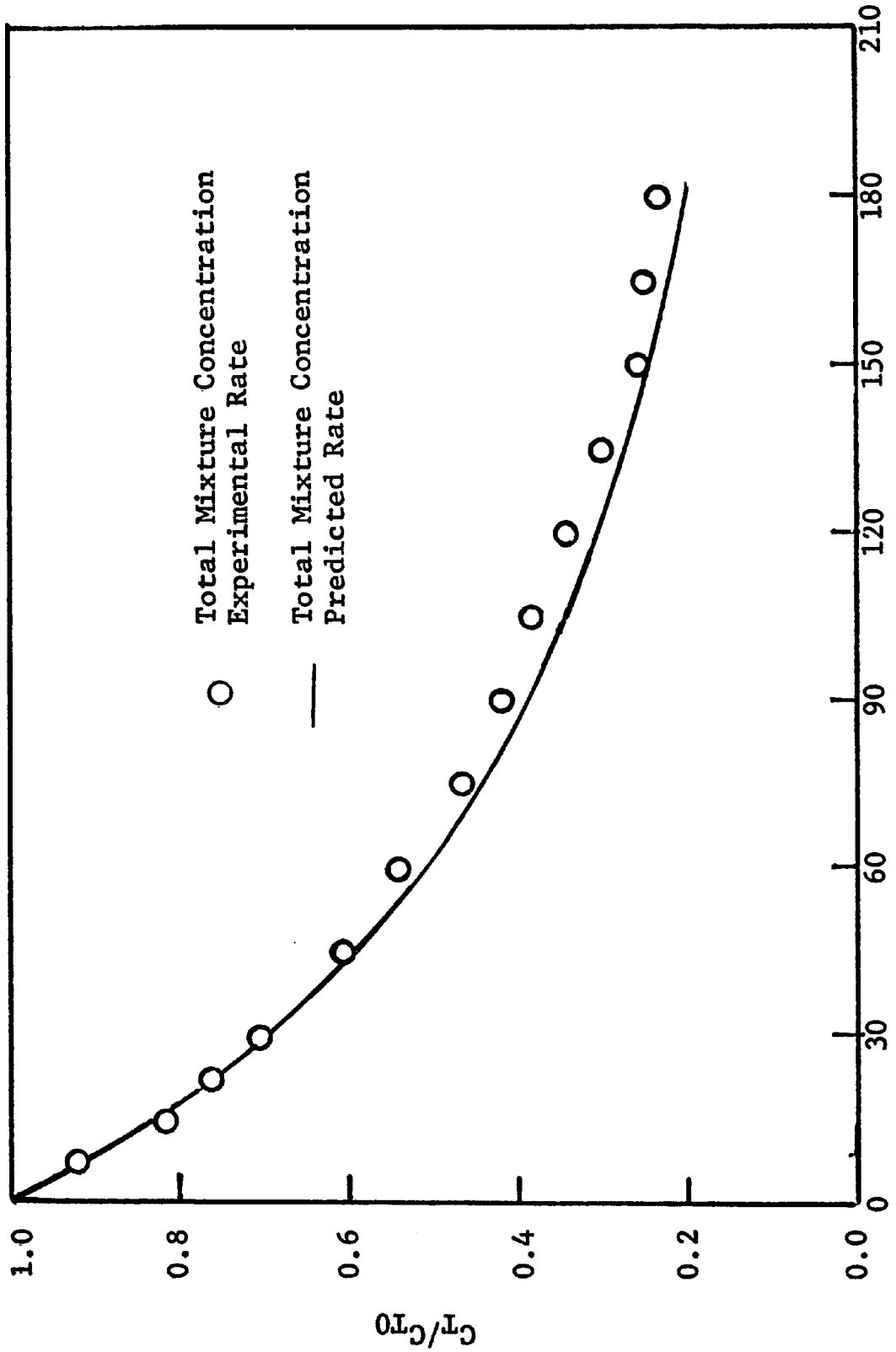


FIGURE 6-14. TOTAL CONCENTRATION PROFILE: PHENOL-DODECYL BENZENE SULFONATE ($C_{10}=C_{20}=5 \times 10^{-5}$ M, CARBON=0.33 g/l, 650 RPM)

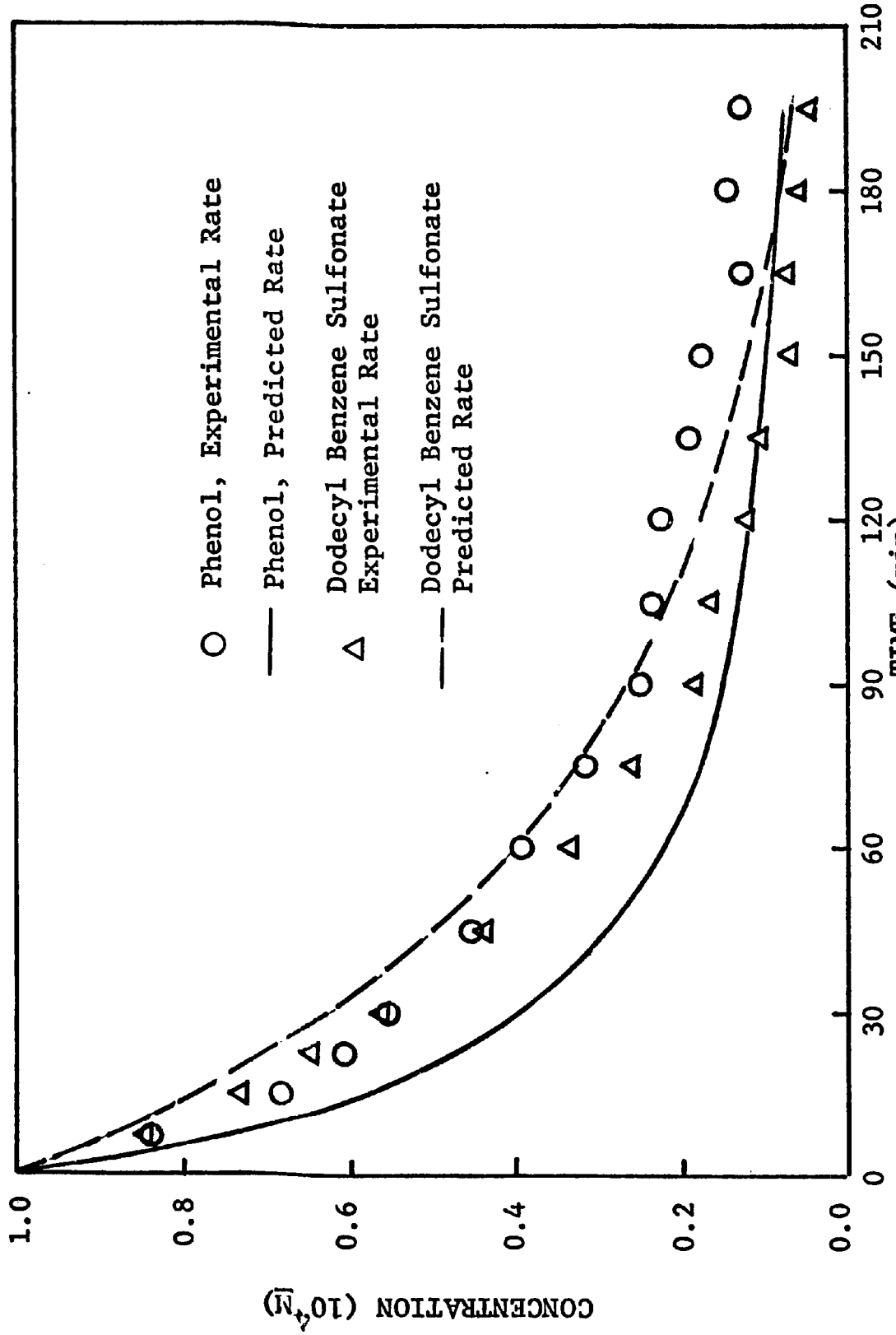


FIGURE 6-15. RATES OF ADSORPTION FROM MIXTURES: PHENOL-DODECYL BENZENE SULFONATE ($C_{10}=C_{20}=10^{-4}$M, CARBON=0.67 g/1, 650 RPM)

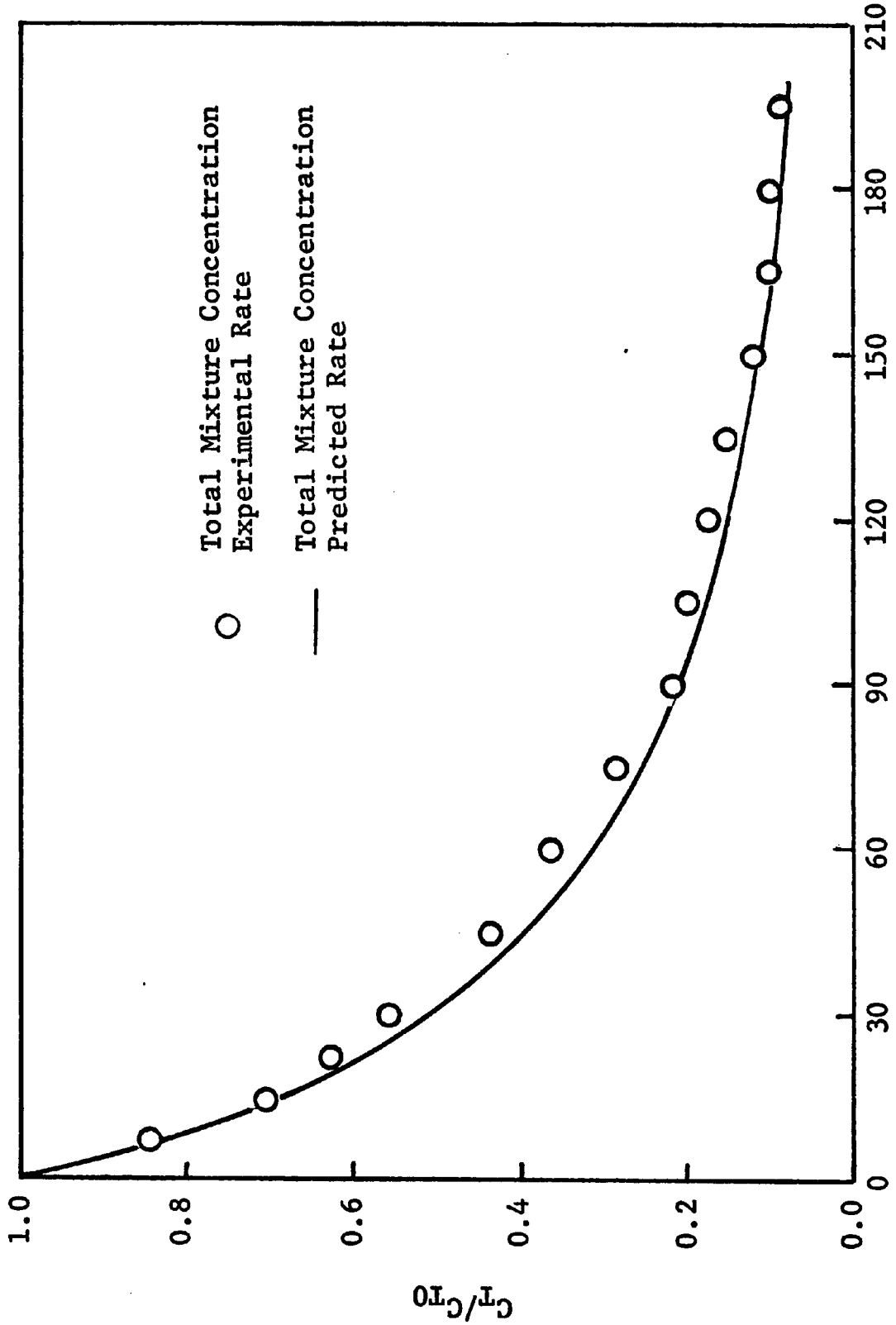


FIGURE 6-16. TOTAL CONCENTRATION PROFILE: PHENOL-DODECYL BENZENE SULFONATE ($C_{10}=C_{20}=10^{-4}$M, CARBON=0.67 g/1, 650 RPM)

Thus, it would appear that solute-solute interactions are affecting the diffusional flux of each solute. Moreover, from Figure 6-14 and 6-16 for the total concentrations, it may be seen that the interaction effects are mutually compensating. The total concentration profiles for both experimental runs agree well with the predicted profiles.

Solute-Solute interactions may affect the diffusion rates in the fluid phase, the solid phase, or both. Toor (65) has used the Stefan-Maxwell equations for steady state mass transfer in multicomponent systems to show that, in the extreme, four different types of diffusion may occur: (1) diffusion barrier, where the rate of diffusion of a component is zero even though its gradient is not zero; (2) osmotic diffusion, where the diffusion rate of a component is not zero even though the gradient is zero; (3) reverse diffusion, where diffusion occurs against the concentration gradient; and, (4) normal diffusion, where diffusion occurs in the direction of the gradient. While such extreme effects are not apparent in this system, it is evident that the adsorption rate of phenol is decreased by dodecyl benzene sulfonate, and that of dodecyl benzene sulfonate increased by phenol.

The diffusional flux of each species in a multicomponent

system may be derived from nonequilibrium thermodynamics (66), and may be represented by equation 6-33.

$$J_i = -\sum_i D_{ij} \nabla C_j \qquad (6\text{-}33)$$

J_i is the flux of each component in the mixture, and is a function of the gradients ∇C_j of all the other components. D_{ii} are the main diffusion coefficients, and D_{ij}, representing interaction, are the cross diffusion coefficients. There are three independent diffusion coefficients for a binary system, and these, in general, vary with the concentration of the components. Kinetic theory of gases may be used to estimate these coefficents for ideal gas mixtures. However, no reliable methods are available for liquid mixtures.

Thus, it is apparent that the inclusion of interaction effects in a multicomponent adsorption model would pose formidable problems in mathematical analysis, and in the application of the model. A qualitative approach is taken here, in the analysis of the phenol - dodecyl benzene sulfonate mixture rate data. The mass transfer coefficients for each solute in the mixture were computed from the initial rates of the component profiles using equation 5-9. The average values from the two rate studies were used in generating the curves in Figures 6-17 to 6-21. It is seen

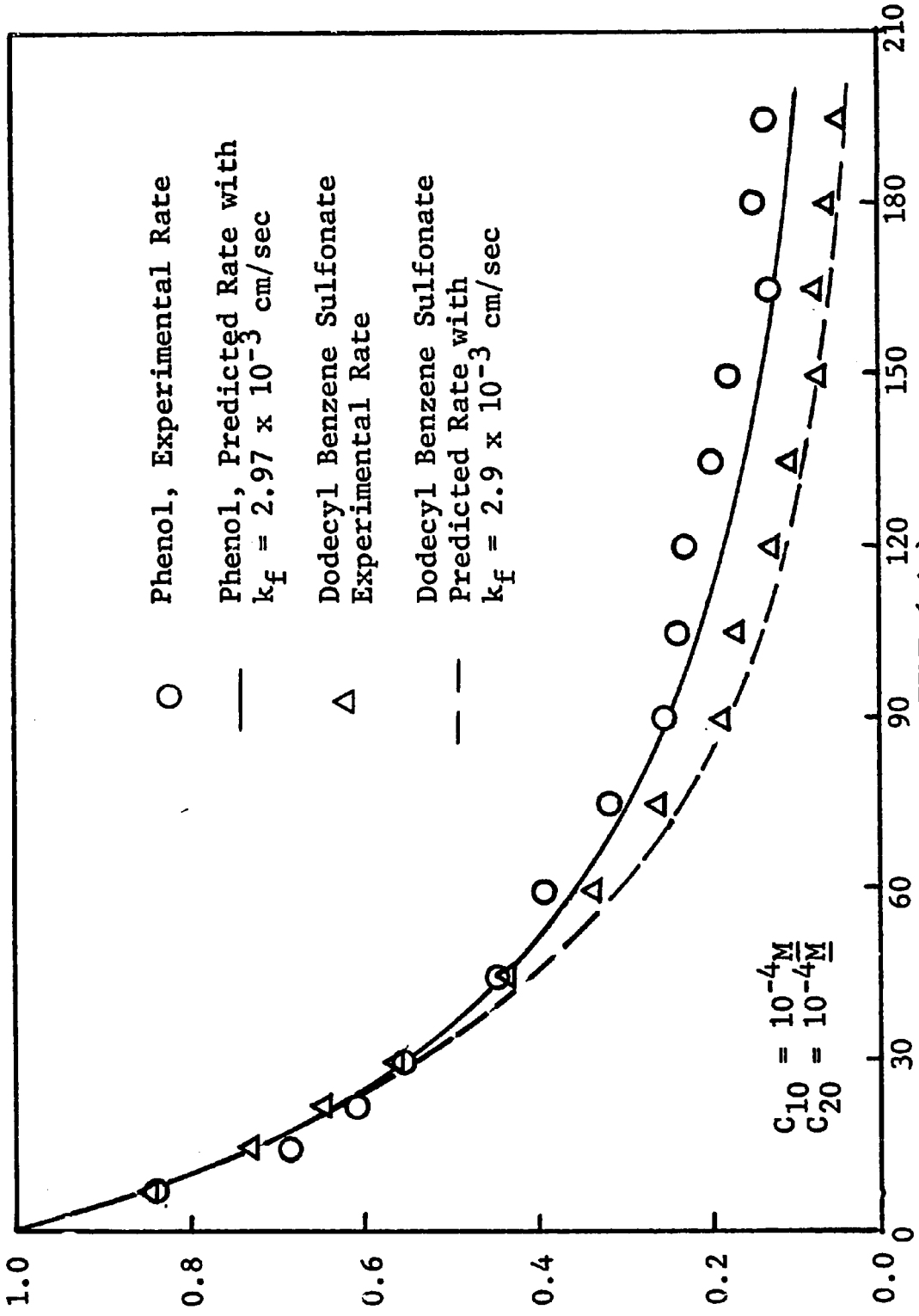


FIGURE 6-17. RATES OF ADSORPTION FROM MIXTURES: PHENOL-DODECYL BENZENE SULFONATE. PREDICTED PROFILES USING k_{fi} FROM MIXTURE RATE DATA

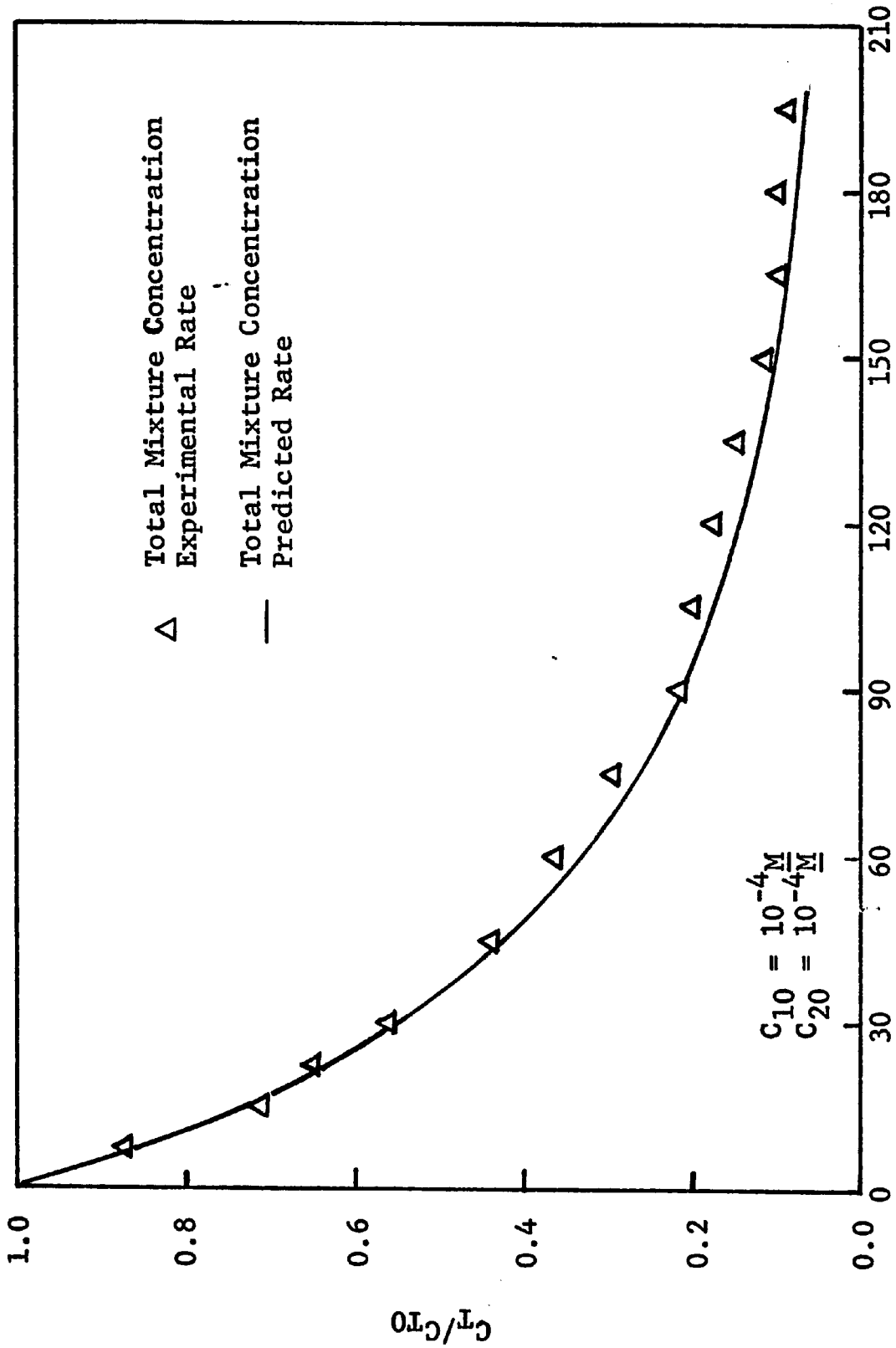


FIGURE 6-18. TOTAL CONCENTRATION PROFILE: PHENOL-DODECYL BENZENE SULFONATE. PREDICTED USING k_{fi} FROM MIXTURE RATE DATA

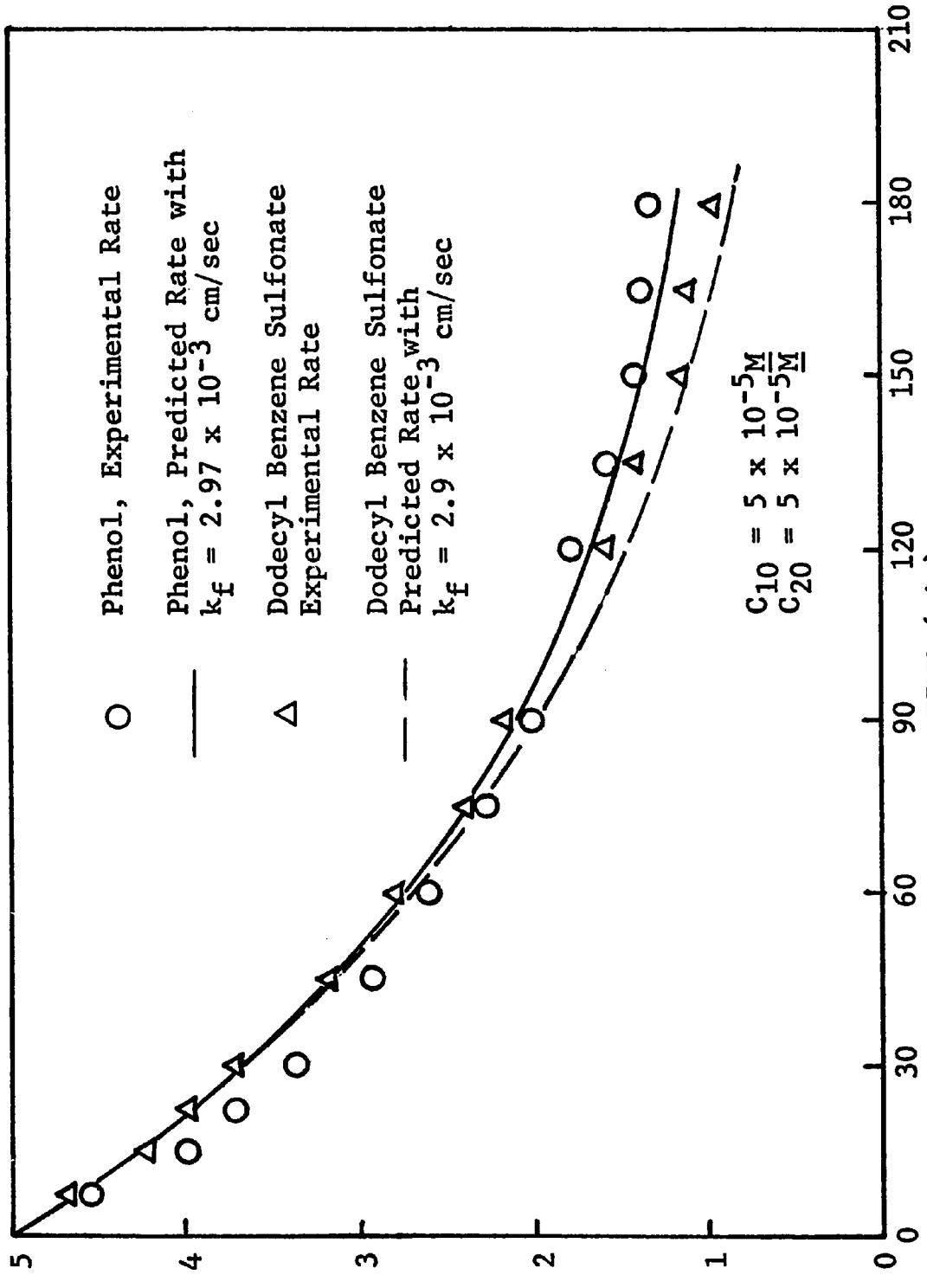


FIGURE 6-19. RATES OF ADSORPTION FROM MIXTURES: PHENOL-DODECYL BENZENE SULFONATE. PREDICTED PROFILES USING k_{fi} FROM MIXTURE RATE DATA

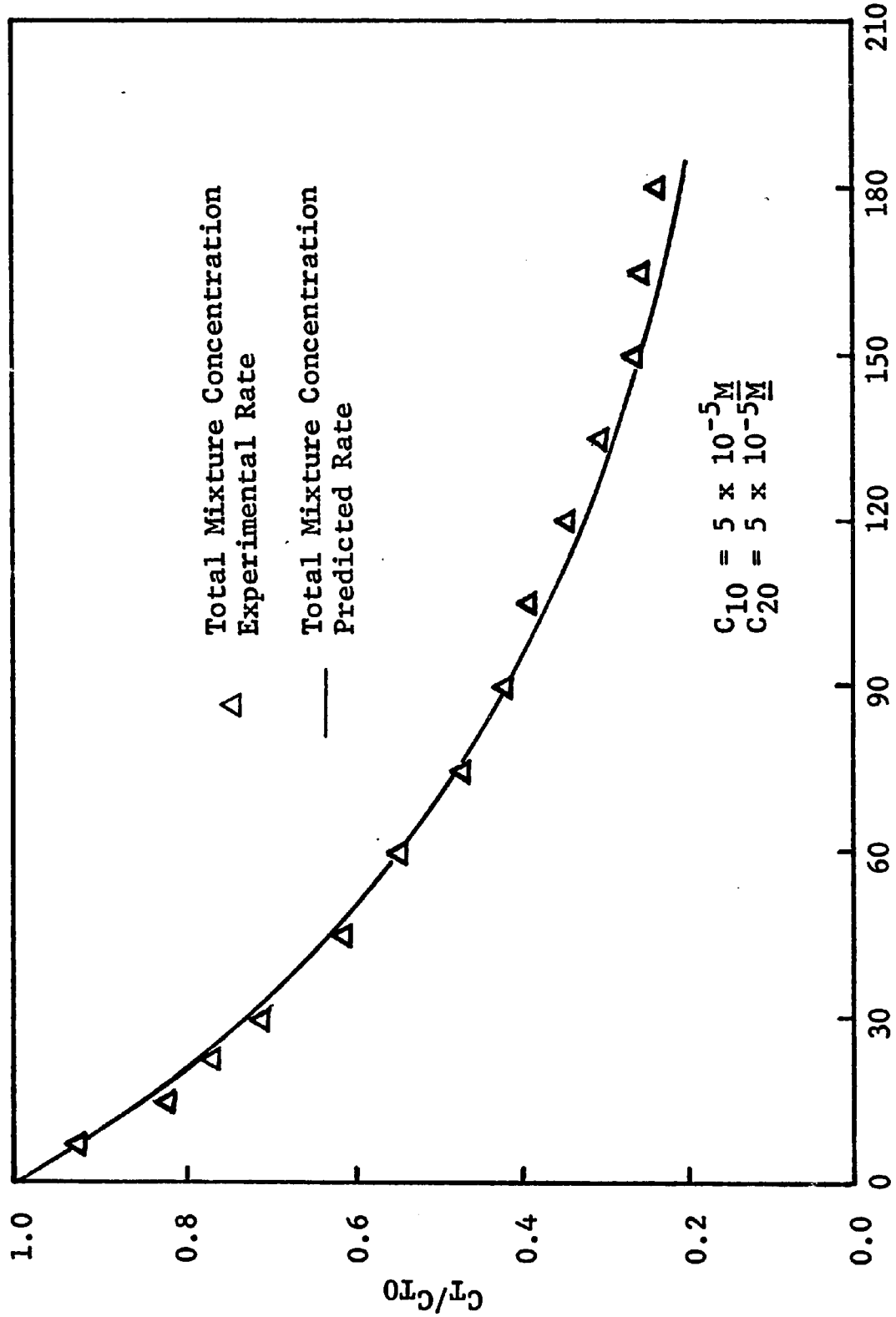


FIGURE 6-20. TOTAL CONCENTRATION PROFILE: PHENOL-DODECYL BENZENE SULFONATE. PREDICTED USING k_{fi} FROM MIXTURE RATE DATA

that for both rate studies, the predicted component profiles the experimental data much better than before. It is thus apparent that a major portion of the interaction is occurring in the fluid phase, in the diffusion boundary layer of each solute. These interactions may be expected to occur in the solid phase also, when the adsorbed phase loading becomes substantial.

Comparison to Single-Resistance Model

The sensitivity of the single solute rate model to film transfer and surface diffusion coefficients was discussed in Chapter 4. It was shown that, in general, the model is sensitive to the film transfer coefficient in the initial period of solute uptake, and to the surface diffusion coefficient in the latter part. The same trends are expected to be followed in the case of multi-solute systems. However, the effects may be different for different solute systems, depending on the multi-solute equilibria, and solute-solute interactions.

The effect of assuming negligible internal diffusion resistance, is shown for the phenol-p-toluene mixture in Figure 6-21. The solid line represents the predicted total concentration using the two-resistance model, and the dotted line represents film-diffusion controlled adsorption. It is seen that the two curves match only up to

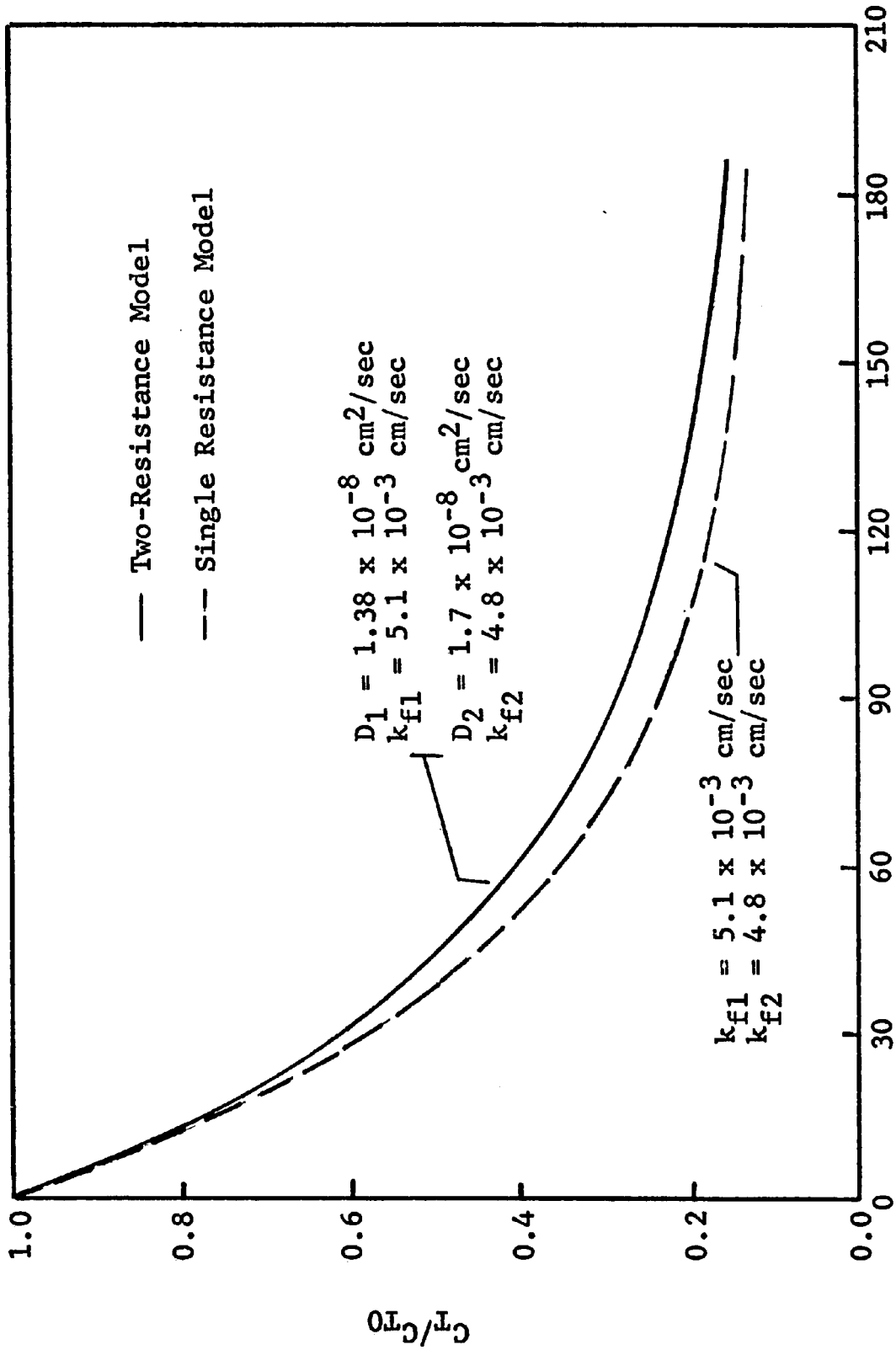


FIGURE 6-21. EFFECT OF INTRAPARTICLE DIFFUSION ON RATES OF ADSORPTION FROM MIXTURES: TOTAL CONCENTRATION PROFILE FOR PHENOL-p-TOLUENE SULFONATE MIXTURE

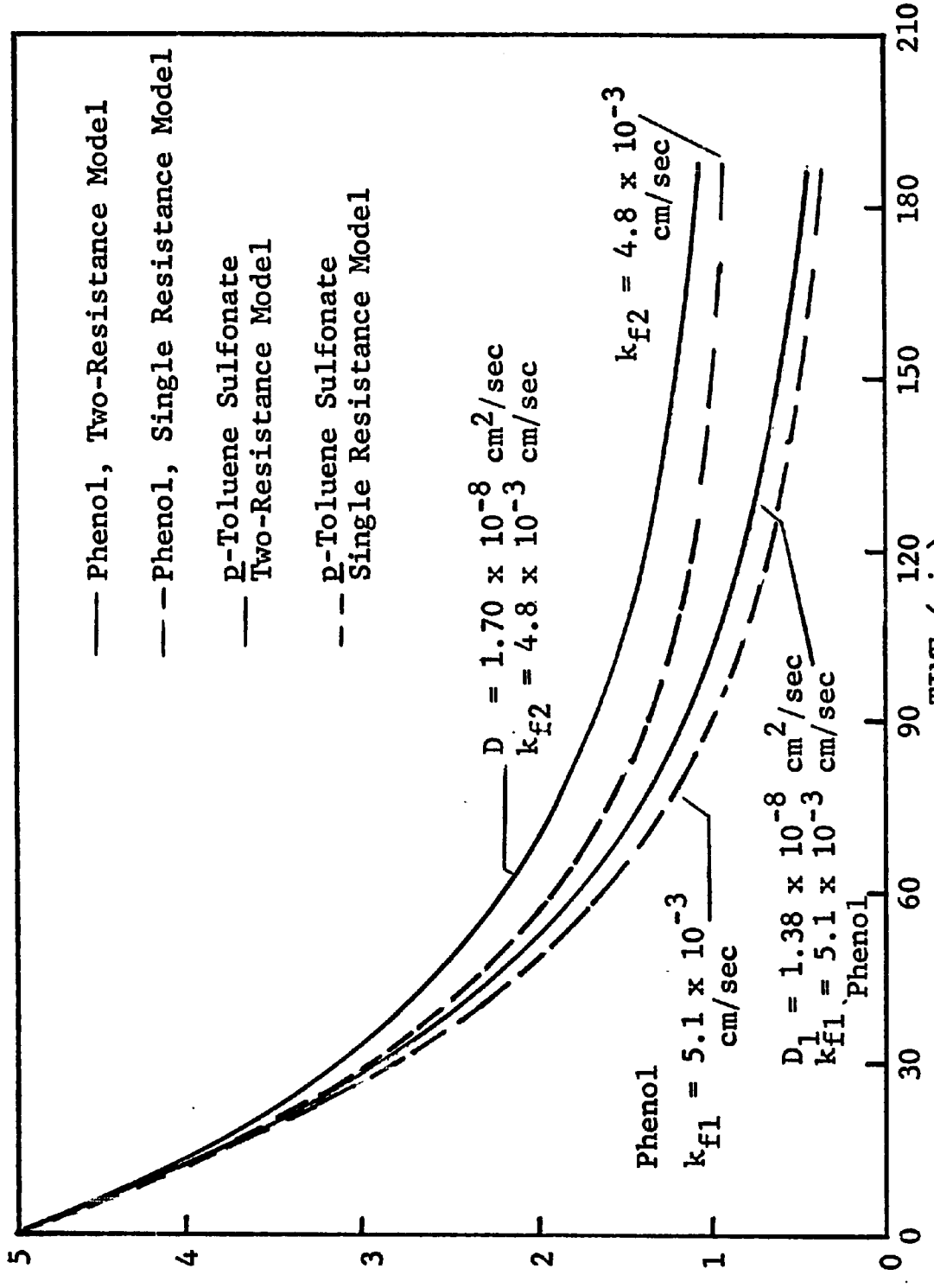


FIGURE 6-22. EFFECT OF INTRAPARTICLE DIFFUSION ON RATES OF ADSORPTION FROM MIXTURES: PHENOL-p-TOLUENE SULFONATE

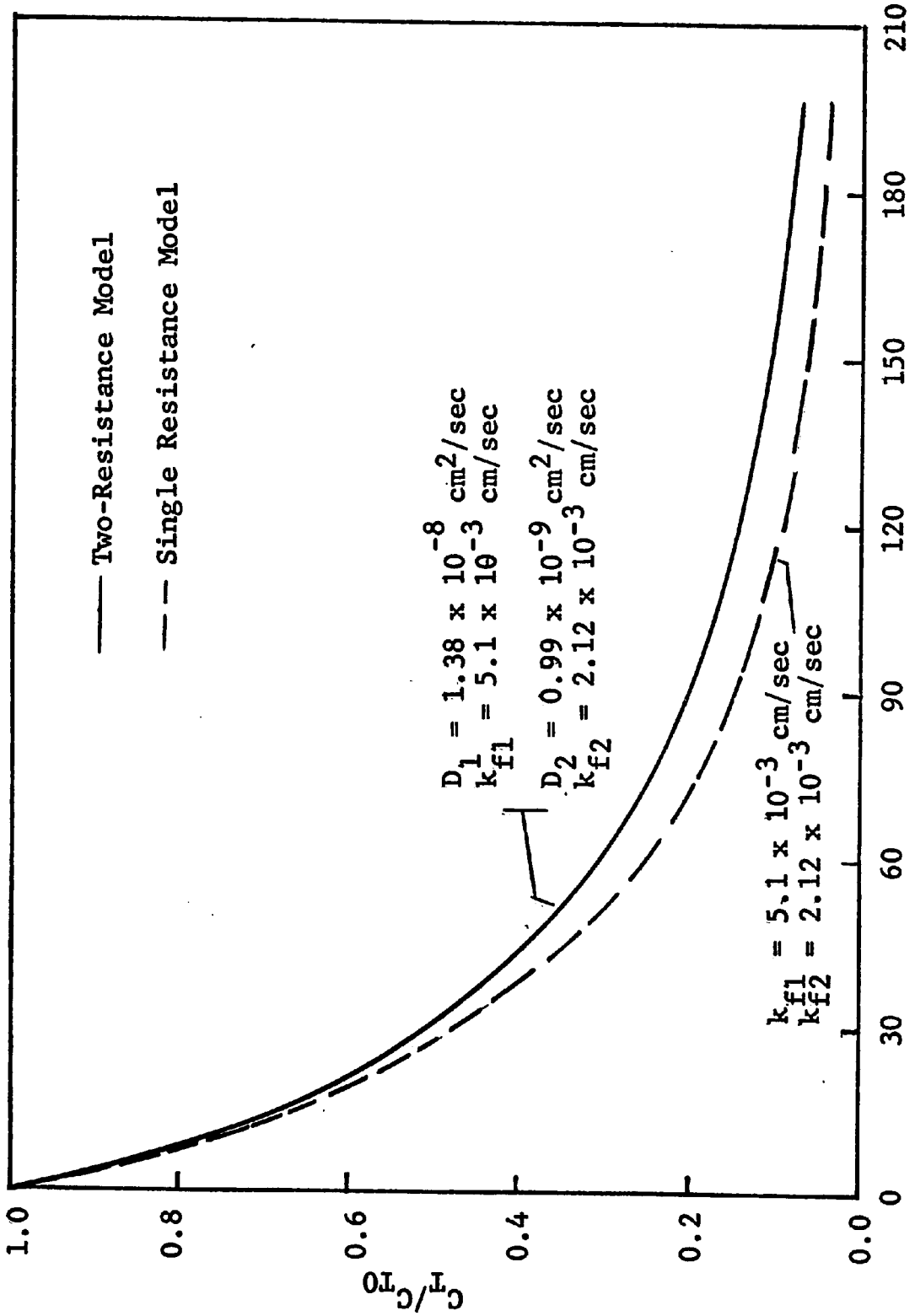


FIGURE 6-23. EFFECT OF INTRAPARTICLE DIFFUSION ON RATES OF ADSORPTION FROM MIXTURES: TOTAL CONCENTRATION PROFILE FOR PHENOL-DODECYL BENZENE SULFONATE MIXTURE

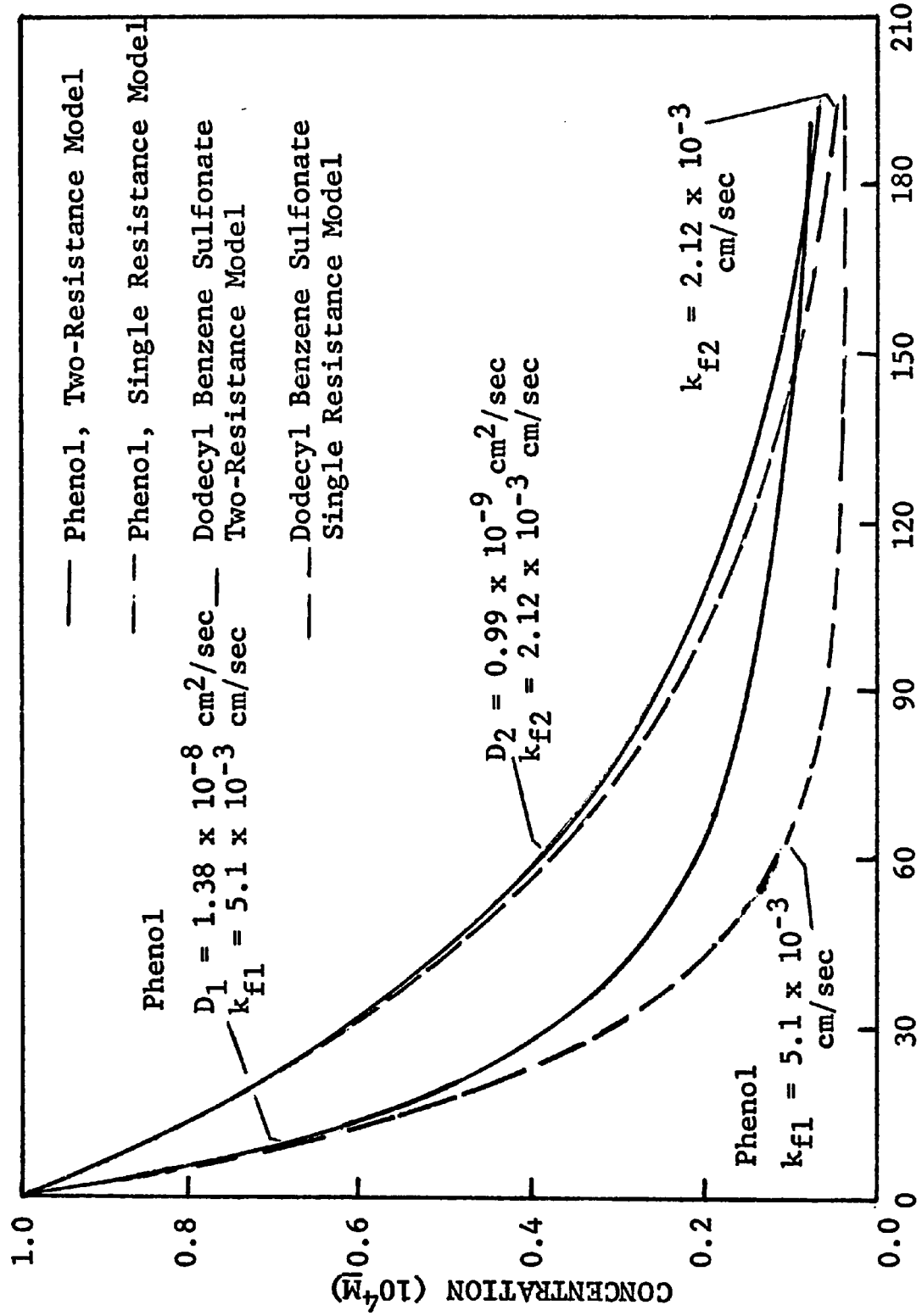


FIGURE 6-24. EFFECT OF INTRAPARTICLE DIFFUSION ON RATES OF ADSORPTION FROM MIXTURES: PHENOL-DODECYL BENZENE SULFONATE

the first 15 minutes. The component profiles for the same system are shown in Figure 6-22. The deviation for p-toluene sulfonate in the mixture is similar to the single solute rate behavior, shown in Figure 5-7. The effect on phenol is less pronounced. This may be due to the fact that the equilibrium adsorption of phenol from its mixture is greater than of p-toluene sulfonate.

In the phenol-dodecyl benzene sulfonate system, the equilibrium distribution of phenol on the solid is less than for dodecyl benzene sulfonate. A comparison of the single and two-resistance models for this system is made in Figures 6-23 and 6-24. The total concentration profile is substantially lower with the single resistance model, and as may be seen from the component profiles, this is mainly due to the effect of assuming an infinite surface diffusion rate for phenol.

CHAPTER 7

SUMMARY AND CONCLUSIONS

The principal objective of this research has been to develop a mathematical model to describe the kinetics of multicomponent adsorption. This has been achieved by integrating systematic developments in the areas of single solute rate modeling, the estimation of rate parameters, and the prediction of multi-solute equilibria.

The single solute model is patterned after the homogeneous solid phase diffusion model of Rosen, and takes into account diffusional processes in both the solid and fluid phases. The transport from the fluid to the solid phase is assumed to occur at a linear rate, and the transport in the solid phase is represented by an unsteady state diffusion equation. The latter representation allows the characterization of particle diffusion rates by the solid phase diffusion coefficient, and this is invariant with particle diameter. The model is sufficiently general to be valid for a wide variety of solutes, since no restrictive assumptions are made.

The equations currently available for representing adsorption equilibrium are inadequate to describe equilibrium

data over a wide concentration range with a single set of parameters. An empirical isotherm is proposed and utilized in this study. This equation reduces to the linear isotherm at low concentrations, and to the Freundlich equation at high concentrations, and can be used to represent data over a wide range of concentration with a single of set of parameters. However, the parameters in the equation must be estimated by least-squares analysis of the experimental data, since the equation can not be linearized.

A numerical procedure was developed to solve the system of equations representing the diffusional rates and equilibrium for single solute adsorption. The procedure may be adapted for the simulation of adsorption in fixed or expanded beds. The concentration-time profiles generated indicate that, in general, film diffusion controls the solute uptake initially, and particle diffusion in the latter stages. The initial uptake rates predicted by this model were compared with those of film diffusion controlled adsorption. It was shown that the assumption of negligible intraparticle resistance is a valid assumption, in the initial period, for solutes that exhibit a large solid to liquid phase equilibrium solute distribution. However, even for such systems, the errors are substantial

beyond the first few minutes, if the agitation power input is high. The assumption of negligible surface accumulation is expected to result in even more deviations, and therefore, the judiciousness of using such models for estimating mass transfer coefficients at high agitation power input is questionable.

The correlations available for predicting solid-liquid mass transfer rates in agitated vessels were reviewed, and it is concluded that external transport rates are a function of both the agitator power input and agitator design. In this study, a direct-search parameter estimation procedure was used to estimate the mass transfer and surface diffusion coefficients from single solute rate data. The procedure is particularly useful for correlating mass transfer coefficients with agitation power input, at high mass transfer rates. From a sensitivity analysis, it was shown that, under such conditions, the assumptions of negligible intraparticle diffusion and negligible surface accumulation could result in lower than actual values for the mass transfer coefficient.

DiGiano has shown that even in rapidly agitated systems, the external diffusion resistance may be of importance and can not be neglected. Besides, for solutes that are highly surface active, it may not be possible to provide rapid

agitation, due to foaming. It is essential then, that in such cases, both film and particle resistances are considered in estimating particle diffusion coefficients.

A number of models were evaluated to obtain a satisfactory description of adsorption equilibria for mixtures. The method of Radke and Prausnitz, using the principles of ideal dilute solution thermodynamics, is particularly suitable for solutes that do not adsorb strongly. However, the computational effort required is substantial unless analytically integrable functions are available for representing single solute equilibrium over a wide concentration range. In this study, the empirical equation proposed for single solutes is extended to multi-solute systems, and is seen to predict satisfactorily the data of Radke and Prausnitz for acetone-propionitrile mixtures, and p-cresol-p-chlorophenol mixtures. For systems that can not be adequately described by this method, a procedure is developed for correlating multi-solute equilibria. This allows the use of experimental mixture equilibrium data in multicomponent rate models.

The multicomponent rate model developed utilizes the rate and equilibrium parameters from single solute rate and equilibrium data, and the mixture equilibrium data

correlation coefficients. The model considers diffusion rates of each solute in the solid and fluid phases, but does not include the effects of solute-solute interactions on the diffusional flows in the two phases. The model was tested by comparing experimental rate profiles for binary systems with profiles predicted by the model. The following three cases were considered: (1) both solutes in the mixture have comparable diffusion rates and equilibria; (2) the solutes have comparable diffusion rates, but differing equilibria; and, (3) the solutes have differing diffusion rates, and differing equilibrium behavior. The first two systems were represented adequately by the model. For the third system, solute-solute interactions are apparent in the fluid phase. However, for all the systems, the total concentration profiles are in good agreement with the experimental data.

Thus, an area for future research that has significant practical utility, is the extension of the model to mixture systems with a large number of compounds by the use of an overall concentration parameter. If the compounds are too numerous and varied in adsorption characteristics, they may be classified into groups that have similar adsorption rate behavior. Each group of these compounds may be described by

a single set of adsorption rate and equilibrium constants, and the multicomponent model may be utilized in the prediction of concentration-time profiles for such systems.

For solutes that have markedly different adsorption rates, the model has to be extended to include solute-solute interactions that affect the diffusion rates. The complexity of models that include diffusional interactions in both fluid and solid phases has been noted in Chapter 6. A valid starting point to investigate such effects may be to study interaction effects in each phase separately by appropriate experimental design so that the transport rate may be characterised by the resistance in one phase.

Single solute adsorption equilibria have for long been represented by the Langmuir isotherm derived on the assumptions of monolayer surface coverage and uniform surface energy. Extension of the method to multilayer adsorption is available in the BET isotherm. An area of research that may be of considerable theoretical and practical interest is the development of equilibrium models that reflect nonuniform energy distributions on the surface. Such developments, particularly if they can be extended to multi-solute systems satisfactorily, will be helpful in eliminating experimentation to generate multi-solute equilibrium data.

The methodology developed in this investigation for the modeling of single and multicomponent kinetics and equilibria, provide a fundamental starting point for the study of systems that involve biological decay. Since the model predicts multicomponent adsorption rates satisfactorily, it may be used in differentiating the effects of adsorption and biological decay in biologically-extended systems. Systematic studies in this area are needed for effecting optimum use of activated carbon adsorption processes in both independent physicochemical treatment systems and in the upgrading of effluents from biological treatment plants.

APPENDIX A

FINITE DIFFERENCE APPROXIMATION TO ADOSRPTION RATE EQUATIONS

Given the partial differential equation A-1,

$$\frac{\delta u}{\delta \tau} = \frac{\delta^2 u}{\delta x^2} \tag{A-1}$$

the Crank-Nicholoson differrence approximation involves replacing the left and right hand sides by equations A-2 and A-3.

$$\frac{\delta u}{\delta \tau} = \frac{1}{\Delta \tau}(u_j^{n+1} - u_j^n) \tag{A-2}$$

$$\frac{\delta^2 u}{\delta x^2} = \frac{1}{2(\Delta x)^2}((u_{j+1}^{n+1} - 2u_j^{n+1} + u_{j-1}^{n+1}) + (u_{j+1}^n - 2u_j^n + u_{j-1}^n)) \tag{A-3}$$

Rearrangement of the resulting expression gives equation 2-37 as the finite difference approximation to the rate equation for solid phase transport.

The surface boundary condition is given by

$$\int_0^1 \frac{\delta u}{\delta \tau} x \, dx = \frac{k_f R}{1000 \rho D (1-\varepsilon)} (C - C_s) \tag{A-4}$$

The integral on the left hand side of equation A-4 is evaluated using the Trapezoidal rule. The Trapezoidal rule for

a finuction f(x) in the interval (0,1) is given by equation A-5.

$$\int_0^1 f(x)\,dx = (\Delta x)\sum_{j=1}^{M} f_j + \frac{\Delta x}{2}(f_1+f_{M+1}) \qquad \text{(A-5)}$$

where, $f_j = f(x_j)$, and $x_j = (j-1)\Delta x$

Thus, equation A-3 becomes

$$(\frac{\delta u}{\delta \tau}\, x)\,dx = (\Delta x)^2\,((\frac{\delta u}{\delta \tau})_{M+1}\,\frac{M}{2} + \sum_{j=2}^{M} (\frac{\delta u}{\delta \tau})_j\,(j-1) \qquad \text{(A-6)}$$

Substituting equation A-7 in A-6 and rearranging, equation

$$(\frac{\delta u}{\delta \tau})_j = \frac{1}{\Delta \tau}(u_j^{n+1} - u_j^n) \qquad \text{(A-7)}$$

A-8 is obtained for the transport at the surface of the particle.

$$u_{M+1}^{n+1} + \frac{2}{M}\sum_{j=1}^{M} u_j^{n+1}\,(j-1) = \frac{(4\lambda/M)k_f R}{1000\rho(1-\varepsilon)D}\,(C-C_s) + \frac{2}{M}\sum_{j=1}^{M} u_j^n\,(j-1) + u_{M+1}^n \qquad \text{(A-8)}$$

The integral in equation 2-36 for the average particle concentration is also evaluated by using the Trapezoidal rule.

APPENDIX B

NEWTON-RAPHSON METHOD COMPUTATIONS FOR RATE AND EQUILIBRIUM MODELS

For two nonlinear equations $F(x,y)=0$, and $G(x,y)=0$, the roots x and y at the (k)th iteration is given by the Newton-Raphson method as

$$x^k = x^{k-1} + \delta_1(x^{k-1}, y^{k-1}) \qquad \text{(B-1)}$$

$$y^k = y^{k-1} + \delta_2(x^{k-1}, y^{k-1}) \qquad \text{(B-2)}$$

where, $$\delta_1 = (-FG_y + GF_y)/(F_xG_y - F_yG_x) \qquad \text{(B-3)}$$

$$\delta_2 = (-F_xG + FG_x)/(F_xG_y - F_yG_x) \qquad \text{(B-4)}$$

Given initial guesses for x and y sufficiently close to the roots, the Newton-Raphson method converges quadratically to the roots.

Equilibria Prediction

The solution of equations 4-33 and 4-36 for the prediction of multi-solute equilibria involves the application of equations B-1 to B-4 to equations 4-33 and 4-36. The partial derivatives needed in equations B-3 and B-4 are given below.

$$F_{C_1^o} = \frac{a_1}{1+b_1(C_1^o)^{\beta_1}} \qquad \text{(B-5)}$$

$$F_{C_2^o} = \frac{-a_2}{1+b_2(C_2^o)^{\beta_2}} \qquad \text{(B-6)}$$

$$G_{C_1^o} = \frac{C_1 C_2}{(C_1^o - C_2)^2} \qquad \text{(B-7)}$$

$$G_{C_2^o} = 1 \qquad \text{(B-8)}$$

Multicomponent Rate Model

The Newton-Raphson method is utilized in the multicomponent rate model to evaluate the equilibrium surface concentrations at each time step using equations 6-5 and 6-6. The partial derivatives of equations 6-5 and 6-6 that are used in eqution B-1 to B-4 are given below.

$$F_{C_{s1}} = 1 - \frac{q_{s1}\eta_1}{a_1} b_1\beta_1 (C_{s1}/\eta_1)^{\beta_1-1} \qquad \text{(B-9)}$$

$$F_{C_{s2}} = - \frac{q_{s1}\eta_1}{a_1} \frac{b_2\beta_2}{\eta_2} (C_{s2}/\eta_2)^{\beta_2-1} \qquad \text{(B-10)}$$

$$G_{C_{s1}} = - \frac{q_{s2}\eta_2}{a_2} \frac{b_1\beta_1}{\eta_1} (C_{s1}/\eta_1)^{\beta_1-1} \qquad \text{(B-11)}$$

$$G_{C_{s2}} = 1 - \frac{q_{s2}\eta_2}{a_2} b_2\beta_2 (C_{s2}/\eta_2)^{\beta_2-1}$$

APPENDIX C

COMPUTER PROGRAMS FOR PARAMETER ESTIMATION AND MULTI-SOLUTE RATE AND EQUILIBRIA PREDICTION

Estimation of Mass Transfer and Surface Diffusion Coefficients from Single Solute Rate Data

```
C.....ESTIMATION OF DIFFUSION AND MASS TRANSFER COEFFICIENTS......
C.....FROM SINGLE SOLUTE ADSORPTION RATE DATA......
C.....M1 DATA SETS  M2 DATA POINTS EACH DATA SET......
C.....N NUMBER OF DISTANCE STEPS  M TIME STEPS......
C.....LPRIN=1 PRINTS INITIAL A MATRIX, INVERSE, AND B VECTOR......
C.....IPRIN=1 PRINTS PARAMETER AND FMIN VALUES IN PRAXIS......
      IMPLICIT REAL*8(A-H,O-Z)
      DIMENSION X(2),ID(18),ID1(18),ETIME(50),CC(50),CE(50),XL(2),XR(2),
     1SCALE(2)
      COMMON ETIME,CC,CE,XL,XR,SCALE,PENALT,ID,L,M2,LPRIN,LO,LP
      EXTERNAL F
C
C.....READ IN EXPERIMENTAL DATA......
C.....SPECIFY RATE DATA AT INTEGER MULTIPLES OF TIME STEP......
      READ(4,1) ID1
    1 FORMAT(18A4)
      READ(4,2) M1
    2 FORMAT(I3)
      READ(4,7) PENALT
    7 FORMAT(E9.4)
      READ(4,2) LPRIN
      READ(4,2) LP
      DO 10 J=1,M1
      READ(4,1) ID
      READ(4,2) M2
      READ(4,4) TC,HC,IPRIN
    4 FORMAT(E9.4,1X,E9.4,1X,I1)
      READ(4,6) X(1),X(2)
    6 FORMAT(E9.4,1X,E9.4)
      READ(4,6) XL(1),XR(1)
      READ(4,6) XL(2),XR(2)
      READ(4,6) SCALE(1),SCALE(2)
      READ(4,3) (ETIME(I),CE(I),I=1,M2)
```

```
 3    FORMAT(E9.4,1X,E9.4)
      NN=2
      L=1
      LO=1
      CC(1)=CE(1)
      DO 620 I=1,NN
      X(I)=X(I)*SCALE(I)
      XL(I)=XL(I)*SCALE(I)
      XR(I)=XR(I)*SCALE(I)
 620  CONTINUE
C
      WRITE(7,103) J
 103  FORMAT(//10X,'DATA SET NO=',I3)
      WRITE(7,104) TO,HO
 104  FORMAT(//10X,'TO=',E10.4,/10X,'HO=',E10.4)
      WRITE(7,111) SCALE(1),SCALE(2)
 111  FORMAT(//10X,'SCALE (1)=',E10.4,/10X,'SCALE(2)=',E10.4)
      WRITE(7,112) IPRIN,LPRIN
 112  FORMAT(//10X,'IPRIN=',I1,/10X,'LPRIN=',I1)
      WRITE(7,113) XL(1),XR(1)
 113  FORMAT(//10X,'XL(1)=',E10.4,/10X,'XL(2)=',E10.4)
      WRITE(7,114) XL(2),XR(2)
 114  FORMAT(/10X,'XL(2)=',E10.4,/10X,'XR(2)=',E10.4)
C
C.....CALL SUBROUTINE PRAXIS FOR MINIMIZATION......
      CALL PRAXIS(TO,HO,NN,IPRIN,X,F,FMIN)
      PRINT 105, FMIN
 105  FORMAT('FMIN=',E10.4)
C
C.....PRINT CALCULATED VALUES WITH ESTIMATED COEFFICIENTS......
      WRITE(7,101)
 101  FORMAT('1')
      WRITE(7,102) ID
 102  FORMAT(//10X,18A4)
      X(1)=X(1)/SCALE(1)
      X(2)=X(2)/SCALE(2)
      WRITE(7,609) X(1),X(2)
 609  FORMAT(//10X,'DIFFUSION COEFFICIENT=',E10.4,' CM SQ/SEC'/10X,'FILM
     1 TRANSFER COEFFICIENT=',E10.4,' CM/SEC')
      WRITE(7,106)
 106  FORMAT(//8X,'TIME',10X,'C EXP',8X,'C CALC')
      WRITE(7,107)
 107  FORMAT(8X,'MIN',9X,'MOLES/L',8X,'MOLES/L')
      WRITE(7,108) (ETIME(I),CE(I),CC(I),I=1,M2)
 108  FORMAT(4X,F10.4,6X,E10.4,3X,E10.4)
 10   CONTINUE
      WRITE(7,608) L
 608  FORMAT(//10X,'NUMBER OF CALLS FOR SOLVE=',I3)
      STOP
      END
      REAL FUNCTION F(X,NN)
C.....FUNCTION TO BE MINIMIZED IS SUM OF SQUARES OF DEVIATIONS......
C.....SUBJECT TO NON-NEGATIVITY CONSTRAINTS......
C
      IMPLICIT REAL*8(A-H,O-Z)
      DIMENSION X(2),ETIME(50),CC(50),CE(50),XL(2),XR(2),ID(18),SCALE(2)
     1,XP1(11),XP2(11),CP(11)
      COMMON ETIME,CC,CE,XL,XR,SCALE,PENALT,ID,L,M2,LPRIN,LO,LP
      IF(L .EQ. 1) GO TO 15
      DO 10 I=1,NN
```

```
      IF(X(I)) 7,7,8
7     C1=PENALT*PENALT*(1.-X(I))
      GO TO 630
8     DIF=XL(I)-X(I)
      IF(DIF) 10,10,11
11    C1=PENALT*(1.+DIF*PENALT)
      GO TO 630
10    CONTINUE
      DO 30 I=1,NN
      IF(X(I)) 9,9,14
9     C1=PENALT*PENALT*(1.-X(I))
      GO TO 630
14    DIF=X(I)-XR(I)
      IF(DIF) 30,30,12
12    C1=PENALT*(1.+DIF*PENALT)
      GO TO 630
30    CONTINUE
15    CALL SOLVE(ETIME,CC,CE,X,SCALE,ID,L,M2,LPRIN)
      C1=0.0D0
      DO 20 I=1,M2
      C1=C1+((CC(I)-CE(I))/CE(I))**2
20    CONTINUE
630   F=C1
      L1=L-L0
      XP1(L1)=X(1)/SCALE(1)
      XP2(L1)=X(2)/SCALE(2)
      CP(L1)=C1
      WRITE(7,641) XP1(L1),XP2(L1),CP(L1)
641   FORMAT(//10X,'X(1)=',E10.4,/10X,'X(2)=',E10.4,/10X,'FMIN=',E10.4)
      IF(L1 .NE. LP) GO TO 640
      L0=L0+LP
      WRITE(6,631)
631   FORMAT(//10X,'X(1)',10X,'X(2)',10X,'FMIN')
      WRITE(6,632) (XP1(I),XP2(I),CP(I),I=1,LP)
632   FORMAT(5X,E10.4,4X,E10.4,4X,E10.4)
      IF(CP(LP)-CP(1))640,634,634
634   WRITE(6,635)
635   FORMAT(/5X,'TYPE IN 1 IF CONSTRAINTS ARE TO BE CHANGED,'/5X,'ELSE
     1TYPE IN 0 AND RETURN')
      READ(5,636) INP
636   FORMAT(I1)
      IF(INP .NE. 1) GO TO 640
      WRITE(6,638)
638   FORMAT(/5X,'ENTER XL(1),XR(1),XL(2),XR(2), WITH FORMAT E9.4,1X,...
     1...')
      READ(5,639) XL(1),XR(1),XL(2),XR(2)
639   FORMAT(E9.4,1X,E9.4,1X,E9.4,1X,E9.4)
640   RETURN
      END
C
      SUBROUTINE SOLVE(ETIME,CC,CE,X,SCALE,ID,L,M2,LPRIN)
C.....SOLUTION OF PARTIAL DIFFERENTIAL EQUATION......
      IMPLICIT REAL*8(A-H,O-Z)
      DIMENSION A(25,25),BB(26),B(25),X(2),ETIME(50),CC(50),CE(50),IPERM
     1(50),ID(18),SCALE(2),Y(2)
      Y(1)=X(1)/SCALE(1)
      Y(2)=X(2)/SCALE(2)
      IF(L .NE. 1) GO TO 400
C
C.....READ IN CONSTANTS......
```

```
      READ(4,1) AI,BI,BETA,RAD
 1    FORMAT(E9.4,1X,E9.4,1X,E9.4,1X,E9.4)
      READ(4,2) N,M
 2    FORMAT(I3,1X,I3)
      READ(4,3) CI,V1,W
 3    FORMAT(E9.4,1X,E9.4,1X,E9.4)
      READ(4,4) DELX,DTIME
 4    FORMAT(E9.4,1X,E9.4)
      READ(4,4) RHO,VOID
      READ(4,5) ERR,NR
 5    FORMAT(E9.4,1X,I3)
      READ(4,7) NPR,LPR
 7    FORMAT(I3,1X,I1)
C
C.....COMPUTE CONSTANTS......
      LENA=25
      LENT=25
      N1=N+1
      N2=N-1
      N3=N/2
      N4=N-2
      DEL=(DELX*DELX)/2.0D0
      DEL1=DEL*6.0D0
C
C.....WRITE INPUT DATA......
      WRITE(7,101)
 101  FORMAT('1')
      WRITE(7,102) ID
 102  FORMAT(//10X,18A4)
      WRITE(7,103) Y(1),Y(2),AI,BI,BETA,RAD,ERR
 103  FORMAT(//10X,'DIFFUSION COEFFICIENT=',E10.4,'CM SQ/SEC',/10X,'FILM
     1 TRANSFER COEFFICIENT=',E10.4,'CM/SEC',/10X,'EQUILIBRIUM CONSTANT
     2A=',E10.4,/10X,'EQUILIBRIUM CONSTANT B=',E10.4,/10X,'EQUILIBRIUM C
     3ONSTANT BETA=',E10.4,/10X,'RADIUS OF PARTICLE=',E10.4,'CM',/10X,'C
     4ONVERGENCE CRITERION ERR=',E10.4)
      WRITE(7,104) DELX,DTIME
 104  FORMAT(//10X,'DISTANCE STEP DELX=',E10.4,/10X,'TIME STEP DELT=',E1
     10.4,'MIN')
      WRITE(7,105) CI,V1,W
 105  FORMAT(//10X,'INITIAL CONCENTRATION=',E10.4,'MOLES/L',/10X,'VOLUME
     1OF REACTOR=',E10.4,'LITERS',/10X,'WEIGHT OF CARBON=',E10.4,'GM')
C
C.....SET UP TO COMPUTE INVERSE OF MATRIX......
 400  DELT=DTIME*Y(1)*6.0D1/(RAD*RAD)
      IF(LPR .NE. 1) GO TO 830
      NPR1=NPR+1
 830  Q=0.0D0
      CS=0.0D0
      QS=0.0D0
      C=CI
      CCLD=CI
      QOLD=0.0D0
      V=V1
      BLAMDA=DELT/(4.0D0*DEL)
      BAM=1.0D0-2.0D0*BLAMDA
      BAM1=1.0D0+2.0D0*BLAMDA
      DO 10 I=1,N2
      B(I)=0.0D0
      DO 20 J=1,N
      A(I,J)=0.D0
```

```
 20   CONTINUE
      A(I,I)=BAM1
 10   CONTINUE
      J1=2
      DO 30 I=1,N2
      A(I,J1)=-BLAMDA
      J1=J1+1
 30   CONTINUE
      I1=2
      DO 40 J=1,N4
      A(I1,J)=-BLAMDA
      I1=I1+1
 40   CONTINUE
      A(N,N)=1.0D0
      DO 200 I=1,N2
      A(N,I)=DFLOAT(I)/N3
 200  CONTINUE
C
C.....WRITE INPUT MATRIX.....
      IF(LPRIN .NE. 1) GO TO 500
      IF(L .NE. 1) GO TO 500
      WRITE(7,221)
 221  FORMAT(//10X,'A MATRIX',/)
      DO 50 I=1,N
      WRITE(7,107) (A(I,J),J=1,N)
 107  FORMAT(5X,(10E10.4))
 50   CONTINUE
C
C.....COMPUTE INVERSE AND PRINT.....
 500  CALL INV(N,LENA,A,IPERM,LENT,A)
      IF(LPRIN .NE. 1) GO TO 600
      IF(L .NE. 1) GO TO 600
      WRITE(7,101)
      WRITE(7,102) ID
      WRITE(7,111)
 111  FORMAT(//10X,'INVERSE OF A MATRIX',/)
      DO 70 I=1,N
      WRITE(7,107) (A(I,J),J=1,N)
 70   CONTINUE
 600  ALPHA=4.0D0*BLAMDA*RAD*Y(2)/(N*Y(1)*RHO*(1.0D0-VOID))
      B(N)=ALPHA*CI
C
C.....WRITE B VECTOR.....
      IF(LPRIN .NE. 1) GO TO 650
      IF(L .NE. 1) GO TO 650
      WRITE(7,101)
      WRITE(7,102) ID
      WRITE(7,108)
 108  FORMAT(//10X,'B VECTOR VALUES',/)
      DO 60 I=1,N
      WRITE(7,109) B(I)
 109  FORMAT(10X,E10.4)
 60   CONTINUE
C
C.....COMPUTATION OF CONCENTRATION FOR EACH TIME STEP.....
 650  DO 80 J=1,N1
      BB(J)=0.D0
 80   CONTINUE
      TIME=0.0D0
      L1=2
```

```
      LET=ETIME(L1)
      DO 120 K=2,M
      TIME=DTIME*(K-1)
C
C.....MULTIPLY B VECTOR WITH A INVERSE.....
      DO 90 I=1,N
      I1=I+1
      BB(I1)=0.D0
      DO 100 J=1,N
      BB(I1)=BB(I1)+B(J)*A(I,J)
  100 CONTINUE
   90 CONTINUE
C
C.....AVERAGE CONCENTRATION OVER THE PARTICLE.....
      Q=N3*BB(N1)
      DO 110 J=2,N
      J1=J-1
      Q=Q+BB(J)*J1
  110 CONTINUE
      Q=Q*DEL1
      C=COLD-W*(Q-QOLD)/V
      LT=TIME
      IF((TIME-LT)-0.5) 811,811,812
  812 LT=LT+1
  811 IF(LT .NE. LET) GO TO 700
      CC(L1)=C
      V=V-5.0D-3
      L1=L1+1
      LET=ETIME(L1)
      IF((ETIME(L1)-LET)-0.5D0) 700,814,814
  814 LET=LET+1
C
C.....COMPUTATION OF EQUILIBRIUM SURFACE CONCENTRATION.....
  700 QSOLD1=QS
      QS=BB(N1)*1.0D3
      IF(K .NE. 2) GO TO 810
      CSOLD=QS/(AI-BI*(QS**BETA))
      QSOLD1=QS*0.5D0
  810 CSOLD1=CSOLD
      CALL ISO(QS,CS,CSOLD,QSOLD1,CSOLD1,AI,BI,BETA,ERR,NR)
      DO 130 I=1,N2
      I1=I+1
      I2=I+2
      B(I)=BLAMDA*BB(I)+BAM*BB(I1)+BLAMDA*BB(I2)
  130 CONTINUE
      B(N)=ALPHA*(C-CS)+BB(N1)
      DO 140 I=2,N
      DI=DFLOAT(I-1)/N3
      B(N)=B(N)+BB(I)*DI
  140 CONTINUE
C
      IF(LPR .NE. 1) GO TO 920
      IF(K .NE. 2) GO TO 820
      WRITE(7,101)
      WRITE(7,102) ID
      WRITE(7,115)
  115 FORMAT(//10X,'TIME',8X,'C CALC',/10X,'MIN',8X,'MOLES/L')
      WRITE(7,116) TIME,C
  820 IF(K .NE. NPR1) GO TO 920
      WRITE(7,116) TIME,C
```

```
  116  FORMAT(6X,E10.4,4X,E10.4)
       NPR1=NPR1+NPR
  920  CCLD=C
       QOLD=Q
  120  CONTINUE
       IF(L .NE. 1) GO TO 640
       WRITE(7,101)
       WRITE(7,102) ID
       WRITE(7,206)
  206  FORMAT(//8X,'TIME',10X,'C EXP',8X,'C CALC')
       WRITE(7,207)
  207  FORMAT(8X,'MIN',9X,'MOLES/L',8X,'MOLES/L')
       WRITE(7,208) (ETIME(I),CE(I),CC(I),I=1,M2)
  208  FORMAT(4X,F10.4,6X,E10.4,3X,E10.4)
  640  L=L+1
       RETURN
       END
       SUBROUTINE ISO(QS,CS,CSOLD,QSOLD1,CSOLD1,AI,BI,BETA,ERR,NR)
C.....COMPUTATION OF EQUILIBRIUM SURFACE CONCENTRATION......
C.....EQUILIBRIUM REPRESENTED BY THREE PARAMETER EQUATION......
C.....NR MAX NUMBER OF STEPS IN NEWTON RAPHSON, ERR CONVERGECE CRITERION
       IMPLICIT REAL*8(A-H,O-Z)
       KIT=0
       CS=CSOLD
       QS1=QS*BETA
  40   DO 10 J=1,NR
       BC=BI*(CS**BETA)
       DNUM=AI*CS-QS*(1.0D0+BC)
       DENOM=AI-QS1*BC/CS
       CS=CS-DNUM/DENOM
       IF(CS) 31,31,32
  31   IF(KIT .EQ. 1) GO TO 50
       CS=(CSOLD1*QS)/QSOLD1
       KIT=1
       GO TO 40
  50   WRITE(6,1)
  1    FORMAT(//10X,'VALUE OF EQUILIBRIUM CONCENTRATION NEGATIVE IN NEWTO
      1N RAPHSON ITERATION')
       WRITE(6,4) CSOLD1,QSOLD1,QS
  4    FORMAT(//10X,'CSOLD1=',E10.4,/10X,'QSOLD1=',E10.4,/10X,'QS=',E10.4)
       WRITE(6,2)
  2    FORMAT(//10X,'INPUT ESTIMATE OF CS, FORMAT E9.4')
       READ(5,3) CS
  3    FORMAT(E9.4)
       GO TO 40
  32   IF((DABS(CS-CSOLD)/CS)-ERR) 21,21,22
  22   CSOLD=CS
  10   CONTINUE
  21   CSOLD=CS
       CS=CS*1.0D-3
       RETURN
       END
```

Estimation of Single Solute Isotherm Constants

```
      REAL FUNCTION F(X,N)
      IMPLICIT REAL*8 (A-H,O-Z)
     DIMENSION X(3),Y(3)
     COMMON C(50),Q(50),SCALE(3),PENALT,M
C.... ESTIMATION OF ISOTHERM CONSTANTS.....
     F=0.D0
     DO 12 I=1,N
     IF(X(I)) 11,12,12
 11  F=PENALT*PENALT*(1.-X(I))
     GO TO 630
 12  CONTINUE
     IF(X(3)-1.D0) 15,15,16
 16  F=PENALT*X(3)
     GO TO 630
 15  DO 20 I=1,N
     Y(I)=X(I)/SCALE(I)
 20  CONTINUE
     DO 10 I=1,M
     F=F+((Q(I)-Y(1)*C(I)/(1.D0+Y(2)*(C(I)**Y(3))))/Q(I))**2
 10  CONTINUE
 630 RETURN
     END
C.....MAIN PROGRAM.....
      IMPLICIT REAL*8 (A-H,O-Z)
     DIMENSION X(3),Y(3),ID(18)
     COMMON C(50),Q(50),SCALE(3),PENALT,M
      EXTERNAL F
      READ(5,1) M1
     READ(5,8) PENALT
 8   FORMAT(E9.4)
     READ(5,8) HO
      DO 40 J=1,M1
      WRITE(6,11) J
      READ(5,21) ID
      WRITE(6,22) ID
 21   FORMAT(18A4)
 22   FORMAT(//10X,18A4)
      READ(5,1) M
 11   FORMAT(//10X,'DATA SET NO=',I3)
 1    FORMAT(I3)
     READ(5,12) N,TO,IPRIN
 12  FORMAT(I2,E9.4,I2)
     READ(5,3) X(1),X(2),X(3)
 3   FORMAT(E9.4,1X,E9.4,1X,E9.4)
     READ(5,3) (SCALE(I),I=1,N)
     DO 60 I=1,N
     X(I)=X(I)*SCALE(I)
 60  CONTINUE
.1   DO 70 I=1,M
 2   READ(5,2) C(I),Q(I)
.3 2 FORMAT(E9.4,1X,E9.4)
.4 70 CONTINUE
      CALL PRAXIS(TO,HO,N,IPRIN,X,F,FMIN)
      PRINT 4, FMIN
 4    FORMAT(' FMIN=',E10.4)
      WRITE(6,5)
 5    FORMAT(//10X,'C',10X,'Q EXP',8X,'Q CALC')
      WRITE(6,6)
 6    FORMAT(8X,'MMOLES/L',4X,'MMOLES/GM',4X,'MMOLES/GM')
     DO 50 I=1,N
     X(I)=X(I)/SCALE(I)
 50  CONTINUE
      DO 30 I=1,M
      Q2=X(1)*C(I)/(1.D0+X(2)*(C(I)**X(3)))
      WRITE(6,7) C(I),Q(I),Q2
 7    FORMAT(7X,E10.4,2X,E10.4,3X,E10.4)
 30   CONTINUE
 40   CONTINUE
      STOP
      END
```

Prediction of Multicomponent Adsorption Rates

```
C.....M1 DATA SETS M2 DATA POINTS EACH SET.....
C.....NC NUMBER OF COMPONENTS  M NUMBER OF TIME STEPS.....
C.....N NUMBER OF DISTANCE STEPS  NR NUMBER OF NEWTON ITERATIONS.....
C.....CI INITIAL CONCENTRATION.....
C.....AI,BI,BETA CONSTANTS FOR THREE PARAMETER ISOTHERM.....
C
      IMPLICIT REAL*8(A-H,O-Z)
      DIMENSION ID1(18),ID(18),DIFF(3),FTC(3),AI(3),BI(3),BETA(3),BET(3)
     1,CI(3),ICOMP(3,18),BLAMDA(3),BAM(3),BAM1(3),ALPHA(3),A(3,25,25),B(
     23,25),BB(3,26),C(3),Q(3),CS(3),CB(3,50),ETIME(50),CC(3,50),IPERM(5
     30),G(25,25),QS(3),CSER(3),COLD(3),QOLD(3),CSOLD(3),QSOLD(3),
     4FACT(3),ETA(3),CCB(3),CCC(3)
      READ(4,1) ID1
    1 FORMAT(18A4)
      READ(4,2) L
      READ(4,2) LC
      READ(4,2) NPR
      READ(4,2) M1
    2 FORMAT(I3)
      READ(4,2) NR
      READ(4,3) ERR
    3 FORMAT(E9.4)
      DO 10 J1=1,M1
      READ(4,1) ID
      READ(4,2) NC
      READ(4,2) M2
      READ(4,4) (FACT(I),I=1,NC)
      READ(4,4) (DIFF(I),I=1,NC)
    4 FORMAT(E9.4,1X,E9.4,1X,E9.4)
      READ(4,4) (FTC(I),I=1,NC)
      READ(4,4) (AI(I),I=1,NC)
      READ(4,4) (BI(I),I=1,NC)
      READ(4,4) (BETA(I),I=1,NC)
      READ(4,4) (ETA(I),I=1,NC)
      READ(4,3) RAD
      READ(4,3) VOID
      READ(4,3) RHO
      READ(4,5) N,M
    5 FORMAT(I3,1X,I3)
      READ(4,4) (CI(I),I=1,NC)
      READ(4,6) DELX,DTIME
    6 FORMAT(E9.4,1X,E9.4)
      DO 11 I=1,NC
   11 READ(4,7) (ICOMP(I,J),J=1,18)
    7 FORMAT(18A4)
      READ(4,6) V,W
      DO 350 J=1,M2
      READ(4,8) ETIME(J),(CB(I,J),I=1,NC)
    8 FORMAT(E9.4,1X,E9.4,1X,E9.4,1X,E9.4)
  350 CONTINUE
C
      N1=N+1
      N2=N-1
      N3=N/2
      N4=N-2
      NPR1=NPR+1
      LENA=25
      LENT=25
C
C.....COMPUTE CONSTANTS.....
```

```
      DELT=DTIME*DIFF(1)*6.0D1/(RAD*RAD)
      DEL=(DELX*DELX)/2.0D0
      DEL1=DEL*6.0D0
      CC(1,1)=CE(1,1)
      C(1)=CI(1)
      COLD(1)=CI(1)
      Q(1)=0.0D0
      QCLD(1)=0.0D0
      QS(1)=0.D0
      CS(1)=0.D0
      BLAMDA(1)=DELT/(4.0D0*DEL)
      BAM(1)=1.0D0-2.0D0*BLAMDA(1)
      BAM1(1)=1.0D0+2.0D0*BLAMDA(1)
      ALPHA(1)=4.0D0*BLAMDA(1)*RAD*FTC(1)/(N*DIFF(1)*RHO*
     1(1.0D0-VOID))
      DO 20 I=2,NC
      C(I)=CI(I)
      COLD(I)=CI(I)
      Q(I)=0.0D0
      CC(I,1)=CE(I,1)
      QCLD(I)=0.0D0
      CS(I)=0.0D0
      QS(I)=0.D0
      BLAMDA(I)=DIFF(I)*BLAMDA(1)/DIFF(1)
      BAM(I)=1.0D0-2.0D0*BLAMDA(I)
      BAM1(I)=1.0D0+2.0D0*BLAMDA(I)
      ALPHA(I)=ALPHA(1)*FTC(I)/FTC(1)
 20   CONTINUE
C
C.....WRITE INPUT DATA.....
      WRITE(7,101)
 101  FORMAT('1')
      WRITE(7,102) ID
 102  FORMAT(//10X,18A4)
      WRITE(7,103) ERR,M1,NC,N,M,NR
 103  FORMAT(//10X,'ERR=',E10.4,/10X,'M1=',I3,/10X,'NC=',I3,/10X,'N=',I3
     1,/10X,'M=',I3,/10X,'NR=',I3)
      DO 30 I=1,NC
      WRITE(7,104) I,(ICOMP(I,J),J=1,18)
 104  FORMAT(//10X,'COMPONENT ',I2,/10X,18A4)
      WRITE(7,105) DIFF(I),FTC(I),ALPHA(I),AI(I),BI(I),BETA(I)
 105  FORMAT(//10X,'DIFFUSION COEFFICIENT=',E10.4,'CM SQ/SEC',/10X,'FILM
     1 TRANSFER COEFFICIENT=',E10.4,'CM/SEC',/10X,
     2    'ALPHA=',E10.4,/10X,'ISOTHERM CONSTANT A=',E10.4,/10X,'ISOTHER
     3M CONSTANT B=',E10.4,/10X,'ISCTHERM CONSTANT BETA=',E10.4)
 30   CONTINUE
      WRITE(7,106) RAD,N,M
 106  FORMAT(//10X,'RADIUS OF PARTICLE=',E10.4,/10X,'N=',I3,/10X,'M=',I3)
C
C.....SET UP TO COMPUTE INVERSE OF MATRIX.....
      DO 40 I=1,NC
      DO 50 J=1,N2
      B(I,J)=0.0D0
      DO 60 K=1,N
      A(I,J,K)=0.0D0
 60   CONTINUE
      A(I,J,J)=BAM1(I)
 50   CONTINUE
      K1=2
      DO 70 J=1,N2
```

```
      A(I,J,K1)=-BLAMDA(I)
      K1=K1+1
   70 CONTINUE
      J2=2
      DO 80 K=1,N4
      A(I,J2,K)=-BLAMDA(I)
      J2=J2+1
   80 CONTINUE
      A(I,N,N)=1.0D0
      B(I,N)=ALPHA(I)*CI(I)
      DO 90 K=1,N2
      A(I,N,K)=DFLOAT(K)/N3
   90 CONTINUE
   40 CONTINUE
C
C.....WRITE INPUT MATRIX AND B VECTOR.....
      IF(L .NE. 1) GO TO 200
      DO 100 I=1,NC
      WRITE(7,101)
      WRITE(7,102) ID
      WRITE(7,121) (ICOMP(I,J),J=1,19)
  121 FORMAT(//10X,'A MATRIX FOR ',18A4)
      DO 110 J=1,N
      WRITE(7,107) (A(I,J,K),K=1,N)
  107 FORMAT(5X,10E10.4)
  110 CONTINUE
      WRITE(7,108) I
  108 FORMAT(//10X,'B VECTOR VALUES FOR COMPONENT ',I3,/)
      DO 120 J=1,N
      WRITE(7,109) B(I,J)
  109 FORMAT(10X,E10.4)
  120 CONTINUE
  100 CONTINUE
C
C.....COMPUTE INVERSE AND PRINT.....
  200 DO 130 I=1,NC
      BB(I,1)=0.0D0
      DO 140 J=1,N
      DO 150 K=1,N
      G(J,K)=A(I,J,K)
  150 CONTINUE
  140 CONTINUE
      CALL INV(N,LENA,G,IPERM,LENT,G)
      IF(L .NE. 1) GO TO 300
      WRITE(7,111) I
  111 FORMAT(//10X,'INVERSE OF MATRIX A FOR COMPONENT ',I2)
      DO 160 J=1,N
      WRITE(7,107) (G(J,K),K=1,N)
  160 CONTINUE
  300 DO 170 J=1,N
      DO 190 K=1,N
      A(I,J,K)=G(J,K)
  190 CONTINUE
  170 CONTINUE
  130 CONTINUE
C
C.....COMPUTATION OF CONCENTRATION FOR EACH TIME STEP.....
      TIME=0.0D0
      L1=2
      LET=ETIME(L1)
```

```
      IF((ETIME(L1)-LET)-0.5DC) 817,818,818
  818 LET=LET+1
  817 IF(LC .NE. 1) GO TO 830
      IF(MC .EQ. 3) GO TO 320
      WRITE(7,115)
  115 FORMAT(//10X,'TIME',10X,'C1',10X,'C2',/10X,'MIN',9X,'MOLES/L',5X,'
     1MOLES/L',2X,'MOLES/GM',2X,'MOLES/GM')
      WRITE(7,117) TIME,(C(I1),I1=1,NC),(Q(I1),I1=1,NC)
      GO TO 830
  320 WRITE(7,116)
  116 FORMAT(//10X,'TIME',10X,'C1',10X,'C2',10X,'C3'/10X,'MIN',9X,'MOLES
     1/L',5X,'MOLES/L',5X,'MOLES/L',2X,'MOLES/GM',2X,'MOLES/GM',2X,'MOLE
     2S/GM')
      WRITE(7,123) TIME,(C(I1),I1=1,NC),(Q(I1),I1=1,NC)
  830 DO 210 K1=2,M
      TIME=DTIME*(K1-1)
      LT=TIME
C
C.....MULTIPLY B VECTOR WITH A INVERSE.....
      DO 220 I=1,NC
      DC 230 J=1,N
      J2=J+1
      BB(I,J2)=C.DC
      DO 240 K=1,N
      BB(I,J2)=BB(I,J2)+B(I,K)*A(I,J,K)
  240 CONTINUE
      QSOLD(I)=QS(I)
      QS(I)=BB(I,N1)*1.0D3
  230 CCNTINUE
C
C.....AVERAGE CONCENTRATION OVER THE PARTICLE.....
      Q(I)=N3*BB(I,N1)
      DC 250 K=2,N
      K2=K-1
      Q(I)=Q(I)+BB(I,K)*K2
  250 CONTINUE
      Q(I)=Q(I)*DEL1
      C(I)=COLD(I)-W*(Q(I)-QOLD(I))/V
      IF(I .NE. NC) GO TO 220
      IF((TIME-LT)-C.5D0)811,812,812
  812 LT=LT+1
  811 IF(LT .NE. LET) GO TO 220
      DC 360 I1=1,NC
      CC(I1,L1)=C(I1)
  360 CONTINUE
      V=V-5.0D-3
      L1=L1+1
      LET=ETIME(L1)
      IF((ETIME(L1)-LET)-0.5DC) 220,816,816
  816 LET=LET+1
  220 CCNTINUE
C
C.....CCMPUTATION OF SURFACE CONCENTRATION.....
      IF(K1 .NE. 2) GO TO 910
      DC 920 I=1,NC
      CSER(I)=QS(I)/(AI(I)-BI(I)*(QS(I)**BETA(I)))
      QSOLD(I)=QS(I)*FACT(I)
  920 CCNTINUE
  910 DO 930 I=1,NC
      CSOLD(I)=CSER(I)
```

```
930   CONTINUE
      CALL ISO(NC,NR,CSER,CS,CSOLD,QS,QSOLD,AI,BI,BETA,ERR,ETA)
      DO 260 I=1,NC
      DO 270 J=1,N2
      J2=J+1
      J3=J+2
      B(I,J)=BLAMDA(I)*BB(I,J)+BAM(I)*BB(I,J2)+BLAMDA(I)*BB(I,J3)
270   CONTINUE
      B(I,N)=ALPHA(I)*(C(I)-CS(I))+BB(I,N1)
      DO 280 J=2,N
      DI=DFLOAT(J-1)/N3
      B(I,N)=B(I,N)+BB(I,J)*DI
280   CONTINUE
260   CONTINUE
      IF(LC .NE. 1) GO TO 1125
      IF(K1 .NE. NPR1) GO TO 1125
      NPR1=NPR1+NPR
      IF(NC .EQ. 3) GO TO 850
      WRITE(7,117) TIME,(C(I1),I1=1,NC),(Q(I1),I1=1,NC)
117   FORMAT(4X,F10.4,6X,E10.4,3X,E10.4,3X,E10.4,3X,E10.4)
      GO TO 1125
850   WRITE(7,123) TIME,(C(I1),I1=1,NC),(Q(I1),I1=1,NC)
123   FORMAT(4X,F10.4,6X,E10.4,3X,E10.4,3X,E10.4,3X,E10.4,3X,E10.4,3X,E1
     10.4)
1125  DO 860 I=1,NC
      IF((DABS(C(I)-COLD(I))/C(I))-ERR)21,21,22
22    DO 970 IJ=I,NC
      COLD(IJ)=C(IJ)
      QOLD(IJ)=Q(IJ)
970   CONTINUE
      GO TO 210
21    IF(I .EQ. NC) GO TO 820
      COLD(I)=C(I)
      QOLD(I)=Q(I)
860   CONTINUE
210   CONTINUE
820   WRITE(7,101)
      WRITE(7,102) ID
      IF(NC .EQ. 3) GO TO 380
      WRITE(7,118)
118   FORMAT(//10X,'TIME',7X,'C1 EXP',7X,'C1 CALC',6X,'C2 EXP',7X,
     1'C2 CALC'/10X,'MIN',8X,'MOLES/L',6X,'MOLES/L',6X,'MOLES/L',
     26X,'MOLES/L')
      DO 870 J=1,M2
      WRITE(7,122) ETIME(J),((CE(I,J),CC(I,J)),I=1,NC)
122   FORMAT(4X,F10.4,6X,E10.4,3X,E10.4,3X,E10.4,3X,E10.4)
870   CONTINUE
      WRITE(6,126)
126   FORMAT(//10X,'TIME',6X,'C1EXP/C0',5X,'C1CALC/C0',5X,
     1'C2EXP/C0',5X,'C2CALC/C0',5X,'CTEXP/C0',5X,'CTCALC/C0')
      CTE0=0.0D0
      DO 880 I=1,NC
      CTE0=CTE0+CE(I,1)
880   CONTINUE
      DO 890 J=1,M2
      CTE=0.0D0
      CTC=0.0D0
      DO 891 I=1,NC
      CCE(I)=CE(I,J)/CE(I,1)
      CCC(I)=CC(I,J)/CE(I,1)
```

```
      CTE=CTE+CE(I,J)
      CTC=CTC+CC(I,J)
  891 CONTINUE
      CTE=CTE/CTE0
      CTC=CTC/CTE0
      WRITE(6,125) ETIME(J),(CCE(I),CCC(I),I=1,NC),CTE,CTC
  125 FORMAT(4X,F10.4,6X,E10.4,3X,E10.4,3X,E10.4,3X,E10.4,
     13X,E10.4,3X,E10.4)
  890 CONTINUE
      GO TO 10
  380 WRITE(7,119)
  119 FORMAT(//10X,'TIME',10X,'C1 EXP',7X,'C1 CALC',6X,'C2 EXP',7X,'C2 C
     1ALC',6X,'C3 EXP',7X,'C3 CALC'/10X,'MIN',7X,'MOLES/L',6X,'MOLES/L',
     36X,'MOLES/L',7X,'MOLES/L',6X,'MOLES/L',7X,'MOLES/L')
      DO 410 J=1,M2
      WRITE(7,124) ETIME(J),((CE(I,J),CC(I,J)),I=1,NC)
  124 FORMAT(4X,F10.4,6X,E10.4,3X,E10.4,3X,E10.4,3X,E10.4,3X,E10.4,3X,E1
     10.4)
  410 CONTINUE
   10 CONTINUE
      STOP
      END
C
      SUBROUTINE ISO(NC,NR,CSER,CS,CSOLD,QS,QSOLD,AI,BI,BETA,ERR,ETA)
C.....EQUILIBRIUM SURFACE CONCENTRATION USING THREE PARAMETER EQUATION..
C.....USES NEWTON RAPHSON METHOD..FIRST TIME STEP READ IN ESTIMATE.....
C.....USES OLD VALUE FOR SUBSEQUENT TIME STEPS.....
      IMPLICIT REAL*8(A-H,O-Z)
      DIMENSION CS(3),QS(3),CSER(3),AI(3),BI(3),BETA(3),QS1(3),QS2(3),DN
     1(3),A(3,3),B(3,3),X(3,3),IPERM(6),CSOLD(3),QSOLD(3),ETA(3)
      KIT=0
      DO 9 I=1,NC
      CS(I)=CSER(I)
      QS1(I)=QS(I)*ETA(I)/AI(I)
    9 CONTINUE
      DO 90 KK=1,NR
  730 DENUM=1.0D0
      DO 10 I=1,NC
      CS1=CS(I)/ETA(I)
      DN(I)=BI(I)*(CS1**BETA(I))
      QS2(I)=DN(I)*BETA(I)/(CS1*ETA(I))
      DENUM=DENUM+DN(I)
   10 CONTINUE
      DO 20 I=1,NC
      DO 30 J=1,NC
      A(I,J)=-QS1(I)*QS2(J)
   30 CONTINUE
      B(I,1)=-(CS(I)-QS1(I)*DENUM)
      A(I,I)=A(I,I)+1.0D0
   20 CONTINUE
      CALL SLE1(NC,3,A,1,3,B,X,IPERM)
      DO 40 I=1,NC
      CS(I)=CS(I)+X(I,1)
      IF(CS(I)) 31,31,40
   31 IF(KIT .EQ. 1) GO TO 50
      DO 710 IL=1,NC
      CS(IL)=(CSOLD(IL)*QS(IL))/QSOLD(IL)
  710 CONTINUE
      KIT=1
      GO TO 730
```

```
50    WRITE(6,1)
      WRITE(6,2)  (CSOLD(IL),QSOLD(IL),QS(IL),IL=1,NC)
2     FORMAT(/10X,'CSOLD=',E10.4,5X,'QSOLD=',E10.4,5X,'QS=',E10.4)
      WRITE(6,3)
1     FORMAT(//10X,'VALUE OF EQUILIBRIUM CONCENTRATION NEGATIVE IN NEWTO
     1N RAPHSON ITERATION')
3     FORMAT(/10X,'INPUT ESTIMATE OF CS(I), FORMAT E9.4,1X..')
      READ(5,4)  (CS(I),I=1,NC)
4     FORMAT(E9.4,1X,E9.4,1X,E9.4)
      GO TO 730
40    CONTINUE
      DO 80 I=1,NC
      IF((DABS((CSER(I)-CS(I))/CS(I)))-ERR) 21,21,22
22    DO 60 J=I,NC
      CSER(J)=CS(J)
60    CONTINUE
      GO TO 90
21    CSER(I)=CS(I)
80    CONTINUE
      GO TO 100
90    CONTINUE
100   DO 70 I=1,NC
      CS(I)=CS(I)*1.0D-3
70    CONTINUE
      RETURN
      END
```

Prediction of Multicomponent Equilibria

```
C.....PRAUSNITZ MODEL......
C.....NEWTON RAPHSON METHOD.. ROMBERG INTEGRATION........
C.....M1 NUMBER OF DATA SETS M NUMBER OF DATA POINTS IN EACH SET........
C.....ERR ERROR CRITERION N MAXIMUM NUMBER OF ITERATIONS IN ROMBERG.....
C.....NR MAXIMUM NUMBER OF NEWTON-RAPHSON ITERATIONS......
      IMPLICIT REAL*8(A-H,O-Z)
      DIMENSION ID1(18),ID(18),ID2(8),ID3(8),IER(50)
      COMMON B,BETA
      EXTERNAL F
C
C.....READ IN CONSTANTS......
      READ(5,1) ID1
 1    FORMAT(18A4)
      READ(5,2) M1
 2    FORMAT(I3)
      READ(5,2) N
      READ(5,2) NR
      READ(5,7) ERR
 7    FORMAT(E9.4)
      DO 10 J=1,M1
      READ(5,1) ID
      READ(5,2) M
      READ(5,3) ID2
 3    FORMAT(8A4)
      READ(5,3) ID3
      READ(5,4) A1,B1,BETA1,A2,B2,BETA2
 4    FORMAT(E9.4,1X,E9.4,1X,E9.4,1X,E9.4,1X,E9.4,1X,E9.4)
C
C.....WRITE INPUT DATA......
      WRITE(6,101)
 101  FORMAT('1')
      WRITE(6,102) ID
 102  FORMAT(//10X,18A4)
      WRITE(6,103)
 103  FORMAT(//10X,'CONSTANTS FOR THE THREE PARAMETER EQUATION')
      WRITE(6,104) ID2
 104  FORMAT(//12X,8A4)
      WRITE(6,105) A1,B1,BETA1
 105  FORMAT(//15X,'A=',E10.4,/15X,'B=',E10.4,/15X,'BETA=',E10.4)
      WRITE(6,104) ID3
      WRITE(6,105) A2,B2,BETA2
      MS=M
      IL=1
      IER(1)=0
C
C.....COMPUTATION OF EQUILIBRIA - PRAUSNITZ MODEL......
      WRITE(6,101)
      WRITE(6,102) ID
      WRITE(6,114)
 114  FORMAT(//10X,'PREDICTED VALUES - PRAUSNITZ MODEL')
      WRITE(6,109)
 109  FORMAT(//10X,'C1',8X,'C2',7X,'Q1 EXP',4X,'Q1 CALC',5X,'Q1 DEV',5X,
     1'Q2 EXP',4X,'Q2 CALC',5X,'Q2 DEV',4X,'QT EXP',5X,'QT CALC',4X,'QT
     2DEV')
      WRITE(6,110)
 110   FORMAT(7X,'MMOLES/L',2X,'MMOLES/L',3X,'MMOLES/GM',1X,'MMOLES/GM',
     114X,'MMOLES/GM',1X,'MMOLES/GM',13X,'MMOLES/GM',2X,'MMOLES/GM')
      QTSUM=0.D0
      Q1SUM=0.D0
```

```
      Q2SUM=0.D0
      IL1=1
      DO 70 I=1,M
      READ(5,5) C1,C2,Q1,Q2
5     FORMAT(E9.4,1X,E9.4,1X,E9.4,1X,E9.4)
      Z1=Q1/(Q1+Q2)
      C10=C1/Z1
      C20=C2/(1.0D0-Z1)
      IJ=0
300   C1ER=C10
      C2ER=C20
      IJ=IJ+1
      IF(IJ-NP)41,41,42
42    IER(IL)=I
      IL=IL+1
      M5=M5-1
      WRITE(6,203) IJ
203   FORMAT(//10X,'NO CONVERGENCE IN ',I3,' ITERATIONS')
      GO TO 70
41    C11=C10-C1
      C12=(C1*C2)/(C11*C11)
      CC1=C20-C10*C2/C11
      B=B1
      BETA=BETA1
      F11=F(C10)*A1
      X1=ROMBER(F,C10,ERR,N)*A1
      B=B2
      BETA=BETA2
      F22=F(C20)*A2
      X2=ROMBER(F,C20,ERR,N)*A2
      DENOM=F11+C12*F22
      DEL1=X1-X2
      DEL=(-DEL1-F22*CC1)/DENOM
      EPS=(DEL1*C12-F11*CC1)/DENOM
      C10=C10+DEL
      C20=C20+EPS
      IF(C10) 31,32,32
32    IF(C20) 31,33,33
31    IER(IL)=I
      IL=IL+1
      M5=M5-1
      WRITE(6,201) I
201   FORMAT(//10X,'C10 OR C20 NEGATIVE FOR DATA POINT NO =',I3)
      GO TO 70
33    IF((DABS(C10-C1ER)/C10)-ERR) 22,22,21
22    IF((DABS(C20-C2ER)/C20)-ERR) 23,23,21
21    GO TO 300
23    Z1=C1/C10
      Z2=1.0D0-Z1
      F22=F(C20)*A2
      B=B1
      BETA=BETA1
      F11=A1*F(C10)
      QT=1.0D0/(Z1/(C10*F11)+Z2/(C20*F22))
      QP1=QT*Z1
      QP2=QT*Z2
      IF(IER(IL1) .NE. I) GO TO 69
      IL1=IL1+1
      GO TO 70
69    QPT=QP1+QP2
```

```
      QP1DEV=(Q1-QP1)/Q1
      QP2DEV=(Q2-QP2)/Q2
      QTEXP=Q1+Q2
      QTDEV=(QTEXP-QPT)/QTEXP
      Q1SUM=Q1SUM+QP1DEV*QP1DEV
      Q2SUM=Q2SUM+QP2DEV*QP2DEV
      QTSUM=QTSUM+QTDEV*QTDEV
      WRITE(6,111) C1,C2,Q1,QP1,QP1DEV,Q2,QP2,QP2DEV,QTEXP,QPT,QTDEV
  111 FORMAT(5X,E10.4,1X,E10.4,1X,E10.4,1X,E10.4,1X,E10.4,1X,E10.4,1X,E1
     10.4,1X,E10.4,1X,E10.4,1X,E10.4,1X,E10.4)
   70 CONTINUE
      WRITE(6,202) M5
  202 FORMAT(//10X,'NUMBER OF VALID DATA POINTS=',I3)
      WRITE(6,112) Q1SUM,Q2SUM,QTSUM
  112 FORMAT(//10X,'SUM OF SQUARES OF DEVIATIONS FOR Q1=',E10.4,/10X,'SU
     1M OF SQUARES OF DEVIATIONS FOR Q2=',E10.4,/10X,'SUM OF SQUARES OF
     1DEVIATIONS FOR QT=',E10.4)
   10 CONTINUE
      STOP
      END
C
      FUNCTION F(X)
      IMPLICIT REAL*8 (A-H,O-Z)
      COMMON B,BETA
      F=1.0D0/(1.0D0+B*(X**BETA))
      RETURN
      END
C.....ROMBERG INTEGRATION.....
      FUNCTION ROMBER(F,C,EPS,N)
      IMPLICIT REAL*8(A-H,O-Z)
      DIMENSION TR(20)
      COMMON A1,B1,BETA1,A2,B2,BETA2,B,BETA,C1,C2,ERR,NR
      CL=C
      TR(1)=C*(1.0D0+F(C))/2.0D0
      N1=1
      KH=1
      DO 10 I=2,N
      H=CL/KH
      TER=TR(1)
      H1=H/2.0D0
      RECT=0.D0
      C=H1
      DO 20 I1=1,N1
      RECT=RECT+F(C)
      C=C+H
   20 CONTINUE
      RECT=H*RECT
      N2=I-1
      TR(I)=(RECT+TR(N2))/2.0D0
      KK=1
      DO 30 I2=1,N2
      I3=I-I2
      I4=I3+1
      TR(I3)=TR(I4)+(TR(I4)-TR(I3))/KK
      KK=KK*4
   30 CONTINUE
      IF((DABS(TR(1)-TER)/TR(1))-EPS) 12,12,11
   11 N1=N1*2
      KH=KH*2
   10 CONTINUE

   12 ROMBER=TR(1)
      RETURN
      END
```

BIBLIOGRAPHY

1. Brian, P.L.T., and Hales, H.B., "Effects of Transpiration and Changing Diameter on Heat and Mass Transfer to Spheres", AIChE J., 15, 419 (1969).

2. Brian, P.L.T., Hales, H.B., and Sherwood, T.K., "Transport of Heat and Mass Between Liquids and Spherical Particles in an Agitated Tank, AIChE J., 15, 727 (1969).

3. Butler, J.A.V., and Ockrent, C., "Studies in Electrocapillarity III", J. Phys. Chem., 34, 2841 (1930).

4. Calderbank, P.H., and Moo-Young, M.B., "The Continuous Phase Heat and Mass Transfer Properties of Dispersions", Chem. Eng. Sci. 16, 39 (1961).

5. Cohen, J.M., "Physical and Chemical Methods", Literature Review, J. Water Poll. Control Fed. 43, 1092 (1971).

6. Crank, J., The Mathematics of Diffusion, Clarendon Press, London (1965).

7. Danckwerts, P.V., "Significance of Liquid-Film Coefficients in Gas Absorption", Ind. Eng. Chem. 43, 1460 (1951).

8. Dedrick, R.L., and Beckman, R.B., "Kinetics of Adsorption by Activated Carbon from Dilute Aqueous Solution", Chem. Eng. Prog. Symp. Ser. 74, 63 68 (1967).

9. DeVault, D.J., "The Theory of Chromatography", J. Am. Chem. Soc. 65, 532 (1943).

10. DeWalle, F.B., and Chian, E.S.K., "Removal of Organic Matter by Activated Carbon Columns", ASCE, J. Sanit. Eng. Div. EE5, 10867 (1974).

11. DiGiano, F.M., and Weber, W.J., Jr., "Mathematical Modeling of Sorption Kinetics in Finite and Infinite Bath Systems", Tech. Publication, Research Project WP-00706, Fed. Water Poll. Control Admin., U.S. Dept. of Interior (April 1969).

12. DiGiano, F.A., and Weber, W.J., Jr., "Sorption Kinetics in Finite-Bath Systems", ASCE, J. Sanit. Eng. Div. 98, SA6, 1021 (1972).

13. DiGiano, F.A., and Weber, W.J., Jr., "Sorption Kinetics in Infinite-Bath Experiments", J. Water Poll. Control Fed. 45, 4 (1973).

14. Edeskuty, F.J., and Amundson, N.R., "Mathematics of Adsorption. IV. Effect of Intraparticle Diffusion in Agitated Systems", J. Phys. Chem. 56, 148 (1952).

15. Environmental Protection Agency 1973 (2): "The Tire and Synthetic Segment of the Rubber Processing Industry", E.P.A. Document No. 440/1-73/013.

16. Ford, D.L., "The Applicability of Carbon Adsorption in the Treatment of Petrochemical Wastes", in Applications of New Concepts of Physical-Chemical Wastewater Treatment, Pergamon Press (1972).

17. Furusawa, T., and Smith, J.M., "Intraparticle Mass Transport in Slurries by Dynamic Adsorption Studies", AIChE J., 20, 88 (1974).

18. Furusawa, T., and Smith, J.M., "Fluid-Particle and Intraparticle Mass Transport Rates in Slurries", Ind. Eng. Chem. Fundamentals 12 197 (1973).

19. Gariepy, R.L., and Zwiebel, I., "Adsorption of Binary Mixtures in Fixed Beds", AIChE Symp. Ser. 67, 117, 17 (1971).

20. Glueckauf, E., "Theory of Chromatography", J. Chem. Soc. , 1315 (1947).

21. Griffin, R.P., and Dranoff, J.S., "The Rate of Glycerol Adsorption by Ion-Exchange Resins", AIChE J. 9, 283 (1963).

22. Harriott, P., "Mass Transfer to Particles: Part I. Suspended in Agitated Tanks", AIChE J. 8, 93 (1962).

23. Hellfferich, F., and Klein, G. Multicomponent Chromatography; Theory of Interference, M.Dekker, Inc. New York (1970).

24. Hiester, N.K., and Vermuelen, T., "Saturation Performance of Ion-Exchange and Adsorption Columns", Chem. Eng. Prog. 48, 505 (1952).

25. Higbie, R., Trans. Am. Inst. Chem. Engrs., 31, 365 (1935).

26. Hougen, O.A., and Marshall, W.R., Jr., "Adsorption from a Fluid Stream Flowing Through a Stationary Granular Bed", Chem. Eng. Prog. 43, 197 (1947).

27. Hougen, O.A., Watson, K.M., and Ragatz, R.A., Chemical Process Principles - Part Two: Thermodynamics, John Wiley and Sons, Inc. (1959).

28. Hsieh, J.S., Turian, R.M., and Tien, C., "Batch Adsorption Kinetics in Sewage-Activated Carbon", ASCE, J. Sanit. Eng. Div. SA4, 505 (1971).

29. Hsieh, J.S., Turian, R.M., and Tien, C., "Experimental Investigation of the Adsorption of Organic Contaminants on Granular Activated Carbon", Res. Rpt. No. 69-1, Grant No. 17020 D20, Fed. Water Poll. Control Admin. (1969).

30. Jain, J.S., and Snoeyink, V.L., "Adsorption from Bisolute Systems on Active Carbon", J. Water Poll. Control Fed. 45, 2463 (1972).

31. Johnson, R.L., Lowes, F.J., Jr., Smith, R.M., and Powers, T.J., "Evaluation of the use of Activated Carbons and Chemical Regenerants in Treatment of Wastewater", Public Health Service Publ. No. 999-WP-13, AWTR-11.

32. Joyce, R.S., and Sukenik, V.S., "Feasibility of Granular Activated-Carbon Adsorption for Wstewater Renovation", Public Health Service Publ. No. 999-WP-12, AWTR-10.

33. Joyce, R.S., and Sukenik, V.S., "Feasibility of Granular Activated-Carbon Adsorption for Wastewater Renovation 2", Public Health Service Publ. No. 999-WP-28, AWTR-15.

34. Kasten, P.R., Lapidus, L., and Amundson, N.R., "Mathematics of Adsorption in Beds. V. Effect of Intraparticle Diffusion in Flow Systems in Fixed Beds", J. Phys. Chem. 56, 683 (1952).

35. Keinath, T.M., and Weber, W.J., Jr., "A Mathematical Model for Prediction of Concentration-Time Profiles for Design of Fluid-Bed Adsorbers", Tech. Publ., Res. Project No. WP-00706, Fed. Water Poll. Control Admin., U.S. Dept. of Interior (April 1968).

36. Keinath, T.M., and Weber, W.J., Jr., "A Predictive Model for the Design of Fluid-Bed Adsorbers", J. Water Poll. Control Fed. 40, 743 (1968).

37. Komiyama, H., and Smith, J.M., "Intraparticle Mass Transport in Liquid-Filled Pores", AIChE J. 20, 728 (1974).

38. Kyte, W.S., "Nonlinear Adsorption in Fixed Beds: the Freundlich Isotherm", Chem. Eng. Sci. 28, 1853 (1973).

39. Letterman, R.D., Quon, J.E., and Gemmel, R.S., "Film Transport Coefficients in Agitated Suspensions of Activated Carbon", J. Water Poll. Control Fed. 46, 2537 (1974).

40. Levich, V.G., Physicochemical Hydrodynamics, Prentice-Hall, Inc. (1962).

41. Levins, D.M., and Glastonbury, J.R., "Application of Kolmogoroff's Theory to Particle-Liquid Mass Transfer in Agitated Vessels", Chem. Eng. Sci. 27, 537 (1972).

42. Marangozis, J., and Johnson, A.I., "A Correlation of Mass Transfer Data of Solid-Liquid Systems in Agitated Vessels", Can. J. Chem. Eng. 40, 231 (1962).

43. Markham, E.D., and Benton, A.F., J. Am. Chem. Soc. 53, 497 (1931).

44. Masamune, S., and Smith, J.M., "Adsorption Rate Studies - Interaction of Diffusion and Surface Processes", AIChE, J. 11, 34 (1965).

45. Masamune, S., and Smith, J.M., "Adsorption Rate Studies - Significance of Pore Diffusion", AIChE, J. 10, 246 (1964).

46. Michaels, A.S., "Simplified Method of Interpreting Kinetic Data in Fixed-Bed Ion-Exchange", Ind. Eng. Chem. 44, 1922 (1952).

47. Miller, D.N., "Liquid Film Controlled Mass Transfer in Agitated Vessels", Ind. Eng. Chem. 56, 18 (1964).

48. Morris, J.C., and Weber, W.J., Jr., "Adsorption of Biochemically Resistant Materials from Solution 2", Public Health Service Publ. No. 999-WP-33, AWTR-16.

49. Myers, A.L., and Prausnitz, J.M., "Thermodynamics of Mixed-Gas Adsorption", AIChE J. 11, 121 (1965).

50. O'Farrell, T.P., Dolloff, F., Bishop, D.F., and Bennet, S.M., "Advanced Waste Treatment at Washington, D.C., Chem. Eng. Prog. Symp. Ser. 65, 251 (1967).

51. Parkhurst, J.D., Dryden, F.D., McDermott, G.N., and English, J., "pomona Activated Carbon Pilot Plant", J. Water Poll. Control Fed. 39, Part 2, R 70 (1967).

52. Ranz, W.E., and Marshall, W.R., "Evaporation from Drops, Part I", Chem. Eng. Prog. 48, 141 (1952).

53. Radke, C.J., and Prausnitz, J.M., "Thermodynamics of Multi-Solute Adsorption from Dilute Liquid Solutions", AIChE J. 18, 761 (1972).

54. Rizzo, J.L., and Schade, R.E., "Secondary Treatment with Granular Activated Carbon", Water and Sewage Works, 116, 307 (1969).

55. Rodman, C.A., and Shunney, E.L., "Bio-regenerated Activated Carbon Treatment of Textile Dye Wasteater", E.P.A. Water Poll. Control Res. Ser. 12090 DWM 01/71 (1971).

56. Rose, J.L., "Advanced Waste Treatment in Nassau County, N.Y.", Water and Wastes Eng. 7, 38 (1970).

57. Rosen, J.B., "Kinetics of a Fixed-Bed System for Solid Diffusion into Spherical Particles", J. Chem. Phys. 20, 387 (1952).

58. Rosen, J.B., "General Numerical Solution for Solid Diffusion into Fixed Beds", Ind. Eng. Chem. 46 1590('54).

59. Schay, G.J., Fejes, F.P., and Szethmary, J., "Studies on the Adsorption of Gas Mixtures, I. Statistical Theory of the Langmuir-type in Multicomponent Systems", Acta Chem. Acad. Sci. Hungary 12, 299 (1957).

60. Snoeyink, V.L., Weber, W.J., Jr., and Mark, H.B., "Sorption of Phenol and Nitrophenol by Active Carbon", Environ. Sci. Tech. 3, 918 (1969).

61. Stuart, F.X., and Camp, D.T., "Solution of the Fixed Bed Physical Adsorption Problem with Two Significant Rate Controlling Steps", AIChE Symp. Ser. 69, 134 33 (1973).

62. Thomas, H.C., "The Kinetics of Ion Exchange", in Ion Exchange, edited by F.C. Nachod, Academic Press, Inc., New York (1949).

63. Tien, C., and Thodos, G., "Ion Exchange Kinetics for Systems of Nonlinear Equilibrium Relationships", AIChE J. 5, 373 (1959).

64. Tien, C., and Thodos, G., "Ion Exchange Kinetics for Systems of Linear Equilibrium Relationships", AIChE J. 6, 364 (1960).

65. Usinowicz, P.J., and Weber, W.J., Jr., "Mathematic Simulation and Prediction of Adsorber Performance for Complex Waste Mixtures", Paper Presented at the 46th Annual Conference of the Water Poll. Control Fed. 8-13 October 1972.

68. Weber, W.J., Jr., Physicochemical Processes for Water Quality Control, Wiley-Interscience, New York (1972).

69. Weber, W.J., Jr., "Adsorption Processes", Int. Union of Pure and Applied Chem. 37, 375 (1974).

70. Weber, W.J.,Jr., Bloom, R., Jr., and Hopkins, C.B., "Expanded-Bed Active-Carbon Adsorption for Wastewater Treatment", Water Res. Symp. 3 294 (1970).

71. Weber, W.J., Jr., Friedman, L.D., and Bloom, R., Jr., "Biologically-Extended Physicochemical Treatment", Proc. of the Sixth Conf. of the Int. Assoc. on Water Poll. Res. Jerusalem, Pergamon Press, Oxford (1972).

72. Weber, W.J., Jr., and Gould, J.P., "Sorption of Organic Pesticides from Aqueous Solution", Adv. Chem. Ser. 60, 280 (1966).

73. Weber, W.J., Jr., Hopkins, C.B., and Bloom, R., Jr., "Physicochemical Treatment of Wastewater", J. Water Poll. Control Fed. 42, 1, 83 (1970).

74. Weber, W.J., Jr., and Keinath, T.M., "Mass Transfer of Perdurable Pollutants from Dilute Aqueous Soltuion in Fluidized Adsorbers", Chem. Eng. Prog. Symp. Ser. 74, 63, 79 (1967).

75. Weber, W.J., Jr., and Morris, J.C., "Kinetics of Adsorption on Carbon from Solution", ASCE, Sanit. Eng. Div. SA2, 31 (1963).

76. Weber, W.J., Jr., and Morris, J.C., "Equilibria and Capacities for Adsorption on Carbon", ASCE, Sanit. Eng. Div. SA3, 79 (1964).

77. Weber, W.J., Jr., and Morris, J.C., "Kinetics of Adsorption in Columns of Fluidized Media", J. Water Poll. Control Fed. 37, 425 (1965).

78. Weber, W.J., Jr., and Rumer, R.R., "Intraparticle Transport of Sulfonated Alkylbenzenes in a Porous Solid: Diffusion with Nonlinear Adsorption", Water Resources Res. 1, 361 (1965).

79. Williamson, J.N., Heit, A.H., and Calmon, O., "Evaluation of Various Adsorbents and Coagulants for Wastewater Renovation", Public Health Service Publ. No. 999-WP-14, AWTR-12.

80. Wilson, H.N., "New Activated Carbon Water Treater Cuts Impurities in Effluents for ARCO", Oil and Gas Journal 69, 16 (1971).

81. Yon, C.M., and Turnock, P.H., "Multicomponent Adsorption Equilibria on Molecular Sieves", AIChE Symp. Ser. 67, 75 (1971).